Universidade do Minho
Escola de Medicina

Joana Catarina Pereira de Sousa

Suppression of Machado-Joseph disease pathogenesis by serotonergic signalling: the contribution of serotonin receptors

Setembro de 2021

Suppression of Machado-Joseph disease pathogenesis by serotonergic signalling: the contribution of serotonin receptors
Joana Catarina Pereira de Sousa
UMinho | 2021

Universidade do Minho
Escola de Medicina

Joana Catarina Pereira de Sousa

Suppression of Machado-Joseph disease pathogenesis by serotonergic signalling: the contribution of serotonin receptors

Tese de Doutoramento em
Ciências da Saúde

Trabalho efetuado sob a orientação da
Doutora Andreia Cristiana Teixeira de Castro
e da
Doutora Luísa Alexandra Meireles Pinto

Setembro de 2021

Agradecimentos / Acknowledgements

À Andreia Castro por todo o apoio incondicional e as horas infindáveis de debate científico, apoio moral e amena cavaqueira sempre que era necessário. Ajudaste-me a crescer como cientista e jamais te poderei retribuir esse favor. • À Luisa Pinto. • À Patrícia Maciel, por todo o *input* científico e sorriso afável. • A toda a malta dos *C. elegans* e do "*Maciel Lab*", "*Five of a kind*" - Raquel, Rui, Célia, Sónia e Filipa – e aos doentes com MJD – com quem tive a sorte de contactar. • Aos meus grandes e eternos amigos Sun, Mariana, Juanita e Dani. • Pai e Mãe, há muito tempo atrás vocês tiveram uma escolha e eram livres de tomar qualquer um dos caminhos, sem medos nem críticas. Mas tiveram o altruísmo de me escolher a mim e proporcionar-me a vida que hoje tenho e que me faz extremamente feliz. Obrigado por tudo, esta é também uma vitória vossa. Estarei para sempre ao vosso lado! • Avô António e avó Ana, apesar de já não estarem por aqui comigo, vocês também foram a causa de tudo o que me tornei. Por isso não poderia completar esta aventura sem um pensamento caloroso e um enorme obrigado. Avó Ana, ensinaste-me a sorrir em todos os momentos da vida e essa foi, sem dúvida, a melhor de todas as lições que aprendi. Avô António, sem o teu apoio talvez o meu sonho em me tornar cientista tivesse ficado apenas por aí, obrigado por isso e por nunca teres escondido o orgulho que sentias por mim. • E como não poderia deixar de ser, um obrigado aos homens da minha vida! Toni por toda a tua paciência e por me teres sempre apoiado incondicionalmente. Nunca achaste que a minha ida para Braga fazer um doutoramento, mesmo com um filho pequeno, fosse má ideia. Estiveste lá, a fazer de pai e mãe, sempre que foi preciso. És grande! Obrigado por estares comigo. Ao meu pequeno Romeu (viste não te chamei bebé!), esta tese também é tua! Obrigado por teres sempre percebido quando a mãe não podia ir buscar-te à escola, nem levar-te aos treinos, e sempre que me atrasei para jantar. És um pequeno excepcional, nunca te esqueças disso. Por fim, ao pequeno Benjamin, tu que ainda nem viste o mundo e a mãe já puxa por ti. Desculpa as longas horas de escrita e as noites mal dormidas, mas foi por um bom motivo. Esta tese é, sem dúvida, tua também (não fosses tu parte de mim neste momento!). Mesmo antes de nasceres, obrigado por ajudares a mãe e não me roubares os neurónios todos. Finally, I would like to acknowledge all members of NERD research domain at Life and Health Sciences Research Institute (ICVS), School of medicine of the university of Minho and Bn'ML – Behavioral & Molecular Lab.[1]

PD/BDE/127834/2016 POCI-01-0145-FEDER-031987

[1] The work presented in this thesis was performed at the Life and Health Sciences Research Institute (ICVS) and at the Bn'ML – Behavioral & Molecular Lab, at the School of Medicine, University of Minho. Financial support was provided by grants from the Portuguese Foundation for Science and Technology (FCT): Doctoral Programme in Applied Health Sciences fellowship (PD/BDE/127834/2016) to J. Pereira-Sousa; and by FEDER, through the Competitiveness Internationalization Operational Programme (POCI) under the scope of the project POCI-01-0145-FEDER-031987 to A. Teixeira-Castro, supported by North Portugal Regional Operational Programme (NORTE 2020), under the PORTUGAL 2020 Partnership Agreement, through the European Regional Development Fund (ERDF) and by ICVS Scientific Microscopy Platform, member of the national infrastructure PPBI Portuguese Platform of Bioimaging (PPBI-POCI-01-0145-FEDER022122); and by National funds, through the FCT - project UIDB/50026/2020 and UIDP/50026/2020. This work was also funded through the National Ataxia Foundation (NAF), USA.

Statement of Integrity

I hereby declare having conducted this academic work with integrity. I confirm that I have not used plagiarism or any form of undue use of information or falsification of results along the process leading to its elaboration.

I further declare that I have fully acknowledged the Code of Ethical Conduct of the University of Minho.

“Supressão da patogénese da doença de Machado-Joseph através da modulação da sinalização serotoninérgica: contribuição dos receptores de serotonina”

Resumo

A doença de Machado-Joseph (DMJ) é uma doença debilitante caracterizada pela perda progressiva do equilíbrio e da coordenação motora. A nível molecular, a DMJ está associada à expansão da repetição de Citosina-Adenina-Guanina (CAG) no gene da ataxina-3. Isto traduz-se num segmento expandido de poliglutaminas na proteína ataxina-3 (ATXN3), que é propenso à auto-associação, sendo a agregação desta proteína uma característica da doença. Apesar dos vários esforços efectuados, não existe cura para esta doença fatal. A modulação da sinalização serotoninérgica foi anteriormente descrita como potencial estratégia terapêutica para a DMJ. O tratamento com citalopram (CIT), um inibidor seletivo da recaptação de serotonina, suprimiu a patogénese da DMJ em vários modelos animais, sendo o efeito do CIT dependente do transportador de serotonina, o seu alvo molecular, com provável contribuição dos receptores serotoninérgicos 5-HT_{1A}/SER-4 e 5-HT_{2}/SER-1. No entanto, o papel de cada receptor serotoninérgico na supressão da proteotoxicidade da ATXN3 mutante não foi ainda elucidado.

Aqui, com o objetivo de determinar a contribuição de cada receptor de serotonina (5-HTR) na supressão da proteotoxicidade da ATXN3 usámos um modelo de *C. elegans* que recapitula as principais características da DMJ, seguindo abordagens químico-genéticas, farmacológicas e bioquímicas, bem como técnicas de microscopia *in vivo*. Inicialmente, explorámos a contribuição do receptor 5-HT_{1A} usando befiradol, um agonista potente e altamente específico destes receptores. A administração crónica e aguda deste composto melhorou a função motora dos mutantes, sendo o ortólogo do receptor 5-HT_{1A} no nematode, o SER-4, necessário para a sua ação. De forma a aprofundar o conhecimento sobre o impacto do tratamento com befiradol na proteotoxicidade da ATXN3, optimizámos ensaios de retardação em filtro e fracionamento bioquímico para avaliar as espécies agregadas da ATXN3, demonstrando-se que ambas as modalidades de tratamento afectaram a solubilidade desta proteína. De realçar que, usando químico-genética e medições de atividade neuronal, foi-nos possível definir os auto- e hetero-receptores 5-HT_{1A}/SER-4 como essenciais para o efeito terapêutico do befiradol e propor o receptor 5-HT_{1A} como novo alvo terapêutico para a DMJ. Além disso, identificámos uma contribuição parcial dos receptores 5-HT_{6}/SER-5 e 5-HT_{7}/SER-7 para a ação do CIT. Surpreendentemente, o antagonismo dos receptores 5-HT_{2}/SER-1, 5-HT_{6}/SER-5 e 5-HT_{7}/SER-7 mostrou-se benéfico para a função motora de animais mutantes, o que é consistente com dados de perfil de expressão de RNA e farmacoterapia multimodal obtidos no nosso laboratório. Embora promissores, são necessários mais estudos para reforçar estes achados e elucidar as vias específicas pelas quais cada 5-HTR individual afecta a proteotoxicidade da ATXN3.

Palavras Chave: SCA3, serotonina, receptores serotoninérgicos, *C. elegans*, ISRS

"Suppression of Machado-Joseph disease pathogenesis by serotonergic signalling: the contribution of serotonin receptors"

Abstract

Machado-Joseph disease (MJD) is a debilitating disease mainly characterized by a progressive loss of balance and motor coordination. At the molecular level, this autosomal dominant disease is associated with an expansion of the Cytosine-Adenine-Guanine (CAG) repeat in the *ataxin-3* gene. This translates into a pathologic polyglutamine tract in the ataxin-3 protein (ATXN3) that is prone to self-associate, aggregation of ATXN3 being a hallmark of the disease. Although several efforts have been made, no cure is yet available for this fatal disorder. Serotonergic signalling modulation, by selective serotonin reuptake inhibitors (SSRIs), was previously described as a potential therapeutical strategy for MJD. Treatment with citalopram (CIT), a SSRI used in the clinics to treat depression, suppressed MJD pathogenesis in a disease-modifying manner, in several animal models. CIT's effect was dependent on its molecular target, the serotonin transporter SERT, likely with the additional need of the serotonin receptors 5-HT_{1A}R/SER-4 and 2-HT_{2}R/SER-1. However, the exact role of each serotonin receptor (5-HTR) in the suppression of mutant ATXN3 proteotoxicity remains to be fully elucidated.

Here, we aimed at determining the contribution of each of the 5-HTRs in the suppression of ATXN3 proteotoxicity using a *C. elegans* model that recapitulates major hallmarks of MJD, by employing chemical genetics, pharmacological- and biochemical- approaches, as well as *in vivo* dynamic imaging techniques. First, we explored the contribution of the 5-HT_{1A}R using a highly specific and potent agonist of these receptors, befiradol. Chronic and acute administration of befiradol rescued the motor function of mutant animals, the 5-HT_{1A}R orthologue in the nematode, SER-4, being required for its action. To further explore the impact of befiradol treatment in ATXN3 proteotoxicity, we optimised filter retardation and biochemical fractionation assays to assess mutant ATXN3 aggregation states, and we showed that both treatment modalities impacted ATXN3 solubility. Importantly, using chemical genetics and single neuron neuronal activity measurements, we defined 5-HT_{1A}R/SER-4 auto- and heteroreceptors' function to be essential to befiradol therapeutic outcome, and the 5-HT_{1A}R as a novel therapeutic target for MJD. Additionally, we found a partial contribution of 5-HT_{6}R/SER-5 and 5-HT_{7}R/SER-7 for CIT action and, surprisingly, antagonism of 5-HT_{2}R/SER-1, 5-HT_{6}R/SER-5 and 5-HT_{7}R/SER-7 showed to be beneficial for motor function of mutant animals, which is consistent with RNA-expression profiling and multimodal pharmacotherapy results obtained in our laboratory. Although promising, further studies are needed to support these findings and to elucidate the specific pathways by which each individual serotonin receptor impacts ATXN3 proteotoxicity.

Keywords: SCA3, serotonin, serotonin receptors, *C. elegans*, SSRI

Table of Contents

List of Abbreviations

#

5-HIAA – 5-hydroxyindoleacetic acid

5-HT – 5-hydroxytryptamine / serotonin

5-HTP – 5-hydroxytryptophan

5-HTR(s) – Serotonin receptor(s)

A

AD – Alzheimer's disease

ALS – Amyotrophic lateral sclerosis

APZ – Aripiprazole

ARS – Ataxia rating scale

ATXN3 – Ataxin-3 protein

ATXN3 – *Ataxin-3* gene

B

BiFC – Bimolecular fluorescence complementation

C

C. elegans – *Caenorhabditis elegans*

CAG – Cytosine-Adenine-Guanine / Citosina-Adenina-Guanina

CIT – Citalopram

CNS – Central nervous system

CRISPR – Clustered regularly interspaced short palindromic repeats

crRNA(s) – CRISPR RNA(s)

D

DAG – Diacylglycerol

DLBD – Diffuse Lewy-Body dementia

DMSO – Dimethyl sulfoxide

DRN – Dorsal raphe nucleus

DRPLA – Dentatorubral pallidoluysian atrophy

E

ER – endoplasmic reticulum

ERAD – endoplasmic reticulum–associated protein degradation

ERK – extracellular signal-regulated kinase

F

FLD – Frontal lobe dementia

FRAP – Fluorescence recovery after photobleaching

FRET – Förster/Fluorescence resonance energy transfer

G

GABA – γ-aminobutyric acid

GAPDH – glyceraldehyde 3-phosphate dehydrogenase

GIRK(s) – G protein-gated inwardly rectifying potassium channel(s)

GPCR(s) – G protein-coupled receptor(s)

I

IP3 – Inositol trisphosphate

L

LB – Luria Broth

LID – L-Dopa induced dyskinesia

M

MAO-A – monoamine oxidase A

MJD / DMJ – Machado-Joseph disease / Doença de Machado-Joseph

MS – Multiple sclerosis

N

ND(s) – Neurodegenerative disorder(s)

NGM – Nematode growth medium

P

PCR – Polymerase chain reaction

PD – Parkinson's disease

PKC – Protein kinase C

polyQ – polyglutamine

PQC - protein quality-control

R

RNAi – RNA interference

S

SCA – Spinocerebellar ataxia

SCA3 – Spinocerebellar ataxia type 3

SDS – Sodium dodecyl sulphate

SERT – Serotonin transporter

SMAX1 / SBMA – spinal bulbar muscular atrophy X-linked type 1

ssODN – Single-stranded oligodeoxynucleotide

SSRI(s) – Selective serotonin reuptake inhibitor(s)

T

TLT – Total length travel

TPS – Total protein staining

U

UIM(s) – Ubiquitin-interacting motif(s)

UPR^{mt} – Unfolded protein response of mitochondria

W

WT – Wild-type

Y

YFP – Yellow fluorescent protein

List of Figures

Chapter 1. General introduction

Chapter 2. Filter retardation and biochemical fractionation assays for detecting and quantifying neuronal polyglutamine aggregates using *C. elegans* protein lysates: protocol development attempts

Chapter 3. Identification of the 5-HT_{1A} serotonin receptor as a novel therapeutic target in a *C. elegans* model of Machado-Joseph disease

List of Tables

Chapter 1. General introduction

Chapter 2. Filter retardation and biochemical fractionation assays for detecting and quantifying neuronal polyglutamine aggregates using *C. elegans* protein lysates: protocol development attempts

Chapter 3. Identification of the 5-HT_{1A} serotonin receptor as a novel therapeutic target in a *C. elegans* model of Machado-Joseph disease

Chapter 4. Addressing the role of serotonin receptors in the suppression of mutant ataxin-3 proteotoxicity

Thesis Aims and Layout

The main aim of this thesis was to address the contribution of each of the serotonin receptors (5-HTRs) in the suppression of mutant ATXN3 proteotoxicity in *C. elegans*. For that, we have established the following specific aims:

- To implement biochemical techniques to analyse mutant ATXN3 aggregation states in *C. elegans*;
- To determine the role of 5-HT_{1A} auto- and hetero-receptors in the suppression of mutant ATXN3 aggregation and proteotoxicity;
- To investigate the potential contribution of other 5-HTRs in citalopram-mediated suppression of Machado-Joseph disease (MJD) pathogenesis;
- To establish potential novel therapeutic targets for MJD.

The present dissertation is organized in 5 chapters. Chapter 1 is the general introduction, the chapters comprising experimental work are presented in Chapter 2 to 4 (in the format of research articles) and Chapter 5 is the general discussion of the work. The research work presented in Chapter 3 was published in *Neurobiology of Disease* journal.

Before addressing the aims of this work, we provide an overview of the literature about MJD, describing the pathological features of the disease, the main pathogenic mechanism(s) and the potential therapeutic strategies discovered in the last decades, focusing mainly on the modulation of the serotonergic neurotransmission. Moreover, we described the serotonergic system in mammals, giving special attention to serotonin receptors, and we established a parallel with the organization of the serotonergic system of the nematode *C. elegans* – **Chapter 1**.

To address the first aim of this thesis and assess the impact of serotonergic system modulation in MJD, we used two major readouts and hallmarks of the disease: mutant ATXN3-mediated motor dysfunction and protein aggregation, using a *C. elegans* model of ATXN3 proteotoxicity. We optimised two biochemical techniques for the assessment of ATXN3 aggregation states, the filter retardation and biochemical fractionation assays. These two techniques explore size and solubility of the aggregates. By introducing internal loading controls, these methods became semi-quantitative, allowing for statistical analysis. We therefore successfully established and improved the laboratory protocol for assessment of ATXN3 aggregation in *C. elegans*. These two methods can complement the information given by *in vivo* confocal dynamic imaging, used to assess aggregation in this model in previous studies – **Chapter 2**.

Since, previously, Teixeira-Castro and colleagues reported a dependency on the nematode serotonin receptor SER-4, the orthologue of the 5-HT_{1A} mammalian receptor, for the effect of CIT on mutant ATXN3-induced motor dysfunction, we first explored the contribution of this receptor to the suppression of MJD pathogenesis using a highly potent and selective 5-HT_{1A} receptor agonist, befiradol – **Chapter 3**.

Next, we determined the dependency on other serotonin receptors for CIT's beneficial effect on ATXN3-induced motor impairment and we started to explore the contribution of the relevant receptors to the suppression of MJD pathogenesis using tool compounds with different intrinsic binding properties to each receptor – **Chapter 4**. We concluded that a complex remodelling of serotonin receptors activity may underlie CIT's action in MJD.

Finally, we integrate the results and describe their relevance in the field, as well as describe future perspectives – **Chapter 5**.

Chapter 1.

General Introduction

1. Machado-Joseph disease – an introduction

1.1. A polyglutamine disorder

Machado-Joseph disease (MJD), also known as Spinocerebellar ataxia (SCA) type 3 [1], is an inherited neurodegenerative disease with autosomal dominant transmission caused by a genetic alteration in the ataxin-3 gene (*ATXN3*) [2]. Clinically, it is characterized by i) progressive cerebellar ataxia, detectable as motor incoordination that affects balance, gait, and speech; ii) peripheral neuropathy; iii) oculomotor abnormalities; iv) facial and lingual fasciculations; v) extrapyramidal signs, including dystonia, rigidity and/or bradykinesia; vi) weight loss and vii) sleep disorders [3; 4; 5; 6]. Among all dominant ataxias worldwide, MJD is the most prevalent, presenting in some countries, like Portugal and Brazil, 58% to 92% of relative frequency within this group of diseases [3; 7; 8].

MJD is one of the polyglutamine (polyQ) disorders, characterized by expansion of a tandem repetition of the Cytosine-Adenine-Guanine triplet (CAG) that encodes the amino acid glutamine (Q) [9]. Within the human proteome polyQ tracts are found in 66 proteins, mainly associated with two biological processes: i) DNA dependent regulation of transcription and ii) neurogenesis [10]. PolyQ disorders include SCA types 1, 2, 6, 7 and 17 and MJD, Huntington's disease, dentatorubral pallidoluysian atrophy (DRPLA) and spinal bulbar muscular atrophy X-linked type 1 (SMAX1/SBMA) [9; 11]. The nine proteins that cause polyQ disorders differ from the other polyQ tract-containing proteins by displaying a higher genomic instability, which causes the stretching of the tandem CAG repeats to a pathological size [12].

The *ATXN3* gene was mapped on chromosome 14q32.1 (initially designated as *MJD1* [13]), and shown to possess a range of CAG units encoding for 10 to 44 glutamines in normal subjects, whereas in MJD patients it presents a polyQ tract containing 61 to 87 residues [14; 15; 16]. Intermediate polyQ lengths are not common but associated with incomplete phenotype penetrance [15]. Furthermore, a negative correlation between expansion size and age at disease onset was found [14].

At the neuropathological level, the expanded polyQ tract makes ataxin-3 protein (ATXN3) prone to aggregation, a hallmark of MJD [17]. ATXN3 is constituted by a N-terminus Josephin domain, two or three ubiquitin-interacting motifs (UIMs) and the polyQ tract, closest to the C-terminus [18; 19]. The Josephin domain makes ATXN3 prone to self-associate, inducing the formation of oligomers. Oligomers of ATXN3 with normal polyQ tracts are SDS-soluble whereas oligomers of expanded ATXN3, with

pathological polyQ tracts, undergo a second step in the aggregation process, resulting in the formation of SDS-insoluble amyloid-like aggregates [20; 21; 22].

Post-mortem, MJD patients' brain typically present atrophy of the cerebellum and brainstem, with a remarkable neuronal depletion at the cerebellar dentate nuclei, pallidum, substantia nigra, thalamus, pontine nuclei, red nuclei, various cranial nerve nuclei, anterior horn cells of the spinal cord, and Clarke's columns [23; 24; 25; 26; 27]. Also, volumetric analyses using MRI have demonstrated atrophy of the cerebellum, basal ganglia, brainstem and pallidum and suggested damage of the cerebellar–thalamocortical and basal ganglia–thalamocortical pathways [28; 29].

The ATXN3 aggregated species are often found in affected areas of MJD patients' brain, as the pons, substantia nigra, globus pallidus, dorsal medulla and dentate nucleus [17; 30]. Nonetheless, aggregates can also be found in brain areas that are typically spared by the disease [30; 31; 32]. In contrast, brain regions in which mutant ATXN3 inclusions are never detected can also undergo cellular death (e.g. the thalamus) [33]. These observations underlie the controversial role of aggregation in MJD, as some researchers consider that aggregation is a cause of the pathologic process, whereas others see it as inert or even as a cellular protective mechanism. One possible explanation for these events could be that in some brain regions the appearance of mutant ATXN3 inclusions precedes toxicity and neuronal cell death, whereas in others, the bigger aggregates are never formed as toxicity overrides aggregation. That could be the case of thalamus, where although with degeneration, the ATXN3 aggregates were not found [33]. In addition, as aggregation can be a controlled-process by quality-control mechanisms of the cell, these large aggregates can function in a way to avoid toxicity and maintained it subthreshold, preventing cell death. This can explain the ATXN3 inclusions in spared brain areas.

1.2. Disruption of protein homeostasis as a mechanism of MJD pathogenesis

The exact mechanism of MJD pathogenesis is still under debate, however it is generally accepted that a gain-of-function of toxic expanded ATXN3 contributes greatly to MJD pathology. Also, it has been proposed that disruption of the protein homeostasis can be an initiating factor of pathogenesis (reviewed in [34] and [35]).

Briefly, the expansion of the polyQ tract leads to the accumulation of the abnormal ATXN3 protein in amorphous aggregates or amyloid fibres. These changes in ATXN3 may lead to a partial loss of its deubiquitylase activity, impact aggresome formation, autophagy, the endoplasmic reticulum–associated protein degradation (ERAD) and the degradation of the proteins by the proteasome, all of which cellular

functions ATXN3 is thought to contribute for. This imbalance will impact protein homeostasis, with important consequences for cellular physiology, affecting the nucleus, mitochondria, endoplasmic reticulum and cellular communication [34].

Protein homeostasis or proteostasis is ensured by a protein quality-control (PQC) network composed of molecular chaperones, proteolytic systems and their regulators [36]. To ensure the correct proteostasis in the cell, this network i) assists the folding of newly synthetized proteins; ii) ensures properly folded proteins are generated at the correct time, cellular location, and with expected stoichiometry to allow assembly of oligomeric protein complexes and iii) prevents protein misfolding and aggregation. In case of aggregate formation, the PQC ensures the refolding or the removal of the aggregated proteins by orchestrating folding, disaggregation, and degradation, by autophagy or proteasome-mediated processes. All this surveillance, performed by the PQC network, avoids the accumulation of dysfunctional proteins and of protein aggregates. However, some insults, such as those that accumulate with aging and genetic mutations that underlie disease, can imbalance these cellular maintenance mechanisms, impairing proteostasis, and a toxic threshold can be achieved [37; 38; 39]. Therefore, any mutations within the genome which increase aggregation propensity, constitute an endogenous stress to neuronal cells and challenges their proteostasis.

The deubiquitinating enzyme activity of ATXN3 [40] consists in the removal of ubiquitin from polyubiquitinated proteins, thus modulating proteasomal and/or autophagic degradation system ([18; 41; 42; 43; 44; 45] reviewed in [45]). By editing polyubiquitin chains, ATXN3 can facilitate the degradation of some proteins or protect others from degradation [46; 47; 48; 49]. ATXN3 also was reported to be involved in the formation of aggresome [47; 50], a structure to which misfolded proteins are transported when the chaperone mediated-refolding and the ubiquitin proteasome systems are overloaded [51]. These aggresomes facilitate the clearance of misfolded proteins by autophagy. Furthermore, ATXN3 is involved in ERAD, being described that expanded ATXN3 binds excessively to VCP, a key protein responsible for extracting ERAD substrates from the endoplasmic reticulum (ER), decreasing ER retrotranslocation and degradation of ERAD substrates [52; 53].

Due to direct and indirect impact on cellular function, as explained above, ATXN3 aggregation causes an imbalance in proteostasis and a cellular burden leading to cell death and degeneration. Therefore, several compounds that modulate pathways of cellular maintenance have been tested as a potential therapy for MJD.

1.3. MJD therapeutics

Currently, there is no effective disease-modifying treatment for this devastating disease. However, several treatments are being investigated and involve i) the direct targeting of ATXN3 gene expression, ii) reducing ATXN3 aggregation, iii) increasing degradation, iv) reducing the nuclear import of ATXN3, v) inhibiting the generation of toxic fragments of the mutant protein, regulating vi) abnormal protein-protein interactions, vii) mitochondrial function, energy availability and oxidative stress or viii) correcting abnormal neuronal firing and neurotransmission (reviewed in [34; 54; 55]).

As referred above, one of the possible treatments explored for MJD relates with neurotransmission modulators. In an unbiased drug screen, Teixeira-Castro and colleagues found that citalopram (CIT), a selective serotonin reuptake inhibitor (SSRI), successfully suppressed MJD pathogenesis in animal models [56]. CIT chronic treatment was able to ameliorate motor symptoms of MJD *C. elegans* and mouse models and decrease ATXN3 aggregation, the effect being dependent on the serotonin transporter (SERT) [56; 57]. The blocking of SERT action resulting from SSRI treatment, likely increases serotonin availability at the synaptic cleft triggering the remodelling of the serotonin receptors [58; 59]. Interestingly, in an ATXN3-proteotoxicity *C. elegans* model, CIT's action was dependent not only on MOD-5, the SERT orthologue in the nematode, but also on SER-4 and SER-1, the orthologs of 5-HT_{1A} and 5-HT_2 receptors, respectively [56].

Although the use of fluoxetine, a less specific SSRI than CIT [58], failed to improve motor function of MJD patients in a small and short term clinical trial [60], other studies with serotonin 5-HT_{1A} receptor partial agonists showed efficacy in ameliorating cerebellar ataxia symptomatology [61; 62]. In these open label clinical trials, two 5-HT_{1A}R partial agonists, buspirone and tandospirone, were used. Tandospirone four-week treatment improved the ataxia rating scale (ARS) and total length travelled (TLT) scores in MJD and SCA6 patients [63]. Furthermore, in another study, MJD patients showed improved gait, posture, kinetic and total ARS [64] but after the withdrawal of the drug the symptomatology returned, showing a non-disease-modifying but rather symptomatic effect of tandospirone treatment in MJD pathogenesis [64]. Treatment with the other 5-HT_{1A}R partial agonist, buspirone, in patients with cerebellar cortical atrophy and olivopontocerebellar atrophy, improved clinical and self-assessment test scores [65], however the effect showed to be only partial and not major [66].

In summary, the serotonergic system is promising and should be further investigated as a potential therapeutic target for MJD. However, further studies are needed to better understand the mode of action of these drugs in the context of this and other neurodegenerative disorders (NDs).

2. Serotonin modulation and the impact on neurodegenerative diseases

Serotonergic system modulation was also shown to be beneficial to other NDs [67; 68; 69; 70; 71]. The common ground among these diseases may be encountered at the pathological level. Despite distinct protein abnormalities are associated with each ND, the formation of insoluble protein aggregates constitutes a common feature, these diseases being collectively often defined as "proteinopathies" [72].

Although none of the known NDs have serotonergic system dysfunction as a sole pathological basis, some reports showed serotonergic degeneration or found evidence of altered serotonin levels as a prognostic factor. Azmitia and Nixon reported a serotonergic axon dystrophy in brains of Parkinson's disease (PD), frontal lobe dementia (FLD) and Diffuse Lewy-Body dementia (DLBD) patients, however the study presented a low sample size and incomplete clinical characterization, as highlighted by the authors [73]. Altered levels of serotonin were also found in the spinal cords of amyotrophic lateral sclerosis (ALS) patients [74], with the serotonin levels in platelets being correlated with survival of these patients [75]. On the other hand, a study in multiple sclerosis (MS) showed that patients treated with fluoxetine show a tendency towards a reduction in the formation of new lesions [71]. Despite these studies pointing towards an involvement of serotonin in these diseases, they are few and the proof of evidence is tenuous. However, a large body of evidence of serotonergic involvement in disease progression and potential for therapy emerged for PD and Alzheimer's disease (AD).

In PD, serotonergic denervation was found in all stages of disease development, albeit failing to correlate with disease progression or patient's disability [76]. However, the involvement of serotonergic system in motor symptoms, as tremors, and non-motor symptoms in PD, as depression, weight loss, fatigue, and visual hallucinations was reported [77; 78; 79]. The most well studied contribution of serotonergic system in PD is in L-Dopa induced dyskinesia (LID). LID is a movement disorder often seen in PD patients due to the prolonged treatment with L-DOPA [80]. Serotonergic neurons located probably in the striatum, have all the enzymatic machinery needed to convert L-DOPA into dopamine. Therefore, in presence of L-DOPA, serotonergic neurons will store and release dopamine as a "false neurotransmitter", potentiating the LID phenotype; they are unable to regulate dopamine release due to the lack of regulatory feedback for this neurotransmitter [79]. In agreement, the administration of serotonergic autoreceptor agonists improves LID by the suppression of serotonin release, and consequently, of the "false neurotransmitter" release [81; 82; 83; 84].

Serotonin also seems to play a role in AD. Decreased levels of serotonin was described in the patients' brains [85; 86] with serotonergic denervation occurring in the raphe nucleus [87; 88; 89; 90;

91]. However, the causality between serotonergic denervation and disease progression was not proven, remaining to be determined if serotonergic neuronal death is a cause or a consequence of an overall degeneration of the AD brain. Nevertheless, serotonergic modulation seems to be a valuable strategy to impact AD pathogenesis [67; 68], and some SSRIs, as escitalopram, that decreases agitation, or 5-HT_6R antagonists, as idalopirdine and intepirdine, that showed to be cognitive enhancers, are being tested as a potential therapy for AD [69]. Also, for SMAX1/SBMA, a polyQ disease, a therapeutic action for Naratriptan, a 5-$HT_{1B/1D}$R agonist, was reported [70].

3. Serotonin

In a pioneering work of 1937, the Italian scientist Vittorio Erspamer extracted a substance from enterochromaffin cells of the gastrointestinal tract that was responsible for smooth muscle contraction and named it enteramine. But in 1952, Erspamer deduced that enteramine was in fact the same substance isolated and characterized by Maurice Rapport and Irvine Page in 1948, 5-hydroxytryptamine (5-HT) also known as serotonin [92; 93; 94; 95]. The name serotonin came from the junction of the Latin word *serum* and the Greek word *tónik*, due to its ability to cause contraction of smooth muscle such as carotid artery, jejunum, and uterus [96; 97]. Serotonin has been identified in several tissues including brain, lung, kidney, platelets, and the gastrointestinal tract, having a regulatory function in virtually all major systems, including digestive, respiratory, circulatory, urinary and reproductive (reviewed in [98]). Additionally, serotonin was later described as a neurotransmitter [99] being involved in several functions in the central nervous system (CNS).

3.1. Serotonin synthesis and metabolism

Serotonin (5-HT) is synthesized by the conversion of the essential amino acid tryptophan. Tryptophan is initially hydroxylated by tryptophan hydroxylase 2 (TPH-2) in the brain, or by tryptophan hydroxylase 1 in the periphery [100], being converted to 5-hydroxytryptophan (5-HTP). Finally, 5-HTP is decarboxylated by tryptophan decarboxylase, generating 5-HT (5-hydroxytryptamine or serotonin) [101]. The limiting step of serotonin synthesis is hydroxylation since tryptophan hydroxylase is specific for tryptophan hydroxylation whereas tryptophan decarboxylase is an L-aromatic amino acid decarboxylase, that also has other L-amino acids as substrates. Furthermore, tryptophan hydroxylase is only found in some tissues where serotonin is produced, as in the brain, enterochromaffin cells and to a less extent in platelets [102]. Besides the biosynthesis of 5-HT, tryptophan is also involved in the kynurenine pathway.

95% of the tryptophan available in the body is converted to kynurenine and its metabolites. The kynurenine pathway has two main branches that culminate in the generation of quinolinic acid and kynurenic acid, being associated with neuropsychiatric disorders and neurodegeneration [103].

The control of 5-HT levels in the body is made not only by regulation of its biosynthesis but also of its degradation [102]. The catabolism of 5-HT is performed mainly by monoamine oxidase A (MAO-A). MAO-A catalyses the conversion of 5-HT to 5-hydroxyindole aldehyde, which is further converted into 5-hydroxyindoleacetic acid (5-HIAA) by aldehyde dehydrogenase [104].

In neurons, 5-HT is synthesized by TPH-2 and released into the synaptic cleft, where it can bind to postsynaptic 5-HT heteroreceptors or to the pre-synaptic 5-HT autoreceptors. The binding of 5-HT to the autoreceptors, expressed in serotonergic neurons, activates a negative feedback signal that causes a decrease in 5-HT production and release [105]. At the synaptic cleft, serotonin can be re-internalized by the highly selective serotonin transporter (SERT) located at the presynaptic membrane, decreasing serotonin levels at the site [106; 107]. Once transported into the pre-synaptic neuron, by SERT, serotonin can be recycled into pre-synaptic vesicles or maintained in the cytosol where is metabolised by MAO-A (Figure 1). The activation of the post synaptic 5-HT heteroreceptors will result in the engagement of several pathways in the target neurons leading to various cellular and behavioural responses.

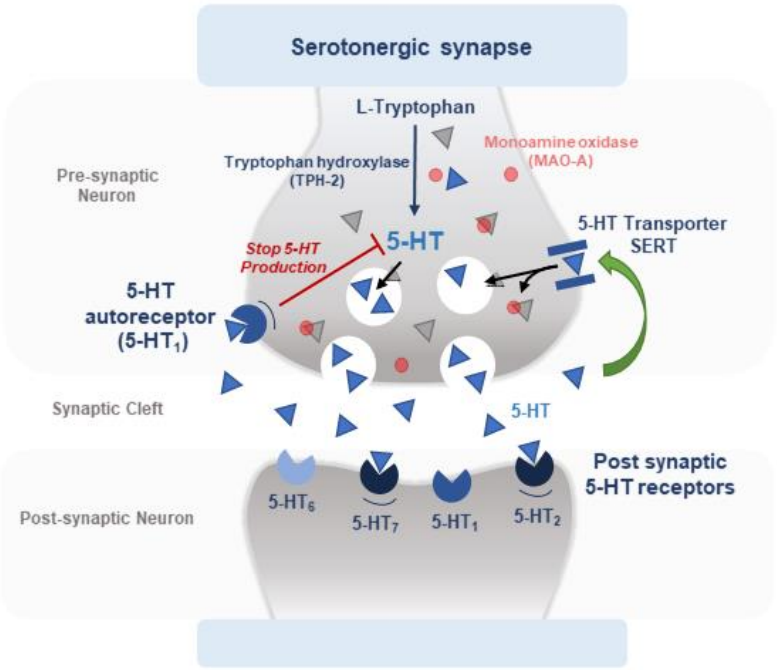

Figure 1. Schematic representation of a serotonergic synapse.

At pre-synaptic serotonergic neuron, serotonin (5-HT) is produced by the enzyme tryptophan hydroxylase (TPH-2) using the amino acid tryptophan. 5-HT is then secreted to the synaptic cleft and activates serotonin receptors (5-HTRs). 5-HTRs present

post- and pre-synaptic localizations. The 5-HT_1R family, expressed in serotonergic cells, is responsible for the triggering of the "stop serotonin production" signalling decreasing 5-HT availability at synaptic cleft. The serotonin transporter (SERT), also with pre-synaptic localization, reuptakes 5-HT that, in the cytosol, is degraded by monoamine oxidase (MAO-A) or re-encapsulated for secretion. The 5-HT in the synaptic cleft also activates the serotonin post-synaptic receptor families 5-HT_1, 5-HT_2, 5-HT_6, 5-HT_7. Only the most relevant receptors for this thesis were represented.

3.2. Serotonin function in the brain

In the mammalian brain, 5-HT is produced mainly in the dorsal raphe nucleus (DRN) located in the midbrain. Serotonergic neurons of the raphe nucleus project to several regions of the brain and spinal cord, however the density of serotonergic fibres is different between these regions. The substantia nigra, nucleus accumbens and hypothalamus present a high density, whereas frontal cortex, caudate-putamen, thalamus, ventral tegmental area, locus coeruleus, hippocampus, amygdala, olfactory bulb and dorsal and ventral horns of spinal cord have moderate to high density of serotonergic fibres. The only brain areas that present low serotonergic innervation are the cortex (with exception of frontal cortex) and the cerebellum [108; 109]. Due to the extent of projections of serotonergic neurons is not surprising this neurotransmitter is involved in several biological functions and behavioural responses. 5-HT generates a modulatory effect on neuronal excitability leading to an increase or suppression of neuronal firing rate. This results in a modulatory impact on the effect of several other neurotransmitters, such as dopamine, glutamate, GABA, etc [79]. This modulation depends on the target brain region, which can be multiple at the same time, as well as on the serotonin receptor type(s) present in the target region (reviewed on [110]). That complex and multifactorial network ensures the fine-tuning of a multiplicity of behavioural responses impacting functions as sleep, feeding, learning and memory, anxiety, mood, aggressiveness, and motor activity (reviewed in [111]).

3.3. Serotonin receptors and signalling

As referred above, serotonergic system presents a multiplicity of functions in the CNS. Despite the low number of serotonergic neurons in the brain, the impact on several responses relies on i) the large number of projections that targets virtually all brain areas and ii) a high number of 5-HTRs, that are expressed in serotonergic and non-serotonergic neurons, which initiate distinct signalling cascades.

Serotonin receptors are divided into seven large groups, represented as 5-HT_1R to 5-HT_7R. Most of these receptors are metabotropic receptors, associated with G proteins being defined as G protein-coupled receptors (GPCRs). Furthermore, each 5-HTR presents several subtypes (Table 1). 5-HT_1Rs and

5-HT_5Rs are coupled with G_i proteins, promoting an inhibitory response in the neurons. These GPCRs, upon ligand binding, elicit a canonical pathway leading to the inhibition of adenylyl-cyclase, causing a decrease in cAMP formation and the opening of G protein-gated inwardly rectifying potassium channels (GIRKs), that lead to the hyperpolarization of neurons and to the inhibition of the opening of calcium channels. Contrarily, 5-HT_2R, 5-HT_4R, 5-HT_6R and 5-HT_7R are associated with $G_{q/11}$ or G_s proteins producing an excitatory effect on neuronal activity. Activation of 5-HT_2R subtypes, that are associated with $G_{q/11}$ proteins, leads to activation of phospholipase C, that results in an increased formation of inositol trisphosphate and diacylglycerol, with further mobilization of intracellular calcium and protein kinase C activation. 5-HT_4R, 5-HT_6R and 5-HT_7R are all associated with G_s proteins, and upon 5-HT binding produce an intracellular increase in adenylyl-cyclase leading to an increase in cAMP formation. 5-HT_3R is the only 5-HT receptor that is ionotropic and mediates rapid synaptic transmission. Despite the canonical pathways referred above it is now known that activation of several 5-HTR subtypes can also elicit non-canonical pathways (summarised on Table 1) dependent or independent on GPCR activity (reviewed in [112; 113; 114]).

Table 1. Non-canonical pathways elicited by the different 5-HT receptors subtypes [112; 113; 114].

Receptor type	Receptor subtype	Non-canonical pathway
5-HT_1	5-HT_{1A}	ERK, CaMKII, Small G-protein
	5-HT_{1B}	ERK, Akt, Small G-protein
	5-HT_{1D}	
	5-HT_{1e}	
	5-HT_{1F}	
5-HT_2	5-HT_{2A}	ERK, PLA_2, PLD, Src/Akt
	5-HT_{2B}	ERK, PLA_2
	5-HT_{2C}	ERK, PLA_2, PLD
5-HT_3	5-HT_{3A}	
	5-HT_{3B}	
	5-HT_{3C}	
5-HT_4		ERK
5-HT_5	5-HT_{5A}	
	5-HT_{5b}	
5-HT_6		ERK, mTOR, Cdk5
5-HT_7		ERK, Small G-protein

Regarding receptor function, it is hard to link each receptor to a specific function or even behavioural pattern, rather several 5-HTR subtypes can play a role in a given behavioural response, often with opposite effects. Overall, 5-HTRs are associated with thermoregulation, antidepressant and anxiolytic effects, modulation of memory and learning, mood, cognition, sleep patterns, addictive behaviours, and impulsivity, as well as pain processing and seizures' thresholds (reviewed in [112]).

Several receptors are involved in anxiolytic and antidepressive behaviours, as the 5-HT_{1A}R, 5-HT_{2B}R, 5-HT_{2C}R and 5-HT_{7}R. Interestingly, due to their regional expression and distinct molecular pathways, the activation or inhibition of these receptors will often end-up in opposite effects. For example, activation of 5-HT_{1A} autoreceptors in the DRN produces an anxiolytic effect but at the same time slows the antidepressive effect elicited by treatment with SSRIs [116], by decreasing serotonin production. Furthermore, the activation of the same 5-HT_{1A}R, expressed in non-serotonergic neurons of the cortex, will produce an antidepressive effect [116] (Figure 2). Even the activation of receptors of the same family can elicit antagonistic responses; as an example, the activation of 5-HT_{2B}R and 5-HT_{2C}R can produce anxiolytic effects and anxiety, respectively [117; 118; 119; 120]. In the case of 5-HT_{4}R, its activation has a fast antidepressant action [121], therefore it is possible that this receptor contributes to the positive action of SSRIs. On the other hand, antagonism of 5-HT_{7}R leads to an antipsychotic and antidepressive-like behaviour in animal models ([122; 123; 124], reviewed in [112]).

This antagonistic effect between several 5-HTRs is not exclusive for anxiety and depression. The same is verified for thermoregulation and food perception. 5-HT_{1A}R activation leads to hypothermia and hyperphagia [125; 126; 127], in contrast with 5-HT_{2C}R activation, which causes hyperthermia and hypophagia [128; 129; 130]. 5-HT_{7}R is also involved in thermoregulation [125; 131]. A role in feeding behaviour was described for 5-HT_{6}R and 5-HT_{4}R, agonism of the latter reveals hypophagy-inducing properties [132; 133; 134; 135].

Impulsivity, memory and learning are other behavioural dimensions that require 5-HTRs' action. Antagonism of 5-HT_{2A}R and agonism of 5-HT_{2C}R decreases impulsivity [136; 137; 138; 139]. Remarkably, a knock-out mouse lacking expression of 5-HT_{2B}R, the other receptor of the 5-HT_{2}R family, presents elevated impulsivity in addition to deficits in sensory-motor gating, social interactions, attention, altered sleep and deficits in learning and memory [140]. Interestingly, 5-HT_{4}R agonism was implicated in memory and learning (reviewed in [141; 142]). Agonism of this receptor showed to be pro-cognitive, reversing cognitive deficits induced by aging and AD-like pathology ([68], reviewed in [141; 142]). On the other hand, the same pro-cognitive effects in learning and memory were found with the antagonism of 5-HT_{6}R (reviewed in [143]). Although some agonists of this receptor can also be pro-cognitive depending on the behavioural paradigm and/or the dimension evaluated by the test and/or the properties of the ligand [144; 145; 146]. Finally, 5-HT_{7}R was also implicated in memory [147].

5-HT_{2B}R, 5-HT_{2C}R and 5-HT_{7}R have been linked with sleep modulation ([140; 148; 149; 150; 151; 152], reviewed in [153]). 5-HT_{1A}R and 5-HT_{7}R were associated with pain processing [154; 155; 156].

Although a large body of knowledge is available for 5-HTRs, the 5-HT_5R, 5-HT_6R and 5-HT_7R functions are mostly still unknown. In the case of 5-HT_5R, the absence of specific and potent drugs contributes to the lack of information regarding its function and molecular pathways, however it is probable that 5-HT_5R can function in a redundant manner to 5-HT_{1A}R in some behavioural responses [157].

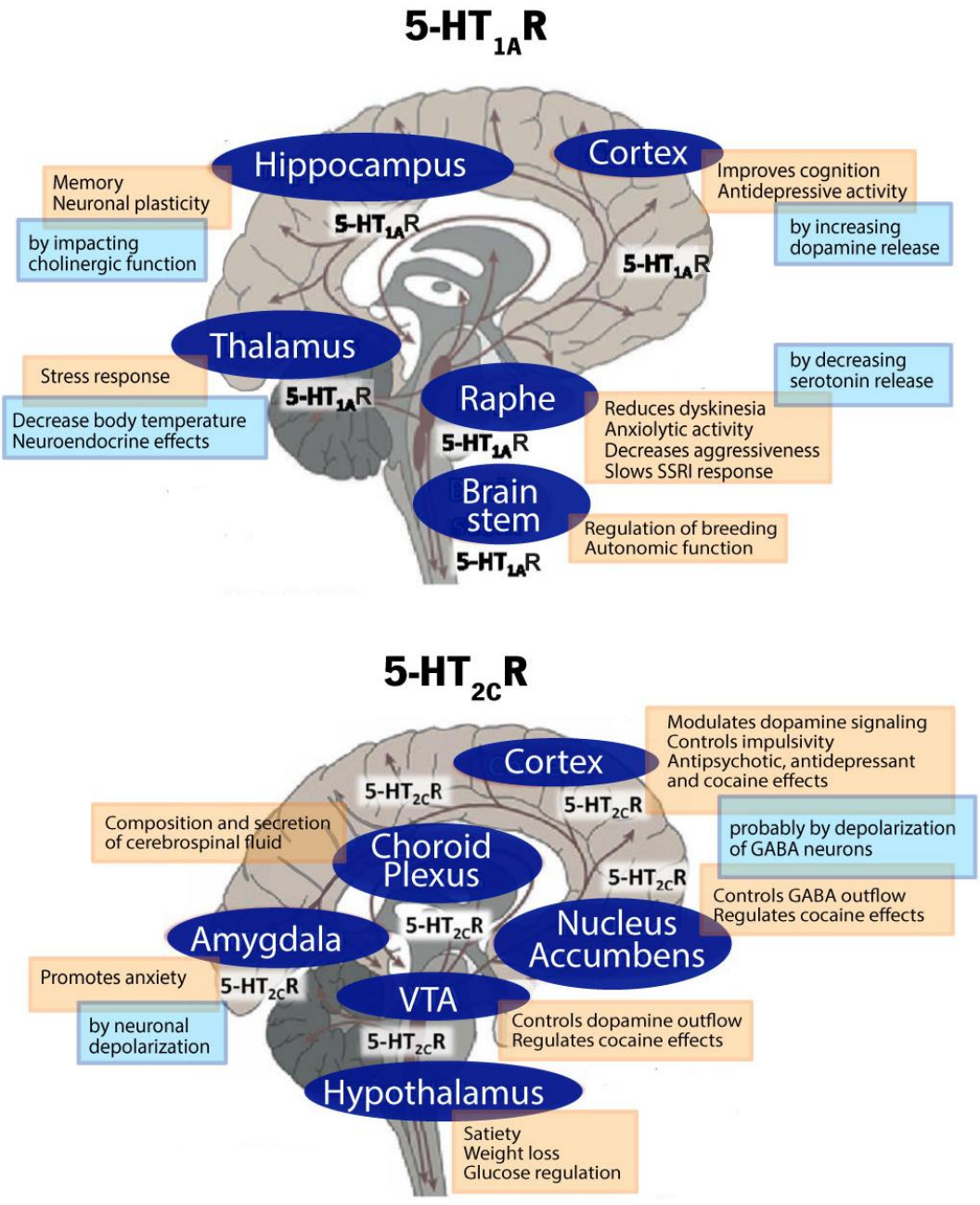

Figure 2. Serotonin receptor localization and physiological responses.

Representation of 5-HT_{1A}R and 5-HT_{2C}R expression and *in vivo* responses as evaluated with biased agonists for 5-HT_{1A}R or agonists for 5-HT_{2C}R. Orange boxes highlight physiological responses and blue boxes show the impact of receptor activation on other neurotransmitters. Adapted, with permission (appendix), from [112].

Although some functions can be attributed to 5-HTRs, as described above, the mechanism by which each receptor acts is mostly unknown. However, the probable answer in the most cases is by the modulation of other neurotransmitter systems. 5-HT_{1A}R modulates several neurotransmitters as dopamine, acetylcholine and is a regulator of the serotonergic system itself (Figure 2). 5-HT_{1B}R also mediates the inhibition of GABA, cholinergic and glutamatergic neurotransmission. The 5-HT_{2}R family plays a role in the modulation of GABA, glutamatergic, and dopaminergic transmission (Figure 2). Lastly, it was shown that 5-HT_{6}R impacts the extracellular levels of acetylcholine, glutamate, GABA, dopamine and norepinephrine (reviewed in [112]).

Therefore, serotonin action in the brain can be difficult to predict, due to the innumerous ways it impacts brain function (by projecting to several areas, the high number of receptors, the multiple signalling pathways – canonical and non-canonical – and by the modulation of other neurotransmitters). Furthermore, it is established that selective agonists of 5-HTRs are prone to bias agonism, which means that the signalling cascade activated by the engaging of drug-receptor is compound specific, and that different agonists can be more prone to activate one cellular response than another [158; 159]. This property can be extremely useful for the design of drugs with less side effects or more specific to treat specific diseases.

One more layer of complexity comes from the concepts of constitutive activity (reviewed in [160]) and homo- and heterodimerization of these receptors (reviewed in [161]). The constitutive activity corresponds to the ability of the receptors to signal, and activate a specific signalling cascade, even in the absence of a ligand. Most of the studies that point to spontaneous activity of 5-HTRs were performed *in vitro*, however some compelling *in vivo* evidence was found for at least the 5-HT_{2C}R (reviewed in [160]). Homo- and heterodimerization of 5-HTRs were also described, and 5-HTRs may dimerize not only with other serotonin receptor types but also with glutamatergic and dopaminergic receptors. The most well described heterodimers are 5-HT_{2A}R-5-HT_{2C}R, 5-HT_{1A}R-5-HT_{7}R, 5-HT_{2A}R-D2, 5-HT_{2A}R-mGlu2. These associations modulate the signalling pathways of the monomeric receptors. As an example, 5-HT_{1A}R-5-HT_{7}R heterodimerization increases 5-HT_{1A}R internalization and decreases G_i canonical signalling but increases 5-HT_{1A}R-mediated ERK signalling (reviewed in [161]). The complexity of signalling modulation by these receptors makes the serotonergic system extremely robust and versatile.

4. *Caenorhabditis elegans* – a small nematode with gigantic possibilities

The complexity of the serotonergic system in mammals increases the level of difficulty in determining the contribution of a specific receptor to a given biological process, not being easy also to predict the mode of action of some drugs *in vivo*. Therefore, simpler model systems can allow a deeper understanding of drug action *in vivo* and in a pathological situation. In this regard, *Caenorhabditis elegans* (*C. elegans*), a small nematode, has long proved to be a potent platform for the study of NDs and a suitable model for drug testing in a high-throughput manner.

C. elegans, as a model organism, was first described by Sydney Brenner. In 1974, Brenner appreciated that to study the functionality of the nervous system "*what was needed was an experimental organism which was suitable for genetical study and in which one could determine the complete structure of the nervous system". "Drosophila,"* – he wrote – *"with about* 10^5 *neurons, is much too large, and, looking for a simpler organism, my choice eventually settled on the small nematode, Caenorhabditis elegans*" [162]. Indeed, the *C. elegans* nervous system in adulthood is composed of 302 neurons with a completely known lineage, structure and connectivity [163; 164; 165]. Despite this apparent simplicity, a single sensory neuron can express up to 14 types of neurotransmitter receptors and 10 neuropeptides [166]. In 1998, the complete sequence of the *C. elegans* genome was revealed [167]; importantly, 83% of this nematode genome presented a homologous sequence in humans, corresponding to 15344 sequences [168], half of these sequences (7943) being orthologs of human genes [169].

C. elegans is a transparent, free-living nematode with about 1 mm in length, with a short life cycle of about 3.5 days from hatching to adulthood (at 20°C). Being a self-fertilizing hermaphrodite, it produces a large number of genetically identical progeny, being for that reason a good choice for high-throughput screening [170]. It is also easily maintained in laboratory conditions, on a diet of *Escherichia coli* bacteria.

The transparency of this animal allows the study of several cellular processes *in vivo*, by tagging proteins with fluorescence tags. Furthermore, it is extremely amenable to genetic manipulation. RNA interference (RNAi) [171] and clustered regularly interspaced short palindromic repeats (CRISPR)/Cas9 technology [172] are well established in the *C. elegans* field, allowing easy genetic manipulation.

The sum of all these features makes *C. elegans* an ideal model organism to study human diseases, and in particular NDs with protein aggregation as molecular basis.

4.1. C. elegans as a model system to study neurodegenerative diseases

Nowadays several models of NDs exist in *C. elegans*, namely of polyQ diseases, including HD, and MJD, as well as AD, Tauopathies, ALS, PD and prion diseases. All the models generated for each disease can, however, vary in specific tissue-driven transgene expression, length of transgene (full protein or truncated forms), mutation and, in the case of polyQ diseases, the expansion size also often varies (reviewed in [173; 174]).

For MJD, a *C. elegans* ATXN3 proteotoxicity model (AT3q130) was generated by Teixeira-Castro and colleagues [175], that addresses construct, face and predicted validity as a model of disease. This strain is a transgenic model in which the human *ATXN3* gene containing an expansion of 130 glutamines is expressed in the nervous system of the animals, having therefore the same genetic cause of the human disease (construct validity). This transgenic insertion in the *C. elegans* genome led to the development of phenotypes that are analogous to the human disease (face validity), namely motor defects and aggregation of the mutant ATXN3 protein. Furthermore, the pathogenicity of mutant ATXN3 correlates positively with the size of the polyQ expansion, animal age, degree of motor dysfunction and aggregation. Moreover, improvement of these phenotypes with specific drug treatments [56; 175; 176; 177] showed to be effective in vertebrate models of the disease [56; 57; 178; 179], and in human patients [180] (predictive validity).

Despite the simplicity of this model organism, the conservation of basic cellular mechanisms, including those related to nervous system function, associated to a validated MJD model, makes it a powerful platform for drug testing and target validation.

4.2. The C. elegans nervous system

C. elegans do not have a proper "brain", their nervous system being organized in ganglia, located in the head and tail, and the ventral nerve cord, that would correspond to the mammalian spinal cord. Its 302 neurons are divided in 118 distinct classes according to their topology and synaptic connections being possible to split them into four functional categories: motor neurons, sensory neurons, interneurons and polymodal neurons (reviewed in [163; 181]).

One third of the total number of neurons in the nematode are motor neurons. These cells make synaptic contacts with muscles and therefore control the locomotor behaviour repertoire, namely crawling, swimming and motility of alimentary and reproductive systems. Motor neurons encompass 8

classes (AS, DA, DB, DD, VA, VB, VC and VD). A and B-types (DA, DB, VA and VB) are cholinergic and excitatory, D-type (DD and VD) neurons produce γ-aminobutyric acid (GABA), an inhibitory neurotransmitter, and C-type (VC) neurons synthetize several neurotransmitters, such as acetylcholine and serotonin.

Sensory neurons are divided into sensillar neurons, that compose the 24 sensillar organs in the nematode, and several isolated sensory neurons. This category of neurons is responsible for the perception of the surrounding environment. Therefore, sensory neurons, as sensory specialized cells, can perceive specific cues of the surrounding, allowing mechanosensation, nociception, chemosensation, thermosensation, as well as light and oxygen sensation.

Interneurons constitute another group of neurons in *C. elegans*. They function as information processors, receiving input from one or more neurons, integrating the information, and transmitting it to the effector neuron. Lastly, polymodal neurons can perform more than one function, combining motor and sensory functions, interneuron and sensory or interneuron and motor functions. As an example, the NSM neuron is simultaneously a neurosecretory and motor neuron, with a sensory function in proprioception.

All these neuronal classes, as in mammals, communicate by chemical or electrical synapses, or neuromuscular junctions. Hence, *C. elegans* synapses can be explored and described by the type of neurotransmitter released by the pre-synaptic neuron. Chemical neurotransmission is accomplished by glutamatergic [182], cholinergic [183], and GABAergic [184] signalling, neuropeptides [185] and by monoaminergic [186] signalling that comprises octopamine, tyramine, dopamine and serotonin.

4.3. Serotonergic signalling in C. elegans

Despite its compact nervous system, *C. elegans* is capable of performing both basic and relatively complex behaviours. Locomotion, foraging, feeding, and defecation are the basic behaviours for animal survival, but they can also discriminate and avoid or prefer some chemicals, odorants, temperatures, and food sources (reviewed in [187]). Complex behaviours can be accomplished by this nematode, such as social feeding behaviour [188], being most of these modulated by associative learning and memory [189].

In *C. elegans*, serotonin-dependent pathways have been described in the modulation of basic behaviours as egg-laying, feeding, locomotion, and olfactory learning [190; 191; 192; 193; 194; 195].

Egg-laying is a well-studied process that involves alteration in the locomotion pattern of the *C. elegans* and is divided in two phases, the active state, where the eggs are laid in clusters, and the inactive state, in which eggs are retained. The transition between the two states was shown to be modulated by 5-HT [196; 197] and more recently by the co-released neuropeptide NLP-3, in an apparently redundant manner [191].

Feeding, as for all living animals, is an indispensable process for *C. elegans* survival. Feeding is accomplished by two processes that take place in the pharynx: pharyngeal pumping and isthmus peristalsis. The action of the serotonergic system in the pharynx was shown to be crucial for both processes, probably through the modulation of the cholinergic system [198; 199; 200]. Locomotion behaviour is not only modulated by 5-HT in the context of egg-laying but also in the context of responsiveness to food. It was shown that the so-called "enhanced slowing response", a behaviour in which food-deprived animals slow dramatically their locomotion when they encounter a food source, is dependent on serotonergic signalling. In this manner, the "enhanced slowing response" allows starved animals not to leave a favourable environment [193; 201]. Furthermore, 5-HT is essential for the learning and discrimination of good and dangerous food sources [189; 194], being involved in the induction of dwelling states of the nematode [202]. Therefore, 5-HT impacts several dimensions of feeding behaviour.

Besides neurochemical action, 5-HT plays a role in neuro-humoral signalling in *C. elegans*. Upon a stress cue, that can be environmental or intrinsic, cellular responses to suppress deregulation of protein homeostasis (namely proteostasis) are triggered and communicated through the different tissues (cell non-autonomous communication), in a process that requires 5-HT release from neurons [203; 204; 205]. It was described that 5-HT can induce the heat-shock response [206] and the unfolded protein response of the mitochondria (UPR^{mt}) [207; 208] in distal tissues, being protective against protein aggregation (Figure 3).

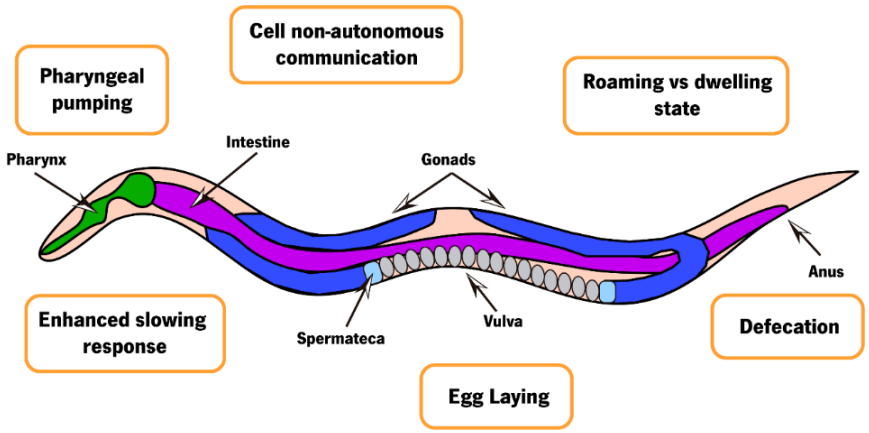

Figure 3. Representation of *C. elegans* anatomy and behaviours controlled by the serotonergic system.
The serotonergic system is involved in the regulation of behaviours represented in the yellow boxes. In the feeding process, upon encountering a loan of bacteria, starved *C. elegans* animals decrease drastically their exploratory movement, by the activation of the "enhanced slowing response" [193; 201]. Also, by the perception of the food in the environment, animals increase pharyngeal pumping [198; 199; 200] and dwelling behaviour, allowing a locally exploration of the food-rich environment increasing the turns and slowing movement [202]. In egg-laying, 5-HT released from the HSN neuron stimulates vulval muscle excitability, triggering the transition from an inactive to an active state, thus promoting egg release [196; 197]. Also, 5-HT is involved in defecation, since exogenous serotonin inhibits expulsion muscle contraction. Upon stress cues, distal tissue communication is ensured by 5-HT release, which causes the activation, in the target tissue, of stress responses and quality control mechanisms, such as the heat-shock response and the mitochondrial unfolded protein response (UPR^{mt}) [203; 204; 205; 206]. The main anatomical features of the nematode *C. elegans* are represented. The digestive tract of the animal is constituted by the pharynx, intestine and anus. The reproductive system, in the hermaphrodite, comprises the gonads, spermatheca and vulval muscles.

In the adult hermaphrodite, 5-HT is present in six types of neurons NSM; HSN; VC4/5; ADF; RIH and AIM (Figure 4). NSM, HSN and ADF being the only neurons that synthesize 5-HT, that is reuptaken by RIH, AIM and possibly by VC4 and VC5 [201; 209; 210]. The NSM is a polymodal neuron located in the pharynx (pharyngeal NeuroSecretory, Motor, sensory neuron). It projects directly to five types of cells in the pharynx; three of them are neurons and the other two are muscle cells. ADF is the only serotonergic sensory neuron in the hermaphrodite animal and may couple food sensing with serotonergic neurotransmission. AIM and RIH are both interneurons with pharyngeal localization, RIH being also a motor neuron. Both interneurons participate in the integration of external cues and modulation of *C. elegans* behaviour, namely on feeding response, locomotion, swimming and mating. HSN and VC4/5 are motor neurons located near the vulva, and they participate in egg-laying behaviour [211]. Similarly to the mammalian system, *C. elegans* serotonergic neurons project to several others that express different neurotransmitters, mainly glutamatergic (30%) and cholinergic (38.3%) neurons (Figure 4), some behaviours being accomplished by serotonergic modulation of these systems [191; 197; 212; 213].

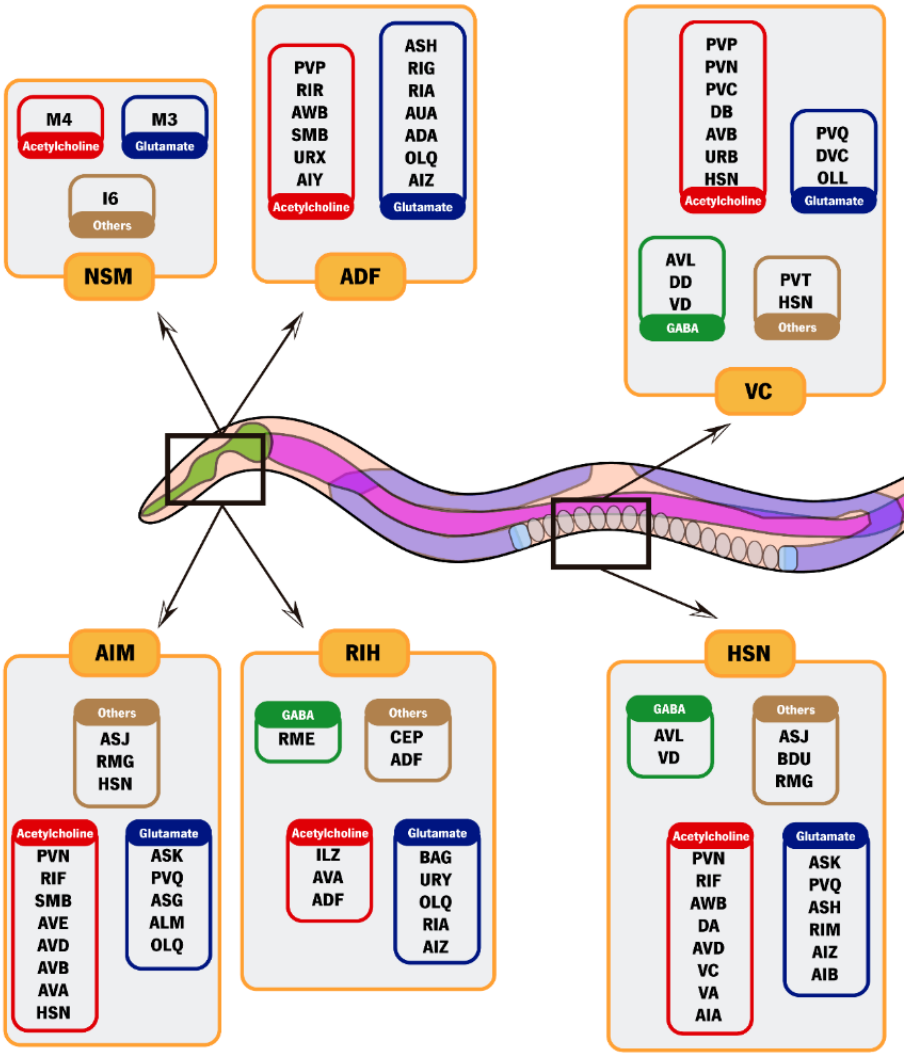

Figure 4. Serotonergic neurons in *C. elegans* hermaphrodite.

Serotonergic neurons (cell bodies) present a pharyngeal and vulval localization (Black boxes). The serotonergic neurons NSM, ADF, VC4/5, AIM, RIH and HSN (yellow boxes) project directly to several other neuronal types that synthesize GABA (green boxes), acetylcholine (red boxes), glutamate (blue boxes) or other (brown boxes) neurotransmitter as dopamine, 5-HT, neuropeptides or PDF. The neurons that do not possess classification in terms of neurotransmitter expression were omitted. From the total direct synapses established by serotonergic neurons, 38.3% are with cholinergic neurons and 30.0% with glutamatergic neurons. Just a small percentage of post-synaptic neurons are GABAergic, corresponding to 6.7%. All other classes of target neurons, that express other neurotransmitters, correspond to 15%, 10% of the synapses being established with neurons without neurotransmitter classification. Information of the neurotransmitters synthesized by the neurons was collected from [211]. Direct synapses established by serotonergic neurons collected from [214].

Until this date, four metabotropic 5-HTRs have been identified in *C. elegans*: SER-1, SER-4, SER-5 and SER-7 with orthology to the mammalian 5-HT$_2$R, 5-HT$_{1A}$R, 5-HT$_6$R and 5-HT$_7$R, respectively [43; 169; 215; 216; 217; 218; 219; 220], to which adds a nematode specific serotonin-gated chloride channel

MOD-1 [221]. These receptors are expressed in several neuronal and muscle cells in the head, vulva and tail of the animal. Overall, the synaptic localization of *C. elegans* serotonin receptors resembles that of its mammalian orthologs, with SER-4 being expressed in serotonergic neurons, as autoreceptors, and in non-serotonergic neurons, as heteroreceptors, as its orthologue 5-HT_{1A}R (Figure 1). SER-1, SER-5, SER-7 and MOD-1 are heteroreceptors expressed in non-serotonergic neurons, as its orthologs 5-HT_2R, 5-HT_6R and 5-HT_7R (Figure 1) [193; 215; 222].

G-proteins associated with *C. elegans* 5-HTRs are also conserved. SER-1 and SER-7 receptors couple to G_q (EGL-30) and G_s (GSA-1), respectively, and the SER-4 receptor couples to G_o (GOA-1) [223]. Interestingly, several of these 5-HTRs synergistically or antagonistically modulate behavioural responses. SER-1, SER-5 and SER-7 are involved in feeding behaviour and increased pharyngeal pumping rate [192; 212; 224]. In another dimension SER-4 and MOD-1 are essential to the "enhanced slowing response" [193]. Regarding egg-laying behaviour, SER-1 is the master receptor for the stimulation of egg-laying [225; 226], however it was reported that SER-7 is also involved in this stimulation [224], and in contrast MOD-1 inhibits egg-laying behaviour [225]. The current model is one where egg-laying can be regulated by all 5-HTRs depending on cell expression localization, MOD-1 and SER-4 having a suppressive effect, and SER-1, SER-7 (and possibly SER-5) an enhancing effect on egg-laying [227]. Antagonistic modulation of two 5-HTRs was also reported for lifespan, with SER-1 inhibition increasing survival of the animals, in opposition to SER-4 inhibition that decreases short to mid-lifespan, measured between day 0 and day 15 post-hatching [228].

5. Relevance of the study

Bearing in mind that i) no treatment is still available for MJD and the nefarious impact of the disease on patients' quality of life, once ii) serotonergic signalling modulation constitutes a promising therapy for this condition, the main aim of this thesis was to address the contribution of each of the 5-HTRs to the suppression of mutant ATXN3 proteotoxicity. For that we used the nematode *C. elegans* that presented a simpler although fully functional serotonergic system, with mammalian defined orthology, and took advantage of a *C. elegans* model of ATXN3 proteotoxicity (the AT3q130 transgenic strain), that mimics key pathologic hallmarks of MJD.

The determination of the role of 5-HT_{1A} auto- and heteroreceptors in the suppression of ATXN3 proteotoxicity and the investigation of the contribution of other 5-HTRs on CIT-mediated action in MJD

pathogenesis may help to deepen the understanding of how serotonergic signalling impacts MJD and potentially reveal new therapeutical targets for this disease.

References

[1] G. Haberhausen, M.S. Damian, F. Leweke, and U. Muller, Spinocerebellar ataxia, type 3 (SCA3) is genetically identical to Machado-Joseph disease (MJD). J Neurol Sci 132 (1995) 71-5. doi: 10.1016/0022-510x(95)90927-i.

[2] L. Lima, and P. Coutinho, Clinical criteria for diagnosis of Machado-Joseph disease: report of a non-Azorena Portuguese family. Neurology 30 (1980) 319-22. doi: 10.1212/wnl.30.3.319.

[3] N. Mendonca, M.C. Franca, Jr., A.F. Goncalves, and C. Januario, Clinical Features of Machado-Joseph Disease. Adv Exp Med Biol 1049 (2018) 255-273. doi: 10.1007/978-3-319-71779-1_13.

[4] H. Paulson, Machado-Joseph disease/spinocerebellar ataxia type 3. Handb Clin Neurol 103 (2012) 437-49. doi: 10.1016/B978-0-444-51892-7.00027-9.

[5] J. Sequeiros, and P. Coutinho, Epidemiology and clinical aspects of Machado-Joseph disease. Adv Neurol 61 (1993) 139-53. http://www.ncbi.nlm.nih.gov/pubmed/8421964

[6] L. Sudarsky, and P. Coutinho, Machado-Joseph disease. Clin Neurosci 3 (1995) 17-22. http://www.ncbi.nlm.nih.gov/pubmed/7614089

[7] L. Schols, G. Amoiridis, J.T. Epplen, M. Langkafel, H. Przuntek, and O. Riess, Relations between genotype and phenotype in German patients with the Machado-Joseph disease mutation. J Neurol Neurosurg Psychiatry 61 (1996) 466-70. doi: 10.1136/jnnp.61.5.466.

[8] I. Silveira, C. Miranda, L. Guimaraes, M.C. Moreira, I. Alonso, P. Mendonca, A. Ferro, J. Pinto-Basto, J. Coelho, F. Ferreirinha, J. Poirier, E. Parreira, J. Vale, C. Januario, C. Barbot, A. Tuna, J. Barros, R. Koide, S. Tsuji, S.E. Holmes, R.L. Margolis, L. Jardim, M. Pandolfo, P. Coutinho, and J. Sequeiros, Trinucleotide repeats in 202 families with ataxia: a small expanded (CAG)n allele at the SCA17 locus. Arch Neurol 59 (2002) 623-9. doi: 10.1001/archneur.59.4.623.

[9] H.T. Orr, and H.Y. Zoghbi, Trinucleotide repeat disorders. Annu Rev Neurosci 30 (2007) 575-621. doi: 10.1146/annurev.neuro.29.051605.113042.

[10] S.L. Butland, R.S. Devon, Y. Huang, C.L. Mead, A.M. Meynert, S.J. Neal, S.S. Lee, A. Wilkinson, G.S. Yang, M.M. Yuen, M.R. Hayden, R.A. Holt, B.R. Leavitt, and B.F. Ouellette, CAG-encoded polyglutamine length polymorphism in the human genome. BMC Genomics 8 (2007) 126. doi: 10.1186/1471-2164-8-126.

[11] A.R. La Spada, and J.P. Taylor, Polyglutamines placed into context. Neuron 38 (2003) 681-4. doi: 10.1016/s0896-6273(03)00328-3.

[12] Y. Takiyama, S. Igarashi, E.A. Rogaeva, K. Endo, E.I. Rogaev, H. Tanaka, R. Sherrington, K. Sanpei, Y. Liang, M. Saito, and et al., Evidence for inter-generational instability in the CAG repeat in the MJD1 gene and for conserved haplotypes at flanking markers amongst Japanese and Caucasian subjects with Machado-Joseph disease. Hum Mol Genet 4 (1995) 1137-46. doi: 10.1093/hmg/4.7.1137.

[13] H.L. Paulson, S.S. Das, P.B. Crino, M.K. Perez, S.C. Patel, D. Gotsdiner, K.H. Fischbeck, and R.N. Pittman, Machado-Joseph disease gene product is a cytoplasmic protein widely expressed in brain. Ann Neurol 41 (1997) 453-62. doi: 10.1002/ana.410410408.

[14] P. Maciel, C. Gaspar, A.L. DeStefano, I. Silveira, P. Coutinho, J. Radvany, D.M. Dawson, L. Sudarsky, J. Guimaraes, J.E. Loureiro, and et al., Correlation between CAG repeat length and clinical features in Machado-Joseph disease. Am J Hum Genet 57 (1995) 54-61. http://www.ncbi.nlm.nih.gov/pubmed/7611296

[15] Y. Kawaguchi, T. Okamoto, M. Taniwaki, M. Aizawa, M. Inoue, S. Katayama, H. Kawakami, S. Nakamura, M. Nishimura, I. Akiguchi, and et al., CAG expansions in a novel gene for Machado-Joseph disease at chromosome 14q32.1. Nat Genet 8 (1994) 221-8. doi: 10.1038/ng1194-221.

[16] H. Maruyama, S. Nakamura, Z. Matsuyama, T. Sakai, M. Doyu, G. Sobue, M. Seto, M. Tsujihata, T. Oh-i, T. Nishio, and et al., Molecular features of the CAG repeats and clinical manifestation of Machado-Joseph disease. Hum Mol Genet 4 (1995) 807-12. doi: 10.1093/hmg/4.5.807.

[17] H.L. Paulson, M.K. Perez, Y. Trottier, J.Q. Trojanowski, S.H. Subramony, S.S. Das, P. Vig, J.L. Mandel, K.H. Fischbeck, and R.N. Pittman, Intranuclear inclusions of expanded polyglutamine protein in spinocerebellar ataxia type 3. Neuron 19 (1997) 333-44. doi: 10.1016/s0896-6273(00)80943-5.

[18] Y. Chai, S.S. Berke, R.E. Cohen, and H.L. Paulson, Poly-ubiquitin binding by the polyglutamine disease protein ataxin-3 links its normal function to protein surveillance pathways. J Biol Chem 279 (2004) 3605-11. doi: 10.1074/jbc.M310939200.

[19] M. Albrecht, D. Hoffmann, B.O. Evert, I. Schmitt, U. Wullner, and T. Lengauer, Structural modeling of ataxin-3 reveals distant homology to adaptins. Proteins 50 (2003) 355-70. doi: 10.1002/prot.10280.

[20] A.E. Bevivino, and P.J. Loll, An expanded glutamine repeat destabilizes native ataxin-3 structure and mediates formation of parallel beta -fibrils. Proc Natl Acad Sci U S A 98 (2001) 11955-60. doi: 10.1073/pnas.211305198.

[21] A.M. Ellisdon, B. Thomas, and S.P. Bottomley, The two-stage pathway of ataxin-3 fibrillogenesis involves a polyglutamine-independent step. J Biol Chem 281 (2006) 16888-96. doi: 10.1074/jbc.M601470200.

[22] L. Gales, L. Cortes, C. Almeida, C.V. Melo, M.C. Costa, P. Maciel, D.T. Clarke, A.M. Damas, and S. Macedo-Ribeiro, Towards a structural understanding of the fibrillization pathway in Machado-Joseph's disease: trapping early oligomers of non-expanded ataxin-3. J Mol Biol 353 (2005) 642-54. doi: 10.1016/j.jmb.2005.08.061.

[23] C. Bettencourt, and M. Lima, Machado-Joseph Disease: from first descriptions to new perspectives. Orphanet J Rare Dis 6 (2011) 35. doi: 10.1186/1750-1172-6-35.

[24] A. Durr, G. Stevanin, G. Cancel, C. Duyckaerts, N. Abbas, O. Didierjean, H. Chneiweiss, A. Benomar, O. Lyon-Caen, J. Julien, M. Serdaru, C. Penet, Y. Agid, and A. Brice, Spinocerebellar ataxia 3 and Machado-Joseph disease: clinical, molecular, and neuropathological features. Ann Neurol 39 (1996) 490-9. doi: 10.1002/ana.410390411.

[25] J.D. Fratkin, and P.J. Vig, Neuropathology of degenerative ataxias. Handb Clin Neurol 103 (2012) 111-25. doi: 10.1016/B978-0-444-51892-7.00005-X.

[26] U. Rub, E.R. Brunt, R.A. de Vos, D. Del Turco, K. Del Tredici, K. Gierga, C. Schultz, E. Ghebremedhin, K. Burk, G. Auburger, and H. Braak, Degeneration of the central vestibular system in spinocerebellar ataxia type 3 (SCA3) patients and its possible clinical significance. Neuropathol Appl Neurobiol 30 (2004) 402-14. doi: 10.1111/j.1365-2990.2004.00554.x.

[27] Y. Takiyama, S. Oyanagi, S. Kawashima, H. Sakamoto, K. Saito, M. Yoshida, S. Tsuji, Y. Mizuno, and M. Nishizawa, A clinical and pathologic study of a large Japanese family with Machado-Joseph disease tightly linked to the DNA markers on chromosome 14q. Neurology 44 (1994) 1302-8. doi: 10.1212/wnl.44.7.1302.

[28] W.O. Arruda, A.T. Meira, S.E. Ono, A. de Carvalho Neto, L. Betting, S. Raskin, C.H.F. Camargo, and H.A.G. Teive, Volumetric MRI Changes in Spinocerebellar Ataxia (SCA3 and SCA10) Patients. Cerebellum 19 (2020) 536-543. doi: 10.1007/s12311-020-01137-3.

[29] P.S. Wang, Y.T. Wu, T.Y. Wang, H.M. Wu, B.W. Soong, and C.W. Jao, Supratentorial and Infratentorial Lesions in Spinocerebellar Ataxia Type 3. Front Neurol 11 (2020) 124. doi: 10.3389/fneur.2020.00124.

[30] T. Schmidt, G.B. Landwehrmeyer, I. Schmitt, Y. Trottier, G. Auburger, F. Laccone, T. Klockgether, M. Volpel, J.T. Epplen, L. Schols, and O. Riess, An isoform of ataxin-3 accumulates in the nucleus of neuronal cells in affected brain regions of SCA3 patients. Brain Pathol 8 (1998) 669-79. doi: 10.1111/j.1750-3639.1998.tb00193.x.

[31] U. Rub, E.R. Brunt, E. Petrasch-Parwez, L. Schols, D. Theegarten, G. Auburger, K. Seidel, C. Schultz, K. Gierga, H. Paulson, C. van Broeckhoven, T. Deller, and R.A. de Vos, Degeneration of ingestion-related brainstem nuclei in spinocerebellar ataxia type 2, 3, 6 and 7. Neuropathol Appl Neurobiol 32 (2006) 635-49. doi: 10.1111/j.1365-2990.2006.00772.x.

[32] U. Rub, R.A. de Vos, C. Schultz, E.R. Brunt, H. Paulson, and H. Braak, Spinocerebellar ataxia type 3 (Machado-Joseph disease): severe destruction of the lateral reticular nucleus. Brain 125 (2002) 2115-24. doi: 10.1093/brain/awf208.

[33] U. Rub, R.A. de Vos, E.R. Brunt, T. Sebesteny, L. Schols, G. Auburger, J. Bohl, E. Ghebremedhin, K. Gierga, K. Seidel, W. den Dunnen, H. Heinsen, H. Paulson, and T. Deller, Spinocerebellar ataxia type 3 (SCA3): thalamic neurodegeneration occurs independently from thalamic ataxin-3 immunopositive neuronal intranuclear inclusions. Brain Pathol 16 (2006) 218-27. doi: 10.1111/j.1750-3639.2006.00022.x.

[34] J.D. Da Silva, A. Teixeira-Castro, and P. Maciel, From Pathogenesis to Novel Therapeutics for Spinocerebellar Ataxia Type 3: Evading Potholes on the Way to Translation. Neurotherapeutics 16 (2019) 1009-1031. doi: 10.1007/s13311-019-00798-1.

[35] H.S. McLoughlin, L.R. Moore, and H.L. Paulson, Pathogenesis of SCA3 and implications for other polyglutamine diseases. Neurobiol Dis 134 (2020) 104635. doi: 10.1016/j.nbd.2019.104635.

[36] W.E. Balch, R.I. Morimoto, A. Dillin, and J.W. Kelly, Adapting proteostasis for disease intervention. Science 319 (2008) 916-9. doi: 10.1126/science.1141448.

[37] M.S. Hipp, P. Kasturi, and F.U. Hartl, The proteostasis network and its decline in ageing. Nat Rev Mol Cell Biol 20 (2019) 421-435. doi: 10.1038/s41580-019-0101-y.

[38] M.S. Hipp, S.H. Park, and F.U. Hartl, Proteostasis impairment in protein-misfolding and -aggregation diseases. Trends Cell Biol 24 (2014) 506-14. doi: 10.1016/j.tcb.2014.05.003.

[39] T. Gidalevitz, A. Ben-Zvi, K.H. Ho, H.R. Brignull, and R.I. Morimoto, Progressive disruption of cellular protein folding in models of polyglutamine diseases. Science 311 (2006) 1471-4. doi: 10.1126/science.1124514.

[40] B. Burnett, F. Li, and R.N. Pittman, The polyglutamine neurodegenerative protein ataxin-3 binds polyubiquitylated proteins and has ubiquitin protease activity. Hum Mol Genet 12 (2003) 3195-205. doi: 10.1093/hmg/ddg344.

[41] E.W. Doss-Pepe, E.S. Stenroos, W.G. Johnson, and K. Madura, Ataxin-3 interactions with rad23 and valosin-containing protein and its associations with ubiquitin chains and the proteasome are consistent with a role in ubiquitin-mediated proteolysis. Mol Cell Biol 23 (2003) 6469-83. doi: 10.1128/mcb.23.18.6469-6483.2003.

[42] J.M. Warrick, L.M. Morabito, J. Bilen, B. Gordesky-Gold, L.Z. Faust, H.L. Paulson, and N.M. Bonini, Ataxin-3 suppresses polyglutamine neurodegeneration in Drosophila by a ubiquitin-associated mechanism. Mol Cell 18 (2005) 37-48. doi: 10.1016/j.molcel.2005.02.030.

[43] F.F. Hamdan, M.D. Ungrin, M. Abramovitz, and P. Ribeiro, Characterization of a novel serotonin receptor from Caenorhabditis elegans: cloning and expression of two splice variants. J Neurochem 72 (1999) 1372-83. doi: 10.1046/j.1471-4159.1999.721372.x.

[44] L.K. Herzog, E. Kevei, R. Marchante, C. Bottcher, C. Bindesboll, A.H. Lystad, A. Pfeiffer, M.E. Gierisch, F.A. Salomons, A. Simonsen, T. Hoppe, and N.P. Dantuma, The Machado-Joseph

disease deubiquitylase ataxin-3 interacts with LC3C/GABARAP and promotes autophagy. Aging Cell 19 (2020) e13051. doi: 10.1111/acel.13051.

[45] A. Ashkenazi, C.F. Bento, T. Ricketts, M. Vicinanza, F. Siddiqi, M. Pavel, F. Squitieri, M.C. Hardenberg, S. Imarisio, F.M. Menzies, and D.C. Rubinsztein, Polyglutamine tracts regulate autophagy. Autophagy 13 (2017) 1613-1614. doi: 10.1080/15548627.2017.1336278.

[46] M. do Carmo Costa, F. Bajanca, A.J. Rodrigues, R.J. Tome, G. Corthals, S. Macedo-Ribeiro, H.L. Paulson, E. Logarinho, and P. Maciel, Ataxin-3 plays a role in mouse myogenic differentiation through regulation of integrin subunit levels. PLoS One 5 (2010) e11728. doi: 10.1371/journal.pone.0011728.

[47] H. Wang, Z. Ying, and G. Wang, Ataxin-3 regulates aggresome formation of copper-zinc superoxide dismutase (SOD1) by editing K63-linked polyubiquitin chains. J Biol Chem 287 (2012) 28576-85. doi: 10.1074/jbc.M111.299990.

[48] H. Liu, X. Li, G. Ning, S. Zhu, X. Ma, X. Liu, C. Liu, M. Huang, I. Schmitt, U. Wullner, Y. Niu, C. Guo, Q. Wang, and T.S. Tang, The Machado-Joseph Disease Deubiquitinase Ataxin-3 Regulates the Stability and Apoptotic Function of p53. PLoS Biol 14 (2016) e2000733. doi: 10.1371/journal.pbio.2000733.

[49] A. Neves-Carvalho, E. Logarinho, A. Freitas, S. Duarte-Silva, C. Costa Mdo, A. Silva-Fernandes, M. Martins, S.C. Serra, A.T. Lopes, H.L. Paulson, P. Heutink, J.B. Relvas, and P. Maciel, Dominant negative effect of polyglutamine expansion perturbs normal function of ataxin-3 in neuronal cells. Hum Mol Genet 24 (2015) 100-17. doi: 10.1093/hmg/ddu422.

[50] B.G. Burnett, and R.N. Pittman, The polyglutamine neurodegenerative protein ataxin 3 regulates aggresome formation. Proc Natl Acad Sci U S A 102 (2005) 4330-5. doi: 10.1073/pnas.0407252102.

[51] J.A. Johnston, C.L. Ward, and R.R. Kopito, Aggresomes: a cellular response to misfolded proteins. J Cell Biol 143 (1998) 1883-98. doi: 10.1083/jcb.143.7.1883.

[52] A. Boeddrich, S. Gaumer, A. Haacke, N. Tzvetkov, M. Albrecht, B.O. Evert, E.C. Muller, R. Lurz, P. Breuer, N. Schugardt, S. Plassmann, K. Xu, J.M. Warrick, J. Suopanki, U. Wullner, R. Frank, U.F. Hartl, N.M. Bonini, and E.E. Wanker, An arginine/lysine-rich motif is crucial for VCP/p97-mediated modulation of ataxin-3 fibrillogenesis. EMBO J 25 (2006) 1547-58. doi: 10.1038/sj.emboj.7601043.

[53] X. Zhong, and R.N. Pittman, Ataxin-3 binds VCP/p97 and regulates retrotranslocation of ERAD substrates. Hum Mol Genet 15 (2006) 2409-20. doi: 10.1093/hmg/ddl164.

[54] A. Neves-Carvalho, S. Duarte-Silva, A. Teixeira-Castro, and P. Maciel, Polyglutamine spinocerebellar ataxias: emerging therapeutic targets. Expert Opin Ther Targets 24 (2020) 1099-1119. doi: 10.1080/14728222.2020.1827394.

[55] S. Duarte-Silva, and P. Maciel, Pharmacological Therapies for Machado-Joseph Disease. Adv Exp Med Biol 1049 (2018) 369-394. doi: 10.1007/978-3-319-71779-1_19.

[56] A. Teixeira-Castro, A. Jalles, S. Esteves, S. Kang, L. da Silva Santos, A. Silva-Fernandes, M.F. Neto, R.M. Brielmann, C. Bessa, S. Duarte-Silva, A. Miranda, S. Oliveira, A. Neves-Carvalho, J. Bessa, T. Summavielle, R.B. Silverman, P. Oliveira, R.I. Morimoto, and P. Maciel, Serotonergic signalling suppresses ataxin 3 aggregation and neurotoxicity in animal models of Machado-Joseph disease. Brain 138 (2015) 3221-37. doi: 10.1093/brain/awv262.

[57] N.S. Ashraf, S. Duarte-Silva, E.D. Shaw, P. Maciel, H.L. Paulson, A. Teixeira-Castro, and M.D.C. Costa, Citalopram Reduces Aggregation of ATXN3 in a YAC Transgenic Mouse Model of Machado-Joseph Disease. Mol Neurobiol 56 (2019) 3690-3701. doi: 10.1007/s12035-018-1331-2.

[58] K. Bezchlibnyk-Butler, I. Aleksic, and S.H. Kennedy, Citalopram–a review of pharmacological and clinical effects. J Psychiatry Neurosci 25 (2000) 241-54. http://www.ncbi.nlm.nih.gov/pubmed/10863884

[59] J. Maj, and E. Moryl, Effects of sertraline and citalopram given repeatedly on the responsiveness of 5-HT receptor subpopulations. J Neural Transm Gen Sect 88 (1992) 143-56. doi: 10.1007/BF01244819.

[60] T.L. Monte, C.R. Rieder, A.B. Tort, I. Rockenback, M.L. Pereira, I. Silveira, A. Ferro, J. Sequeiros, and L.B. Jardim, Use of fluoxetine for treatment of Machado-Joseph disease: an open-label study. Acta Neurol Scand 107 (2003) 207-10. doi: 10.1034/j.1600-0404.2003.02132.x.

[61] M. Ogawa, Pharmacological treatments of cerebellar ataxia. Cerebellum 3 (2004) 107-11. doi: 10.1080/14734220410003233l.

[62] A. Takei, T. Hamada, I. Yabe, and H. Sasaki, Treatment of cerebellar ataxia with 5-HT1A agonist. Cerebellum 4 (2005) 211-5. doi: 10.1080/14734220500222318.

[63] A. Takei, S. Hamada, S. Homma, K. Hamada, K. Tashiro, and T. Hamada, Difference in the effects of tandospirone on ataxia in various types of spinocerebellar degeneration: an open-label study. Cerebellum 9 (2010) 567-70. doi: 10.1007/s12311-010-0199-0.

[64] A. Takei, T. Fukazawa, T. Hamada, H. Sohma, I. Yabe, H. Sasaki, and K. Tashiro, Effects of tandospirone on "5-HT1A receptor-associated symptoms" in patients with Machado-Josephe disease: an open-label study. Clin Neuropharmacol 27 (2004) 9-13. doi: 10.1097/00002826-200401000-00005.

[65] J.S. Lou, L. Goldfarb, L. McShane, P. Gatev, and M. Hallett, Use of buspirone for treatment of cerebellar ataxia. An open-label study. Arch Neurol 52 (1995) 982-8. doi: 10.1001/archneur.1995.00540340074015.

[66] P. Trouillas, J. Xie, P. Adeleine, D. Michel, A. Vighetto, J. Honnorat, R. Dumas, N. Nighoghossian, and B. Laurent, Buspirone, a 5-hydroxytryptamine1A agonist, is active in cerebellar ataxia. Results of a double-blind drug placebo study in patients with cerebellar cortical atrophy. Arch Neurol 54 (1997) 749-52. doi: 10.1001/archneur.1997.00550180059013.

[67] B. Benhamu, M. Martin-Fontecha, H. Vazquez-Villa, L. Pardo, and M.L. Lopez-Rodriguez, Serotonin 5-HT6 receptor antagonists for the treatment of cognitive deficiency in Alzheimer's disease. J Med Chem 57 (2014) 7160-81. doi: 10.1021/jm5003952.

[68] S. Claeysen, J. Bockaert, and P. Giannoni, Serotonin: A New Hope in Alzheimer's Disease? ACS Chem Neurosci 6 (2015) 940-3. doi: 10.1021/acschemneuro.5b00135.

[69] L.K. Huang, S.P. Chao, and C.J. Hu, Clinical trials of new drugs for Alzheimer disease. J Biomed Sci 27 (2020) 18. doi: 10.1186/s12929-019-0609-7.

[70] M. Minamiyama, M. Katsuno, H. Adachi, H. Doi, N. Kondo, M. Iida, S. Ishigaki, Y. Fujioka, S. Matsumoto, Y. Miyazaki, F. Tanaka, H. Kurihara, and G. Sobue, Naratriptan mitigates CGRP1-associated motor neuron degeneration caused by an expanded polyglutamine repeat tract. Nat Med 18 (2012) 1531-8. doi: 10.1038/nm.2932.

[71] J.P. Mostert, F. Admiraal-Behloul, J.M. Hoogduin, J. Luyendijk, D.J. Heersema, M.A. van Buchem, and J. De Keyser, Effects of fluoxetine on disease activity in relapsing multiple sclerosis: a double-blind, placebo-controlled, exploratory study. J Neurol Neurosurg Psychiatry 79 (2008) 1027-31. doi: 10.1136/jnnp.2007.139345.

[72] T.A. Bayer, Proteinopathies, a core concept for understanding and ultimately treating degenerative disorders? Eur Neuropsychopharmacol 25 (2015) 713-24. doi: 10.1016/j.euroneuro.2013.03.007.

[73] E.C. Azmitia, and R. Nixon, Dystrophic serotonergic axons in neurodegenerative diseases. Brain Res 1217 (2008) 185-94. doi: 10.1016/j.brainres.2008.03.060.

[74] O. Bertel, S. Malessa, E. Sluga, and O. Hornykiewicz, Amyotrophic lateral sclerosis: changes of noradrenergic and serotonergic transmitter systems in the spinal cord. Brain Res 566 (1991) 54-60. doi: 10.1016/0006-8993(91)91680-y.

[75] L. Dupuis, O. Spreux-Varoquaux, G. Bensimon, P. Jullien, L. Lacomblez, F. Salachas, G. Bruneteau, P.F. Pradat, J.P. Loeffler, and V. Meininger, Platelet serotonin level predicts survival in amyotrophic lateral sclerosis. PLoS One 5 (2010) e13346. doi: 10.1371/journal.pone.0013346.

[76] M. Politis, K. Wu, C. Loane, L. Kiferle, S. Molloy, D.J. Brooks, and P. Piccini, Staging of serotonergic dysfunction in Parkinson's disease: an in vivo 11C-DASB PET study. Neurobiol Dis 40 (2010) 216-21. doi: 10.1016/j.nbd.2010.05.028.

[77] M. Politis, and F. Niccolini, Serotonin in Parkinson's disease. Behav Brain Res 277 (2015) 136-45. doi: 10.1016/j.bbr.2014.07.037.

[78] G. Pagano, F. Niccolini, P. Fusar-Poli, and M. Politis, Serotonin transporter in Parkinson's disease: A meta-analysis of positron emission tomography studies. Ann Neurol 81 (2017) 171-180. doi: 10.1002/ana.24859.

[79] A. Munoz, A. Lopez-Lopez, C.M. Labandeira, and J.L. Labandeira-Garcia, Interactions Between the Serotonergic and Other Neurotransmitter Systems in the Basal Ganglia: Role in Parkinson's Disease and Adverse Effects of L-DOPA. Front Neuroanat 14 (2020) 26. doi: 10.3389/fnana.2020.00026.

[80] S. Pandey, and P. Srivanitchapoom, Levodopa-induced Dyskinesia: Clinical Features, Pathophysiology, and Medical Management. Ann Indian Acad Neurol 20 (2017) 190-198. doi: 10.4103/aian.AIAN_239_17.

[81] R. Depoortere, T.H. Johnston, S.H. Fox, J.M. Brotchie, and A. Newman-Tancredi, The selective 5-HT1A receptor agonist, NLX-112, exerts anti-dyskinetic effects in MPTP-treated macaques. Parkinsonism Relat Disord 78 (2020) 151-157. doi: 10.1016/j.parkreldis.2020.08.009.

[82] R. Fisher, A. Hikima, R. Morris, M.J. Jackson, S. Rose, M.A. Varney, R. Depoortere, and A. Newman-Tancredi, The selective 5-HT1A receptor agonist, NLX-112, exerts anti-dyskinetic and anti-parkinsonian-like effects in MPTP-treated marmosets. Neuropharmacology 167 (2020) 107997. doi: 10.1016/j.neuropharm.2020.107997.

[83] H. Iderberg, A.C. McCreary, M.A. Varney, M.S. Kleven, W. Koek, L. Bardin, R. Depoortere, M.A. Cenci, and A. Newman-Tancredi, NLX-112, a novel 5-HT1A receptor agonist for the treatment of L-DOPA-induced dyskinesia: Behavioral and neurochemical profile in rat. Exp Neurol 271 (2015) 335-50. doi: 10.1016/j.expneurol.2015.05.021.

[84] A.C. McCreary, M.A. Varney, and A. Newman-Tancredi, The novel 5-HT1A receptor agonist, NLX-112 reduces l-DOPA-induced abnormal involuntary movements in rat: A chronic administration study with microdialysis measurements. Neuropharmacology 105 (2016) 651-660. doi: 10.1016/j.neuropharm.2016.01.013.

[85] M. Garcia-Alloza, F.J. Gil-Bea, M. Diez-Ariza, C.P. Chen, P.T. Francis, B. Lasheras, and M.J. Ramirez, Cholinergic-serotonergic imbalance contributes to cognitive and behavioral symptoms in Alzheimer's disease. Neuropsychologia 43 (2005) 442-9. doi: 10.1016/j.neuropsychologia.2004.06.007.

[86] C.G. Gottfries, Disturbance of the 5-hydroxytryptamine metabolism in brains from patients with Alzheimer's dementia. J Neural Transm Suppl 30 (1990) 33-43. doi: 10.1007/978-3-7091-3345-3_4.

[87] G.G. Kovacs, S. Kloppel, I. Fischer, S. Dorner, E. Lindeck-Pozza, P. Birner, I.C. Botefur, P. Pilz, B. Volk, and H. Budka, Nucleus-specific alteration of raphe neurons in human neurodegenerative disorders. Neuroreport 14 (2003) 73-6. doi: 10.1097/00001756-200301200-00014.

[88] T. Yamamoto, and A. Hirano, Nucleus raphe dorsalis in Alzheimer's disease: neurofibrillary tangles and loss of large neurons. Ann Neurol 17 (1985) 573-7. doi: 10.1002/ana.410170608.

[89] M.A. Aletrino, O.J. Vogels, P.H. Van Domburg, and H.J. Ten Donkelaar, Cell loss in the nucleus raphes dorsalis in Alzheimer's disease. Neurobiol Aging 13 (1992) 461-8. doi: 10.1016/0197-4580(92)90073-7.

[90] C.P. Chen, S.L. Eastwood, T. Hope, B. McDonald, P.T. Francis, and M.M. Esiri, Immunocytochemical study of the dorsal and median raphe nuclei in patients with Alzheimer's disease prospectively assessed for behavioural changes. Neuropathol Appl Neurobiol 26 (2000) 347-55. doi: 10.1046/j.1365-2990.2000.00254.x.
[91] G.M. Halliday, H.L. McCann, R. Pamphlett, W.S. Brooks, H. Creasey, E. McCusker, R.G. Cotton, G.A. Broe, and C.G. Harper, Brain stem serotonin-synthesizing neurons in Alzheimer's disease: a clinicopathological correlation. Acta Neuropathol 84 (1992) 638-50. doi: 10.1007/BF00227741.
[92] V. Erspamer, and B. Asero, Identification of enteramine, the specific hormone of the enterochromaffin cell system, as 5-hydroxytryptamine. Nature 169 (1952) 800-1. doi: 10.1038/169800b0.
[93] M.M. Rapport, A.A. Green, and I.H. Page, Crystalline Serotonin. Science 108 (1948) 329-30. doi: 10.1126/science.108.2804.329.
[94] M.M. Rapport, A.A. Green, and I.H. Page, Partial purification of the vasoconstrictor in beef serum. J Biol Chem 174 (1948) 735-41. http://www.ncbi.nlm.nih.gov/pubmed/18865641
[95] M.M. Rapport, A.A. Green, and I.H. Page, Serum vasoconstrictor, serotonin; isolation and characterization. J Biol Chem 176 (1948) 1243-51. http://www.ncbi.nlm.nih.gov/pubmed/18100415
[96] G. Reid, and M. Rand, Pharmacological actions of synthetic 5-hydroxytryptamine (serotonin, thrombocytin). Nature 169 (1952) 801-2. doi: 10.1038/169801a0.
[97] M.B. Zucker, A STUDY OF THE SUBSTANCES IN BLOOD SERUM AND PLATELETS WHICH STIMULATE SMOOTH MUSCLE. American Journal of Physiology-Legacy Content 142 (1944) 12-26. doi: 10.1152/ajplegacy.1944.142.1.12.
[98] M. Berger, J.A. Gray, and B.L. Roth, The expanded biology of serotonin. Annu Rev Med 60 (2009) 355-66. doi: 10.1146/annurev.med.60.042307.110802.
[99] B.B. Brodie, and P.A. Shore, A concept for a role of serotonin and norepinephrine as chemical mediators in the brain. Ann N Y Acad Sci 66 (1957) 631-42. doi: 10.1111/j.1749-6632.1957.tb40753.x.
[100] X. Zhang, J.M. Beaulieu, T.D. Sotnikova, R.R. Gainetdinov, and M.G. Caron, Tryptophan hydroxylase-2 controls brain serotonin synthesis. Science 305 (2004) 217. doi: 10.1126/science.1097540.
[101] C.T. Clark, H. Weissbach, and S. Udenfriend, 5-Hydroxytryptophan decarboxylase: preparation and properties. J Biol Chem 210 (1954) 139-48. http://www.ncbi.nlm.nih.gov/pubmed/13201577
[102] G.M. Tyce, Origin and metabolism of serotonin. J Cardiovasc Pharmacol 16 Suppl 3 (1990) S1-7. http://www.ncbi.nlm.nih.gov/pubmed/1369709
[103] J. Savitz, The kynurenine pathway: a finger in every pie. Mol Psychiatry 25 (2020) 131-147. doi: 10.1038/s41380-019-0414-4.
[104] D. Keszthelyi, F.J. Troost, and A.A. Masclee, Understanding the role of tryptophan and serotonin metabolism in gastrointestinal function. Neurogastroenterol Motil 21 (2009) 1239-49. doi: 10.1111/j.1365-2982.2009.01370.x.
[105] P.R. Albert, and F. Vahid-Ansari, The 5-HT1A receptor: Signaling to behavior. Biochimie 161 (2019) 34-45. doi: 10.1016/j.biochi.2018.10.015.
[106] R.D. Blakely, H.E. Berson, R.T. Fremeau, Jr., M.G. Caron, M.M. Peek, H.K. Prince, and C.C. Bradley, Cloning and expression of a functional serotonin transporter from rat brain. Nature 354 (1991) 66-70. doi: 10.1038/354066a0.
[107] B.J. Hoffman, E. Mezey, and M.J. Brownstein, Cloning of a serotonin transporter affected by antidepressants. Science 254 (1991) 579-80. doi: 10.1126/science.1948036.
[108] Y. Charnay, and L. Leger, Brain serotonergic circuitries. Dialogues Clin Neurosci 12 (2010) 471-87. http://www.ncbi.nlm.nih.gov/pubmed/21319493

[109] K.A. Michelsen, C. Schmitz, and H.W. Steinbusch, The dorsal raphe nucleus–from silver stainings to a role in depression. Brain Res Rev 55 (2007) 329-42. doi: 10.1016/j.brainresrev.2007.01.002.

[110] G. Di Giovanni, A. Chagraoui, R. Bharatiya, and P. De Deurwaerdère, Chapter 10 - Serotonergic control of excitability: from neuron to networks. in: C.P. Müller, and K.A. Cunningham, (Eds.), Handbook of Behavioral Neuroscience, Elsevier, 2020, pp. 197-215.Book Section doi: 10.1016/B978-0-444-64125-0.00010-4.

[111] J. Bacque-Cazenave, R. Bharatiya, G. Barriere, J.P. Delbecque, N. Bouguiyoud, G. Di Giovanni, D. Cattaert, and P. De Deurwaerdere, Serotonin in Animal Cognition and Behavior. Int J Mol Sci 21 (2020). doi: 10.3390/ijms21051649.

[112] N.M. Barnes, G.P. Ahern, C. Becamel, J. Bockaert, M. Camilleri, S. Chaumont-Dubel, S. Claeysen, K.A. Cunningham, K.C. Fone, M. Gershon, G. Di Giovanni, N.M. Goodfellow, A.L. Halberstadt, R.M. Hartley, G. Hassaine, K. Herrick-Davis, R. Hovius, E. Lacivita, E.K. Lambe, M. Leopoldo, F.O. Levy, S.C.R. Lummis, P. Marin, L. Maroteaux, A.C. McCreary, D.L. Nelson, J.F. Neumaier, A. Newman-Tancredi, H. Nury, A. Roberts, B.L. Roth, A. Roumier, G.J. Sanger, M. Teitler, T. Sharp, C.M. Villalon, H. Vogel, S.W. Watts, and D. Hoyer, International Union of Basic and Clinical Pharmacology. CX. Classification of Receptors for 5-hydroxytryptamine; Pharmacology and Function. Pharmacol Rev 73 (2021) 310-520. doi: 10.1124/pr.118.015552.

[113] T. Sharp, and N.M. Barnes, Central 5-HT receptors and their function; present and future. Neuropharmacology 177 (2020) 108155. doi: 10.1016/j.neuropharm.2020.108155.

[114] J. Bockaert, S. Claeysen, A. Dumuis, and P. Marin, Classification and Signaling Characteristics of 5-HT Receptors, 2010. doi: 10.1016/S1569-7339(10)70073-4.

[115] J. Masson, M.B. Emerit, M. Hamon, and M. Darmon, Serotonergic signaling: multiple effectors and pleiotropic effects. Wiley Interdisciplinary Reviews: Membrane Transport and Signaling 1 (2012) 685-713. doi: 10.1002/wmts.50.

[116] J. De Vry, R. Schreiber, C. Melon, M. Dalmus, and K.R. Jentzsch, 5-HT1A receptors are differentially involved in the anxiolytic- and antidepressant-like effects of 8-OH-DPAT and fluoxetine in the rat. Eur Neuropsychopharmacol 14 (2004) 487-95. doi: 10.1016/j.euroneuro.2004.01.004.

[117] M.B. Gatch, Discriminative stimulus effects of m-chlorophenylpiperazine as a model of the role of serotonin receptors in anxiety. Life Sci 73 (2003) 1347-67. doi: 10.1016/s0024-3205(03)00422-3.

[118] G.A. Kennett, F. Bright, B. Trail, G.S. Baxter, and T.P. Blackburn, Effects of the 5-HT2B receptor agonist, BW 723C86, on three rat models of anxiety. Br J Pharmacol 117 (1996) 1443-8. doi: 10.1111/j.1476-5381.1996.tb15304.x.

[119] G.A. Kennett, B. Trail, and F. Bright, Anxiolytic-like actions of BW 723C86 in the rat Vogel conflict test are 5-HT2B receptor mediated. Neuropharmacology 37 (1998) 1603-10. doi: 10.1016/s0028-3908(98)00115-4.

[120] S. Sevy, S.L. Brown, S. Wetzler, M. Kotler, A. Molcho, R. Plutchik, and H.M. van Praag, Effects of alprazolam on increases in hormonal and anxiety levels induced by meta-chlorophenylpiperazine. Psychiatry Res 53 (1994) 219-29. doi: 10.1016/0165-1781(94)90051-5.

[121] G. Lucas, V.V. Rymar, J. Du, O. Mnie-Filali, C. Bisgaard, S. Manta, L. Lambas-Senas, O. Wiborg, N. Haddjeri, G. Pineyro, A.F. Sadikot, and G. Debonnel, Serotonin(4) (5-HT(4)) receptor agonists are putative antidepressants with a rapid onset of action. Neuron 55 (2007) 712-25. doi: 10.1016/j.neuron.2007.07.041.

[122] R. Galici, J.D. Boggs, K.L. Miller, P. Bonaventure, and J.R. Atack, Effects of SB-269970, a 5-HT7 receptor antagonist, in mouse models predictive of antipsychotic-like activity. Behav Pharmacol 19 (2008) 153-9. doi: 10.1097/FBP.0b013e3282f62d8c.

[123] B. Pouzet, M. Didriksen, and J. Arnt, Effects of the 5-HT(7) receptor antagonist SB-258741 in animal models for schizophrenia. Pharmacol Biochem Behav 71 (2002) 655-65. doi: 10.1016/s0091-3057(01)00744-4.

[124] A. Wesolowska, A. Nikiforuk, K. Stachowicz, and E. Tatarczynska, Effect of the selective 5-HT7 receptor antagonist SB 269970 in animal models of anxiety and depression. Neuropharmacology 51 (2006) 578-86. doi: 10.1016/j.neuropharm.2006.04.017.

[125] P.B. Hedlund, L. Kelly, C. Mazur, T. Lovenberg, J.G. Sutcliffe, and P. Bonaventure, 8-OH-DPAT acts on both 5-HT1A and 5-HT7 receptors to induce hypothermia in rodents. Eur J Pharmacol 487 (2004) 125-32. doi: 10.1016/j.ejphar.2004.01.031.

[126] S. Hjorth, Hypothermia in the rat induced by the potent serotoninergic agent 8-OH-DPAT. J Neural Transm 61 (1985) 131-5. doi: 10.1007/BF01253058.

[127] C.T. Dourish, P.H. Hutson, G.A. Kennett, and G. Curzon, 8-OH-DPAT-induced hyperphagia: its neural basis and possible therapeutic relevance. Appetite 7 Suppl (1986) 127-40. doi: 10.1016/s0195-6663(86)80058-7.

[128] P. Mazzola-Pomietto, C.S. Aulakh, K.M. Wozniak, and D.L. Murphy, Evidence that m-chlorophenylpiperazine-induced hyperthermia in rats is mediated by stimulation of 5-HT2C receptors. Psychopharmacology (Berl) 123 (1996) 333-9. doi: 10.1007/BF02246643.

[129] A. Hayashi, M. Suzuki, M. Sasamata, and K. Miyata, Thermogenic effect of YM348, a novel 5-HT2C-receptor agonist, in rats. J Pharm Pharmacol 56 (2004) 1551-6. doi: 10.1211/0022357044841.

[130] D.D. Lam, M.J. Przydzial, S.H. Ridley, G.S. Yeo, J.J. Rochford, S. O'Rahilly, and L.K. Heisler, Serotonin 5-HT2C receptor agonist promotes hypophagia via downstream activation of melanocortin 4 receptors. Endocrinology 149 (2008) 1323-8. doi: 10.1210/en.2007-1321.

[131] V.S. Naumenko, E.M. Kondaurova, and N.K. Popova, On the role of brain 5-HT7 receptor in the mechanism of hypothermia: comparison with hypothermia mediated via 5-HT1A and 5-HT3 receptor. Neuropharmacology 61 (2011) 1360-5. doi: 10.1016/j.neuropharm.2011.08.022.

[132] A. Fisas, X. Codony, G. Romero, A. Dordal, J. Giraldo, R. Merce, J. Holenz, N. Vrang, R.V. Sorensen, D. Heal, H. Buschmann, and P.J. Pauwels, Chronic 5-HT6 receptor modulation by E-6837 induces hypophagia and sustained weight loss in diet-induced obese rats. Br J Pharmacol 148 (2006) 973-83. doi: 10.1038/sj.bjp.0706807.

[133] V. Compan, M. Zhou, R. Grailhe, R.A. Gazzara, R. Martin, J. Gingrich, A. Dumuis, D. Brunner, J. Bockaert, and R. Hen, Attenuated response to stress and novelty and hypersensitivity to seizures in 5-HT4 receptor knock-out mice. J Neurosci 24 (2004) 412-9. doi: 10.1523/JNEUROSCI.2806-03.2004.

[134] A. Jean, G. Conductier, C. Manrique, C. Bouras, P. Berta, R. Hen, Y. Charnay, J. Bockaert, and V. Compan, Anorexia induced by activation of serotonin 5-HT4 receptors is mediated by increases in CART in the nucleus accumbens. Proc Natl Acad Sci U S A 104 (2007) 16335-40. doi: 10.1073/pnas.0701471104.

[135] A. Jean, L. Laurent, J. Bockaert, Y. Charnay, N. Dusticier, A. Nieoullon, M. Barrot, R. Neve, and V. Compan, The nucleus accumbens 5-HTR(4)-CART pathway ties anorexia to hyperactivity. Transl Psychiatry 2 (2012) e203. doi: 10.1038/tp.2012.131.

[136] P.J. Fletcher, M. Tampakeras, J. Sinyard, and G.A. Higgins, Opposing effects of 5-HT(2A) and 5-HT(2C) receptor antagonists in the rat and mouse on premature responding in the five-choice serial reaction time test. Psychopharmacology (Berl) 195 (2007) 223-34. doi: 10.1007/s00213-007-0891-z.

[137] G.A. Higgins, M. Enderlin, M. Haman, and P.J. Fletcher, The 5-HT2A receptor antagonist M100,907 attenuates motor and 'impulsive-type' behaviours produced by NMDA receptor antagonism. Psychopharmacology (Berl) 170 (2003) 309-319. doi: 10.1007/s00213-003-1549-0.

[138] P.L. Rock, C.J. Harmer, S.F. McTavish, G.M. Goodwin, and R.D. Rogers, Short-term quetiapine treatment alters the use of reinforcement signals during risky decision-making and promotes the choice of negative expected values in healthy adult males. J Neurosci 33 (2013) 15588-95. doi: 10.1523/JNEUROSCI.5721-11.2013.

[139] C.A. Winstanley, D.E. Theobald, J.W. Dalley, J.C. Glennon, and T.W. Robbins, 5-HT2A and 5-HT2C receptor antagonists have opposing effects on a measure of impulsivity: interactions with global 5-HT depletion. Psychopharmacology (Berl) 176 (2004) 376-85. doi: 10.1007/s00213-004-1884-9.

[140] P.M. Pitychoutis, A. Belmer, I. Moutkine, J. Adrien, and L. Maroteaux, Mice Lacking the Serotonin Htr2B Receptor Gene Present an Antipsychotic-Sensitive Schizophrenic-Like Phenotype. Neuropsychopharmacology 40 (2015) 2764-73. doi: 10.1038/npp.2015.126.

[141] J. Bockaert, S. Claeysen, V. Compan, and A. Dumuis, 5-HT(4) receptors: history, molecular pharmacology and brain functions. Neuropharmacology 55 (2008) 922-31. doi: 10.1016/j.neuropharm.2008.05.013.

[142] J. Bockaert, S. Claeysen, V. Compan, and A. Dumuis, 5-HT(4) receptors, a place in the sun: act two. Curr Opin Pharmacol 11 (2011) 87-93. doi: 10.1016/j.coph.2011.01.012.

[143] E.S. Mitchell, and J.F. Neumaier, 5-HT6 receptors: a novel target for cognitive enhancement. Pharmacol Ther 108 (2005) 320-33. doi: 10.1016/j.pharmthera.2005.05.001.

[144] I. Kendall, H.A. Slotten, X. Codony, J. Burgueno, P.J. Pauwels, J.M. Vela, and K.C. Fone, E-6801, a 5-HT6 receptor agonist, improves recognition memory by combined modulation of cholinergic and glutamatergic neurotransmission in the rat. Psychopharmacology (Berl) 213 (2011) 413-30. doi: 10.1007/s00213-010-1854-3.

[145] M. Pereira, B.J. Martynhak, R. Andreatini, and P. Svenningsson, 5-HT6 receptor agonism facilitates emotional learning. Front Pharmacol 6 (2015) 200. doi: 10.3389/fphar.2015.00200.

[146] S. Woods, N.N. Clarke, R. Layfield, and K.C. Fone, 5-HT(6) receptor agonists and antagonists enhance learning and memory in a conditioned emotion response paradigm by modulation of cholinergic and glutamatergic mechanisms. Br J Pharmacol 167 (2012) 436-49. doi: 10.1111/j.1476-5381.2012.02022.x.

[147] G. Sarkisyan, and P.B. Hedlund, The 5-HT7 receptor is involved in allocentric spatial memory information processing. Behav Brain Res 202 (2009) 26-31. doi: 10.1016/j.bbr.2009.03.011.

[148] M.G. Frank, M.P. Stryker, and L.H. Tecott, Sleep and sleep homeostasis in mice lacking the 5-HT2c receptor. Neuropsychopharmacology 27 (2002) 869-73. doi: 10.1016/S0893-133X(02)00353-6.

[149] P.B. Hedlund, S. Huitron-Resendiz, S.J. Henriksen, and J.G. Sutcliffe, 5-HT7 receptor inhibition and inactivation induce antidepressantlike behavior and sleep pattern. Biol Psychiatry 58 (2005) 831-7. doi: 10.1016/j.biopsych.2005.05.012.

[150] S. Kantor, R. Jakus, B. Balogh, A. Benko, and G. Bagdy, Increased wakefulness, motor activity and decreased theta activity after blockade of the 5-HT2B receptor by the subtype-selective antagonist SB-215505. Br J Pharmacol 142 (2004) 1332-42. doi: 10.1038/sj.bjp.0705887.

[151] J.M. Monti, and H. Jantos, Effects of the 5-HT(7) receptor antagonist SB-269970 microinjected into the dorsal raphe nucleus on REM sleep in the rat. Behav Brain Res 167 (2006) 245-50. doi: 10.1016/j.bbr.2005.09.025.

[152] D.R. Thomas, S. Melotto, M. Massagrande, A.D. Gribble, P. Jeffrey, A.J. Stevens, N.J. Deeks, P.J. Eddershaw, S.H. Fenwick, G. Riley, T. Stean, C.M. Scott, M.J. Hill, D.N. Middlemiss, J.J. Hagan, G.W. Price, and I.T. Forbes, SB-656104-A, a novel selective 5-HT7 receptor antagonist, modulates REM sleep in rats. Br J Pharmacol 139 (2003) 705-14. doi: 10.1038/sj.bjp.0705290.

[153] J.M. Monti, Serotonin control of sleep-wake behavior. Sleep Med Rev 15 (2011) 269-81. doi: 10.1016/j.smrv.2010.11.003.

[154] A.F. Almeida-Santos, R.C. Ferreira, I.D. Duarte, D.C. Aguiar, T.R. Romero, and F.A. Moreira, The antipsychotic aripiprazole induces antinociceptive effects: Possible role of peripheral dopamine D2 and serotonin 5-HT1A receptors. Eur J Pharmacol 765 (2015) 300-6. doi: 10.1016/j.ejphar.2015.08.053.

[155] L. Fei, L. Abrardi, and R.D. Mediati, Unexpected effect of aripiprazole on nociceptive pain. Ther Adv Psychopharmacol 2 (2012) 211-2. doi: 10.1177/2045125312451271.

[156] T. Meuser, C. Pietruck, A. Gabriel, G.X. Xie, K.J. Lim, and P. Pierce Palmer, 5-HT7 receptors are involved in mediating 5-HT-induced activation of rat primary afferent neurons. Life Sci 71 (2002) 2279-89. doi: 10.1016/s0024-3205(02)02011-8.

[157] N.M. Goodfellow, C.D. Bailey, and E.K. Lambe, The native serotonin 5-HT(5A) receptor: electrophysiological characterization in rodent cortex and 5-HT(1A)-mediated compensatory plasticity in the knock-out mouse. J Neurosci 32 (2012) 5804-9. doi: 10.1523/JNEUROSCI.4849-11.2012.

[158] G. Becker, R. Bolbos, N. Costes, J. Redoute, A. Newman-Tancredi, and L. Zimmer, Selective serotonin 5-HT1A receptor biased agonists elicitdistinct brain activation patterns: a pharmacoMRI study. Sci Rep 6 (2016) 26633. doi: 10.1038/srep26633.

[159] A. Newman-Tancredi, Biased agonism at serotonin 5-HT1A receptors: Preferential postsynaptic activity for improved therapy of CNS disorders. Neuropsychiatry 1 (2011) 149-164. doi: 10.2217/npy.11.12.

[160] P. De Deurwaerdere, R. Bharatiya, A. Chagraoui, and G. Di Giovanni, Constitutive activity of 5-HT receptors: Factual analysis. Neuropharmacology 168 (2020) 107967. doi: 10.1016/j.neuropharm.2020.107967.

[161] U. Shah, H. Pincas, S.C. Sealfon, and J. González-Maeso, Chapter 11 - Structure and function of serotonin GPCR heteromers. in: C.P. Müller, and K.A. Cunningham, (Eds.), Handbook of Behavioral Neuroscience, Elsevier, 2020, pp. 217-238.Book Section doi: 10.1016/B978-0-444-64125-0.00011-6.

[162] S. Brenner, The genetics of Caenorhabditis elegans. Genetics 77 (1974) 71-94. http://www.ncbi.nlm.nih.gov/pubmed/4366476

[163] J.G. White, E. Southgate, J.N. Thomson, and S. Brenner, The structure of the nervous system of the nematode Caenorhabditis elegans. Philos Trans R Soc Lond B Biol Sci 314 (1986) 1-340. doi: 10.1098/rstb.1986.0056.

[164] S.J. Cook, T.A. Jarrell, C.A. Brittin, Y. Wang, A.E. Bloniarz, M.A. Yakovlev, K.C.Q. Nguyen, L.T. Tang, E.A. Bayer, J.S. Duerr, H.E. Bulow, O. Hobert, D.H. Hall, and S.W. Emmons, Whole-animal connectomes of both Caenorhabditis elegans sexes. Nature 571 (2019) 63-71. doi: 10.1038/s41586-019-1352-7.

[165] O. Hobert, Neurogenesis in the nematode Caenorhabditis elegans. WormBook (2010) 1-24. doi: 10.1895/wormbook.1.12.2.

[166] J.F. Etchberger, A. Lorch, M.C. Sleumer, R. Zapf, S.J. Jones, M.A. Marra, R.A. Holt, D.G. Moerman, and O. Hobert, The molecular signature and cis-regulatory architecture of a C. elegans gustatory neuron. Genes Dev 21 (2007) 1653-74. doi: 10.1101/gad.1560107.

[167] C.e.S. Consortium, Genome sequence of the nematode C. elegans: a platform for investigating biology. Science 282 (1998) 2012-8. doi: 10.1126/science.282.5396.2012.

[168] C.H. Lai, C.Y. Chou, L.Y. Ch'ang, C.S. Liu, and W. Lin, Identification of novel human genes evolutionarily conserved in Caenorhabditis elegans by comparative proteomics. Genome Res 10 (2000) 703-13. doi: 10.1101/gr.10.5.703.

[169] W. Kim, R.S. Underwood, I. Greenwald, and D.D. Shaye, OrthoList 2: A New Comparative Genomic Analysis of Human and Caenorhabditis elegans Genes. Genetics 210 (2018) 445-461. doi: 10.1534/genetics.118.301307.

[170] T. Kaletta, and M.O. Hengartner, Finding function in novel targets: C. elegans as a model organism. Nat Rev Drug Discov 5 (2006) 387-98. doi: 10.1038/nrd2031.
[171] A. Fire, S. Xu, M.K. Montgomery, S.A. Kostas, S.E. Driver, and C.C. Mello, Potent and specific genetic interference by double-stranded RNA in Caenorhabditis elegans. Nature 391 (1998) 806-11. doi: 10.1038/35888.
[172] D.J. Dickinson, J.D. Ward, D.J. Reiner, and B. Goldstein, Engineering the Caenorhabditis elegans genome using Cas9-triggered homologous recombination. Nat Methods 10 (2013) 1028-34. doi: 10.1038/nmeth.2641.
[173] K.M. Van Pelt, and M.C. Truttmann, Caenorhabditis elegans as a model system for studying aging-associated neurodegenerative diseases. Translational Medicine of Aging 4 (2020) 60-72. doi: 10.1016/j.tma.2020.05.001.
[174] X. Chen, J.W. Barclay, R.D. Burgoyne, and A. Morgan, Using C. elegans to discover therapeutic compounds for ageing-associated neurodegenerative diseases. Chem Cent J 9 (2015) 65. doi: 10.1186/s13065-015-0143-y.
[175] A. Teixeira-Castro, M. Ailion, A. Jalles, H.R. Brignull, J.L. Vilaca, N. Dias, P. Rodrigues, J.F. Oliveira, A. Neves-Carvalho, R.I. Morimoto, and P. Maciel, Neuron-specific proteotoxicity of mutant ataxin-3 in C. elegans: rescue by the DAF-16 and HSF-1 pathways. Hum Mol Genet 20 (2011) 2996-3009. doi: 10.1093/hmg/ddr203.
[176] F. Pohl, A. Teixeira-Castro, M.D. Costa, V. Lindsay, J. Fiuza-Fernandes, M. Goua, G. Bermano, W. Russell, P. Maciel, and P. Kong Thoo Lin, GST-4-Dependent Suppression of Neurodegeneration in C. elegans Models of Parkinson's and Machado-Joseph Disease by Rapeseed Pomace Extract Supplementation. Front Neurosci 13 (2019) 1091. doi: 10.3389/fnins.2019.01091.
[177] D. Vilasboas-Campos, M.D. Costa, A. Teixeira-Castro, R. Rios, F.G. Silva, C. Bessa, A.C.P. Dias, and P. Maciel, Neurotherapeutic effect of Hyptis spp. leaf extracts in Caenorhabditis elegans models of tauopathy and polyglutamine disease: Role of the glutathione redox cycle. Free Radic Biol Med 162 (2021) 202-215. doi: 10.1016/j.freeradbiomed.2020.10.018.
[178] S. Duarte-Silva, A. Silva-Fernandes, A. Neves-Carvalho, C. Soares-Cunha, A. Teixeira-Castro, and P. Maciel, Combined therapy with m-TOR-dependent and -independent autophagy inducers causes neurotoxicity in a mouse model of Machado-Joseph disease. Neuroscience 313 (2016) 162-73. doi: 10.1016/j.neuroscience.2015.11.030.
[179] A. Silva-Fernandes, S. Duarte-Silva, A. Neves-Carvalho, M. Amorim, C. Soares-Cunha, P. Oliveira, K. Thirstrup, A. Teixeira-Castro, and P. Maciel, Chronic treatment with 17-DMAG improves balance and coordination in a new mouse model of Machado-Joseph disease. Neurotherapeutics 11 (2014) 433-49. doi: 10.1007/s13311-013-0255-9.
[180] L.F. Lei, G.P. Yang, J.L. Wang, D.M. Chuang, W.H. Song, B.S. Tang, and H. Jiang, Safety and efficacy of valproic acid treatment in SCA3/MJD patients. Parkinsonism Relat Disord 26 (2016) 55-61. doi: 10.1016/j.parkreldis.2016.03.005.
[181] Z.F. Altun, D.H. Hall, and L.A. Herndon, WormAtlas Hermaphrodite Handbook - Nervous System - General Description. WormAtlas (2005). doi: 10.3908/wormatlas.1.18.
[182] P.J. Brockie, and A.V. Maricq, Ionotropic glutamate receptors: genetics, behavior and electrophysiology. WormBook (2006) 1-16. doi: 10.1895/wormbook.1.61.1.
[183] J.B. Rand, Acetylcholine. WormBook (2007) 1-21. doi: 10.1895/wormbook.1.131.1.
[184] E.M. Jorgensen, Gaba. WormBook (2005) 1-13. doi: 10.1895/wormbook.1.14.1.
[185] C. Li, and K. Kim, Neuropeptides. WormBook (2008) 1-36. doi: 10.1895/wormbook.1.142.1.
[186] D.L. Chase, and M.R. Koelle, Biogenic amine neurotransmitters in C. elegans. WormBook (2007) 1-15. doi: 10.1895/wormbook.1.132.1.
[187] M. de Bono, and A.V. Maricq, Neuronal substrates of complex behaviors in C. elegans. Annu Rev Neurosci 28 (2005) 451-501. doi: 10.1146/annurev.neuro.27.070203.144259.

[188] M. de Bono, Molecular approaches to aggregation behavior and social attachment. J Neurobiol 54 (2003) 78-92. doi: 10.1002/neu.10162.
[189] A.C. Giles, J.K. Rose, and C.H. Rankin, Investigations of learning and memory in Caenorhabditis elegans. Int Rev Neurobiol 69 (2006) 37-71. doi: 10.1016/S0074-7742(05)69002-2.
[190] Y. Zhang, H. Lu, and C.I. Bargmann, Pathogenic bacteria induce aversive olfactory learning in Caenorhabditis elegans. Nature 438 (2005) 179-84. doi: 10.1038/nature04216.
[191] J.C. Brewer, A.C. Olson, K.M. Collins, and M.R. Koelle, Serotonin and neuropeptides are both released by the HSN command neuron to initiate Caenorhabditis elegans egg laying. PLoS Genet 15 (2019) e1007896. doi: 10.1371/journal.pgen.1007896.
[192] S. Srinivasan, L. Sadegh, I.C. Elle, A.G. Christensen, N.J. Faergeman, and K. Ashrafi, Serotonin regulates C. elegans fat and feeding through independent molecular mechanisms. Cell Metab 7 (2008) 533-44. doi: 10.1016/j.cmet.2008.04.012.
[193] G. Gurel, M.A. Gustafson, J.S. Pepper, H.R. Horvitz, and M.R. Koelle, Receptors and other signaling proteins required for serotonin control of locomotion in Caenorhabditis elegans. Genetics 192 (2012) 1359-71. doi: 10.1534/genetics.112.142125.
[194] C.H. Rankin, Nematode behavior: the taste of success, the smell of danger! Curr Biol 16 (2006) R89-91. doi: 10.1016/j.cub.2006.01.025.
[195] L. Segalat, D.A. Elkes, and J.M. Kaplan, Modulation of serotonin-controlled behaviors by Go in Caenorhabditis elegans. Science 267 (1995) 1648-51. doi: 10.1126/science.7886454.
[196] K.M. Collins, A. Bode, R.W. Fernandez, J.E. Tanis, J.C. Brewer, M.S. Creamer, and M.R. Koelle, Activity of the C. elegans egg-laying behavior circuit is controlled by competing activation and feedback inhibition. Elife 5 (2016). doi: 10.7554/eLife.21126.
[197] L.E. Waggoner, G.T. Zhou, R.W. Schafer, and W.R. Schafer, Control of alternative behavioral states by serotonin in Caenorhabditis elegans. Neuron 21 (1998) 203-14. doi: 10.1016/s0896-6273(00)80527-9.
[198] B.M. Song, and L. Avery, The pharynx of the nematode C. elegans: A model system for the study of motor control. Worm 2 (2013) e21833. doi: 10.4161/worm.21833.
[199] B.M. Song, and L. Avery, Serotonin activates overall feeding by activating two separate neural pathways in Caenorhabditis elegans. J Neurosci 32 (2012) 1920-31. doi: 10.1523/JNEUROSCI.2064-11.2012.
[200] N.F. Trojanowski, D.M. Raizen, and C. Fang-Yen, Pharyngeal pumping in Caenorhabditis elegans depends on tonic and phasic signaling from the nervous system. Sci Rep 6 (2016) 22940. doi: 10.1038/srep22940.
[201] E.R. Sawin, R. Ranganathan, and H.R. Horvitz, C. elegans locomotory rate is modulated by the environment through a dopaminergic pathway and by experience through a serotonergic pathway. Neuron 26 (2000) 619-31. doi: 10.1016/s0896-6273(00)81199-x.
[202] S.W. Flavell, D.M. Raizen, and Y.-J. You, Behavioral States. Genetics 216 (2020) 315-332. doi: 10.1534/genetics.120.303539.
[203] C.I. Nussbaum-Krammer, and R.I. Morimoto, Caenorhabditis elegans as a model system for studying non-cell-autonomous mechanisms in protein-misfolding diseases. Dis Model Mech 7 (2014) 31-9. doi: 10.1242/dmm.013011.
[204] V. Prahlad, T. Cornelius, and R.I. Morimoto, Regulation of the cellular heat shock response in Caenorhabditis elegans by thermosensory neurons. Science 320 (2008) 811-4. doi: 10.1126/science.1156093.
[205] V. Prahlad, and R.I. Morimoto, Neuronal circuitry regulates the response of Caenorhabditis elegans to misfolded proteins. Proc Natl Acad Sci U S A 108 (2011) 14204-9. doi: 10.1073/pnas.1106557108.

[206] M.C. Tatum, F.K. Ooi, M.R. Chikka, L. Chauve, L.A. Martinez-Velazquez, H.W.M. Steinbusch, R.I. Morimoto, and V. Prahlad, Neuronal serotonin release triggers the heat shock response in C. elegans in the absence of temperature increase. Curr Biol 25 (2015) 163-174. doi: 10.1016/j.cub.2014.11.040.

[207] K.M. Berendzen, J. Durieux, L.W. Shao, Y. Tian, H.E. Kim, S. Wolff, Y. Liu, and A. Dillin, Neuroendocrine Coordination of Mitochondrial Stress Signaling and Proteostasis. Cell 166 (2016) 1553-1563 e10. doi: 10.1016/j.cell.2016.08.042.

[208] Q. Zhang, X. Wu, P. Chen, L. Liu, N. Xin, Y. Tian, and A. Dillin, The Mitochondrial Unfolded Protein Response Is Mediated Cell-Non-autonomously by Retromer-Dependent Wnt Signaling. Cell 174 (2018) 870-883 e17. doi: 10.1016/j.cell.2018.06.029.

[209] G. Jafari, Y. Xie, A. Kullyev, B. Liang, and J.Y. Sze, Regulation of extrasynaptic 5-HT by serotonin reuptake transporter function in 5-HT-absorbing neurons underscores adaptation behavior in Caenorhabditis elegans. J Neurosci 31 (2011) 8948-57. doi: 10.1523/JNEUROSCI.1692-11.2011.

[210] H.R. Horvitz, M. Chalfie, C. Trent, J.E. Sulston, and P.D. Evans, Serotonin and octopamine in the nematode Caenorhabditis elegans. Science 216 (1982) 1012-4. doi: 10.1126/science.6805073.

[211] Z.F. Altun, L.A. Herndon, C.A. Wolkow, C. Crocker, R. Lints, N.E. Schroeder, and D.H. Hall, WormAtlas, http://www.wormatlas.org 2002-2021; Accessed March 2021,

[212] K.A. Cunningham, Z. Hua, S. Srinivasan, J. Liu, B.H. Lee, R.H. Edwards, and K. Ashrafi, AMP-activated kinase links serotonergic signaling to glutamate release for regulation of feeding behavior in C. elegans. Cell Metab 16 (2012) 113-21. doi: 10.1016/j.cmet.2012.05.014.

[213] Y. Ishita, T. Chihara, and M. Okumura, Serotonergic modulation of feeding behavior in Caenorhabditis elegans and other related nematodes. Neurosci Res 154 (2020) 9-19. doi: 10.1016/j.neures.2019.04.006.

[214] N. Bhatla, An Interactive Visualization of the C. elegans Neural Network, http://wormweb.org/neuralnet#c=NSM&m=1, 2009 - accessed March 2021,

[215] M. Carre-Pierrat, D. Baillie, R. Johnsen, R. Hyde, A. Hart, L. Granger, and L. Segalat, Characterization of the Caenorhabditis elegans G protein-coupled serotonin receptors. Invert Neurosci 6 (2006) 189-205. doi: 10.1007/s10158-006-0033-z.

[216] G.P. Harris, V.M. Hapiak, R.T. Wragg, S.B. Miller, L.J. Hughes, R.J. Hobson, R. Steven, B. Bamber, and R.W. Komuniecki, Three distinct amine receptors operating at different levels within the locomotory circuit are each essential for the serotonergic modulation of chemosensation in Caenorhabditis elegans. J Neurosci 29 (2009) 1446-56. doi: 10.1523/JNEUROSCI.4585-08.2009.

[217] R.J. Hobson, J. Geng, A.D. Gray, and R.W. Komuniecki, SER-7b, a constitutively active Galphas coupled 5-HT7-like receptor expressed in the Caenorhabditis elegans M4 pharyngeal motorneuron. J Neurochem 87 (2003) 22-9. doi: 10.1046/j.1471-4159.2003.01967.x.

[218] B. Olde, and W.R. McCombie, Molecular cloning and functional expression of a serotonin receptor from Caenorhabditis elegans. J Mol Neurosci 8 (1997) 53-62. doi: 10.1007/BF02736863.

[219] C.M. Dempsey, S.M. Mackenzie, A. Gargus, G. Blanco, and J.Y. Sze, Serotonin (5HT), fluoxetine, imipramine and dopamine target distinct 5HT receptor signaling to modulate Caenorhabditis elegans egg-laying behavior. Genetics 169 (2005) 1425-36. doi: 10.1534/genetics.104.032540.

[220] J. Xie, S. Dernovici, and P. Ribeiro, Mutagenesis analysis of the serotonin 5-HT2C receptor and a Caenorhabditis elegans 5-HT2 homologue: conserved residues of helix 4 and helix 7 contribute to agonist-dependent activation of 5-HT2 receptors. J Neurochem 92 (2005) 375-87. doi: 10.1111/j.1471-4159.2004.02867.x.

[221] R. Ranganathan, S.C. Cannon, and H.R. Horvitz, MOD-1 is a serotonin-gated chloride channel that modulates locomotory behaviour in C. elegans. Nature 408 (2000) 470-5. doi: 10.1038/35044083.

[222] S. Dernovici, T. Starc, J.A. Dent, and P. Ribeiro, The serotonin receptor SER-1 (5HT2ce) contributes to the regulation of locomotion in Caenorhabditis elegans. Dev Neurobiol 67 (2007) 189-204. doi: 10.1002/dneu.20340.

[223] R.W. Fernandez, K. Wei, E.Y. Wang, D. Mikalauskaite, A. Olson, J. Pepper, N. Christie, S. Kim, S. Weissenborn, M. Sarov, and M.R. Koelle, Cellular Expression and Functional Roles of All 26 Neurotransmitter GPCRs in the C. elegans Egg-Laying Circuit. J Neurosci 40 (2020) 7475-7488. doi: 10.1523/JNEUROSCI.1357-20.2020.

[224] R.J. Hobson, V.M. Hapiak, H. Xiao, K.L. Buehrer, P.R. Komuniecki, and R.W. Komuniecki, SER-7, a Caenorhabditis elegans 5-HT7-like receptor, is essential for the 5-HT stimulation of pharyngeal pumping and egg laying. Genetics 172 (2006) 159-69. doi: 10.1534/genetics.105.044495.

[225] L. Carnell, J. Illi, S.W. Hong, and S.L. McIntire, The G-protein-coupled serotonin receptor SER-1 regulates egg laying and male mating behaviors in Caenorhabditis elegans. J Neurosci 25 (2005) 10671-81. doi: 10.1523/JNEUROSCI.3399-05.2005.

[226] H. Xiao, V.M. Hapiak, K.A. Smith, L. Lin, R.J. Hobson, J. Plenefisch, and R. Komuniecki, SER-1, a Caenorhabditis elegans 5-HT2-like receptor, and a multi-PDZ domain containing protein (MPZ-1) interact in vulval muscle to facilitate serotonin-stimulated egg-laying. Developmental Biology 298 (2006) 379-391. doi: 10.1016/j.ydbio.2006.06.044.

[227] V.M. Hapiak, R.J. Hobson, L. Hughes, K. Smith, G. Harris, C. Condon, P. Komuniecki, and R.W. Komuniecki, Dual excitatory and inhibitory serotonergic inputs modulate egg laying in Caenorhabditis elegans. Genetics 181 (2009) 153-63. doi: 10.1534/genetics.108.096891.

[228] H. Murakami, and S. Murakami, Serotonin receptors antagonistically modulate Caenorhabditis elegans longevity. Aging Cell 6 (2007) 483-8. doi: 10.1111/j.1474-9726.2007.00303.x.

Chapter 2.

Filter retardation and biochemical fractionation assays for detecting and quantifying neuronal polyglutamine aggregates using *C. elegans* protein lysates: protocol development attempts

Data from this chapter is included in the following manuscripts:

Jalles, A.*; Vieira, C.*; Pereira-Sousa, J.; Vilasboas-Campos, D.; Mota, A.F.; Vasconcelos, S.; Ferreira-Lomba, B.; Da Silva, J. D.; Maciel P.; Teixeira-Castro, A. "Aripiprazole offsets mutant ATXN3-induced motor dysfunction by targeting dopamine D2 and serotonin 1A and 2A receptors in *C. elegans*" (under revision – *Frontiers in Molecular Neuroscience*)

Duarte-Silva, S.; Vilasboas-Campos, D.; Neves-Carvalho, A.; Pereira-Sousa, J.; Teixeira-Castro, A. and Maciel, P. "The current lead molecular tweezer CLR-01: impact on *in vivo* models of MJD" (manuscript in preparation)

Note:

All data presented in this chapter was generated by the author of this thesis. Importantly, the techniques developed here were also used in the article presented in Chapter 3.

Filter retardation and biochemical fractionation assays for detecting and quantifying neuronal polyglutamine aggregates using *C. elegans* protein lysates: protocol development attempts

Joana Pereira-Sousa[1,2,3], Daniela Vilasboas-Campos[1,2], Patricia Maciel[1,2], Andreia Teixeira-Castro[1,2]

[1]Life and Health Sciences Research Institute (ICVS), School of Medicine, University of Minho, Braga

[2]ICVS/3B's - PT Government Associate Laboratory Braga/Guimarães, Portugal

[3]Behavioural and Molecular Lab (Bn'ML), University of Minho, Braga

Abstract

Alzheimer's, Parkinson's and Machado-Joseph diseases are a set of neurodegenerative disorders collectively known as proteinopathies. The commonality of these diseases resides in the accumulation of specific proteins in the brain. Regardless of whether proteinopathies share, or not, a common disease mechanism is generally accepted that the strong tendency to aggregation of the specific proteins is tightly linked to pathogenesis and disease progression. For this reason, the ability to detect and quantify protein aggregation is of utmost importance. Several techniques allow the study of aggregation *in vitro* and in *vivo*, however assessment of the aggregation process continues to be very challenging. The most used *in vivo* technologies are based on the imaging of fluorescent proteins. These methods include confocal dynamic imaging, Förster/Fluorescence Resonance Energy Transfer (FRET) or Bimolecular Fluorescence Complementation (BiFC) and explore the propensity of the monomeric proteins to form immobile aggregates with fluorescent emission and puncta formation. Nonetheless, other characteristics of aggregates can be evaluated using biochemical techniques. Filter retardation assay and biochemical fractionation techniques explore the differential size and solubility of the different multimeric and aggregation species. Although these biochemical methods have been already applied to study aggregation in several model systems, they were generally used in a qualitative manner.

Here, we optimised filter retardation assay and biochemical fractionation protocols, and by adding internal loading controls to the assays, made them more suitable to semi-quantification and statistical analysis. Furthermore, we explored the amenability of a combinatory strategy comprising confocal dynamic imaging, filter retardation assay and biochemical fractionation to assess aggregation of mutant ATXN3 in *C. elegans*, through a systematic approach that can be easily applied to other proteins. Using a *C. elegans* model of ATXN3 proteotoxicity and taking advantage of a known genetic modifier of ATXN3 aggregation, *mod-5*, previously described by us, we optimised the biochemical methods as proposed. We showed a decrease in ATXN3 SDS-insoluble large aggregates, measured by filter retardation assay, with a concomitant decrease in SDS-resistant species assessed by biochemical fractionation. These

biochemical methods provided complementary information, about the nature of the aggregated species, to that determined by confocal dynamic imaging, as demonstrated also in the case of pharmacological treatments with aripiprazole and the molecular tweezer CLR-01.

1. Introduction

Several neurodegenerative disorders are characterized by the accumulation of specific proteins in the brain, being collectively known as proteinopathies (reviewed in [1]). Regardless of whether proteinopathies share, or not, a common disease mechanism [2], it is generally accepted that the aggregation process is tightly linked to pathogenesis and disease progression [3; 4] and several compounds that modulate protein aggregation have been tested in these diseases [5]. For that reason, the ability to detect and quantify protein disease-relevant aggregation species is of utmost need.

The study of the different aggregated species has been largely explored in the last decades (reviewed in [6; 7; 8]). Electron and atomic force microscopy or circular dichroism enabled the determination of morphology and structural conformation of aggregates (reviewed in [6; 7; 8]). These techniques can be complemented with others, including the determination of molecular weight, by PAGE, size exclusion chromatography or light scattering, and by kinetic methods such as Thioflavin T and Congo Red (reviewed in [6; 7; 8]), which allow the determination of the nature of aggregates. However, none of these methods are suitable to study the aggregation process *in vivo*.

The study of aggregation *in vivo* is extremely important due to the complexity of the cellular environment, that affects protein aggregation and homeostasis. The most widely used methods are based on fluorescent reporters coupled with spectroscopic imaging techniques, including Förster/Fluorescence Resonance Energy Transfer (FRET) and Bimolecular Fluorescence Complementation (BiFC) [9] or on the use of conformation-sensitive fluorescent dyes, such as Thioflavin-S that allows the detection of amyloid-like aggregates, in intact cells, by flow cytometry (reviewed in [10; 11]). In FRET, energy is transferred from an excited molecular fluorophore, the donor, to another fluorophore, the acceptor, by means of intermolecular long-range dipole–dipole coupling [12]. When expressed in heterologous systems, as cells, in fusion with the protein/peptide of interest, these fluorophores allow the detection and monitoring of aggregated species in native states or in different conditions [13; 14]. In the BiFC assay, two non-fluorescent fragments of a fluorescent reporter are fused with the proteins of interest, which ones when in proximity, achieved by protein interaction, allow the formation of a bimolecular complex with emission of fluorescent signal [15]. This technique allows the *in vivo* visualization and monitoring of

dimerization/early stage oligomerization and aggregation processes in several animal models [16; 17], however a careful characterization of the system is advised since, depending the cell type or protein of study, just some specific protein conformations can be detected [18].

Machado-Joseph disease (MJD) is characterized by the aggregation of the ataxin-3 (ATXN3) protein, that in pathologic conditions presents an expanded polyglutamine (polyQ) tract that makes ATXN3 prone to self-associate and aggregate [19; 20; 21].

To study ATXN3 aggregation *in vivo*, Teixeira-Castro and colleagues generated a humanized *C. elegans* model that expresses an expanded form of the ATXN3 protein, with 130 polyQs, in fusion with Yellow Fluorescent Protein (YFP), in all *C. elegans* neurons. This transgenic strain recapitulates several features of MJD pathogenesis, showing an age-dependent progressive motor dysfunction, and increase in ATXN3 aggregation, the severity of these phenotypes also being proportional to the size of the polyQ expansion [22]. In this model system, mutant ATXN3 aggregation can be readily assessed by *in vivo* confocal dynamic imaging and fluorescence recovery after photobleaching (FRAP) techniques [23]. ATXN3 aggregation can be studied *in vivo* throughout the animals' development and ageing. Moreover, it is amenable for genetic or drug screenings, being a suitable model to identify possible modifier genes of MJD pathogenesis, as well as therapeutic targets. Studies from our laboratory showed that alterations in ATXN3 aggregation can be achieved by pharmacological modulation or by genetic ablation of key components of the serotonergic signalling. Ablation of *mod-5/ SERT* gene or citalopram pharmacological treatment (SERT inhibitor) reduced mutant ATXN3 aggregation [24; 25]. Also using an hypothesis-free approach, Costa et al described aripiprazole (APZ), an atypical-antipsychotic that targets the serotonin receptors 5-HT_{1A} and 5-HT_2, and the D_2 dopaminergic receptor [26], as a modulator of ATXN3 abundance and aggregation in *Drosophila* and in transgenic MJD mice [27]; however, the functional impact of this treatment was not addressed.

As demonstrated for MJD, as for other proteinopathies, an impact on aggregation, either by avoidance of its toxic self-assembly or by promotion of its elimination, can be key to halt disease progression (reviewed in [28; 29]). "Molecular tweezers" are small molecules described as selective lysine residue receptors, that act as broad-spectrum inhibitors of the assembly and toxicity of amyloid proteins. Treatment with CLR-01, a well-known molecular tweezer, demonstrated therapeutic effect by decreasing aggregation in several models of proteinopathies such as Alzheimer's and Parkinson's diseases (reviewed in [30]).

In this work, we aimed at improving biochemical techniques to assess protein aggregation states in *C. elegans* upon different stimuli. For that purpose, we used a *C. elegans* ATXN3-proteotoxicity model to optimize two biochemical methods, previously used to investigate mutant ATXN3 aggregation, the filter retardation and biochemical fractionation assays, turning it more suitable for semi-quantification and statistical analysis. After validation of these techniques, using the previously described genetic modifier of ATXN3 proteotoxicity, the ablation of *mod-5* gene, we explored the impact of pharmacological treatments, namely with APZ and CLR-01, on ATXN3 aggregation. Our results showed that filter retardation assay and biochemical fractionation robustly detected changes on ATXN3 aggregation upon *mod-5* ablation, with a clear decrease in large ATXN3 aggregates measured by the filter retardation assay and a concomitant decrease in ATXN3 SDS-resistant species assessed by biochemical fractionation. The pharmacological treatments tested, however, resulted in a higher variability in ATXN3 aggregation states despite the significant amelioration of motor dysfunction of mutant animals upon treatment.

2. Material and methods

2.1. Caenorhabditis elegans strains and maintenance

Caenorhabditis elegans (*C. elegans*) strains used, and abbreviations are listed in Table 1. All the strains were backcrossed to Bristol strain N2 (WT) at least five times. Standard methods were used for culturing and observing *C. elegans* [31]. Nematodes were grown on nematode growth medium (NGM) plates seeded with *Escherichia coli* (*E. coli*) OP50 strain at 20°C.

Table 1. *C. elegans* strains used in this study.

ID number	Strain name	Genotype
N2 (Bristol)	WT	Wild-type
MAC037/AM599	ATXN3 WT (AT3q75)	*rmIs238* [$P_{regf\text{-}1}$::AT3v1-1q75::YFP]
MAC001/AM685	ATXN3 mutant (AT3q130)	*rmIs263* [$P_{regf\text{-}1}$::AT3v1-1q130::YFP] II
MAC074	*mod-5*Δ; ATXN3 mutant	*mod-5(n3314)* I; *rmIs263* [$P_{regf\text{-}1}$::AT3v1-1q130::YFP] II

2.2. Drug preparation

In this study two different drugs were used, both previously identified as modulators of aggregation, CLR-01 and aripiprazole (APZ) (CAS #129722-12-9, Kemprotec UK). The molecular tweezer

CLR-01 was kindly provided by Dr. Gal Bitan (UCLA). CLR-01 and APZ were diluted to a final concentration of 0.1 µM and 10 µM, respectively, in 1% dimethyl sulfoxide (DMSO, Sigma).

2.3. Nematode culturing conditions, drug assay and motility assay

To collect animals to measure ATXN3 steady-state protein levels, and to perform biochemical fractionation, filter retardation assay and confocal dynamic imaging assays, animals were grown in liquid culture and a drug assay was performed in a 96-well plate format [32]. Each well contained a final volume of 60 µl, comprising 20–25 animals of the following strains: wild-type (WT, N2), wild-type ATXN3 (ATXN3 WT), and *mod-5Δ*; ATXN3 mutant (AT3q130), or 40-45 animals of ATXN3 mutant (AT3q130) in the egg stage in a total volume of 15 µl (increased egg number of AT3q130 are needed to ensure similar number of animals post-hatching, comparing with WT, ATXN3 WT, and *mod-5Δ*; AT3q130 strains); 25 µl of drug vehicle (DMSO 1%), CLR-01 or APZ at the appropriate concentration; and 20 µl of *E. coli* OP50 bacteria to a final OD_{595nm} of 0.9 measured in a microplate reader (Tecan Infinite 200 Microplate Reader).

To obtain an age synchronized population of eggs, four-day-old gravid adults were treated with alkaline hypochlorite solution (0.5 M NaOH, ~2.6% NaClO) for five minutes. The eggs were then washed in M9 buffer and resuspended in S-medium complete (S-Basal buffer, 10 mM potassium citrate pH 6, 10X trace metal solution, 3 mM $CaCl_2$, 3 mM $MgSO_4$) to the appropriate egg number in 15 µl and transferred into a 96-well plate, to a total animal number of 2500 for CLR-01- and APZ-treated condition, and *mod-5Δ*; ATXN3 mutant, and 4000 for ATXN3 mutant strain. OP50 bacteria were grown overnight at 37°C and 150 rpm in Luria Broth (LB) media, pelleted by centrifugation, inactivated by three cycles of flash-freeze (−190°C) / thawing at 37°C and then resuspended in S-medium complete supplemented with 0.004 mg/ml cholesterol, 0.5X Pen-strep (Sigma) and 0.5X nystatin (Sigma). Animals were grown with continuous shaking at 180 rpm at 20°C (Shel Lab) for four days.

To ensure drug efficacy, a motility assay at 20°C was performed, as previously described [22], in a sample of the animals used for aggregation analysis. Briefly, four-day-old animals were transferred from the 96-well plates onto an unseeded NGM plate (equilibrated at 20°C). Plates were dried for 45 minutes before starting the motility assays. Ten animals were placed simultaneously in the centre of a freshly seeded 30 mm plate (equilibrated at 20°C). Animals remaining inside the 1 cm circle after one minute were scored as locomotion defective. Motor behaviour assays were run with at least 50 animals tested per drug treatment or genotype, per biological replicate.

2.4. Immunoblotting analysis

For determination of ATXN3 steady-state levels, four-day-old animals were collected from 96-well plates, washed three times with M9, and flash-frozen in liquid nitrogen. After extraction with 50 µl of non-denaturating protein buffer (50 mM HEPES, pH 7.4, 150 mM NaCl, 1 mM EDTA, 0.5% Triton X-100) freshly supplemented with an EDTA-free protease inhibitor cocktail (Roche), animals were disrupted by mechanic force using glass beads (Sigma) in a FastPrep®-24 (MP Biomedicals) (six cycles of 6.5 ms for 45 s followed by 5 min on ice). After a centrifugation at 500 g during 1 min, the supernatant was collected, and the total protein quantified by the Bradford assay (Bio-Rad). For tubulin versus total protein staining experiments, four-day-old animals of each condition were transferred from the liquid culture onto an unseeded NGM plate (equilibrated at 20°C). After 45 minutes, 25 individual young adult animals were picked into a 1.5 mL tube with a screw cap. Animal samples or protein/ aggregate lysates were boiled for 15 min in sodium dodecyl sulphate (SDS) sample buffer (to destroy all the aggregates) and the resulting extracts resolved on a 10% SDS gel, as previously described [22; 33]. Immunoblots were probed with mouse anti-ATXN3 antibody (1:1000) (Millipore Cat# MAB5360) or α-tubulin (1:5000) (Sigma Cat#T5168) and detected with horseradish peroxidase-coupled secondary antibodies (Bio-Rad) and chemiluminescence (Radiance ECL, Azure biosystems). Total protein staining (TPS) was detected on the membrane, right after transferring, using AzureRed Fluorescent Total Protein Dye (Azure biosystems), according to the manufacturer's instructions. Capturing of chemiluminescence and TPS signals was performed using the Sapphire Biomolecular Imager (Azure biosystems), and Western-blot quantifications were performed using AzureSpot Analysis Software (Azure biosystems), according to the manufacturer's instructions.

2.5. C. elegans confocal dynamic imaging

Vehicle- and drug-treated mutant ATXN3 (AT3q130) animals were grown in liquid culture in a 96-well plate format, as described above. Four-day-old animals were transferred from the 96-well plates onto unseeded NGM plates (equilibrated at 20°C). After 45 minutes, live animals were immobilized with 3 mM levamisole (Sigma) and mounted on a 3% agarose pad. All images were captured using an Olympus LPS Confocal FV1000 microscope (Confocal microscope, Olympus, FV1000) under a 60X oil (NA = 1.35). Z-series imaging was acquired for vehicle- and CLR-01- or APZ-treated animals, using a 515 nm laser excitation line for YFP fusion proteins. The pinhole was adjusted to 1.0 Airy unit of optical slice, and a scan was taken every ~0.5 µm along the z-axis. The quantification of the aggregates was performed as

previously described [22; 23]. Three parameters were extracted from analysis: area occupied by the aggregates in the head/ total area of the animal's head; number of aggregates in the head/ total area of the animal's head and total area of the animal's head. Values shown are the mean (normalized to vehicle treated control). Number of animals used in each assay are shown in Supplementary table 1 and in figure legends.

2.6. Biochemical methods to assess aggregation

In this section, we will extensively describe the methods used for aggregation assessment and quantification, namely a) filter retardation assay and b) biochemical fractionation.

2.6.1. Filter retardation assay

Four-day-old animals were collected from 96-well plates and washed three times with M9 to eliminate OP50 bacteria and progeny. In the final wash, M9 was freshly supplemented with an EDTA-free protease inhibitor cocktail (Roche). After the removal of the excess M9 buffer, animal pellets were flash-frozen in liquid nitrogen. For protein/ aggregate extraction, a 50 µl of cold non-denaturing protein buffer (50 mM HEPES, pH 7.4, 150 mM NaCl, 1 mM EDTA, 0.5% Triton X-100) freshly supplemented with an EDTA-free protease inhibitor cocktail (Roche) [34] was added and animals were disrupted by mechanic force using glass beads (Sigma) in a FastPrep®-24 (MP Biomedicals) (six cycles of 6 ms for 25 s followed by 5 min on ice). After a centrifugation at 500 g during 1 min, for elimination of cellular debris, the supernatant was collected, and the total protein quantified by the Bradford assay (Bio-Rad). A total of 100 µg of protein was treated with SDS at a final concentration of 1% [34] and loaded onto a cellulose acetate membrane (0.2 µm pore size, ref. 10404180, Whatman) assembled in a Bio-Dot® Microfiltration Apparatus (Bio-Rad). After applying low vacuum driving SDS-soluble proteins to pass through the membrane, these were washed with 0.1% SDS/ PBS 1X two times [35]. After blocking with 5% non-fat milk in TBS 1X, membranes were incubated with mouse anti-ATXN3 antibody (1:1000) (Millipore Cat# MAB5360) diluted in 5% non-fat milk in TBS 1X. After overnight incubation, at 4°C, with primary antibody, membranes were washed three times with TBS 1X and incubated with horseradish peroxidase-coupled secondary antibodies (Bio-Rad) during 1h at room temperature (RT). Anti-ATXN3 antibody signals were detected by chemiluminescence (ECL Radiance, Azure biosystems), the acquisition being performed in the Sapphire Biomolecular Imager (Azure biosystems) and quantified using the AzureSpot Analysis Software (Azure biosystems), according to the manufacturer's instructions.

As loading control, 5 µg of protein extracts were transferred to an Eppendorf tube with a screw cap, supplemented with Laemmli Buffer to a final concentration of 1X and boiled for 15 minutes. The samples were resolved in a 10% SDS-gel, as previously described [22; 33], for drug treatments. Gel was then incubated with AzureRed Fluorescent Total Protein Stain (Azure biosystems), following the manufacturer instructions, to determine total protein staining (TPS) signals. Total protein quantification was done in AzureSpot Analysis Software (Azure biosystems), according to the manufacturer's instructions. For *mod-5* KO animals, loading controls were resolved in an SDS-PAGE gel prepared with TGX™ FastCast™ Acrylamide Kit, 10% (Bio-Rad) to detect total protein staining, following the manufacturer's instructions. Quantification of the gel images obtained in Image lab software (BioRad) in Tiff format, was performed using AzureSpot Analysis Software (Azure biosystems), according to the manufacturer's instructions. After quantification, filter retardation ATXN3 densitometry values were normalized by TPS ratio.

2.6.2. Biochemical fractionation

Four-day-old animals were collected from 96-well plates and washed three times with M9, to eliminate OP50 bacteria and progeny, the last wash being supplemented with an EDTA-free protease inhibitor cocktail (Roche), and flash-frozen in liquid nitrogen. For protein/ aggregate extraction 150 µl of cold RIPA Buffer (50 mM Tris pH 7.5, 150 mM NaCl, 25 mM EDTA, 0.2% Triton X-100) freshly supplemented with an EDTA-free protease inhibitor cocktail (Roche) was added and animals were disrupted by mechanic force using glass beads (Sigma) in a FastPrep®-24 (MP Biomedicals) (six cycles of 6 ms for 25 s followed by 5 min on ice). After a centrifugation at 500 g during 1 min, the supernatant was collected, and the total protein quantified by the Bradford assay (Bio-Rad). Protein concentration was adjusted to 4 µg/µl and a loading control fraction, corresponding to 50 µg of protein, was collected. The rest of the protein sample was submitted to a 22000 g centrifugation for 30 min at 4°C. The pellet fraction was separated from the supernatant (soluble fraction). Pellets were then homogenized in 150 µl RIPA buffer supplemented with 2% SDS, at RT, by pipetting up-and-down. A second centrifugation step at RT was performed at 22000 g for 30 min. The supernatant (SDS-soluble fraction) was collected, and the remaining pellet were incubated for 16 hours in 100% formic acid at 50°C, allowing formic acid evaporation [24; 36]. This sample was dissolved in 50 µl of Laemmli buffer (0.1 M Tris, pH 6.8, 16% glycerol, 2% SDS, β-mercaptoethanol and bromophenol blue powder) (SDS-resistant fraction). Fractions collected during the biochemical fractionation protocol were submitted to SDS-PAGE and Western-blot against ATXN3. To do so, 50 µg of protein of loading control fraction, 50 µg of protein of soluble fraction,

40 µl of SDS-soluble fraction and the complete SDS-resistant fraction were loaded in a 10% SDS gel. After wet transfer, TPS was determined using AzureRed Fluorescent Total Protein dye (Azure biosystems), according to the manufacturer's instructions. The membrane was then blocked with 5% non-fat milk in TBS 1X during 1h at room temperature. To detect ATXN3 protein, the membrane was incubated overnight at 4°C with mouse anti-ATXN3 antibody (1:1000) (Millipore Cat# MAB5360). After washing with TBS 1X, the membrane was incubated 1h at RT with horseradish peroxidase-coupled anti-mouse antibody (Bio-Rad). Chemiluminescence (ECL western-blotting detection reagents, Bio-Rad or ECL Radiance, Azure biosystems) was used and detected using Sapphire Biomolecular Imager (Azure biosystems). TPS was detected in the same apparatus following the manufacturer's instructions, prior to the chemiluminescence assay. Quantification was done in AzureSpot Analysis Software (Azure biosystems), according to the manufacturer's instructions. After quantification, the ATXN3 signal of each fraction was normalized to TPS of the loading control fraction of the corresponding treatment. The values shown in the violin plots are the ratio of ATXN3 (normalised to TPS of the loading control fraction) divided by ATXN3 values of the ATXN3 mutant animals (for *mod-5*) or vehicle-treated mutant ATXN3 animals (for drug treatments), for each fraction. Quartiles (Q1 and Q3) and median (M) were represented.

2.7. Statistical analysis

All statistical analysis was performed using the IBM SPSS statistics 23 software (SPSS) and GraphPad Prism 8.0.1 software. Normal distribution of continuous variables was analysed according with the Shapiro-Wilk or Kolmogorov-Smirnov normality test, depending on sample size, and histogram plot distribution. Levene's test assessment was performed to confirm homogeneity of variances between groups. When both assumptions were verified, groups were compared using One-Way ANOVA followed by post-hoc analysis by Tukey (Fig. 1C), Dunnett (Fig. 2A, Fig. 3D, Fig. 4B – number of aggregates/ TA assay 2 and area occupied by aggregates/ TA assay 2, Fig. 4D, Supplementary fig. 2, Supplementary fig. 3A, Supplementary fig. 4 – genetic modifiers), or using independent sample t-test when just two groups were compared (Fig. 3B – assay 2 and 3, Fig. 3B - area occupied by aggregates/ TA assay 1, Fig. 3C, Fig. 4B – assay 1 and 3, Fig. 4C – total area and area occupied by aggregates/ TA, Supplementary fig. 3B and 3C, Supplementary fig. 4 – CLR-01). For biochemical fractionation, a one-sample t-test with Bonferroni correction versus the value of 1 was applied (Fig. 2B, Fig. 3E, Fig. 4E).

For samples with normal distribution but not displaying homogeneity of variances, Welch correction for independent sample t-test was reported (Fig. 4C – number of aggregates/ TA, Supplementary fig. 4 – APZ).

When the data did not display a normal distribution, bootstrap with BCA correction was performed. Bootstrap sampling was followed by an independent sample t-test test with bias correction (Fig. 3B – number of aggregates/ TA assay 1).

Detailed statistics for all experiments are shown in Supplementary table 1.

3. Results

3.1. Total protein determination – detection of smaller variations with high dynamic range

To compare total protein staining (TPS) and tubulin loading controls in *C. elegans* lysates, we conducted SDS-PAGE followed by Western blot analysis using α-tubulin antibody in parallel with detection of TPS, using AzureRed® total protein dye in lysates from WT, ATXN3 mutant, *mod-5*Δ; ATXN3 mutant and ATXN3 mutant animals treated with APZ.

In all samples, tubulin load linearly correlated with TPS with a coefficient of determination (r^2) of 0.7203 that supported the direct proportional relationship between the two variables, however without a perfect fit (Figure 1A). Interestingly, the evaluation of the coefficient of variation between the two variables, that measures the distance of each individual value from the average, showed a smaller variation of TPS of ≈14.8%, in contrast with a 23.8% variation in α-tubulin, a difference of almost 9% between the two methods (Figure 1B). Quantification of α-tubulin levels across the different genotypes showed a significant increase in the expression of this protein in mutant ATXN3 animals when compared to WT (Figure 1C).

Furthermore, analysis of serial dilutions of protein samples from WT animals revealed a limited dynamic range of tubulin that was overcome by the dynamic range of TPS (Figure 1D), which allowed the detection of analytical differences among the close protein concentrations tested. Evaluation of the curves slope showed that TPS measurements are almost 10 times more sensitive allowing clear discrimination of slightly increasing protein loads within its linear range. Taking together, we opted for TPS as a standard internal loading control, at the expense of the use of α-tubulin as an internal loading control due to its low dynamic range, higher variability, and its marginal increased expression in the disease model (ATXN3 mutant strain).

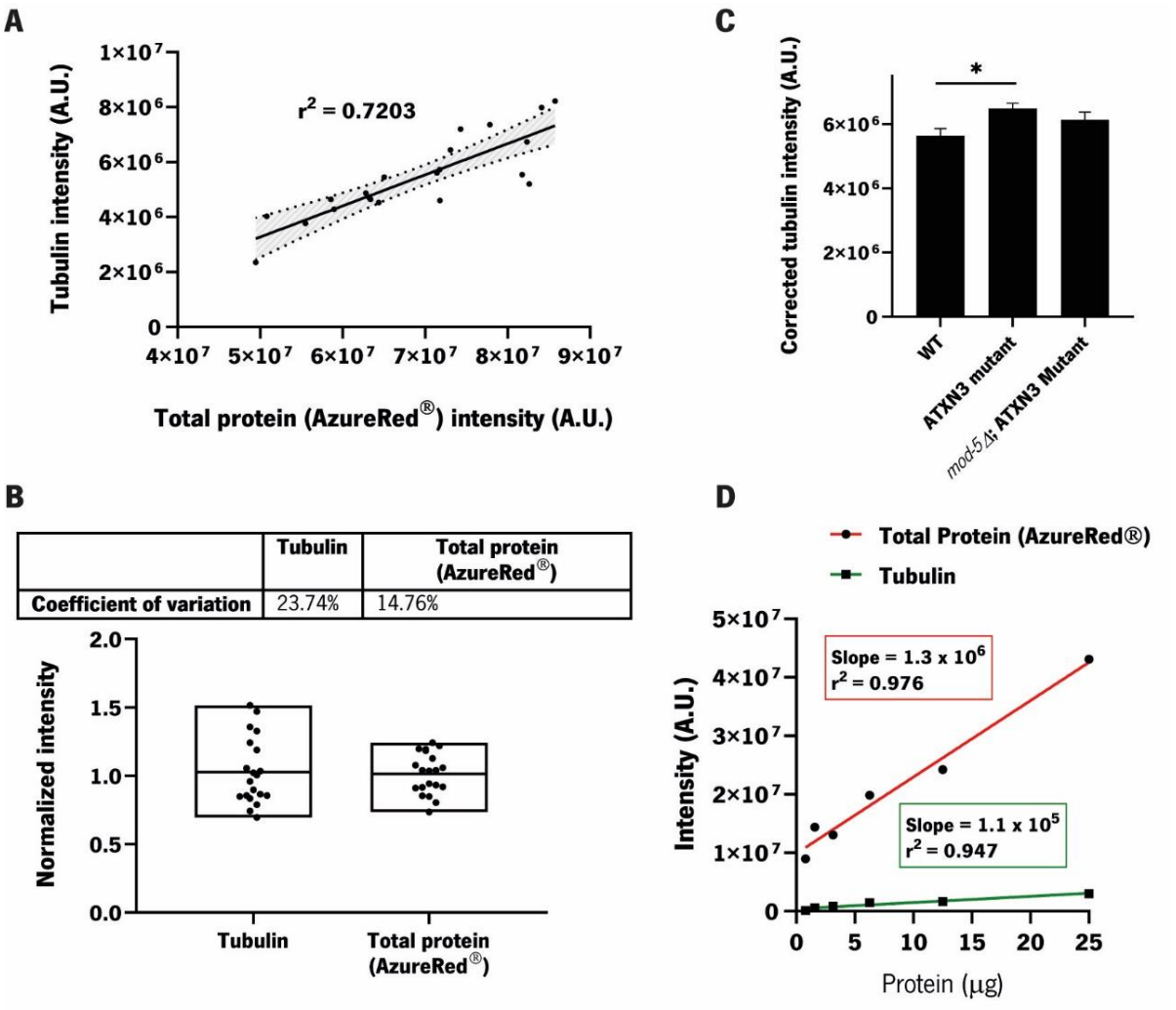

Figure 1. Tubulin versus total protein staining signals as loading control strategies in western-blotting of *C. elegans* lysates.

(A) Tubulin intensity correlates with total protein staining (TPS) intensity, however without a perfect fit presenting a r^2 of 0.7203 being **(B)** TPS much less variable than tubulin. **(C)** Tubulin intensity and expression is increased in ATXN3-mutant animals when compared with WT animals, when corrected to TPS. **(D)** Evaluation of the dynamic range of each loading control strategy showed that TPS (red) presented ten times higher dynamic range than tubulin (green) (10^5 in tubulin versus to 10^6 in TPS). (C) (n = 4, ± SEM), *P = 0.050, (ANOVA, Tukey).

3.2. Confocal dynamic imaging, filter retardation assay and biochemical fractionation to assess ATXN3 aggregation in C. elegans

Previously, our laboratory showed that the ATXN3-proteotoxicity *C. elegans* model has a neuron-specific pattern of aggregation, as in some neurons mutant ATXN3 proteins remain in their soluble state, whereas in others there is the formation of protein aggregates [22]. Since in these animals mutant ATXN3 proteins are expressed in fusion with YFP, aggregation can be assessed by dynamic confocal imaging and

quantified using MeVisLab [23]. Dynamic confocal imaging has great advantages, including the fact that can be performed in live animals and allows the study of the dynamics of protein foci *in vivo*. However, this technique is also time consuming, as it evaluates the aggregation load in individual animals, being highly dependent on the efficacy of the anaesthetic during acquisition to avoid animal movement. So, to complement the study of aggregation in this model, we explored two biochemical techniques: (a) filter retardation assay that captures large agglomerates of proteins which, because of their size, cannot pass through a membrane and (b) biochemical fractionation assay, that through the usage of different buffers separates protein species by their solubility.

3.2.1. Impact of genetic modifiers

Previous studies showed that serotonergic signalling modulation, by citalopram (CIT) treatment, impacts on MJD pathogenesis, decreasing ATXN3 aggregation in several disease models. Interestingly, genetic ablation of the serotonin transporter in *C. elegans*, *mod-5*, was shown to mimic CIT treatment [24], *mod-5* mutation being a potent suppressor of ATXN3 aggregation. To evaluate the ability of the biochemical techniques in study to detect alterations in ATXN3 aggregation in *C. elegans*, we performed filter retardation assay and biochemical fractionation of ATXN3 mutant animals in the background of *mod-5* ablation.

To fulfil the need of quantification, we optimised the filter retardation assay protocol by collecting a loading sample of 5 µg of total protein prior to the samples loading into the cellulose acetate membrane. These loading control samples were resolved into SDS-PAGE gels and stained to total protein (Supplementary figure 1A – bottom panel). The ratios between TPS within the gels were used to normalize the ATXN3 signal in filter retardation membranes. We detected higher ATXN3 aggregation in ATXN3 mutant animals that decreased in the absence of *mod-5* (Figure 2A and Supplementary figure 1A). Normalization of ATXN3 signals by TPS did not alter the statistical results but allowed important correction for eventual errors in protein loading, which can significantly affect results interpretation (Supplementary figure 2).

Similarly, to turn biochemical fractionation assay more prone to quantification and statistical analysis, a loading control sample was added to the SDS-PAGE gel and TPS signals were measured. Also, to avoid variations among biological replicates (due to chemiluminescence-based detection of ATXN3 intensity), intensity values of each fraction were normalized to TPS-corrected ATXN3 control levels (ATXN3 mutant animals), having control always a ratio of 1. For this reason, statistical analysis was based on one-

sample t-test against value of 1. With this change in protocol, we managed to semi-quantify biochemical fractionation experiments and showed that mutation in *mod-5* gene in *mod-5*Δ; ATXN3 mutant animals consistently decreased ATXN3 SDS-resistant species of mutant ATXN3 animals (Figure 2B), this shift in ATXN3 aggregated species being accompanied by improvement of motor function of the animals (Supplementary figure 3A), but not altering ATXN3 steady-state levels in whole animal lysates (Supplementary figure 4).

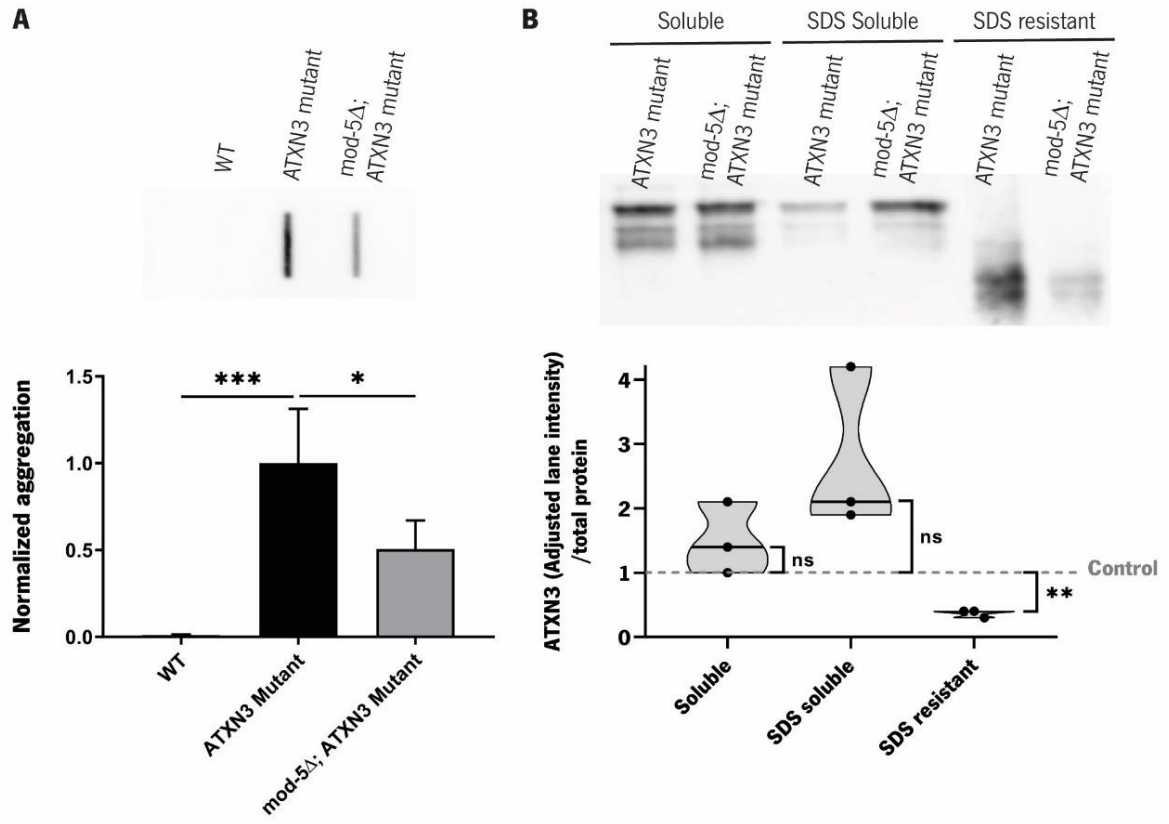

Figure 2. Biochemical methods, filter retardation assay and biochemical fractionation, are suitable to measure ATXN3 aggregation.

Evaluation of ATXN3 aggregation by **(A)** filter retardation assay upon *mod-5* ablation corroborates the suppression of aggregation previously reported by confocal live imaging techniques. **(B)** Biochemical fractionation of *mod-5*Δ; ATXN3 mutant showed a marked decrease in ATXN3 SDS-resistant species. For filter retardation assay (A): ATXN3 densitometry values in each sample were plotted as the mean of each sample (normalized to TPS) divided by the average of ATXN3 mutant animals. (n = 3 - 4, ± SD), *P < 0.05 ***P < 0.001, (ANOVA, Dunnett); For biochemical fractionation (B): ratio of ATXN3 divided by ATXN3 values of the ATXN3 mutant animals (control), for each fraction, were plotted (n = 3, Q1 – M – Q3), **P < 0.01 (one sample t-test, with Bonferroni correction vs value 1).

3.2.2. Impact of drug treatment

To test the impact of APZ treatment on a *C. elegans* model of mutant ATXN3 proteotoxicity, we evaluated aggregation of ATXN3 by confocal dynamic imaging, as well as using filter retardation assay and biochemical fractionation.

Live confocal imaging of at least 8 animals per condition was performed in triplicates (three independent assays). Assay 2 presented an increase in the number and size of mutant ATXN3 foci upon APZ treatment, however assays 1 and 3 showed limited impact of drug treatment (Figure 3A and 3B). Pool of the three assays, normalized to control, revealed no overall impact of APZ treatment on mutant ATXN3 foci (Figure 3C). Drug efficacy was ensured in the same animals by measuring motor function of the animals upon treatment (Supplementary figure 3B). When aggregation was assessed by the filter retardation assay, using a significantly higher number of animals per assay (≈ 3000 animals) and with a total of six independent replicates tested, no significant statistical effect on aggregation was observed, however, we showed a tendency for APZ treatment to increase ATXN3 aggregation ($p = 0.054$) with four out of six replicates presenting higher aggregation compared to control (Figure 3D and Supplementary figure 1B). To further explore the effects of APZ treatment on ATXN3 aggregation, we performed a biochemical fractionation assay of ATXN3 mutant animals in the presence of the compound. Although no statistical differences were found when comparing treated and untreated animals, there was also a tendency to a decrease in ATXN3 SDS-soluble species, with a parallel increase in ATXN3 SDS-resistant species upon treatment (Figure 3E). No alterations in ATXN3 steady-state level were found upon APZ treatment (Supplementary figure 4).

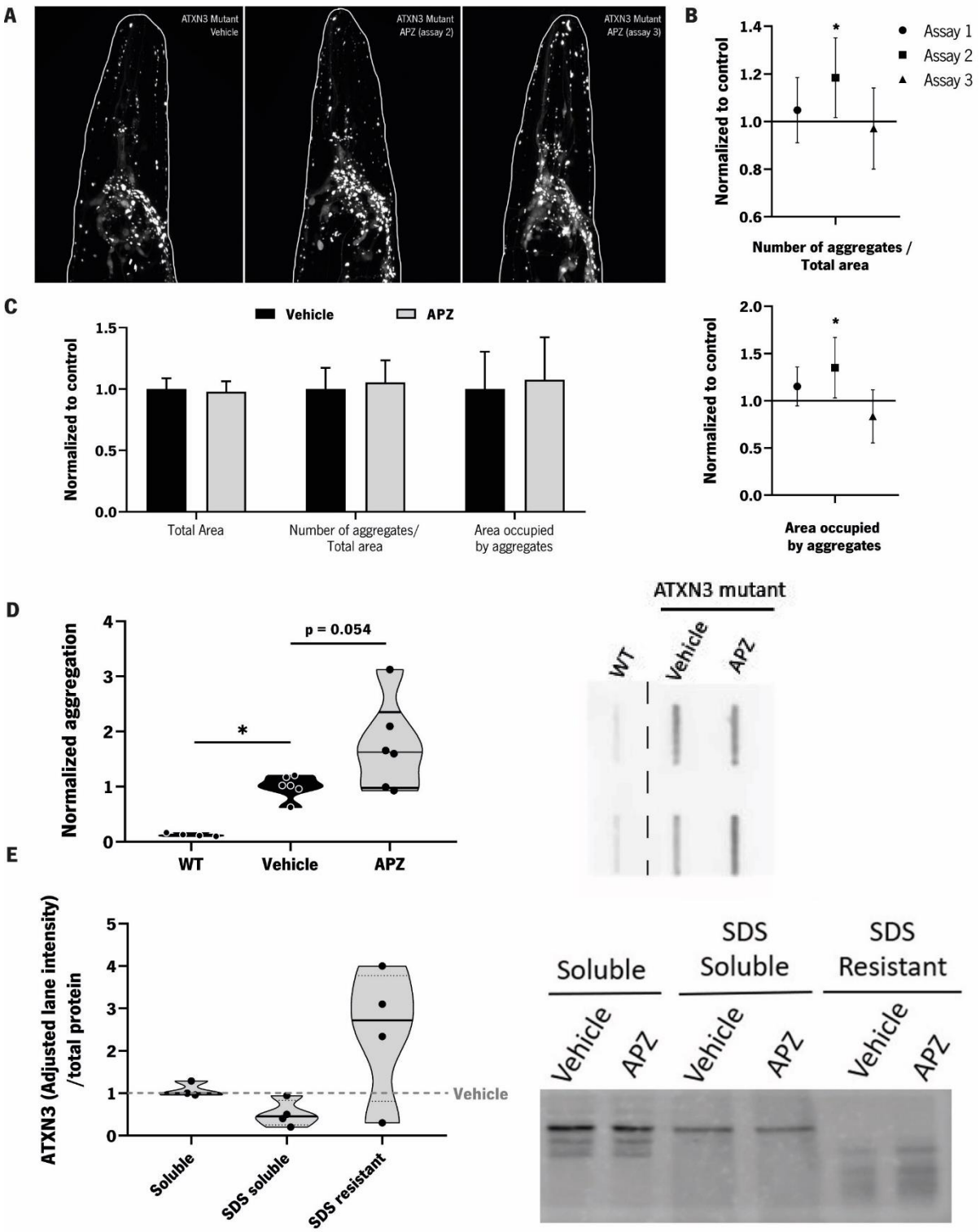

Figure 3. APZ treatment had a limited impact on mutant ATXN3 aggregation.

(A) Mutant ATXN3 expression pattern in the animals' head upon treatment, obtained by confocal dynamic imaging. **(B)** One of the three independent assays performed by confocal dynamic imaging showed an increase in the number of ATXN3 aggregates (top) and size (bottom), however, **(C)** the pool of the three assays, normalized by the results of daily control, did not reach statistical significance. **(D)** Filter retardation analysis showed that four out of six samples presented higher aggregation than average of control animals with a borderline tendency to APZ treatment-mediated increase in ATXN3

aggregation. **(E)** APZ treatment had a limited impact on ATXN3 aggregation, when evaluated by biochemical fractionation, however three out of four assays point to an increase of SDS-resistant species. For confocal dynamic imaging: (B) Assay 1 (n = 9 - 10, ± SD) (unpaired t-test corrected for BCA); Assay 2 (n = 9, ± SD) *P < 0.05 (unpaired t-test); Assay 3 (n = 8 - 13, ± SD) (unpaired t-test). (C) Total area (n = 28 - 32, ± SD) (unpaired t-test); number of aggregates / Total area (n = 27 to 31, ± SD), (unpaired t-test); area occupied by aggregates / Total area (n = 26 to 31, ± SD), (unpaired t-test). For filter retardation assay (D): ATXN3 densitometry values were normalized to TPS measured by AzureRed® (Azure Biosystems) and the results were plotted dividing each individual normalized sample value by the vehicle average. (n = 4 - 6, Q1 – M – Q3), *P < 0.05, (ANOVA, Dunnett); For biochemical fractionation (E): ratio of ATXN3 divided by ATXN3 values of the vehicle, for each fraction, were plotted. (n = 3 - 4, Q1 – M – Q3), (one sample t-test, with Bonferroni correction vs value 1).

Similarly, to address the possible impact of the molecular tweezer CLR-01 on ATXN3 aggregation we employed the same protocols as for APZ treatment. One out of the three assays, obtained by confocal dynamic imaging, showed a decrease in number of aggregates upon CLR-01 treatment (Figure 4A and B). The pool of those three assays showed a decrease in the number of ATXN3 foci ($p = 0.049$) (Figure 4C). However, aggregation of ATXN3 was not significantly changed when assessed by filter retardation assay (Figure 4D and Supplementary figure 1C), differences in ATXN3 solubility not being found upon CLR-01 treatment, by biochemical fractionation, however the majority of the assays show a tendency to a decrease in all ATXN3 species (soluble, SDS-soluble and SDS-resistant) (Figure 4E). As for APZ, CLR-01 treatment efficacy was ensured by determining the impact of drug treatment in animals motor function, prior to animals' collection for the aggregation assays (Supplementary figure 3C). Alterations of ATXN3 steady-state levels were not found upon CLR-01 treatment (Supplementary figure 4).

Overall, these results suggested that the techniques used here can detect potential alterations in mutant ATXN3 aggregation and inform about ATXN3 solubility, in semi-quantitative manner. These techniques are limited by inter-individual variability among a population, which is clearly lower upon genetic modifications of strong effect, such as the deletion of *mod-5*, in comparison to drug treatments, in which each individual may respond differently to compound treatment.

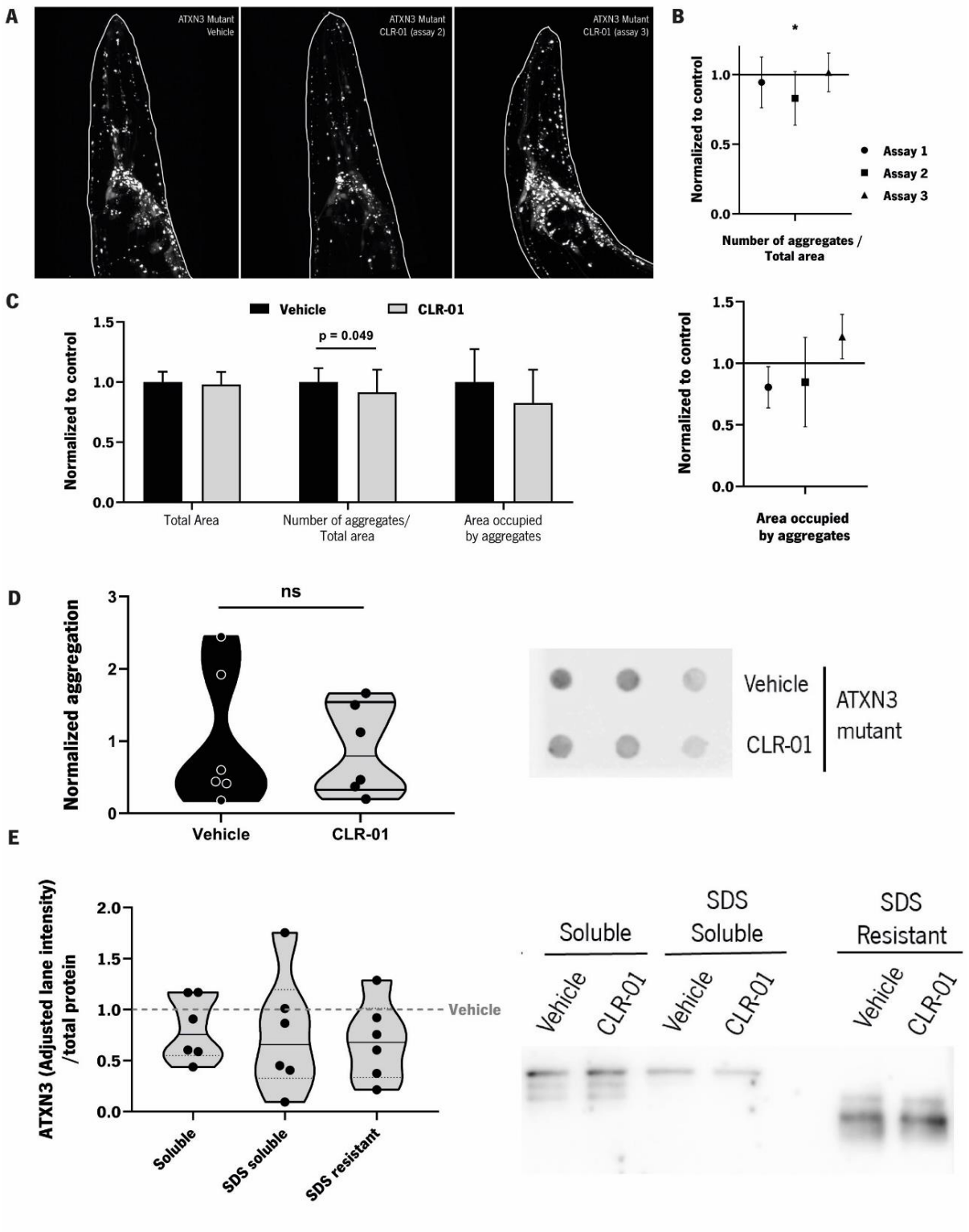

Figure 4. CLR-01 treatment showed a limited impact on ATXN3 aggregation.

(A) Mutant ATXN3 expression pattern in the animals' head upon CLR-01 treatment, obtained by confocal dynamic imaging. **(B)** One of the three independent assays performed by confocal dynamic imaging showed a decrease in ATXN3 aggregates number (top) without altering the area occupied by the aggregates (bottom). **(C)** Pool of the three assays normalized by the respective control animals showed a marginal decrease in the number of ATXN3 aggregates in the animals' head, however **(D)** filter retardation and **(E)** biochemical fractionation analyses showed a limited impact of CLR-01 treatment in ATXN3

aggregates. For confocal dynamic imaging: (B) Assay 1 (n = 5 to 11, ± SD) (unpaired t-test); Assay 2 (n = 10 to 11, ± SD) *P < 0.05 (ANOVA, Dunnett); Assay 3 (n = 6 to 9, ± SD) (unpaired t-test). (C) Total area (n = 24 to 28, ± SD) (unpaired t-test); number of aggregates / Total area (n = 24 to 28, ± SD), p = 0.049, (unpaired t-test with Welch correction); area occupied by aggregates / Total area (n = 15 to 22, ± SD), p = 0.067 (unpaired t-test). For filter retardation assay (D): ATXN3 densitometry values were normalized to TPS measured by AzureRed® (Azure Biosystems) and the results were plotted dividing each normalized sample value by the vehicle average. (n = 6, Q1 – M – Q3) ns – non significant (ANOVA, Dunnett); For biochemical fractionation (E): ratio of ATXN3 divided by ATXN3 values of the vehicle, for each fraction, were plotted. (n = 6, Q1 – M – Q3), (one sample t-test, with Bonferroni correction vs value 1).

4. Discussion

Evaluation of protein aggregation states in proteinopathies is crucial to better understand the pathogenic mechanism(s) of each disease, as well as to evaluate therapeutic potential of new or repurposed drugs. Although a large number of techniques is available to study aggregation *in vitro* and *in vivo*, there are still many limitations regarding quantification and determination of the degree of toxicity among aggregation intermediates (reviewed in [37]).

In this work we explored the amenability of two biochemical methods to assess aggregation in *C. elegans*, i) filter retardation and ii) biochemical fractionation assays. Previous reports used these two methods to assess aggregation in *C. elegans*, however in a more qualitative manner [24; 34; 35]. Here, we improved the described methods by controlling for total protein loading to allow semi-quantification of ATXN3 aggregation, enabling statistical treatment of the results.

Western blot is the most widely used technique for detection and quantification of specific proteins in biological samples. However, a large debate arose in the past decade regarding internal loading controls, which should be used to guarantee, as much as possible, equal loading of the samples. Housekeeping proteins, such as tubulin, actin or glyceraldehyde 3-phosphate dehydrogenase (GAPDH) are often used as internal loading control in several publications, assuming limited to no changes in expression in different physiological conditions or upon external stimuli. However, it is now known that in several neurological diseases, such as in Alzheimer's disease and spinal cord injury, as well as in cancer, there are changes in the expression of these housekeeping proteins (reviewed in [38]). Moreover, different tissues and cell lines can present significant differences in actin and tubulin protein content (reviewed in [39]). In addition, one of the most widely recognized limitation of the use of housekeeping protein signals is their limited dynamic range, which precludes the detection of small changes. For this reason, new methods of protein loading control were developed to overcome these limitations [38; 39; 40]. Our data

pointed to an overall superiority of the TPS to control for loading differences, in comparison to the use of tubulin quantification by immunoblotting. Despite both tubulin and TPS signals correlated in all samples, TPS showed lower variation around the mean and a higher dynamic range. Furthermore, tubulin was increased in *C. elegans* expressing mutant ATXN3 protein when compared to WT animals, further supporting the previously described possible unbalance of cytoskeletal dynamics in the absence of a full functional ATXN3 protein [41] eventually stemming from the known interaction between ATXN3 and tubulin [42]. Therefore, here, we suggest TPS as a more accurate method to control for protein loading in biochemical methods to assess ATXN3 aggregation.

Only a few techniques allow the study of protein aggregation in live organisms including *C. elegans*. In reporter strains, the protein of interest is often fused with a fluorescent tag, that upon self-association will generate an increase in fluorescent signals with consequent visualization of protein *foci*. These foci can, however, be constituted by mobile and soluble protein, not forming true aggregates. FRAP and FRET methods are microscopy-based techniques that can identify aggregated species due to the immobile nature of protein aggregates [9; 12; 13; 14; 15; 16; 17; 18; 22; 43]. Although with obvious advantages, as the fact that they are performed in live animals and allow monitorization of the aggregation process over time and in specific cells, these microscopy live imaging based-techniques are time consuming, only evaluating the pattern of aggregation in a limited number of cells and in a small number of animals (reduced sampling). On the other hand, in the case of live animals, the quality of the images is highly dependent on the efficacy of anaesthetics to avoid animal movement during image acquisition, this being often achieved with the application of neurotoxic drugs not compatible with the study of protein aggregation, when expressed in the nervous system.

Aggregates are by definition, among other features, immobile, insoluble in SDS and present increased size compatible with protein agglomerates [44]. The biochemical methods further optimised in this work took advantage of these two later characteristics. Filter retardation assay (or filter trap assay) retained the SDS-insoluble large aggregates on a cellulose acetate membrane separating them from the monomeric soluble protein [45]. After immunoblotting, using specific antibodies against the protein of interest, aggregates can be detected and quantified making this method suitable for fast throughput screenings. However, filter retardation assays do not allow the detection of intermediate forms in the process of aggregation being just suitable for the detection of large aggregates, higher than 0.2 μm. On the other hand, biochemical fractionation explores the differential solubility of the protein species in different detergents and combine it with a sedimentation assay, where insoluble proteins form a pellet

during centrifugation [24; 36]. In this method, SDS-soluble and resistant species can be assessed independently of aggregate size. Therefore, and taking into account the advantages and limitations of each method, here we propose to use a combinatory approach to assess aggregation in *C. elegans*.

To explore the amenability of these existing methods for *C. elegans* protein samples, we assessed ATXN3 aggregation by these techniques in presence of a known genetic modifier of ATXN3 proteotoxicity, *mod-5*, and in two drug treatments, using APZ and CLR-01, described as protein aggregation modulators. *mod-5* ablation in the ATXN3-proteotoxicity *C. elegans* model, was previously reported to decrease aggregation *in vivo*, as assessed using confocal dynamic imaging [24]. APZ treatment was reported as modulator of high molecular weight ATXN3 species abundance in mice and fly MJD models [27]. CLR-01, on the other hand, is a molecular tweezer that was described to reduce aggregation or self-assembly of multiple pathogenic proteins as huntingtin, α-synuclein and superoxide dismutase 1 [46; 47; 48]. Here, we showed that with filter retardation assay, biochemical fractionation, and dynamic confocal imaging, we can detect alterations in mutant ATXN3 aggregation and inform about ATXN3 solubility, in a semi-quantitative manner. Therefore, we fulfil the need of improving these biochemical methods by adding internal controls in line with what was then proposed by other groups [35; 49]. However, a high variability within each technique was still observed mostly in the case of drug treatments, that is much less pronounced when ATXN3 aggregation was evaluated in presence of a strong genetic modifier. The inter-populational variability, in which each population may respond differently to compound treatment can be related with host-microbiota interactions, the impact of food heat-inactivation on drug efficacy, or by transgenerational effect since the maternal environment is transmitted to the offspring [50; 51], and may reflect the intrinsic variability of each assay. Consistently with these results the limited impact of the drugs here tested on ATXN3 aggregation was previously suggested, since no impact on highly insoluble ATXN3 aggregates was seen in the brain of MJD mice upon APZ treatment [27] and preliminary experiments, performed in our laboratory, treating a different MJD mouse model with CLR-01 failed to impact ATXN3 inclusion load in the spinal cord (S. Duarte-Silva, personal communication).

In conclusion, we successfully improved filter retardation and biochemical fractionation assays to semi-quantifiable methods, although, in the case of drug treatments these methods are limited by some variability. Therefore, we propose the evaluation of the aggregation, in *C. elegans*, using a combinatory strategy comprising multiple methods.

Acknowledgments

We are grateful to members of the Maciel laboratory for sharing reagents, for critical analysis of the data and result discussion. To Dr. Gal Bitan (UCLA) for kindly providing the experimental drug CLR-01. Thanks to the *Caenorhabditis Genetics Center* (CGC), which is funded by NIH Office of Research Infrastructure Programs (P40 OD010440) for providing some of the nematode strains used in this study.

Funding

This work was funded by FEDER, through the Competitiveness Internationalization Operational Programme (POCI), and by National funds, through the Foundation for Science and Technology (FCT), under the scope of the project POCI-01-0145-FEDER-0 31987, NORTE-010145-FEDER-000013 and NORTE-01-0145-FEDER-000023, supported by the Northern Portugal Regional Operational Programme (NORTE 2020), under the Portugal 2020 Partnership Agreement, through the European Regional Development Fund (ERDF) and by ICVS Scientific Microscopy Platform, member of the national infrastructure PPBI Portuguese Platform of Bioimaging (PPBI-POCI-01-0145-FEDER022122); by National funds, through the Foundation for Science and Technology (FCT) - project UIDB/50026/2020 and UIDP/50026/2020. Additionally, this project was supported by National Ataxia Foundation (NAF) and the FCT individual fellowship PD/BDE/127834/2016 (For Pereira-Sousa, J.).

References

[1] T.A. Bayer, Proteinopathies, a core concept for understanding and ultimately treating degenerative disorders? Eur Neuropsychopharmacol 25 (2015) 713-24. doi: 10.1016/j.euroneuro.2013.03.007.

[2] A.P. Marsh, Molecular mechanisms of proteinopathies across neurodegenerative disease: a review. Neurological Research and Practice 1 (2019) 35. doi: 10.1186/s42466-019-0039-8.

[3] C.A. Ross, and M.A. Poirier, Protein aggregation and neurodegenerative disease. Nat Med 10 Suppl (2004) S10-7. doi: 10.1038/nm1066.

[4] C. Soto, Unfolding the role of protein misfolding in neurodegenerative diseases. Nat Rev Neurosci 4 (2003) 49-60. doi: 10.1038/nrn1007.

[5] V. Kumar, N. Sami, T. Kashav, A. Islam, F. Ahmad, and M.I. Hassan, Protein aggregation and neurodegenerative diseases: From theory to therapy. Eur J Med Chem 124 (2016) 1105-1120. doi: 10.1016/j.ejmech.2016.07.054.

[6] K.A. Bruggink, M. Muller, H.B. Kuiperij, and M.M. Verbeek, Methods for analysis of amyloid-beta aggregates. J Alzheimers Dis 28 (2012) 735-58. doi: 10.3233/JAD-2011-111421.

[7] H.C. Mahler, W. Friess, U. Grauschopf, and S. Kiese, Protein aggregation: pathways, induction factors and analysis. J Pharm Sci 98 (2009) 2909-34. doi: 10.1002/jps.21566.

[8] J.T. Pedersen, and N.H. Heegaard, Analysis of protein aggregation in neurodegenerative disease. Anal Chem 85 (2013) 4215-27. doi: 10.1021/ac400023c.

[9] A. Kitamura, K. Nagata, and M. Kinjo, Conformational analysis of misfolded protein aggregation by FRET and live-cell imaging techniques. Int J Mol Sci 16 (2015) 6076-92. doi: 10.3390/ijms16036076.

[10] D. Ami, A. Natalello, M. Lotti, and S.M. Doglia, Why and how protein aggregation has to be studied in vivo. Microb Cell Fact 12 (2013) 17. doi: 10.1186/1475-2859-12-17.

[11] A. Espargaro, R. Sabate, and S. Ventura, Thioflavin-S staining coupled to flow cytometry. A screening tool to detect in vivo protein aggregation. Mol Biosyst 8 (2012) 2839-44. doi: 10.1039/c2mb25214g.

[12] R.B. Sekar, and A. Periasamy, Fluorescence resonance energy transfer (FRET) microscopy imaging of live cell protein localizations. J Cell Biol 160 (2003) 629-33. doi: 10.1083/jcb.200210140.

[13] C.H. Lo, N.K. Pandey, C.K. Lim, Z. Ding, M. Tao, D.D. Thomas, R. Langen, and J.N. Sachs, Discovery of Small Molecule Inhibitors of Huntingtin Exon 1 Aggregation by FRET-Based High-Throughput Screening in Living Cells. ACS Chem Neurosci 11 (2020) 2286-2295. doi: 10.1021/acschemneuro.0c00226.

[14] F. Miraglia, V. Valvano, L. Rota, C. Di Primio, V. Quercioli, L. Betti, G. Giannaccini, A. Cattaneo, and E. Colla, Alpha-Synuclein FRET Biosensors Reveal Early Alpha-Synuclein Aggregation in the Endoplasmic Reticulum. Life (Basel) 10 (2020). doi: 10.3390/life10080147.

[15] T.K. Kerppola, Bimolecular fluorescence complementation (BiFC) analysis as a probe of protein interactions in living cells. Annu Rev Biophys 37 (2008) 465-87. doi: 10.1146/annurev.biophys.37.032807.125842.

[16] E.K. Don, A. Maschirow, R.A.W. Radford, N.M. Scherer, A. Vidal-Itriago, A. Hogan, C. Maurel, I. Formella, J.J. Stoddart, T.E. Hall, A. Lee, B. Shi, N.J. Cole, A.S. Laird, A.P. Badrock, R.S. Chung, and M. Morsch, In vivo Validation of Bimolecular Fluorescence Complementation (BiFC) to Investigate Aggregate Formation in Amyotrophic Lateral Sclerosis (ALS). Mol Neurobiol 58 (2021) 2061-2074. doi: 10.1007/s12035-020-02238-0.

[17] S. Shin, D. Kim, J.Y. Song, H. Jeong, S.J. Hyeon, N.W. Kowall, H. Ryu, A.N. Pae, S. Lim, and Y.K. Kim, Visualization of soluble tau oligomers in TauP301L-BiFC transgenic mice demonstrates the progression of tauopathy. Prog Neurobiol (2020) 101782. doi: 10.1016/j.pneurobio.2020.101782.

[18] B. Frey, A. AlOkda, M.P. Jackson, N. Riguet, J.A. Duce, and H.A. Lashuel, Monitoring alpha-synuclein oligomerization and aggregation using bimolecular fluorescence complementation assays: What you see is not always what you get. J Neurochem 157 (2021) 872-888. doi: 10.1111/jnc.15147.

[19] A.E. Bevivino, and P.J. Loll, An expanded glutamine repeat destabilizes native ataxin-3 structure and mediates formation of parallel beta -fibrils. Proc Natl Acad Sci U S A 98 (2001) 11955-60. doi: 10.1073/pnas.211305198.

[20] A.M. Ellisdon, B. Thomas, and S.P. Bottomley, The two-stage pathway of ataxin-3 fibrillogenesis involves a polyglutamine-independent step. J Biol Chem 281 (2006) 16888-16896. doi: 10.1074/jbc.M601470200.

[21] L. Gales, L. Cortes, C. Almeida, C.V. Melo, M.C. Costa, P. Maciel, D.T. Clarke, A.M. Damas, and S. Macedo-Ribeiro, Towards a structural understanding of the fibrillization pathway in Machado-Joseph's disease: trapping early oligomers of non-expanded ataxin-3. J Mol Biol 353 (2005) 642-54. doi: 10.1016/j.jmb.2005.08.061.

[22] A. Teixeira-Castro, M. Ailion, A. Jalles, H.R. Brignull, J.L. Vilaca, N. Dias, P. Rodrigues, J.F. Oliveira, A. Neves-Carvalho, R.I. Morimoto, and P. Maciel, Neuron-specific proteotoxicity of mutant ataxin-3 in C. elegans: rescue by the DAF-16 and HSF-1 pathways. Hum Mol Genet 20 (2011) 2996-3009. doi: 10.1093/hmg/ddr203.

[23] A. Teixeira-Castro, N. Dias, P. Rodrigues, J.F. Oliveira, N.F. Rodrigues, P. Maciel, and J.L. Vilaça, An Image Processing Application for Quantification of Protein Aggregates in Caenorhabditis Elegans,

Springer Berlin Heidelberg, Berlin, Heidelberg, 2011, pp. 31-38, doi: 10.1007/978-3-642-19914-1_5.

[24] A. Teixeira-Castro, A. Jalles, S. Esteves, S. Kang, L. da Silva Santos, A. Silva-Fernandes, M.F. Neto, R.M. Brielmann, C. Bessa, S. Duarte-Silva, A. Miranda, S. Oliveira, A. Neves-Carvalho, J. Bessa, T. Summavielle, R.B. Silverman, P. Oliveira, R.I. Morimoto, and P. Maciel, Serotonergic signalling suppresses ataxin 3 aggregation and neurotoxicity in animal models of Machado-Joseph disease. Brain 138 (2015) 3221-37. doi: 10.1093/brain/awv262.

[25] N.S. Ashraf, S. Duarte-Silva, E.D. Shaw, P. Maciel, H.L. Paulson, A. Teixeira-Castro, and M.D.C. Costa, Citalopram Reduces Aggregation of ATXN3 in a YAC Transgenic Mouse Model of Machado-Joseph Disease. Mol Neurobiol 56 (2019) 3690-3701. doi: 10.1007/s12035-018-1331-2.

[26] D.A. Shapiro, S. Renock, E. Arrington, L.A. Chiodo, L.X. Liu, D.R. Sibley, B.L. Roth, and R. Mailman, Aripiprazole, a novel atypical antipsychotic drug with a unique and robust pharmacology. Neuropsychopharmacology 28 (2003) 1400-11. doi: 10.1038/sj.npp.1300203.

[27] M.D.C. Costa, N.S. Ashraf, S. Fischer, Y. Yang, E. Schapka, G. Joshi, T.J. McQuade, R.M. Dharia, M. Dulchavsky, M. Ouyang, D. Cook, D. Sun, M.J. Larsen, J.E. Gestwicki, S.V. Todi, M.I. Ivanova, and H.L. Paulson, Unbiased screen identifies aripiprazole as a modulator of abundance of the polyglutamine disease protein, ataxin-3. Brain 139 (2016) 2891-2908. doi: 10.1093/brain/aww228.

[28] A. Neves-Carvalho, S. Duarte-Silva, A. Teixeira-Castro, and P. Maciel, Polyglutamine spinocerebellar ataxias: emerging therapeutic targets. Expert Opinion on Therapeutic Targets 24 (2020) 1099-1119. doi: 10.1080/14728222.2020.1827394.

[29] P. Sweeney, H. Park, M. Baumann, J. Dunlop, J. Frydman, R. Kopito, A. McCampbell, G. Leblanc, A. Venkateswaran, A. Nurmi, and R. Hodgson, Protein misfolding in neurodegenerative diseases: implications and strategies. Translational Neurodegeneration 6 (2017). doi: 10.1186/s40035-017-0077-5.

[30] A. Attar, and G. Bitan, Disrupting self-assembly and toxicity of amyloidogenic protein oligomers by "molecular tweezers" - from the test tube to animal models. Curr Pharm Des 20 (2014) 2469-83. doi: 10.2174/13816128113199990496.

[31] S. Brenner, The genetics of Caenorhabditis elegans. Genetics 77 (1974) 71-94. http://www.ncbi.nlm.nih.gov/pubmed/4366476

[32] C. Voisine, H. Varma, N. Walker, E.A. Bates, B.R. Stockwell, and A.C. Hart, Identification of potential therapeutic drugs for huntington's disease using Caenorhabditis elegans. PLoS One 2 (2007) e504. doi: 10.1371/journal.pone.0000504.

[33] T. Gidalevitz, T. Krupinski, S. Garcia, and R.I. Morimoto, Destabilizing protein polymorphisms in the genetic background direct phenotypic expression of mutant SOD1 toxicity. PLoS genetics 5 (2009) e1000399. doi: 10.1371/journal.pgen.1000399.

[34] D. Vilchez, I. Morantte, Z. Liu, P.M. Douglas, C. Merkwirth, A.P. Rodrigues, G. Manning, and A. Dillin, RPN-6 determines C. elegans longevity under proteotoxic stress conditions. Nature 489 (2012) 263-8. doi: 10.1038/nature11315.

[35] O. Sin, A. Mata-Cabana, R.I. Seinstra, and E.A.A. Nollen, Filter Retardation Assay for Detecting and Quantifying Polyglutamine Aggregates Using Caenorhabditis elegans Lysates. Bio-protocol 8 (2018). doi: 10.21769/BioProtoc.3042.

[36] P. Koch, P. Breuer, M. Peitz, J. Jungverdorben, J. Kesavan, D. Poppe, J. Doerr, J. Ladewig, J. Mertens, T. Tuting, P. Hoffmann, T. Klockgether, B.O. Evert, U. Wullner, and O. Brustle, Excitation-induced ataxin-3 aggregation in neurons from patients with Machado-Joseph disease. Nature 480 (2011) 543-6. doi: 10.1038/nature10671.

[37] S. Gregoire, J. Irwin, and I. Kwon, Techniques for Monitoring Protein Misfolding and Aggregation in Vitro and in Living Cells. Korean J Chem Eng 29 (2012) 693-702. doi: 10.1007/s11814-012-0060-x.

[38] R. Li, and Y. Shen, An old method facing a new challenge: re-visiting housekeeping proteins as internal reference control for neuroscience research. Life Sci 92 (2013) 747-51. doi: 10.1016/j.lfs.2013.02.014.

[39] R.E. Ferguson, H.P. Carroll, A. Harris, E.R. Maher, P.J. Selby, and R.E. Banks, Housekeeping proteins: a preliminary study illustrating some limitations as useful references in protein expression studies. Proteomics 5 (2005) 566-71. doi: 10.1002/pmic.200400941.

[40] C.P. Moritz, Tubulin or Not Tubulin: Heading Toward Total Protein Staining as Loading Control in Western Blots. Proteomics 17 (2017). doi: 10.1002/pmic.201600189.

[41] A.J. Rodrigues, M. do Carmo Costa, T.L. Silva, D. Ferreira, F. Bajanca, E. Logarinho, and P. Maciel, Absence of ataxin-3 leads to cytoskeletal disorganization and increased cell death. Biochim Biophys Acta 1803 (2010) 1154-63. doi: 10.1016/j.bbamcr.2010.07.004.

[42] S. Mazzucchelli, A. De Palma, M. Riva, A. D'Urzo, C. Pozzi, V. Pastori, F. Comelli, P. Fusi, M. Vanoni, P. Tortora, P. Mauri, and M.E. Regonesi, Proteomic and biochemical analyses unveil tight interaction of ataxin-3 with tubulin. Int J Biochem Cell Biol 41 (2009) 2485-92. doi: 10.1016/j.biocel.2009.08.003.

[43] J. Hinz, L. Lehnhardt, S. Zakrzewski, G. Zhang, and Z. Ignatova, Polyglutamine expansion alters the dynamics and molecular architecture of aggregates in dentatorubropallidoluysian atrophy. J Biol Chem 287 (2012) 2068-78. doi: 10.1074/jbc.M111.318915.

[44] L.O. Narhi, J. Schmit, K. Bechtold-Peters, and D. Sharma, Classification of protein aggregates. J Pharm Sci 101 (2012) 493-8. doi: 10.1002/jps.22790.

[45] E.E. Wanker, E. Scherzinger, V. Heiser, A. Sittler, H. Eickhoff, and H. Lehrach, Membrane filter assay for detection of amyloid-like polyglutamine-containing protein aggregates. Methods Enzymol 309 (1999) 375-86. doi: 10.1016/s0076-6879(99)09026-6.

[46] M. Herrera-Vaquero, D. Bouquio, M. Kallab, K. Biggs, G. Nair, J. Ochoa, A. Heras-Garvin, C. Heid, I. Hadrovic, W. Poewe, G.K. Wenning, F.G. Klarner, T. Schrader, G. Bitan, and N. Stefanova, The molecular tweezer CLR01 reduces aggregated, pathologic, and seeding-competent alpha-synuclein in experimental multiple system atrophy. Biochim Biophys Acta Mol Basis Dis 1865 (2019) 165513. doi: 10.1016/j.bbadis.2019.07.007.

[47] R. Malik, H. Meng, P. Wongkongkathep, C.I. Corrales, N. Sepanj, R.S. Atlasi, F.G. Klarner, T. Schrader, M.J. Spencer, J.A. Loo, M. Wiedau, and G. Bitan, The molecular tweezer CLR01 inhibits aberrant superoxide dismutase 1 (SOD1) self-assembly in vitro and in the G93A-SOD1 mouse model of ALS. J Biol Chem 294 (2019) 3501-3513. doi: 10.1074/jbc.RA118.005940.

[48] T. Vopel, K. Bravo-Rodriguez, S. Mittal, S. Vachharajani, D. Gnutt, A. Sharma, A. Steinhof, O. Fatoba, G. Ellrichmann, M. Nshanian, C. Heid, J.A. Loo, F.G. Klarner, T. Schrader, G. Bitan, E.E. Wanker, S. Ebbinghaus, and E. Sanchez-Garcia, Inhibition of Huntingtin Exon-1 Aggregation by the Molecular Tweezer CLR01. J Am Chem Soc 139 (2017) 5640-5643. doi: 10.1021/jacs.6b11039.

[49] O. Sin, T. de Jong, A. Mata-Cabana, M. Kudron, M.A. Zaini, F.A. Aprile, R.I. Seinstra, E. Stroo, R.W. Prins, C.N. Martineau, H.H. Wang, W. Hogewerf, A. Steinhof, E.E. Wanker, M. Vendruscolo, C.F. Calkhoven, V. Reinke, V. Guryev, and E.A. Nollen, Identification of an RNA Polymerase III Regulator Linked to Disease-Associated Protein Aggregation. Mol Cell 65 (2017) 1096-1108 e6. doi: 10.1016/j.molcel.2017.02.022.

[50] T.A. Scott, L.M. Quintaneiro, P. Norvaisas, P.P. Lui, M.P. Wilson, K.Y. Leung, L. Herrera-Dominguez, S. Sudiwala, A. Pessia, P.T. Clayton, K. Bryson, V. Velagapudi, P.B. Mills, A. Typas, N.D.E.

Greene, and F. Cabreiro, Host-Microbe Co-metabolism Dictates Cancer Drug Efficacy in C. elegans. Cell 169 (2017) 442-456 e18. doi: 10.1016/j.cell.2017.03.040.

[51] K.B. Pho, and L.T. MacNeil, Biology is the root of variability: cautionary tales in Caenorhabditis elegans biology. Biochem Soc Trans 47 (2019) 887-896. doi: 10.1042/BST20190001.

[52] W. Lenhard, and A. Lenhard, Computation of Effect Sizes (2017), http://www.psychometrica.de/effect_size.html Accessed June 2021, doi: 10.13140/RG.2.2.17823.92329.

[53] J.O. Uanhoro, Effect size calculators (2017), https://effect-size-calculator.herokuapp.com/ Accessed June 2021.

Supplementary Material

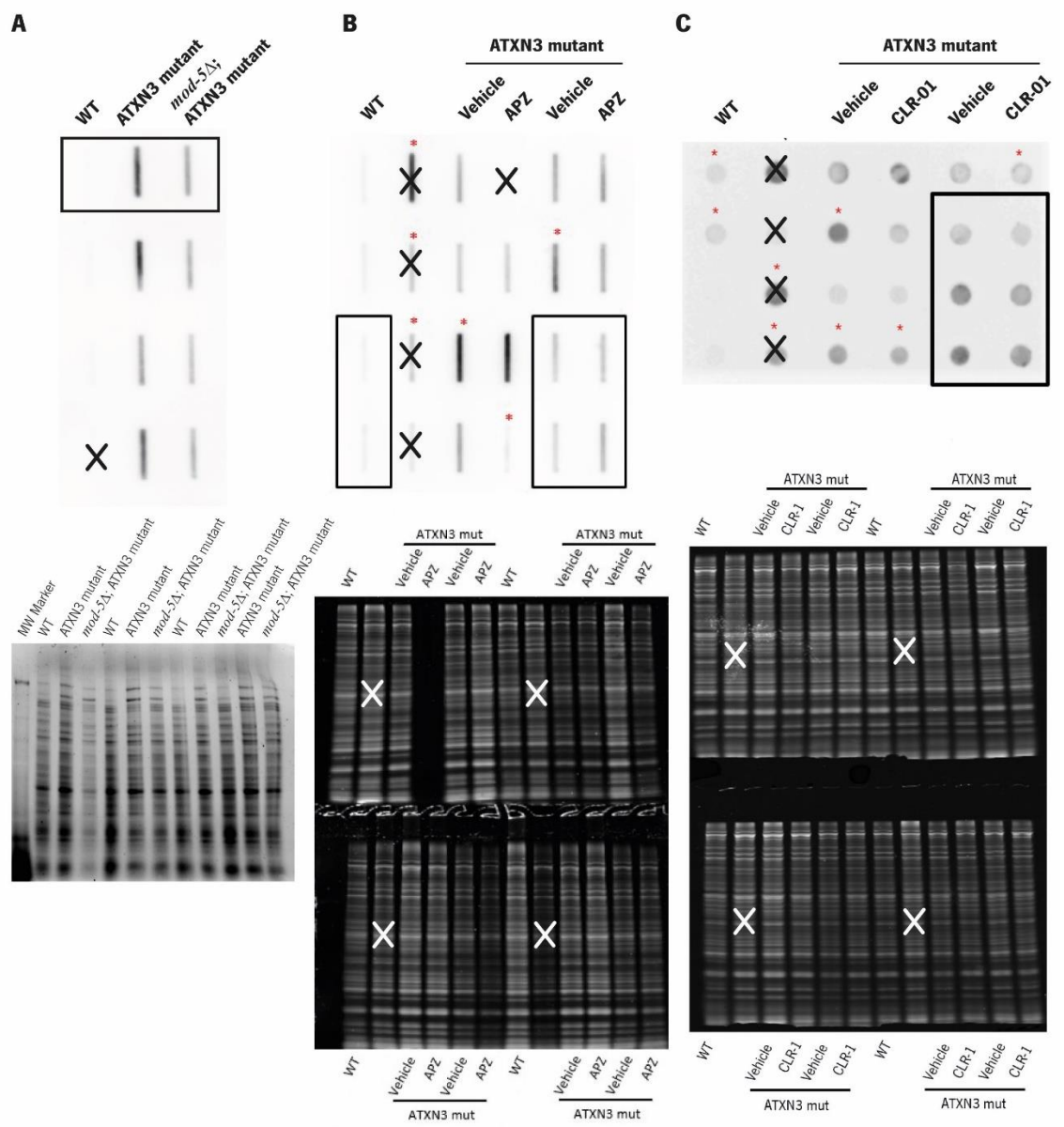

Supplementary figure 1. Filter retardation membranes and SDS-page total protein gels.

Filter retardation membranes (upper panel) and SDS-PAGE total protein loading controls (bottom panel) for **(A)** genetic modifier *mod-5*, **(B)** APZ and **(C)** CLR-01 treatments after ATXN3 Western blot probing. Highlighted rectangles are shown in the main Figures 2A, 3D and 4D. * Discarded samples, due to probable membrane clogging (assumed by reduced solvent flux upon vacuum initiation).

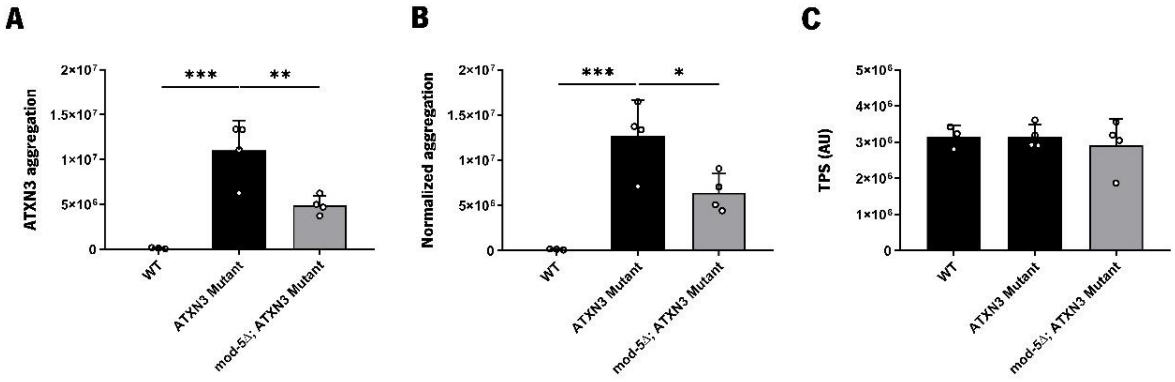

Supplementary figure 2. Quantification and statistical analysis of filter retardation assay of *mod-5Δ*; ATXN3 mutant animals.

(A) ATXN3 intensity signals as a measure of ATXN3 aggregation, without TPS normalization, were decreased in *mod-5Δ*; ATXN3 mutant animals in comparison with ATXN3 mutant animals. **(B)** The difference is maintained upon normalization of ATXN3 signals, using TPS. **(C)** TPS did not significantly differ among genotypes, however some experimental variability can be detected. (A): (n = 3 - 4, ± SD), **P < 0.01 ***P < 0.001, (ANOVA, Dunnett); (B): (n = 3 - 4, ± SD), *P < 0.05 ***P < 0.001, (ANOVA, Dunnett); (C): (n = 3 - 4, ± SD), (ANOVA, Dunnett).

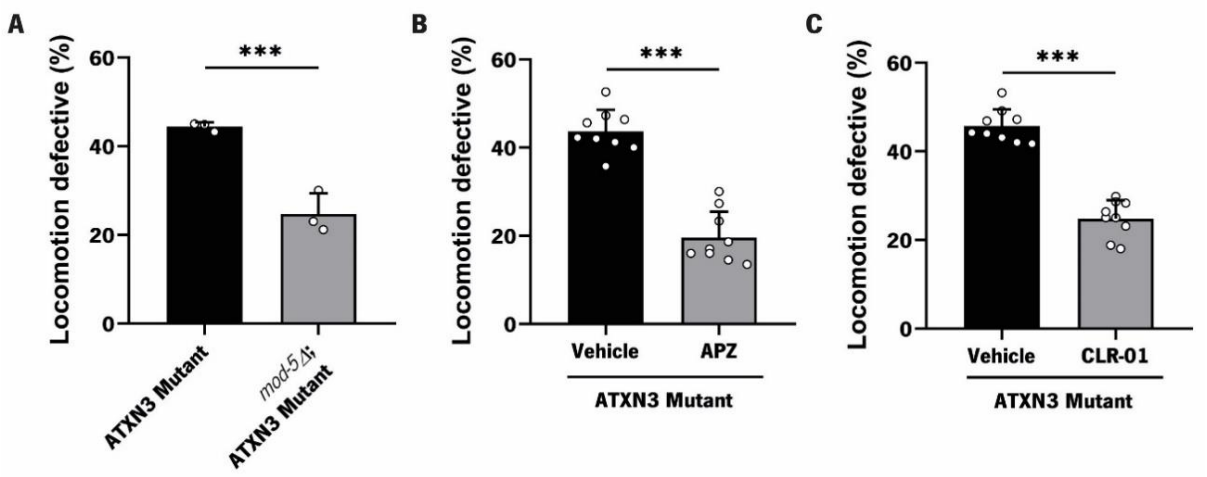

Supplementary figure 3. Motility assay performed in animals collected for filter retardation assay and biochemical fractionation experiments.

Motor assessment demonstrating motor improvement in **(A)** genetic ablation of *mod-5* in ATXN3 mutant background and drug efficacy of **(B)** APZ and **(C)** CLR-01 treatments. For *mod-5Δ*; ATXN3 mutant (A) (n = 3, ± SD) ***P < 0.001 (ANOVA, Dunnett test); for drug treatments (B) (n = 9, ± SD) ***P < 0.001 (unpaired t-test); (C) (n = 9, ± SD) ***P < 0.001 (unpaired t-test).

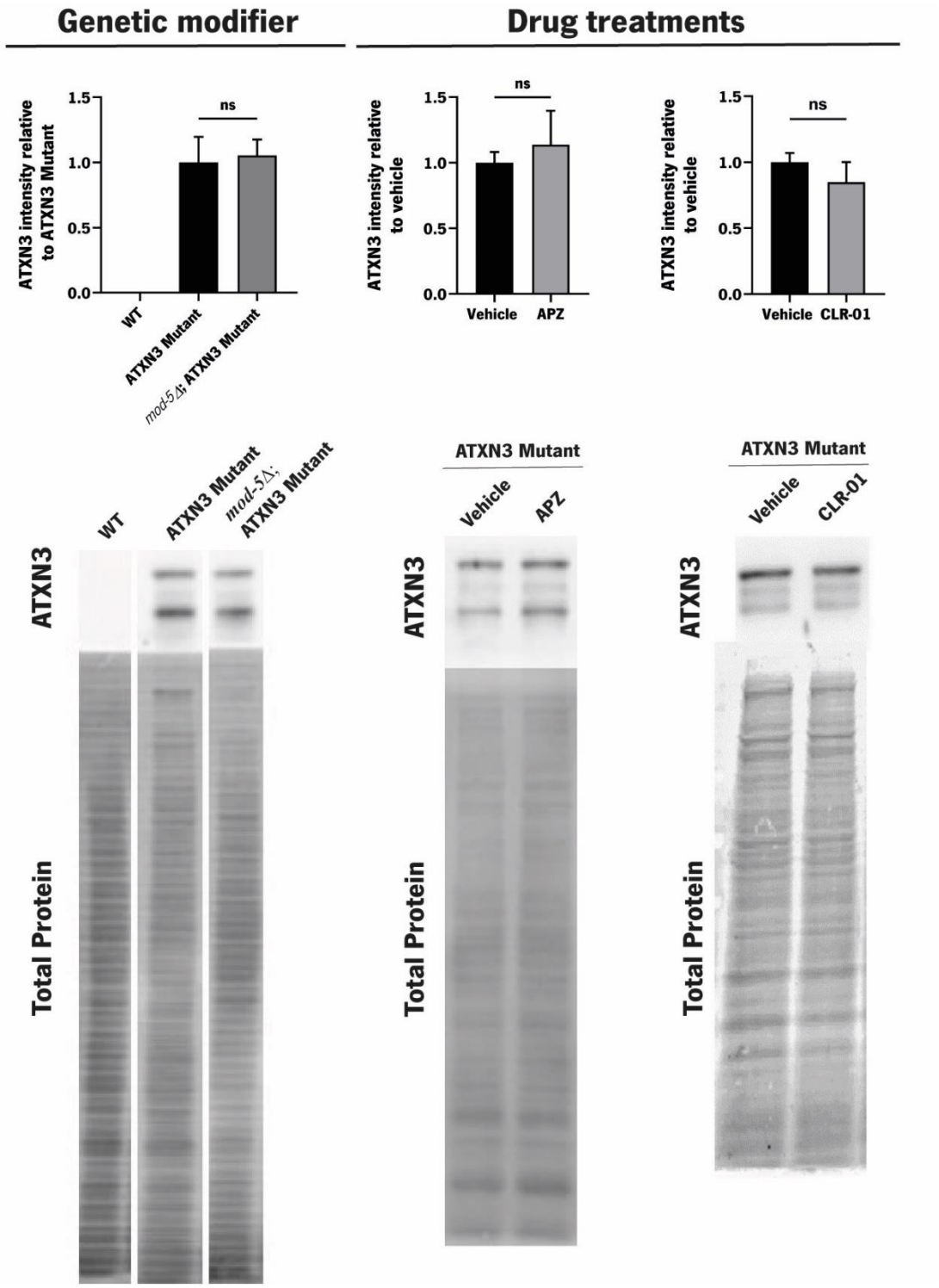

Supplementary figure 4. Total steady-state levels of ATXN3 protein promoted by the genetic modifier *mod-5* or drug treatments.

No alterations were found in ATXN3 full-length protein levels. For genetic modifier (n = 4, ± SEM) ns – non-significant differences (ANOVA, Dunnett test); for drug treatments (APZ) (n = 6, ± SEM) ns – non-significant differences (unpaired t-test with welch correction); (CLR-01) (n = 6, ± SEM) ns – non-significant differences (unpaired t-test). Chart representation (top). Membrane of ATXN3 and total protein staining obtained (bottom).

Supplementary table 1. Statistical report.

Effect sizes reported calculated as [52; 53].

Figure number		Statistics	Sample size
Fig. 1	C	F (2, 9) = 3,946, p = 0.0588, ω^2p = 0.329	4
Fig. 2	A	F (2, 8) = 17.98, p = 0.0011, ω^2p = 0.755	3 to 4
	B - Soluble	T(2) = 1.555, $p_{corrected}$ = 0.7803, *d* = 0.898	3
	B - SDS soluble	T(2) = 2.356, $p_{corrected}$ = 0.4278, *d* = 1.360	3
	B - SDS resistant	T(2) = 19.00, $p_{corrected}$ = 0.0084, *d* = -10.97	3
Fig. 3	B – number of aggregates / Total area - Assay 1	T(17) = -0.611, p = 0.552, *d* = -0.281	9 to 10
	B – number of aggregates / Total area - Assay 2	T(16) = -2.420, p = 0.028, *d* = -1.141	9
	B – number of aggregates / Total area - Assay 3	T(19) = 0.369, p = 0.716, *d* = 0.166	8 to 13
	B – area occupied by aggregates / Total area Assay 1	T(16) = -1.624, p = 0.124, *d* = -0.766	9
	B – area occupied by aggregates / Total area Assay 2	T(16) = -2.292, p = 0.036, *d* = -1.08	9
	B – area occupied by aggregates / Total area Assay 3	T(19) = 1.095, p = 0.287, *d* = 0.492	8 to 13
	C – Total area	T(58) = 0.9583, p = 0.342, *d* = 0.248	28 to 32
	C – number of aggregates / Total area	T(56) = 1.186, p = 0.240, *d* = 0.312	27 to 31
	C – area occupied by aggregates / Total area	T(55) = 0.8746, p = 0.3856, *d* = 0.233	26 to 31
	D	F (2, 13) = 11.53, p = 0.0013, ω^2p = 0.568	4 to 6
	E - Soluble	T(2) = 0.8012, $p_{corrected}$ > 0.999, *d* = 0.462	3
	E – SDS soluble	T(3) = 3.119, $p_{corrected}$ = 0.157, *d* = -1.560	4
	E – SDS resistant	T(3) = 1.820, $p_{corrected}$ = 0.499, *d* = 0,910	4
Fig. 4	B – number of aggregates / Total area - Assay 1	T(14) = 0.6492, p = 0.5267, *d* = 0.350	5 to 11
	B – number of aggregates / Total area - Assay 2	F (2, 29) = 8.332, p = 0.0014, ω^2p = 0.314	10 to 11
	B – number of aggregates / Total area - Assay 3	T(13) = 0.2388, p = 0.8150, *d* = 0.126	6 to 9

	B – area occupied by aggregates / Total area Assay 1	T(14) = 2.014, p = 0.0636, *d* = 1.086	5 to 11
	B – area occupied by aggregates / Total area Assay 2	F (2, 29) = 6.512, p = 0.0046, ω^2p = 0.256	10 to 11
	B – area occupied by aggregates / Total area Assay 3	T(13) = 1.732, p = 0.1069, *d* = 0.913	6 to 9
	C – Total area	T(50) = 0.7581, p = 0.4520, *d* = 0.211	24 to 28
	C – number of aggregates / Total area	T(45.66) = 2.020, p = 0.0493, *d* = 0.562	24 to 28
	C – area occupied by aggregates / Total area	T(35) = 1.890, p = 0.067, *d* = 0.633	15 to 22
	D	F (3, 11) = 0.9075, p= 0.4686, ω^2p = -0.019	6
	E - Soluble	T(5) = 1.459, $p_{corrected}$ = 0.6132, *d* = -0,595	6
	E – SDS soluble	T(5) = 0.9864, $p_{corrected}$ > 0.9999, *d* = -0,403	6
	E – SDS resistant	T(5) = 1.945, $p_{corrected}$ = 0.3192, *d* = -0,794	6
Supplementary Fig. 2	A	F(2, 8) = 22.80, p < 0.001, ω^2p = 0.798	3 to 4
	B	F(2, 8) = 17.98, p = 0.0011, ω^2p = 0.755	3 to 4
	C	F(2, 8) = 0.2736, p = 0.767, ω^2p = -0.152	3 to 4
Supplementary Fig. 3	A	F(2, 5) = 74.78, p < 0.001, ω^2p = 0.949	3
	B	T(16) = 9.454, p < 0.001, *d* = 4.457	9
	C	T(16) = 11.18, p < 0.001, *d* = 5.270	9
Supplementary Fig. 4	Genetic modifier	F(2, 9) = 19.50, p < 0.001, ω^2p = 0.755	4
	APZ	T(5.985) = 0.5101, p = 0.6282, *d* = 0.295	6
	CLR-01	T(10) = 0.9033, p = 0.3876, *d* = 0.522	6

Chapter 3.

Identification of the 5-HT_{1A} serotonin receptor as a novel therapeutic target in a *C. elegans* model of Machado-Joseph disease

Neurobiology of Disease 152 (2021) 105278

Contents lists available at ScienceDirect

Neurobiology of Disease

journal homepage: www.elsevier.com/locate/ynbdi

Identification of the 5-HT$_{1A}$ serotonin receptor as a novel therapeutic target in a *C. elegans* model of Machado-Joseph disease

Joana Pereira-Sousa [a,b,c], Bruna Ferreira-Lomba [a,b], Aina Bellver-Sanchis [a,b,1], Daniela Vilasboas-Campos [a,b], Jorge H. Fernandes [a,b], Marta D. Costa [a,b], Mark A. Varney [d], Adrian Newman-Tancredi [d], Patrícia Maciel [a,b,*,2], Andreia Teixeira-Castro [a,b,*,2]

[a] Life and Health Sciences Research Institute (ICVS), School of Medicine, University of Minho, Braga, Portugal
[b] ICVS/3B's - PT Government Associate Laboratory Braga/Guimarães, Portugal
[c] Behavioral & Molecular Lab (Bn'ML), University of Minho, Braga, Portugal
[d] Neurolixis Inc., Park Ridge, NJ 07656, USA

ARTICLE INFO

Keywords:
Befiradol
NLX-112
5-HT$_{1A}$ receptor agonist
Spinocerebellar ataxia type 3
Ataxin-3 aggregation
Serotonin
Therapy

ABSTRACT

Machado-Joseph disease (MJD) or Spinocerebellar ataxia type 3 (SCA3) is a progressive neurodegenerative disorder that affects movement coordination leading to a premature death. Despite several efforts, no disease-modifying treatment is yet available for this disease. Previous studies pinpointed the modulation of serotonergic signaling, through pharmacological inhibition of the serotonin transporter SERT, as a promising therapeutic approach for MJD/SCA3. Here, we describe the 5-HT$_{1A}$ receptor as a novel therapeutic target in MJD, using a *C. elegans* model of ATXN3 proteotoxicity. Chronic and acute administration of befiradol (also known as NLX-112), a highly specific 5-HT$_{1A}$ agonist, rescued motor function and suppressed mutant ATXN3 aggregation. This action required the 5-HT$_{1A}$ receptor orthologue in the nematode, SER-4. Tandospirone, a clinically tested 5-HT$_{1A}$ receptor partial agonist, showed a limited impact on animals' motor dysfunction on acute administration and a broader receptor activation profile upon chronic treatment, its effect depending on 5-HT$_{1A}$ but also on the 5-HT$_6$/SER-5 and 5-HT$_7$/SER-7 receptors. Our results support high potency and specificity of befiradol for activation of 5-HT$_{1A}$/SER-4 receptors and highlight the contribution of the auto- and hetero-receptor function to the therapeutic outcome in this MJD model. Our study deepens the understanding of serotonergic signaling modulation in the suppression of ATXN3 proteotoxicity and suggests that a potent and selective 5-HT$_{1A}$ receptor agonist such as befiradol could constitute a promising therapeutic agent for MJD.

1. Introduction

Machado-Joseph disease (MJD) or Spinocerebellar ataxia type 3 (SCA3) is a dominantly inherited neurodegenerative disease caused by an abnormal expansion of the cytosine-adenosine-guanine triplet (CAG) that encodes the amino acid glutamine in the ataxin-3 protein (ATXN3). Although the genetic alteration that causes MJD was described more than 25 years ago (Kawaguchi et al., 1994), currently, there is no treatment available for this severe and ultimately fatal disorder. MJD is the most prevalent form of dominant cerebellar ataxia worldwide and its clinical symptoms include progressive cerebellar ataxia, pyramidal syndrome, peripheral neuropathy, oculomotor abnormalities, extrapyramidal signs and sleep perturbation (Mendonca et al., 2018). At the molecular level, the abnormal expansion of the CAG repeat in the ataxin-3 gene translates into a polyglutamine tract of 61 to 87 glutamines that renders ATXN3 prone to self-assembly, and thus to form aggregates, and makes it toxic to neurons. The pathophysiology of MJD has been widely studied in the last decades, pointing to the misfolding of mutant ATXN3 and the disruption of protein homeostasis as the hub of MJD pathogenesis (reviewed in (Da Silva et al., 2019)).

In an attempt to counteract MJD progression, several studies were carried out using targeted- or hypothesis-free strategies to find disease-

* Corresponding authors at: Life and Health Sciences Research Institute (ICVS), School of Medicine, University of Minho, Braga, Portugal.
E-mail addresses: pmaciel@med.uminho.pt (P. Maciel), accastro@med.uminho.pt (A. Teixeira-Castro).
[1] Current affiliation: Pharmacology Section, Department of Pharmacology, Toxicology and Therapeutic Chemistry, Faculty of Pharmacy and Food Sciences, Institut de Neurociències—Universitat de Barcelona, Avda. Joan XXIII, 27. 08028 Barcelona, Spain.
[2] Authors share senior authorship.

https://doi.org/10.1016/j.nbd.2021.105278
Received 27 October 2020; Received in revised form 15 January 2021; Accepted 24 January 2021
Available online 28 January 2021

modifying compounds capable of ameliorating core symptoms of the disease (Da Silva et al., 2019; Neves-Carvalho et al., 2020). Some of the compounds described in these studies are neuromodulators including compounds that target the neuropeptide Y, and the adenosinergic, dopaminergic or serotonergic systems (Costa et al., 2016; Duarte-Neves et al., 2015; Goncalves et al., 2017; Teixeira-Castro et al., 2015). Previously, in an unbiased in vivo screening, we found that treatment with citalopram, a selective serotonin reuptake inhibitor (SSRI) that targets the serotonin transporter (SERT), suppressed mutant ATXN3 proteotoxicity in *C. elegans* and in two distinct transgenic mouse models of MJD (Ashraf et al., 2019; Esteves et al., 2019; Teixeira-Castro et al., 2015). Consistently with the pharmacological effect of citalopram, the molecular ablation of the *C. elegans* SERT homologue, MOD-5, suppressed mutant ATXN3 aggregation and motor impairments. Treatment efficacy was dependent on SERT/MOD-5 but also on serotonin (5-HT) receptors, their direct targeting, using pharmacological modulators, being sufficient to significantly reduce the motor dysfunction of the nematode MJD model (Teixeira-Castro et al., 2015).

Although citalopram and other SSRIs directly bind and inhibit SERT, thereby increasing the 5-HT availability at the synapse, there is, at least in the context of depression treatment, a delay in time to first response (Schatzberg, 2002). This is likely due to the molecular dynamics of 5-HT_{1A} receptors (5-HT_{1A}Rs). 5-HT_{1A}R is one of the most abundant and widely expressed 5-HT receptors in the brain (Albert et al., 1990; Garcia-Garcia et al., 2014; Pompeiano et al., 1992). There are two distinct populations of 5-HT_{1A}Rs: the presynaptic autoreceptors located on the cell body and dendrites of 5-HT neurons of the dorsal raphe nuclei (DRN); and the postsynaptic somatodendritic heteroreceptors expressed at 5-HT projecting areas (Kia et al., 1996; Riad et al., 2000). 5-HT_{1A} autoreceptors negatively regulate the 5-HT system. Serotonin released from the DRN activates 5-HT_{1A} autoreceptors, which exert a feedback inhibition on the firing of 5-HT neurons (Albert and Vahid-Ansari, 2019; Invernizzi et al., 1988; Prinssen et al., 2002; Stahl, 1998). In addition to their direct effect at the serotonin transporter, the chronic administration of SSRIs is accompanied by the downregulation of the 5-HT_{1A} autoreceptors and the subsequent suppression of the negative feedback mechanism of the serotonergic system, increasing neuronal firing rate (Kulikov et al., 2018; Stahl, 1998). Release of serotonin in target brain regions, in contrast, activates 5-HT heteroreceptors, including the 5-HT_{1A} heteroreceptor, which are associated to multiple regulatory functions including neuronal plasticity and synaptogenesis (Albert and Vahid-Ansari, 2019). Moreover, 5-HT_{1A}R can play a role in motor fine tuning and coordination, and it has been shown that several 5-HT_{1A}R agonists exhibited pronounced neuroprotective properties in models of cell injury, by causing a reduction in glutamate release and through the regulation of anti-apoptotic activities and the expression of protective proteins (Berends et al., 2005; Druse et al., 2005; Miyazaki and Asanuma, 2016; Oosterink et al., 2003; Thampi et al., 2012).

Tandospirone, a partial 5-HT_{1A}R agonist, has been used in the clinic to treat anxiety and depression and was put forward as a candidate for the treatment of other central nervous system disorders, including Parkinson, Alzheimer's and schizophrenia (Huang et al., 2017). Furthermore, treatment with tandospirone reduced ataxia, pain, insomnia and depressive symptoms in spinocerebellar ataxia (SCA) patients (Takei et al., 2003; Takei et al., 2010; Takei et al., 2005), focusing attention on the 5-HT_{1A} receptor as a promising target for the treatment of SCAs, including MJD.

Befiradol (NLX-112, F-13640) is a selective, full agonist that displays high selectivity and maximum potency at 5-HT_{1A}R (Colpaert et al., 2002; Newman-Tancredi et al., 2017), binding preferentially to subcortical regions of the brain in several species including non-human primates (Vidal et al., 2018). Other animal studies showed therapeutic efficacy in a range of models of movement disorders, including efficacious anti-dystonic activity in rat, namely by eliminating the catalepsy induced by the neuroleptic drug, haloperidol, and the complete reversal of L-DOPA-induced dyskinesia in parkinsonian rats (Iderberg et al., 2015). These effects appear to translate well to higher species, because befiradol also elicits potent and efficacious anti-dyskinetic and anti-parkinsonian-like properties in MPTP-treated marmosets and MPTP-treated macaques (Depoortere et al., 2020; Fisher et al., 2020). Furthermore, previous clinical trials of befiradol indicate that it is well-tolerated and safe (EU_Clinical_Trials, 2009; Paillard et al., 2020), suggesting that it has potential for treating CNS disorders involving serotonergic transmission.

Here, we take advantage of the *C. elegans* model of ATXN3-proteotoxicity (ATXN3 mutant), to test the effect of befiradol in motor dysfunction and aggregation, not only under chronic treatment but also upon acute administration of the drug. In this animal model, a mutant form of human ATXN3 with 130 glutamines, expressed in *C. elegans* neurons, leads to protein aggregation and motor dysfunction phenotypes, which, as in humans, is highly dependent on the size of the polyQ expansion and progresses with aging (Teixeira-Castro et al., 2011a). Despite its simplicity and relatively small number of neurons, the short life cycle, the conservation of basic cellular mechanisms and the phenotypic similarities with human MJD pathogenesis, conjugated with the possibility of genetic manipulation, make *C. elegans* a potent platform for drug testing and target validation *in vivo*. In addition to the therapeutic effect of befiradol treatment, we show high selectivity of this drug for the 5-HT_{1A}R orthologue SER-4 in *C. elegans*, in comparison with tandospirone that shows limited effect under acute treatment and an additional requirement for the presence of the 5-HT_6 and 5-HT_7 (SER-5 and SER-7, respectively) receptors activity at chronic administration. The finding that befiradol is a potent and selective disease-modifying compound for MJD may be relevant for future treatment of this and other disorders of protein conformation.

2. Materials & methods

2.1. Nematode strains and general methods

Strains used in this work and abbreviations are listed in Supplementary Table 1. All the strains were backcrossed to Bristol strain N2 (WT) five to twelve times. Standard methods were used for culturing and observing *C. elegans*, unless otherwise noted (Brenner, 1974). Nematodes were grown on nematode growth medium (NGM) plates seeded with Escherichia coli OP50 strain at 20 °C.

2.2. Drug assay

The drug assay was performed in a 96-well plate format, in liquid culture (Voisine et al., 2007). Each well contained a final volume of 60 µl, comprising 20–25 animals for wild-type (WT, N_2) and wild-type ATXN3 (ATXN3 WT), or 40–45 animals for mutant ATXN3 (ATXN3 mutant or AT3q130) in egg stage in 15 µl, 25 µl of drug at the appropriate concentration and 20 µl of OP50 bacteria to a final optical density at 595 nm (OD_{595}) of 0·9 measured in the microplate reader (Tecan Infinite 200 Microplate Reader).

To obtain an age synchronized population of eggs, four-day-old gravid adults were treated with alkaline hypochlorite solution (0·5 M NaOH, ~2·6% NaClO) for five minutes. The animals were then washed in M9 buffer, resuspended in S-medium (S-Basal, 10 mM potassium citrate pH 6, 10× trace metals solution, 3 mM $CaCl_2$, 3 mM $MgSO_4$) to the appropriate egg number and transferred into the 96-well plate. The OP50 bacteria were grown overnight at 37 °C and 150 rpm in Luria Broth (LB) media, pelleted by centrifugation, inactivated by three cycles of freeze/thawing, frozen at −80 °C and then resuspended in S-medium supplemented with 0·004 mg/ml cholesterol, 0·5× Pen-strep (Sigma) and 0·5× nystatin (Sigma). Worms were grown with continuous shaking at 180 rpm at 20 °C (Shel Lab) for four days.

2.3. Compound preparation

Compounds used in this study were provided by Neurolixis or were obtained from the commercial vendors indicated below and were used without further purification. To define the optimal concentration of the compounds, befiradol (a.k.a. NLX-112 or F13640; Neurolixis, CAS# 208110–64-9) and tandospirone (Aris Pharmaceuticals or Chemvon Industries CAS# 112457–95-1) were serially diluted in a range between 50 mM and 0·00001 mM in 100% dimethyl sulphoxide (DMSO, Sigma). Each concentration was then diluted in MiliQ purified water to obtain, in the well, a final concentration ranged between 500 μM and 0·01 nM in 1% DMSO. Further assays, with chronic or acute treatment protocols, were performed using 10 μM concentration of befiradol or tandospirone. Estrone (Sigma, CAS# 53-16-7) was diluted to a 25 μM concentration, WAY-100635 maleate (Tocris Bioscience, CAS# 1092679-51-0) was diluted to a 0·1 μM, 1 μM and 10 μM concentrations. 17-DMAG (Tocris Bioscience, CAS# 467214-21-7) was diluted to 1 μM concentration in water and CCI779 (LC Laboratories, CAS# 162635-04-3) was diluted to 1 μM concentration in 0·02% ethanol.

2.4. Food clearance assay

WT worms were subjected to a drug assay as described above, except for the OP50 bacteria OD_{595} adjusted to 0·7 (Voisine et al., 2007). Worms were grown with continuous shaking at 180 rpm at 20 °C (Shel Lab) for seven days. Befiradol and tandospirone stock concentrations were prepared in 100% DMSO (Sigma) and tested at dilutions corresponding to a maximum concentration of 1% DMSO to avoid solvent-specific developmental defects and toxicity. Tested concentrations ranged between 500 μM and 0·01 nM. The effect of compounds on *C. elegans* physiology was monitored by the rate at which the OP50 suspension was consumed, as a read out for *C. elegans* growth, survival, or fecundity. The OD_{595} was measured daily. OP50-only (S-medium, no vehicle), DMSO 1% (vehicle) and DMSO 5% (toxic condition) controls were used.

2.5. C. elegans assays

2.5.1. Motility assay and motor index determination

Four-day-old animals were transferred from the 96-well plates onto an unseeded NGM plate (equilibrated at 20 °C). Plates were allowed to dry for 45 min before starting the motility assays. Motility assays were performed at 20 °C as previously described (Teixeira-Castro et al., 2011a). Five animals were placed simultaneously in the center of a freshly seeded 30 mm plate, equilibrated at 20 °C. Animals remaining inside the 1 cm circle after one minute were scored as locomotion-defective. Motor behavior assays were run in triplicates or quadruplicates (n = 3 or 4), with a total of at least 150 animals tested per compound concentration.

Motor index establishes a score, in which treated animals that display the same motor behavior as mutant ATXN3 had a 0% index and when animals improve motor coordination comparable with ATXN3 WT expressing animals obtain an index of 100%. All results shown in the figures are calculated using the following formula

$$\text{Motor index } (\%) = \frac{\text{LD mutant ATXN3}_{\text{vehicle}} - \text{LD mutant ATXN3}_{\text{drug}}}{\text{LD mutant ATXN3}_{\text{vehicle}} - \text{LD ATXN3 WT}_{\text{vehicle}}}$$

LD- locomotion-defective.

2.5.2. Velocity assay

Wild-type (WT), wild-type ATXN3 (ATXN3 WT) and mutant ATXN3 (ATXN3 mutant or AT3q130) animals were grown in liquid culture in a 96-well plate format as described above. Four-day-old animals grown in vehicle (1% DMSO) or treated chronically with 10 μM befiradol or 10 μM tandospirone were transferred to climatized NGM plates without OP50 and after 45 min velocity assays were performed. For the velocity assay set up, the recording system comprised a stereo microscope (SZX7, Olympus), a digital camera (SC30, Olympus) and an imaging software (Olympus cellSens Software, RRID:SCR_016238) and 30 mm seeded NGM plates with a cooper ring in the center (assay plate) were used to avoid the escape of worms from the camera field. The assay was performed at 20 °C. Ten to 15 animals were transferred to the middle of the assay plate and movements were recorded immediately. A 0·8 X zoom lens was used to maximize the recorded field. Animals were recorded during 1 min at a rate of 15 frames per second. Recorded images were analysed by ImageJ (ImageJ, RRID:SCR_003070) and wrMTrck (plugin for ImageJ: www.phage.dk/plugins). The locomotion velocity was obtained in μm per second and corrected for the size of the animal (Body Length per second (BLPS) data in wrMTrck) (Nussbaum-Krammer et al., 2015). Animals that were recorded for less than 25 s were discarded.

2.5.3. C. elegans assays for aggregation

For confocal dynamic imaging and quantification of ATXN3 aggregation, mutant ATXN3 animals were grown in liquid culture in a 96-well plate format, with 10 μM befiradol or 10 μM tandospirone, as described above. For this assay, drugs were added at egg stage (chronic treatment) or 2 h before the acquisition (acute treatment). Four-day-old animals were transferred from the 96-well plates onto unseeded NGM plates (equilibrated at 20 °C). After 45 min, live animals were immobilized with 3 mM levamisole (Sigma) and mounted on a 3% agarose pad. All images were captured using an Olympus LPS Confocal FV1000 microscope (Confocal microscope, Olympus, FV1000, RRID:SCR_016840) under a 60× oil (NA = 1·35) objective. *Z*-series imaging was acquired for all vehicle- and befiradol-treated and tandospirone-treated animals, using a 515 nm laser excitation line for yellow fluorescent protein fusion proteins. The pinhole was adjusted to 1·0 Airy unit of optical slice, and a scan was acquired every ~0·5 μm along the z-axis. The quantification of the aggregates was performed as previously described (Teixeira-Castro et al., 2011a; Teixeira-Castro et al., 2011b). Three parameters were extracted from analysis: area of aggregates/total area; number of aggregates/total area and total area. Values shown are the mean (normalized to vehicle treated control) of nine or more animals per group, unless otherwise noted.

For filter trap assay and biochemical fractionation, worms were grown in liquid culture in a 96-well plate format, treated chronically or acutely with 10 μM befiradol, as described before. A total of 1500 eggs were plated for WT, ATXN3 WT and *mod-5*Δ; AT3q130 strains and 2500 eggs were plated for mutant ATXN3 vehicle-treated and befiradol-treated conditions. Four-day-old animals were collected and washed three times with M9, to eliminate OP50 bacteria and progeny, and flash-frozen in liquid nitrogen. For protein/aggregates extraction, a 50 μl of non-denaturating protein buffer (50 mM HEPES, pH 7·4, 150 mM NaCl, 1 mM EDTA, 0·5% Triton X-100) or 150 μl of RIPA buffer (50 mM Tris, pH 7·5, 150 mM NaCl, 25 mM EDTA, 0·2% Triton X-100), for filter trap or biochemical fractionation respectively, freshly supplemented with EDTA-free protease inhibitor cocktail (Roche) was added and worms were disrupted by mechanic force using glass beads (Sigma) in a FastPrep®-24 (MP Biomedicals) (six cycles of 6·5 ms for 45 s followed by 1 min on ice). After a centrifugation of 500 *g* during 1 min, the supernatant was collected, and the total protein quantified by the Bradford assay (Bio-Rad). For filter trap, a total of 100 μg of protein was treated with SDS at a final concentration of 1% and loaded onto a cellulose acetate membrane assembled in a slot blot apparatus (Bio-Rad). The membrane was washed with 0·1% SDS and retained ATXN3 protein detected with anti-ATXN3 mouse (1:1000) (Millipore Cat# MAB5360, RRID: AB_2129339) and with horseradish peroxidase-coupled secondary antibodies (Bio-Rad) and chemiluminescence (ECL Radiance, Azure Biosystems). For biochemical fractionation, protein concentration was adjusted to 4 μg/μl and followed by a 22,000 *g* centrifugation for 30 min at 4 °C. The pellet fractions were separated from supernatants (Triton X-100-soluble fraction) and homogenized in 150 μl RIPA buffer

supplemented with 2% SDS, followed by a second centrifugation step at room temperature. The supernatants (SDS-soluble fraction) were removed, and the remaining pellets were incubated for 16 h in 100% formic acid at 37 °C allowing formic acid evaporation. Pellet was dissolved in 50 µl of Laemmli buffer (0·1 M Tris (pH = 6·8), 16% glycerol, 2% SDS, β-mercaptoethanol and bromophenol blue powder) (SDS-insoluble fraction). For SDS–polyacrylamide gel electrophoresis 50 µg of the Triton X-100 fraction, 40 µl of the SDS-soluble fraction and the complete SDS-insoluble fraction were loaded in a 10% SDS gel. ATXN3 protein was detected with anti-ATXN3 mouse (1:1000) (Millipore Cat# MAB5360, RRID: AB_2129339) and with horseradish peroxidase-coupled secondary antibodies (Bio-Rad) and chemiluminescence (ECL western-blotting detecting reagents, Bio-Rad or ECL Radiance, Azure Biosystems). The capture of chemiluminescence signals was performed in the Sapphire Biomolecular Imager (Azure Biosystems), and Western blot quantifications were performed using AzureSpot Analysis Software (Azure Biosystems), according to the manufacturer's instructions.

2.5.4. *C. elegans* ratiometric calcium dynamic imaging

Ratiometric calcium imaging was performed as previously described (Collins et al., 2016; Ravi et al., 2018b). Briefly, for ratiometric Ca^{2+} dynamic imaging and quantification in the HSN neuron, *nlp-3*::GcAMP5 animals were grown in liquid culture in a 96-well plate format, with 10 µM befiradol as described above. Drugs were added at the egg stage (chronic treatment) or 2 h before image acquisition (acute treatment). Four-day-old animals were immobilized with 5 mM levamisole (Sigma) and mounted on a 3% agarose pad. After 30 min, images were captured using a Confocal Laser Scanning Microscope FV3000 (Olympus Confocal Laser Scanning Microscope Fluoview FV3000, RRID:SCR_017015) with the resonant scanner running at 8000 Hz and collected at 30 fps at 512 × 512 pixel resolution, 16-bit depth after 2× digital zoom, under a 60× oil (NA = 1·35) objective. Time-series images were acquired for all vehicle- and befiradol-treated animals at each 30 ms during 15 min, using a 488 nm laser excitation line for GcAMP5, and 651 nm laser excitation line for mCherry. Both proteins expressed, under the same promoter (*nlp-3*), in the HSN neuron. Acquisition of each channel was done simultaneously. The pinhole was adjusted to 1·15 Airy unit of optical slice. The quantification of fluorescence intensity for both channels was performed using Fiji ImageJ software (Fiji, RRID: SCR_002285). After subtraction of background intensity, R and ΔR/R values were calculated using the following formulas:

$$R = \frac{F_{GcAMP5}}{F_{mCherry}} \quad \Delta R/R = \frac{R_{t(x)} - R_{t(lowestR)}}{R_{t(lowestR)}}$$

2.6. SDS-PAGE and Western blot

For determination of the steady-state protein levels of ATXN3, mutant ATXN3 animals were incubated in liquid culture with vehicle (1% DMSO), 10 µM befiradol or 10 µM tandospirone in a 96-well plate format as already mentioned. For chronic treatment, four-day-old animals were transferred from the liquid culture onto an unseeded NGM plate (equilibrated at 20 °C). After 45 min, 25 individual young adult animals were picked into a screwed Eppendorf tube, boiled for 15 min in sodium dodecyl sulphate (SDS) sample buffer (to destroy all the aggregates) and the resulting extracts resolved on a 10% SDS gel, as previously described (Gidalevitz et al., 2009; Teixeira-Castro et al., 2011a). Immunoblots were probed with anti-ATXN3 mouse (1:1000) (Millipore Cat# MAB5360, RRID: AB_2129339) and anti-tubulin mouse antibodies (1:3000) (Sigma-Aldrich Cat# T5168, RRID: AB_477579); and detected with horseradish peroxidase-coupled secondary antibodies (Bio-Rad) and chemiluminescence (ECL Western-blotting detecting reagents, Bio-Rad). To capture chemiluminescence signal were used Chemidoc XRS Software (Bio-Rad) and Western blot quantifications were performed using ImageLab Software (Bio-Rad, RRID: SCR_014210), according to the manufacturer's instructions. For acute treatment, four-day-old animals treated with befiradol or tandospirone during 2 h in adulthood, were collected and washed three times with M9, and flash-frozen in Liquid Nitrogen. After extraction with 50 µl of non-denaturating protein buffer (50 mM HEPES, pH 7·4, 150 mM NaCl, 1 mM EDTA, 0·5% Triton X-100) freshly supplemented with EDTA-free protease inhibitor cocktail (Roche), worms were disrupted by mechanic force using glass beads (Sigma) in a FastPrep®-24 (MP Biomedicals) (six cycles of 6·5 ms for 45 s followed by 1 min on ice). After a centrifugation of 500 *g* during 1 min, the supernatant was collected, and the total protein quantified by the Bradford assay (Bio-Rad). 5 µg of total protein were transferred to an Eppendorf screw tube, supplemented with Laemmli Buffer to final 1× concentration and boiled for 15 min. The samples were resolved in a 10% SDS-gel, as previously described (Gidalevitz et al., 2009; Teixeira-Castro et al., 2011a). After transfer, membrane was incubated with AzureRed Fluorescent Total Protein Stain (Azure Biosystems) as manufacturer instructions. Immunoblots were probed with anti-ATXN3 mouse (1:1000) (Millipore Cat# MAB5360, RRID: AB_2129339) and detected with horseradish peroxidase-coupled secondary antibodies (Bio-Rad) and chemiluminescence (Radiance ECL, Azure Biosystems). To capture chemiluminescence signal were used Sapphire Biomolecular Imager (Azure Biosystems) and Western blot quantifications were performed using AzureSpot Analysis Software (Azure Biosystems), according to the manufacturer's instructions.

2.7. Generation of *C. elegans* double mutant strains

Males of *ser-5*Δ (tm2654), *ser-7*Δ (DA2100), mod-*1*Δ (MT9668), *dop-1*Δ (LX636) and *dop-2*Δ (LX702) were generated by mating with N2 (WT) males. To generate double mutant strains, thirteen males and three hermaphrodites L4 stage of ATXN3 mutant (AT3q130) (MAC001/AM685) animals were placed in NGM 30 mm seeded plate at 16 °C for 24 h. Hermaphrodites were singled out and male progeny were evaluated three days later. 24 to 32 L4 stage animals, from plates with 50% male progeny, were singled out and after 24 h worm lysis and single-worm PCR was performed to evaluate animals' genotype.

To generate double mutant strain lacking *tph-1* gene into ATXN3 mutant background, CRISPR/Cas9 technology was used as previously described (Paix et al., 2015). To generate *tph-1*Δ(mnh5) CRISPR RNAs (crRNAs) were designed using the Custom Alt-R® CRISPR-Cas9 guide RNA tool (Integrated DNA Technologies, Coralville, IA) and crRNAs with high on-target efficiency and low off-target prediction scores were chosen. To delete the complete gene sequence without altering regulatory regions, two crRNAs were designed, one to cut the 5′ region close to ATG start codon (cattgctctcttcaatcata) and another for the 3′ region near the stop codon triplet (ctacatcctgtagtttgagt). A single-stranded oligodeoxynucleotide (ssODN) comprising a fusion of the 5′ and 3′ regions flanking ATG and STOP codon triplet, respectively, (ctttggtttttaggtag-cattgctctcttcaatcattttgagtttccgtgtttttttatttttttttatttgg) was used as a repair template. crRNA and ssODN repair template for *dpy-10* was co-injected with *tph-1* specific oligos and was used as a marker for efficiency of Cas9 activity. The injection mix, constituted by crRNAs, ssODNs and EnGen® Cas9 NLS, S. pyogenes enzyme (New England BioLabs, Ipswich, MA), was placed at 37 °C for 15 min, and young adult ATXN3 mutant (AT3q130) animals were injected, as previously described (Mello et al., 1991). Injected animals were placed at 25 °C and their progeny was screened for the roller phenotype 72 h later. Non-roller animals were singled out to avoid *dpy-10* mutation and screened by PCR for the *tph-1* deletion.

To lysate, each animal was placed in 10 µl of worm lysis buffer (50 mM KCl, 10 mM Tris-HCl (pH 8·3), 2·5 mM $MgCl_2$, 0·45% Nonidet P-40, 0·45% Tween 20, 0·01% (*w/v*) gelatin) supplemented with 0·01 µl of 20 mg/ml Proteinase-K and heated at 65 °C during 1 h. After Proteinase-k inactivation (95 °C, 15 min), 2 µl of worm lysate were used as template for Polymerase Chain Reaction (PCR) [1× Supreme NZYTaq II Green Master Mix, 200 nM primers (Supplementary table 2)]. PCR products were analysed in 1·5% agarose gel. 24 to 32 adult worms from

heterozygous plates were singled out and after genotype confirmation, by single worm PCR, and YFP fluorescence screening to confirm ATXN3 mutant (AT3q130) homozygosity in progeny, the double mutant strains and the ATXN3 mutant (AT3q130) post-crossing control were isolated.

For CRISPR/Cas9 *tph-1*Δ double mutant deletion was confirmed by Sanger sequencing.

2.8. Reverse-transcriptase quantitative PCR

Worm pellets from four-day-old animals were obtained by bleaching synchronization and washed four times with M9, resuspended in TRIzol™ (Invitrogen) and stored after flash freezing in liquid nitrogen. After thawing, worms were disrupted by mechanic force using glass beads (Sigma) in a FastPrep®-24 (MP Biomedicals) (six cycles of 4 ms for 30 s followed by one minute on ice). Beads were removed from the homogenate and a phase separation was conducted using chloroform retrieving the aqueous phase. RNA was extracted using RNeasy plus mini kit (Qiagen) according to the manufacturer's instructions. Samples were treated with DNase I (Thermo Scientific), RNA concentration was quantified by spectrophotometry, and RNA quality was tested through electrophoresis. cDNA was synthesized from 1 μg purified RNA using the iScript™ cDNA synthesis kit (Bio-Rad). The quantitative PCR was then carried out using the 5× HOT FIREPol® EvaGreen® qPCR Mix Plus (ROX) (Solis BioDyne) with 1 μl of cDNA. The used primers are listed in supplementary table 3. PCR reaction was run in Applied Biosystems™ 7500 Real-Time PCR System (Applied Biosystems) and raw data was extracted using 7500 software v2·3 (7500 Real-Time PCR Software, RRID:SCR_014596). Statistical analysis was conducted using $2^{-\Delta CT}$ values and plots was reported in Fold Change ($2^{-\Delta\Delta CT}$) (Livak and Schmittgen, 2001).

2.12. Statistical analysis

All statistical analysis was performed using the IBM SPSS statistics 23 software (SPSS, RRID:SCR_002865) and GraphPad Prism 8·0·1 software. Normal distribution of continuous variables was analysed according with Shapiro-Wilk or Kolmogorov-Smirnov normality test, depending on sample size, and histogram plot distribution. Levene's test assessment was performed to confirm homogeneity of variances between groups. When both assumptions were verified, groups were compared using independent sample *t*-test (Fig. 2b, c and d – befiradol chronic), one-way or two-way ANOVA followed by Dunnett (Fig. 1a – befiradol; Fig. 1b; Fig. 1d; Fig. 2d – acute and tandospirone chronic; Fig. 2g; Fig. 2h; Supplementary Fig. 2d), Tukey (Fig. 1b; Fig. 3; Supplementary Fig. 2a and b; Supplementary Fig. 4c and 2e) or Sidak post-hoc tests (Fig. 1c; Fig. 1d; Fig. 5b; Supplementary Fig. 4d; Supplementary Fig. 5). For Biochemical fractionation one-sample t-test with Bonferroni correction *versus* the value of 1 was applied (Fig. 2e and f).

When previous assumptions were not verified, a robust ANOVA (using R batch for SPSS) with Brown-Forsythe (if sample size less than 6) or Welch correction was reported and bootstrap with BCA were performed. Bootstrap sampling was followed by one-way ANOVA with

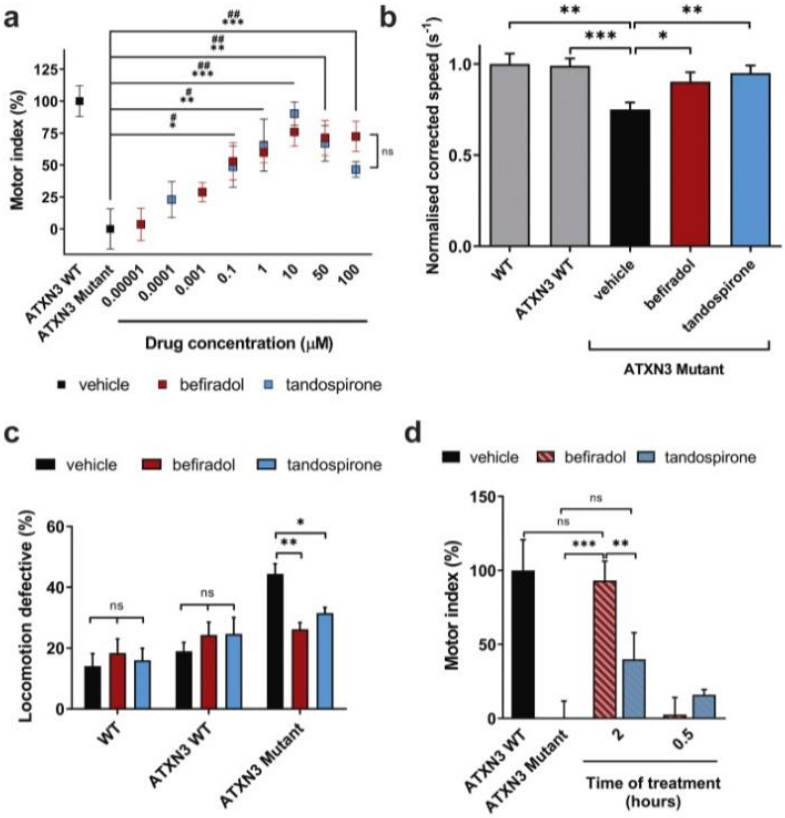

Fig. 1. Treatment with befiradol ameliorates motor dysfunction of ATXN3 mutant (AT3q130) animals. (a) befiradol (red) and tandospirone (blue) showed a positive impact on animals' motor dysfunction in the range of concentrations from 100 nM to 100 μM, the maximum effect being obtained at a 10 μM concentration for both drugs. (b) AT3q130 (ATXN3 mutant) animals presented a decreased corrected speed when compared to WT and ATXN3 WT animals. After chronic treatment with befiradol or tandospirone there was an increase in animals' velocity. (c) Chronic treatment with befiradol or with tandospirone did not change motor behavior of WT and ATNX3 WT animals. (d) Treatment of AT3q130 (ATXN3 mutant) animals during 2 h with befiradol ameliorates motor dysfunction. For dose-response (a): befiradol - (n = 7, ± SEM) $^{*}P < 0{\cdot}05$, $^{**}P < 0{\cdot}01$, $^{***}P < 0{\cdot}001$ (ANOVA, Dunnett test); tandospirone – (n = 6, ± SEM) $^{\#}P < 0{\cdot}05$, $^{\#\#}P < 0{\cdot}01$ (ANOVA, SIDAK test corrected for BCA). Velocity assay (b): (n = 18–43, ± SEM), $^{*}P < 0{\cdot}05$, $^{**}P < 0{\cdot}01$, $^{***}P < 0{\cdot}001$ (ANOVA, Dunnett test). Drug effects on wild-type animals (c): (n = 4, ± SEM) $^{*}P < 0{\cdot}05$, $^{**}P < 0{\cdot}01$, ns – non-significant (ANOVA, SIDAK test). Acute treatment assay (d): (n = 3, ± SEM) $^{**}P < 0{\cdot}01$, $^{***}P < 0{\cdot}001$, ns – non-significant (Factorial ANOVA, SIDAK test and Dunnett test).

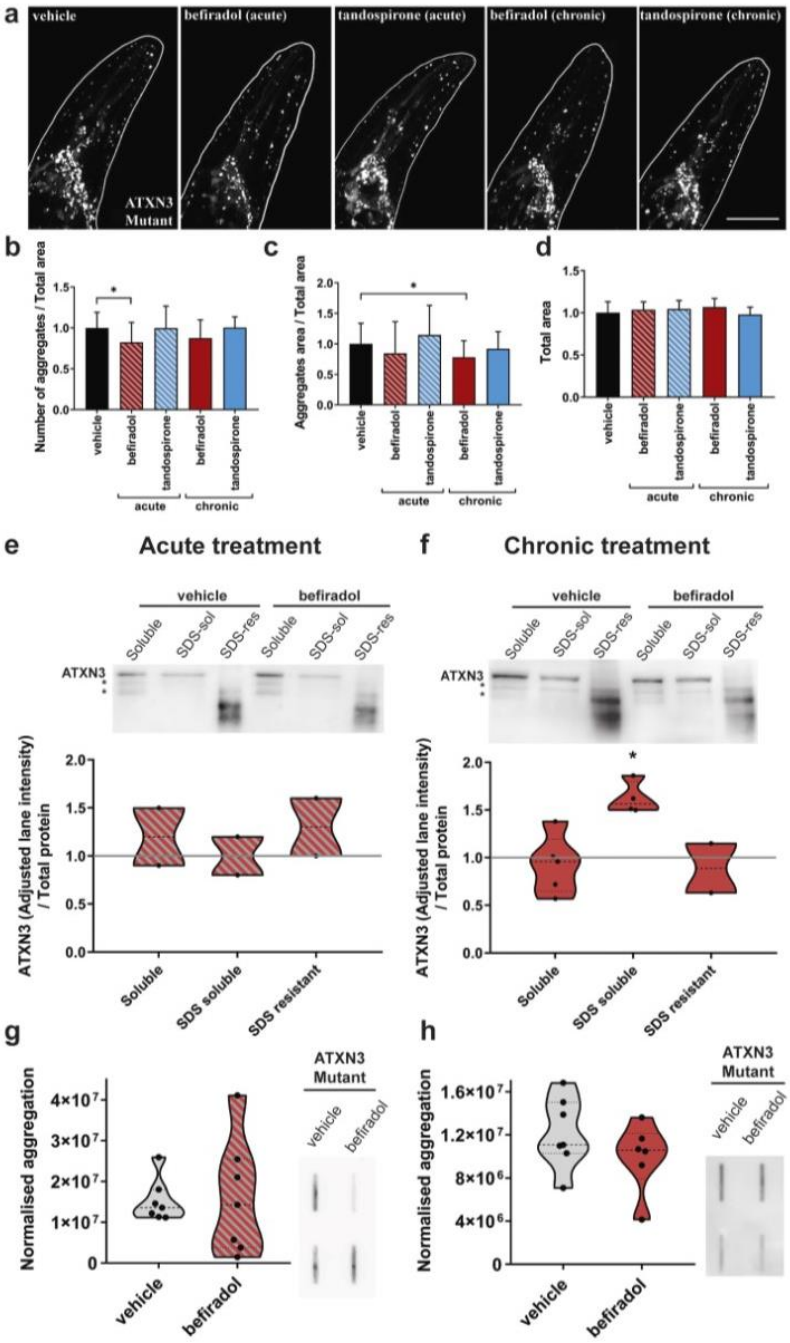

Fig. 2. Befiradol treatment decreases mutant ATXN3 aggregation. (a) Mutant ATXN3 expression pattern in the animals' head upon treatment, obtained by confocal live imaging. Scale bar: 100 μm. (b) Number of aggregates and (c) area of aggregates was decreased upon acute and chronic treatments with befiradol, respectively, with no changes in (d) total area of the animal's heads. Biochemical fractionation assay of AT3q130 (ATXN3 mutant) animals upon (f) chronic administration of the drug increases the ATXN3 species soluble in SDS. (e) Upon acute administration of befiradol no differences were found in solubility of mutant ATXN3. Filter trap retardation assay of AT3q130 (ATXN3 mutant) upon (g) acute or (h) chronic administration of befiradol. For confocal microscopy live imaging: (n = 11–37, ± SD – pool of 3 individual experiments), *P < 0·05 (Kruskal-Wallis with Dunn post-hoc test or One-Way ANOVA with Dunnett post-hoc test or t-test). For filter trap: ATXN3 densitometry values were divided by the total amount of protein measures by AzureRed®, Azure Biosystems. (n = 6–8, Q1 – Q2 – Q3). For biochemical fractionation: (n = 2–5, Q1 – Q2 – Q3), *P < 0·05 (one sample t-test, with Bonferroni correction *vs* value 1).

Sidak post-hoc test with bias correction (Fig. 1a – tandospirone; Fig. 4; Fig. 5a and c; Supplementary Fig. 6). When normal distribution and homogeneity of variances failed to be verified, Kruskal-Wallis with Dunn post-hoc test was applied (Fig. 2b and c – acute and tandospirone chronic treatments; Supplementary Fig. 4a and b).

For samples with normal distribution but not displaying homogeneity of variances, Brown-Forsythe were reported and Dunnett3 post-hoc test was applied (Supplementary Fig. 2c).

Toxicity assay results were compared using a non-linear regression approach (Supplementary Fig. 1) tacking in account IC50, HillSlope and Top and Bottom values.

Detailed statistics for all experiments can be consulted at supplementary table 4.

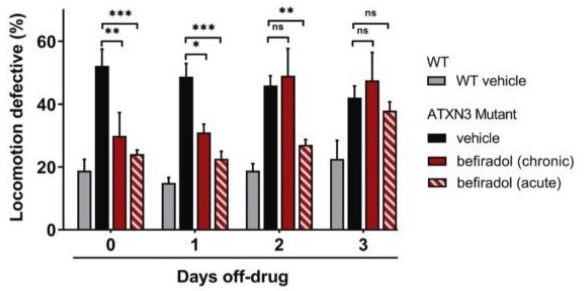

Fig. 3. Persistence of effect of befiradol treatment of ATXN3 mutant animals upon drug removal. OFF-drug effect on motor behavior of AT3q130 (ATXN3 mutant) animals treated with befiradol for either 4 days or 2 h, showing that improvements in motor performance persist at least at day 1 and day 2 post drug treatment discontinuation. After 2 days (for chronic treatment protocol) or 3 days (for acute treatment protocol) of drug withdrawal, the beneficial effect of befiradol on motor behavior declined and neurotoxicity returned. (n = 3, ± SD), *P < 0·05, **P < 0·01, ns – non-significant (Two-Way ANOVA, Tukey post-hoc test).

3. Results

3.1. Chronic and acute treatment with befiradol ameliorates mutant ATXN3-mediated neuronal dysfunction

To evaluate the impact of the activation of the 5-HT_{1A} receptor on mutant ATXN3-mediated pathogenesis, we used a *C. elegans* model of MJD proteotoxicity (ATXN3 mutant) in which the expanded form of ATXN3 (AT3q130) is expressed in neuronal cells causing progressive motor dysfunction and mutant ATXN3 aggregation (Teixeira-Castro et al., 2011a). Safe concentrations of befiradol and tandospirone to be used in subsequent assays were defined using wild-type *C. elegans* (WT, N_2) in a toxicity assay (Voisine et al., 2007). In this assay, consumption of food, assessed by the variation in the optical density of bacteria throughout time, was used as a measure of normal development and well-being of the animals. The majority of the befiradol and tandospirone concentrations tested were safe to the animals, with the exception of treatment with 500 μM of befiradol that caused a deficit in body fitness and a slight decrease in the food consumption rate (Supplementary Fig. 1). To assess motor function in *C. elegans*, we performed a motility assay where animals were placed in the centre of a plate, in the presence of food, and allowed to explore freely the environment for 1 min. After this time, the animals that did not cross 1 cm circumference were scored as motor defective. The motor index for each condition was calculated using the motor performance of wild-type ataxin-3 (ATXN3 WT, 100%) and mutant ataxin-3 (ATXN3 mutant, 0%) animals as reference. Chronic treatment of ATXN3 mutant (AT3q130) animals with befiradol or tandospirone improved motor behavior of the animals with a dose response profile and a large effect size of 0·616 and 0·605, respectively (Supplementary table 4, ω^2p). Both drugs showed a positive impact on animals' motor dysfunction in the range of concentrations of 100 nM to 100 μM, the maximum effect being obtained at 10 μM treatment (Fig. 1a). No significant differences were found in treatment efficacy between drugs. The concentration of 10 μM was used in subsequent experiments for both compounds. To further assess the impact of drug treatment on motor behavior of ATXN3 mutant animals, we evaluated an intrinsic characteristic of movement, the velocity of the animals. To do this, we filmed WT, ATXN3 WT and mutant ATXN3 animals in the presence of food, after chronic drug administration (four days). Indeed, ATXN3 mutant animals presented a decreased size-corrected speed when compared with WT animals. After chronic treatment with befiradol or tandospirone, we observed a restoration of animals' velocity (Fig. 1b). Furthermore, motility of WT or ATXN3 WT animals was not changed by any of the drug treatments, suggesting that their action specifically targets mutant ATXN3-mediated pathogenesis (Fig. 1c). To test the potential of befiradol and tandospirone treatments to revert motor impairment of adult ATXN3 mutant animals, we conducted a time course assay in which adult worms already showing core motor deficits were treated with each drug during the indicated time periods. Interestingly, acute treatment with befiradol for 2 h was sufficient to restore motor function of the animals to WT levels. In contrast, acute treatment with tandospirone did not show a statistically significant effect on motor behavior (Fig. 1d), suggesting a higher potency of befiradol for 5-HT_{1A}Rs and/or a different mode-of-action of the two drugs.

3.2. Treatment with befiradol decreases aggregation of mutant ATXN3 protein

The impact of 5-HT_{1A}R activation on mutant ATXN3 aggregation was assessed using three different techniques: *in vivo* confocal imaging, which allowed the quantification of the number and size of mutant ATXN3 *foci* (Teixeira-Castro et al., 2011a; Teixeira-Castro et al., 2011b); a biochemical fractionation assay, which discriminated ATXN3 species with distinct detergent solubilities (Koch et al., 2011); and a filter trap assay, whereby aggregates were immobilized in a cellulose acetate 0·2 μm membrane, allowing the separation of the large SDS-resistant aggregates from the soluble smaller species (Vilchez et al., 2012). Our results showed a decrease in the number or area of ATXN3 aggregates upon befiradol acute (Fig. 2a, b) and chronic (Fig. 2a, c) treatments, respectively. These changes in aggregation occurred without alteration in the ATXN3 protein steady-state levels (Supplementary Fig. 2a, b) neither in animal size, upon drug treatments (Fig. 2d). Tandospirone, however, showed limited impact on aggregation (Fig. 2a-c) in both treatment modalities. Unlike acute treatment (Fig. 2e, g), there was an increase in SDS-soluble ATXN3 species upon chronic treatment with befiradol, as assessed by biochemical fractionation (Fig. 2f). No changes were found in ATXN3 aggregation measured by filter trap (Fig. 2g, h and Supplementary Fig. 3) upon befiradol supplementation; however, blocking 5-HT re-uptake genetically (by SERT/MOD-5 ablation) significantly suppressed the levels of SDS-resistant mutant ATXN3 species, being this a positive control of the technique (Supplementary Fig. 2c). Drug efficacy was monitored in all aggregation assays by evaluating motor performance of the same animals upon treatment (Supplementary Fig. 2d). To evaluate the sustainability of drug effect after treatment withdrawal, we treated animals chronically for four days or acutely for 2 h and maintained the animals off-drug during the indicated days. Both treatment protocols maintained efficacy for at least 1 to 3 days post interruption of the treatment, further supporting a disease-modifying effect of befiradol (Fig. 3).

3.3. Befiradol acts via 5-HT_{1A}R orthologue SER-4 to mitigate motor dysfunction in C. elegans

Although with different potencies, befiradol and tandospirone are described in mammals to act as agonists of the 5-HT_{1A}R (Bollinger et al., 2010; Hamik et al., 1990; Llado-Pelfort et al., 2012). In *C. elegans*, SER-4 has been described as a putative orthologue of human 5-HT_{1A} receptors (Olde and McCombie, 1997). To verify the conservation of specific protein domains between species, we aligned human 5-HT_{1A}R (Uniprot #P08908) with SER-4 (Uniprot #G5EGH0) proteins using T-COFFEE Multiple Sequence Alignment Server (Notredame et al., 2000). Indeed, SER-4 presented a high degree of conservation of ligand binding sites and a fully conserved G-coupled protein receptor (GPCR) binding motif (DRY motif) and activation site (NPxxY motif) (Fig. 4a). The overall percentage of aminoacid similarity (Stothard, 2000) between the *C. elegans* receptor and the human 5-HTR_{1A}R is of 47·5%. The *C. elegans* serotonergic system includes at least three other GPCR: SER-1, SER-5 and SER-7, presenting high homology to human 5-HT_2R, 5-HT_6R and 5-HT_7R (Hamdan et al., 1999; Harris et al., 2009; Hobson et al., 2003),

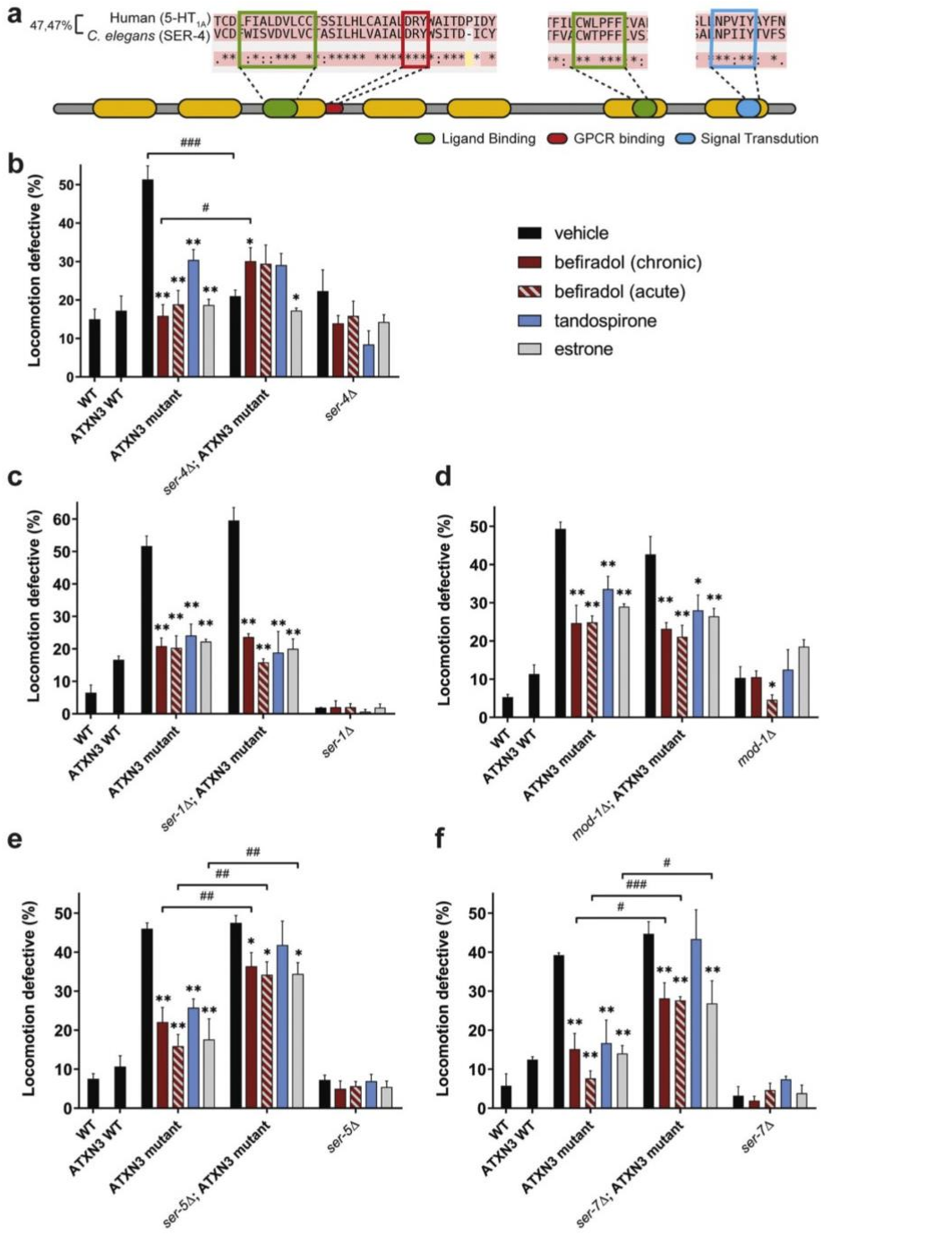

Fig. 4. *C. elegans* SER-4 receptors are molecular targets of befiradol. (a) Alignment of *Homo sapiens* (human) 5-HT$_{1A}$R protein with the *C. elegans* orthologue SER-4 showing conserved regions of the receptor like ligand binding motif (green), GPCR binding DRY motif (red) and signal transduction NPXXY motif (blue). Pharmacological treatment of *C. elegans* strains lacking (b) *ser-4*, (c) *ser-1*, (d) *mod-1*, (e) *ser-5* or (f) *ser-7* receptors showed that SER-4 is likely to be the molecular target of befiradol, tandospirone's effect being dependent on SER-4, SER-5 and SER-7 activity. Both drugs' action was independent of *ser-1* and *mod-1* receptors. For alignment: t-coffee multiple sequence alignment server was used (http://tcoffee.crg.cat). For pharmacogenetics: (n = 3–4, ± SD), *P < 0·05, **P < 0·01, ***P < 0·001 comparing drug treatment with vehicle, $^{\#}$P < 0·05, $^{\#\#}$P < 0·01, $^{\#\#\#}$P < 0·001 comparing strain effect within the same drug treatment (Factorial ANOVA, Sidak test corrected for BCA).

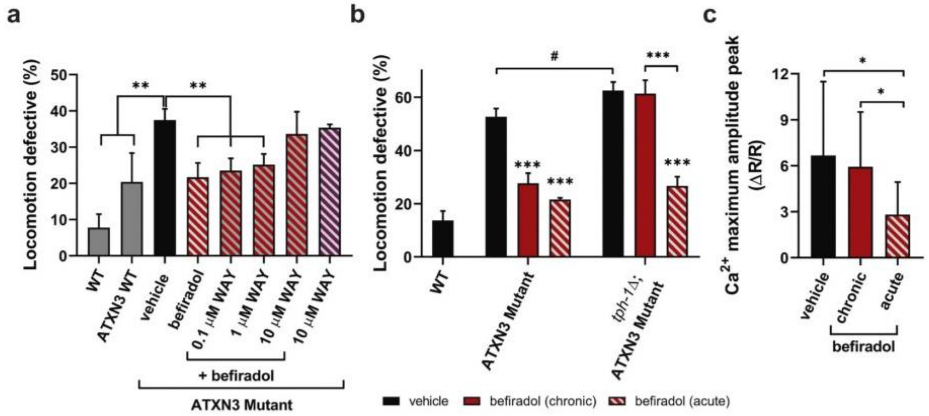

Fig. 5. 5-HT_{1A} auto- and heteroreceptors' function contribute to befiradol treatment efficacy of ATXN3 mutant animals. (a) The effect of befiradol on motor dysfunction showed to be dependent on the activation of the 5-HT_{1A} receptor. The occupation of the binding site of the receptor 5-HT_{1A} by its specific antagonist WAY 100635 precluded the effect of befiradol on mutant ATXN3-expressing animals upon acute treatment. (b) Acute befiradol treatment ameliorated motor dysfunction of mutant ATXN3 animals, even in the absence of serotonin synthesis and release, highlighting the contribution of 5-HT_{1A} heteroreceptors activation. (c) Chronic and acute administration of befiradol differently impacted HSN Ca^{2+} dynamics. Acute treatment with the drug decreased the Ca^{2+} maximum peak amplitude, which was not observed upon chronic treatment, supporting a differential response of the receptor dependent on drug treatment duration. For co-treatment (a): (n = 2–3, ± SD) **P < 0·01 (ANOVA, SIDAK test corrected for BCA). For *tph-1* pharmacogenetics (b): (n = 3, ± SD) ***P < 0·001 comparing drug treatment with vehicle, #P < 0·05 comparing strain effect within the same drug treatment (ANOVA, SIDAK test). For HSN calcium dynamics (c): (n = 11–12, ± SD) *P < 0·05 (ANOVA, SIDAK test corrected for BCA).

respectively; and one chloride channel gate receptor, MOD-1, exclusive of the *C. elegans* genome (Ranganathan et al., 2000).

To investigate the molecular targets of befiradol and of tandospirone in *C. elegans* and their role in the suppression of mutant ATXN3-mediated toxicity, we generated double mutant strains with ablation of the individual 5-HT receptors in the ATXN3 mutant background. The ablation of *ser-4* receptor reduced locomotion impairments of transgenic ATXN3 mutant animals (Fig. 4b), as previously described (Teixeira-Castro et al., 2015). This is consistent with its role as autoreceptor, loss and/or desensitization of which would lead to a disinhibition of serotonin production and release (Teixeira-Castro et al., 2015). No compensatory effects in mRNA expression level of the other serotonergic receptors were observed in *ser-4* mutant strains (Supplementary Fig. 4). By combining compound treatment with genetic tools, we found that befiradol and tandospirone treatments did not further improve motor performance of the animals, compatible with SER-4 receptors being cellular targets of both drugs. In contrast, treatment of *ser-4Δ*; ATXN3 mutant animals with estrone (a steroid hormone) was able to cause a further reduction in their motility impairment, consistent with an independent mechanism-of-action for this compound (Fig. 4b). Ablation of *ser-1* and of *mod-1* genes, however, did not have an impact on drug action for any of the compounds and treatment modalities (Fig. 4c and d). The role of SER-5/5-HT_6 and SER-7/5-HT_7 receptors in mutant ATXN3-mediated proteotoxicity discriminated the mode-of-action of the two compounds (Fig. 4e and f). Ablation of SER-5 and SER-7 precluded tandospirone-mediated amelioration of motor performance of ATXN3 mutant animals, in contrast with befiradol that still maintained its therapeutic action. The partial loss of efficacy of befiradol in the absence of SER-5 and SER-7 is mirrored upon estrone treatment, as well as with 17-DMAG and CCI779 treatments, two drugs with well-defined molecular targets (HSP90 and mTORC1 complex, respectively (Mellatyar et al., 2018; Peralba et al., 2003)) (Supplementary Fig. 5), possibly suggesting an intrinsic effect in the double mutants independent of drug action. Despite of these observations, a partial contribution of SER-5 and SER-7 receptors in befiradol action cannot be excluded. The potential drug interaction with dopaminergic signaling pathways, mostly proposed for tandospirone (Hamik et al., 1990), fails to impact on mutant ATXN3-mediated proteotoxicity (Supplementary Fig. 6). Taken together, these results support the idea that befiradol is mitigating motor dysfunction and aggregation in the *C. elegans* model of ATXN3 proteotoxicity through selective targeting of the 5-HT_{1A}R. This hypothesis was further supported by the co-treatment of ATXN3 mutant animals with befiradol and WAY-100635. WAY-100635 is a potent and selective 5-HT_{1A} antagonist (Gozlan et al., 1995; Laporte et al., 1994; Mathis et al., 1994), that upon acute administration occupies the ligand binding site of 5-HT_{1A}R without altering 5-HT release (Gurling et al., 1994). Upon administration of befiradol alone and in combination with increasing dosages of WAY 100635, we observed a dose-dependent loss of befiradol effect on the amelioration of motor dysfunction of ATXN3 mutant animals, suggesting a direct competition for the 5-HT_{1A}R ligand binding site (Fig. 5a).

3.4. Addressing 5HT_{1A} auto- and heteroreceptor contribution to befiradol's therapeutic action

The role of 5HT_{1A} auto- and heteroreceptors on mutant ATXN3 proteotoxicity was examined using pharmacogenetic approaches (Fig. 5b). Genetic ablation of the 5-HT_{1A}R orthologue SER-4 led to a suppression in proteotoxicity of mutant ATXN3-expressing animals (Fig. 4b), possibly consistent with a net effect of abrogation of the negative regulation of serotonin production mediated by autoreceptors located at serotonergic neurons. Next, we asked whether the 5-HT_{1A} heteroreceptors activity could also contribute to the effect of the drug. We tested this hypothesis by ablating the *tph-1* gene in ATXN3 mutant background. TPH-1 is the orthologue of human tryptophan hydroxylase 1 (Sze et al., 2000), the enzyme responsible for the first step of 5-HT biosynthesis, limiting the rate conversion of tryptophan into 5-HT. In *C. elegans*, a null mutation on the *tph-1* gene, the sole tryptophan hydroxylase enzyme, abolishes all 5-HT production (Sze et al., 2000), therefore making the modulatory role of 5-HT_{1A} autoreceptors on 5-HT synthesis irrelevant, but still allowing activation of 5-HT_{1A} heteroreceptors and of their downstream signaling pathways by exogenous agonists. Importantly for the mechanism of action of befiradol, upon acute treatment with this drug there was an amelioration of motor dysfunction of ATXN3 mutant animals, both in the presence or absence of TPH-1. In contrast, upon chronic administration, befiradol showed a

limited impact on the motor behavior of *tph-1Δ*; ATXN3 mutant animals (Fig. 5b). These results suggest that the beneficial effect of befiradol chronic treatment is predominantly dependent on 5-HT_{1A} autoreceptor function, likely by desensitization of these receptors in serotonergic neurons and disinhibition of serotonin release, whereas acute treatment may predominantly act through activation of the heteroreceptors in non-serotonergic neurons even in the absence of endogenous serotonin, culminating in the suppression of mutant ATXN3-associated phenotypes (Fig. 6). This is consistent with the differential impact caused by chronic or acute administration of befiradol on Ca^{2+} dynamics of HSN neurons (Fig. 5c and Supplementary Fig. 7). While acute treatment elicited a decrease in HSN activity, chronic treatment failed to do so, suggesting a desensitization of the receptor.

4. Discussion

In this study, we evaluated befiradol, a novel 5-HT_{1A} receptor full agonist, as a potential modulator of MJD pathogenesis, comparing its effects with tandospirone, a 5-HT_{1A}R partial agonist, using a *C. elegans* model of mutant ATXN3 proteotoxicity. Our results showed that befiradol treatment ameliorates core pathological features in this model, including mutant ATXN3-mediated motor dysfunction and protein aggregation in neurons upon chronic and acute administration. Hence, we propose befiradol as a disease-modifying agent and the 5-HT_{1A}R as a therapeutic target for MJD. Comparing its effect with tandospirone, befiradol presents higher potency, notably at acute administration, and high target specificity, its therapeutic effect being likely dependent on 5-

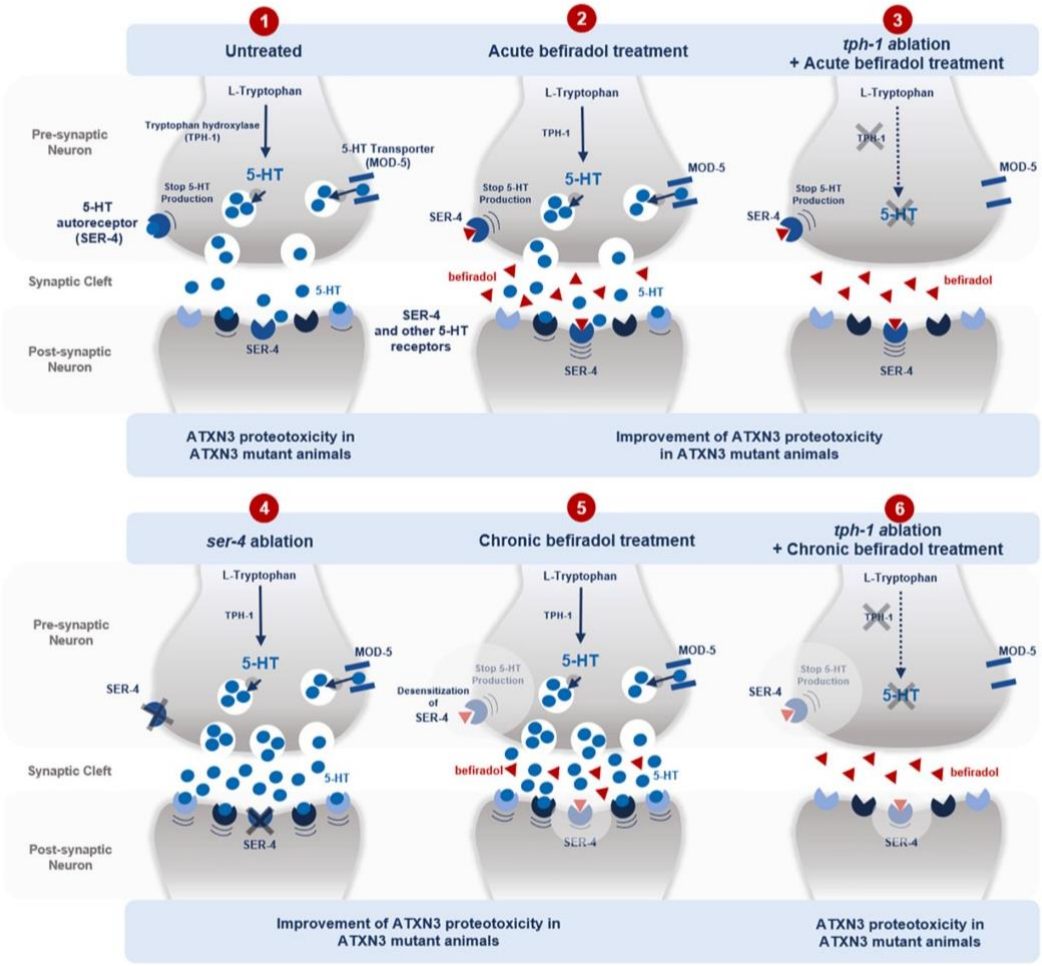

Fig. 6. Hypothetical model of befiradol action in a *C. elegans* model of ATXN3 proteotoxicity. Schematic of serotonergic synapses showing that 5-HT is synthesized and released into the synaptic cleft, where it activates postsynaptic 5-HT receptors, activating the regulatory signaling coupled with the different 5-HT hetero-receptors. Serotonin also binds the 5-HT autoreceptor SER-4, eliciting the "stop 5-HT production" signal mediated by 5-HT autoreceptors in presynaptic neurons (1). Acute treatment with befiradol rapidly targeted 5-HT_{1A}/SER-4 receptors, activating protective cellular pathways against mutant ATXN3-mediated neuronal dysfunction (2). In the absence of endogenous serotonin, through ablation of the *tph-1* gene, acute treatment with befiradol still improved motor function, suggesting a contribution of 5-HT_{1A} hetero-receptors signaling for the suppression of mutant ATXN3-associated phenotypes (3). *ser-4* ablation also suppressed proteotoxicity, consistent with a possible disinhibition of serotonin synthesis and release, likely increasing its availability, as described previously for chronic treatment with selective serotonin re-uptake inhibitors (4). Chronic treatment with befiradol suppressed mutant ATXN3 pathogenesis through activation of 5-HT_{1A}/SER-4 receptors, an effect which we hypothesize includes the disinhibition of serotonin release, likely by desensitization of the 5-HT_{1A}/SER-4 auto-receptor at the pre-synapse (5). In the absence of endogenous serotonin, through ablation of the *tph-1* gene, chronic treatment with befiradol was insufficient to suppress ATXN3 proteotoxicity, further supporting a possible role of the disinhibition of serotonin release upon chronic treatment with befiradol (6).

HT_{1A} auto- and hetero-receptors (Fig. 6).

Pharmacologic and genetic modulation of serotonergic signaling was previously shown to impact MJD pathogenesis, being able to suppress mutant ATXN3 aggregation and to restore motor function in three distinct MJD animal models exposed to chronic administration of citalopram (Ashraf et al., 2019; Esteves et al., 2019; Teixeira-Castro et al., 2015). Interestingly, this effect was dependent not only of SERT/MOD-5, the citalopram molecular target, but also on the 5-HT_{1A}/SER-4 and 5-HT_2/SER-1 receptors (Teixeira-Castro et al., 2015). Although the mechanism of action of citalopram is not fully understood, there is evidence that the therapeutic effects of SSRIs are modulated by 5-HT_{1A}R function (Kulikov et al., 2018; Stahl, 1998). Specifically, citalopram chronic treatment was shown to lead to 5-HT_{1A} auto-receptor desensitization, increasing 5-HT availability (Invernizzi et al., 1994), and to increase the functional sensitivity of post-synaptic 5-HT_{1A} hetero-receptors (Moulin-Sallanon et al., 2009). In addition, enhancement of the signaling cascades downstream of 5-HT_{1A}R, upon chronic citalopram treatment and direct targeting of 5-HT_{1A}R, has a modulatory effect on glutamatergic (Cervantes-Ramirez et al., 2019), dopaminergic and noradrenergic signaling pathways, further supporting a broad and overarching mode-of-action of the serotonergic system in the brain (Kaneko et al., 2016). The adaptation of the serotonergic system, in particular 5-HT_{1A}R desensitization, needed for citalopram action, could explain the delay in phenotypic amelioration seen in depression upon treatment with this drug. Often, patients with major depression discontinue citalopram use due to anxiety symptoms in the first weeks of treatment, this emotional imbalance being associated with 5-HT_{1A}R activation at the Dorsal Raphe Nucleus (DRN), as seen in a PET and functional MRI study (Selvaraj et al., 2018). This close relationship between citalopram action and 5-HT_{1A} receptor signaling further supported the hypothesis that direct modulation of 5-HT_{1A}Rs could suppress MJD pathogenesis. Indeed, previous studies in patients showed efficacy of two 5-HT_{1A}R agonists, buspirone and tandospirone, in amelioration of cerebellar ataxia symptomatology (Ogawa, 2004; Takei et al., 2005). Buspirone led to an improvement of clinical and self-assessment test scores in patients with cerebellar cortical atrophy and olivopontocerebellar atrophy (Lou et al., 1995), however this effect was shown to be partial and not major (Trouillas et al., 1997). Tandospirone treatment improved the ataxia rating scale (ARS) scores in MJD and SCA6 patients (Takei et al., 2010). In the MJD cohort, patients showed improved gait, posture, kinetic and total ARS during the 3 to 4 weeks of treatment (Takei et al., 2004). However, the withdrawal of tandospirone reverted symptom amelioration, showing a non-modulatory short-term effect of tandospirone treatment in MJD pathogenesis (Takei et al., 2004). Interestingly, buspirone and tandospirone were classified as partial agonists of 5-HT_{1A} hetero-receptors (Huang et al., 2017; Yocca, 1990), making it plausible that a potent and selective 5-HT_{1A}R agonist (Colpaert et al., 2002) might increase efficacy. Accordingly, this study shows that although befiradol elicited the same effect size as tandospirone upon chronic treatment, befiradol also suppressed MJD pathogenesis on acute administration, contrary to tandospirone. This is consistent with the description of tandospirone as a partial agonist of 5-HT_{1A} hetero-receptors and with the primary effect of acute treatment with befiradol being predominantly mediated by the activation of 5-HT_{1A} hetero-receptors and independent of the serotonin synthesis downregulation signal mediated by autoreceptors. In addition to a decreased agonism effect (60%) compared to a selective 5-HT_{1A} agonist (Hamik et al., 1990), tandospirone may also be a suboptimal therapeutic agent in view of its interactions with multiple cellular targets, namely serotonin 5-HT_2, dopamine D_2 and alpha-adrenergic receptors, which our data suggest are not essential for the therapeutic effects of 5-HT_{1A}R-targeting drugs in MJD.

The pattern of binding and activation by befiradol in the brain has been extensively studied in rat, cat, macaque and, more recently, in human using a variety of *in vitro*, *ex vivo*, PET imaging and fMRI techniques (Bardin et al., 2005; Colom et al., 2020; Levigoureux et al., 2019; Llado-Pelfort et al., 2012; Vidal et al., 2019; Vidal et al., 2018). Since the 5-HT_{1A}R is highly expressed in the DRN, the serotonergic core of the brain, not surprisingly, befiradol binds to the 5-HT_{1A} autoreceptors of DRN neurons (Levigoureux et al., 2019; Vidal et al., 2019; Vidal et al., 2018) and decreases the neuronal firing rate (Llado-Pelfort et al., 2012) through activation of the negative feedback loop of serotonin production. The desensitization of these autoreceptors is probably accounting for the effect of befiradol chronic treatment in mutant ATXN3-expressing animals, by increasing serotonin availability (Fig. 6). However, befiradol not only activates 5-HT_{1A} autoreceptors but also heteroreceptors (Llado-Pelfort et al., 2012). Extensive PET/fRMI studies, using several species, showed activity of befiradol for thalamus, cingulate cortex and hippocampus (Vidal et al., 2019; Vidal et al., 2018), the receptor occupancy being correlated with changes in activation of these regions, and in the occipital lobe, amygdala, sub-regions of the brainstem and right motor cortex (Vidal et al., 2018). A study with conscious rats showed a more detailed pattern of befiradol binding-selectivity with activation of the pontine nuclei and cerebellum, and an inhibition in the brainstem, piriform cortex and striatum (Levigoureux et al., 2019). Some of these areas have been described as atrophic or damaged in MJD, like the thalamus (Paulson, 2012), and cerebellar–thalamocortical and basal ganglia–thalamocortical pathways (Wang et al., 2020a), or related with ataxic dysfunction and severity, including the cingulate cortex, cerebellum (Hernandez-Castillo et al., 2017) and brainstem (Jafari et al., 2011).

In *C. elegans*, serotonin is present in eight classes of neurons: NSM, HSN, $VC_{4,5}$, ADF, RIH and AIM (Chase and Koelle, 2007), the production of serotonin occurring in NSM, HSN and ADF neurons (Horvitz et al., 1982; Jafari et al., 2011). As in the vertebrate brain, these serotonin-producing neurons project to and regulate non-serotonergic cells that express serotonin receptors. The effect of befiradol proved to be dependent on SER-4, the 5-HT_{1A} orthologue (Olde and McCombie, 1997), which is expressed in neurons, like serotonergic neuron NSM (Gurel et al., 2012), cholinergic (RIB and DVA), glutamatergic (DVC and AIB) and GABAergic (RIS) interneurons (Gurel et al., 2012; Tsalik et al., 2003), but also in a type II vulval muscle cell (vm2) (Gurel et al., 2012; Ravi et al., 2018a), SER-4 expression being required for the effects of endogenous serotonin in locomotion (Gurel et al., 2012).

Importantly, the suppression of ATXN3 aggregation caused by pharmacological modulation of the serotonergic system by citalopram (Ashraf et al., 2019; Teixeira-Castro et al., 2015) and befiradol treatment (this work) are mimicked by genetic ablation of their respective cellular targets. Their effect on protein folding and aggregation suggests that protein homeostasis mechanism(s) may be a link between serotonergic signaling and neurodegeneration associated with proteotoxicity. The exact mechanism of proteostasis modulation by serotonin is unknown, however some candidate pathways have been proposed. HSP90 inhibition improved balance and motor coordination of a MJD mice model (Silva-Fernandes et al., 2014), and the abundance of Hsp90β was directly correlated with ATXN3 high molecular weight species upon citalopram treatment (Ashraf et al., 2019). Interestingly, serotonin was shown to be indispensable for inter-tissue or non-cell autonomous communication of the folding status of an organism (Berendzen et al., 2016; Tatum et al., 2015; Zhang et al., 2018). In this process, the proteotoxic stress caused by the expression of mutant polyQ proteins in neuronal cells was communicated to distal tissues to improve organism proteostasis *via* the activation of the unfolded protein response of mitochondria (UPR^{mt}) (Berendzen et al., 2016). This communication was found to occur *via* WNT signaling and to require serotonin release from serotonergic neurons (Zhang et al., 2018), further supporting that serotonin regulates protein homeostasis at an inter-cellular level. The modulation of protein homeostasis upon serotonergic signaling activation could, therefore, have a positive impact not only on MJD pathogenesis but also in other proteinopathies, such as Parkinson's Disease (PD) and Alzheimer's Disease (AD) (Bayer, 2015; Ross and Poirier, 2004). Indeed, serotonergic signaling dysfunction was recently reported

in PD (Fazio et al., 2020), ALS (reviewed in (Vermeiren et al., 2018)) and AD (Pena-Bautista et al., 2020; Snowden et al., 2019). Interestingly, AD patients present low SERT binding in the limbic regions of the brain (van der Zande et al., 2020) and decreased expression of 5-HT_{1A} receptor (Lanctot et al., 2007). It has been shown that serotonergic signaling modulation by tandospirone (Sato et al., 2007), citalopram (Meyer et al., 2019) or its enantiomer escitalopram impacts on AD pathogenesis (Wang et al., 2016). Interestingly, escitalopram attenuated beta-amyloid-induced tau hyperphosphorylation through 5-HT_{1A} receptor-mediated Akt/GSK-3β pathway (Wang et al., 2020b; Wang et al., 2016), possibly underlying the beneficial effects seen in cognition of AD and vascular dementia patients (Ramirez et al., 2014; Xie et al., 2019). In PD, befiradol treatment reverted L-DOPA-induced dyskinesia (Depoortere et al., 2020; Iderberg et al., 2015; McCreary et al., 2016), a side-effect caused by prolonged administration of L-DOPA. 5-HT_{1A}R agonism and befiradol treatment very efficaciously activated inhibitory somatodendritic 5-HT_{1A} autoreceptors in the DRN. This decreases 5-HT release and blocks the "false neurotransmitter" surge of DA release elicited by L-DOPA administration from 5-HT neurons — an effect that underlies the potent antidyskinetic action of befiradol. Befiradol also activated cortical 5-HT_{1A} heteroreceptors, which can be associated with the beneficial properties seen in models of mood and cognition deficits (Iderberg et al., 2015). Recently, it was found that befiradol can have some anti-parkinsonism properties in MPTP-treated macaques (Fisher et al., 2020), coherent with the findings that 5-HT_{1A}R agonism, by 8-OH-DPAT or buspirone, ameliorated haloperidol-induced catalepsy and bradykinesia (Mohajjel Nayebi and Sheidaei, 2010; Ohno et al., 2008). Therefore, serotonergic signaling stimulation seems to be also effective for parkinsonism, L-DOPA-induced dyskinesia, cognitive impairment and neurodegeneration of dopaminergic neurons (Ohno, 2011; Ohno et al., 2015).

In conclusion, our results strengthen interest in the modulation of serotonergic signaling as a promising therapeutic approach for MJD, presenting befiradol as a potent and selective 5-HT_{1A}R agonist *in vivo*. In the future, in-depth studies and translational analysis using MJD mouse models will be required to further validate befiradol use as therapeutic agent and to dissect the involvement of 5-HT_{1A} receptors signaling in the suppression of MJD pathogenesis.

Contributors

J.P-S, A.T-C and P.M. contributed to the study design. J.P-S, B.F-L, A. B-S, D.V-C, J.H.F, M.D.C and A.T-C collected the data. Interpretation of data was made by J.P-S, A.T-C and P.M. The first draft was written by J. P-S, which was critically commented by A.T-C, A.N-T, M.A.V. and P.M. All authors revised and approved the final version of the manuscript.

Data sharing statement

Data sets can be shared by request to the corresponding author.

Declaration of interests

J.P-S, B.F-L, A.B-S, D.V-C, J.H.F, M.D.C, A.T-C, P.M declare no conflict of interest. Mark A. Varney, Adrian Newman-Tancredi are stockholders of Neurolixis.

Acknowledgements

We are grateful to members of the Maciel laboratory for sharing reagents, for critical analysis of the data and discussions on the manuscript. Thanks to the Caenorhabditis Genetics Center (CGC), which is funded by NIH Office of Research Infrastructure Programs (P40 OD010440), and to National Bioresource Project for the Experimental Animal "Nematode *C. elegans*" (NBRP) for providing some of the nematode strains used in this study.

This work was funded by FEDER, through the Competitiveness Internationalization Operational Programme (POCI), and by National funds, through the Foundation for Science and Technology (FCT), under the scope of the project POCI-01-0145-FEDER-0 31987, NORTE-01-0145-FEDER-000013 and NORTE-01-0145-FEDER-000023, supported by the Northern Portugal Regional Operational Programme (NORTE 2020), under the Portugal 2020 Partnership Agreement, through the European Regional Development Fund (ERDF) and by ICVS Scientific Microscopy Platform, member of the national infrastructure PPBI - Portuguese Platform of Bioimaging (PPBI-POCI-01-0145-FEDER-022122); by National funds, through the Foundation for Science and Technology (FCT) - project UIDB/50026/2020 and UIDP/50026/2020. Additionally, this project was supported by National Ataxia Foundation (NAF) and the FCT individual fellowship PD/BDE/127834/2016 (For J. P-S).

Appendix A. Supplementary data

Supplementary data to this article can be found online at https://doi.org/10.1016/j.nbd.2021.105278.

References

Albert, P.R., Vahid-Ansari, F., 2019. The 5-HT1A receptor: signaling to behavior. Biochimie. 161, 34–45.
Albert, P.R., et al., 1990. Cloning, functional expression, and mRNA tissue distribution of the rat 5-hydroxytryptamine1A receptor gene. J. Biol. Chem. 265, 5825–5832.
Ashraf, N.S., et al., 2019. Citalopram reduces aggregation of ATXN3 in a YAC transgenic mouse model of Machado-Joseph disease. Mol. Neurobiol. 56, 3690–3701.
Bardin, L., et al., 2005. Dual, hyperalgesic, and analgesic effects of the high-efficacy 5-hydroxytryptamine 1A (5-HT1A) agonist F 13640 [(3-chloro-4-fluoro-phenyl)-[4-fluoro-4-{[(5-methyl-pyridin-2-ylmethyl)-amino]-me thyl}piperidin-1-yl] methanone, fumaric acid salt]: relationship with 5-HT1A receptor occupancy and kinetic parameters. J. Pharmacol. Exp. Ther. 312, 1034–1042.
Bayer, T.A., 2015. Proteinopathies, a core concept for understanding and ultimately treating degenerative disorders? Eur. Neuropsychopharmacol. 25, 713–724.
Berends, A.C., et al., 2005. A review of the neuroprotective properties of the 5-HT1A receptor agonist repinotan HCl (BAYx3702) in ischemic stroke. CNS Drug Rev. 11, 379–402.
Berendzen, K.M., et al., 2016. Neuroendocrine coordination of mitochondrial stress signaling and proteostasis. Cell. 166 (1553–1563), e10.
Bollinger, S., et al., 2010. Novel pyridylmethylamines as highly selective 5-HT(1A) superagonists. J. Med. Chem. 53, 7167–7179.
Brenner, S., 1974. The genetics of *Caenorhabditis elegans*. Genetics. 77, 71–94.
Cervantes-Ramirez, V., et al., 2019. Citalopram reduces glutamatergic synaptic transmission in the auditory cortex via activation of 5-HT1A receptors. Neuroreport. 30, 1316–1322.
Chase, D.L., Koelle, M.R., 2007. Biogenic amine neurotransmitters in *C. elegans*. In: WormBook, pp. 1–15.
Collins, K.M., et al., 2016. Activity of the *C. elegans* egg-laying behavior circuit is controlled by competing activation and feedback inhibition. Elife 5.
Colom, M., et al., 2020. (18)F-F13640 PET imaging of functional receptors in humans. Eur. J. Nucl. Med. Mol. Imaging 47, 220–221.
Colpaert, F.C., et al., 2002. Large-amplitude 5-HT1A receptor activation: a new mechanism of profound, central analgesia. Neuropharmacology. 43, 945–958.
Costa, M.D.C., et al., 2016. Unbiased screen identifies aripiprazole as a modulator of abundance of the polyglutamine disease protein, ataxin-3. Brain. 139, 2891–2908.
Da Silva, J.D., et al., 2019. From pathogenesis to novel therapeutics for spinocerebellar ataxia type 3: evading potholes on the way to translation. Neurotherapeutics. 16, 1009–1031.
Depoortere, R., et al., 2020. The selective 5-HT1A receptor agonist, NLX-112, exerts anti-dyskinetic effects in MPTP-treated macaques. Parkinsonism Relat. Disord. 78, 151–157.
Druse, M., et al., 2005. Signaling pathways involved with serotonin1A agonist-mediated neuroprotection against ethanol-induced apoptosis of fetal rhombencephalic neurons. Brain Res. Dev. Brain Res. 159, 18–28.
Duarte-Neves, J., et al., 2015. Neuropeptide Y mitigates neuropathology and motor deficits in mouse models of Machado-Joseph disease. Hum. Mol. Genet. 24, 5451–5463.
Esteves, S., et al., 2019. Preclinical evidence supporting early initiation of citalopram treatment in Machado-Joseph disease. Mol. Neurobiol. 56, 3626–3637.
EU_Clinical_Trials, 2009. EU Clinical Trials Register [Internet]: Amsterdam: European Medicines Agency (EU): Identifier EUCTR2009-012123-28. A Dose-finding Study of Efficacy and Safety of F13640 in Patients With Moderate to Severe Painful Peripheral Diabetic Polyneuropathy. https://www.clinicaltrialsregister.eu/ctr-search/search?query=2009-012123-28. (Accessed September 2020).
Fazio, P., Ferreira, D., Svenningsson, P., et al., 2020. High-resolution PET imaging reveals subtle impairment of the serotonin transporter in an early non-depressed

Parkinson's disease cohort. Eur. J. Nucl. Med. Mol. Imaging 47, 2407–2416. https://doi.org/10.1007/s00259-020-04683-4.
Fisher, R., et al., 2020. The selective 5-HT1A receptor agonist, NLX-112, exerts anti-dyskinetic and anti-parkinsonian-like effects in MPTP-treated marmosets. Neuropharmacology. 167, 107997.
Garcia-Garcia, A.L., et al., 2014. 5-HT(1A) [corrected] receptors in mood and anxiety: recent insights into autoreceptor versus heteroreceptor function. Psychopharmacology 231, 623–636.
Gidalevitz, T., et al., 2009. Destabilizing protein polymorphisms in the genetic background direct phenotypic expression of mutant SOD1 toxicity. PLoS Genet. 5, e1000399.
Goncalves, N., et al., 2017. Caffeine alleviates progressive motor deficits in a transgenic mouse model of spinocerebellar ataxia. Ann. Neurol. 81, 407–418.
Gozlan, H., et al., 1995. The selective 5-HT1A antagonist radioligand [3H]WAY 100635 labels both G-protein-coupled and free 5-HT1A receptors in rat brain membranes. Eur. J. Pharmacol. 288, 173–186.
Gurel, G., et al., 2012. Receptors and other signaling proteins required for serotonin control of locomotion in *Caenorhabditis elegans*. Genetics. 192, 1359–1371.
Gurling, J., M., A.A.-P., Dourish, C.T., Routledge, C., 1994. Effects of acute and chronic treatment with the selective 5-HT1A receptor antagonist WAY-100635 on hippocampal 5-HT release in vivo. Br. J. Pharmacol. 112, 299 P.
Hamdan, F.F., et al., 1999. Characterization of a novel serotonin receptor from *Caenorhabditis elegans*: cloning and expression of two splice variants. J. Neurochem. 72, 1372–1383.
Hamik, A., et al., 1990. Analysis of tandospirone (SM-3997) interactions with neurotransmitter receptor binding sites. Biol. Psychiatry 28, 99–109.
Harris, G.P., et al., 2009. Three distinct amine receptors operating at different levels within the locomotory circuit are each essential for the serotonergic modulation of chemosensation in *Caenorhabditis elegans*. J. Neurosci. 29, 1446–1456.
Hernandez-Castillo, C.R., et al., 2017. Neural correlates of ataxia severity in spinocerebellar ataxia type 3/Machado-Joseph disease. Cerebellum Ataxias. 4, 7.
Hobson, R.J., et al., 2003. SER-7b, a constitutively active Galphas coupled 5-HT7-like receptor expressed in the *Caenorhabditis elegans* M4 pharyngeal motorneuron. J. Neurochem. 87, 22–29.
Horvitz, H.R., et al., 1982. Serotonin and octopamine in the nematode *Caenorhabditis elegans*. Science. 216, 1012–1014.
Huang, X., et al., 2017. Role of tandospirone, a 5-HT1A receptor partial agonist, in the treatment of central nervous system disorders and the underlying mechanisms. Oncotarget. 8, 102705–102720.
Iderberg, H., et al., 2015. NLX-112, a novel 5-HT1A receptor agonist for the treatment of L-DOPA-induced dyskinesia: behavioral and neurochemical profile in rat. Exp. Neurol. 271, 335–350.
Invernizzi, R.W., et al., 1988. 8-Hydroxy-2-(di-n-propylamino) tetralin, a selective serotonin1A receptor agonist, blocks haloperidol-induced catalepsy by an action on raphe nuclei medianus and dorsalis. Neuropharmacology. 27, 515–518.
Invernizzi, R., et al., 1994. Chronic treatment with citalopram facilitates the effect of a challenge dose on cortical serotonin output: role of presynaptic 5-HT1A receptors. Eur. J. Pharmacol. 260, 243–246.
Jafari, G., et al., 2011. Regulation of extrasynaptic 5-HT by serotonin reuptake transporter function in 5-HT-absorbing neurons underscores adaptation behavior in *Caenorhabditis elegans*. J. Neurosci. 31, 8948–8957.
Kaneko, F., et al., 2016. Long-term citalopram treatment alters the stress responses of the cortical dopamine and noradrenaline systems: the role of cortical 5-HT1A receptors. Int. J. Neuropsychopharmacol. 19.
Kawaguchi, Y., et al., 1994. CAG expansions in a novel gene for Machado-Joseph disease at chromosome 14q32.1. Nat. Genet. 8, 221–228.
Kia, H.K., et al., 1996. Immunocytochemical localization of serotonin1A receptors in the rat central nervous system. J. Comp. Neurol. 365, 289–305.
Koch, P., et al., 2011. Excitation-induced ataxin-3 aggregation in neurons from patients with Machado-Joseph disease. Nature. 480, 543–546.
Kulikov, A.V., et al., 2018. Interplay between the key proteins of serotonin system in SSRI antidepressants efficacy. Expert Opin. Ther. Targets 22, 319–330.
Lanctot, K.L., et al., 2007. A positron emission tomography study of 5-hydroxytryptamine-1A receptors in Alzheimer disease. Am. J. Geriatr. Psychiatry 15, 888–898.
Laporte, A.M., et al., 1994. Selective in vivo labelling of brain 5-HT1A receptors by [3H] WAY 100635 in the mouse. Eur. J. Pharmacol. 271, 505–514.
Levigoureux, E., et al., 2019. Serotonin 5-HT1A receptor biased agonists induce different cerebral metabolic responses: a [(18)F]-fluorodesoxyglucose positron emission tomography study in conscious and anesthetized rats. ACS Chem. Neurosci. 10, 3108–3119.
Livak, K.J., Schmittgen, T.D., 2001. Analysis of relative gene expression data using real-time quantitative PCR and the 2(-Delta Delta C(T)) method. Methods. 25, 402–408.
Llado-Pelfort, L., et al., 2012. In vivo electrophysiological and neurochemical effects of the selective 5-HT1A receptor agonist, F13640, at pre- and postsynaptic 5-HT1A receptors in the rat. Psychopharmacology 221, 261–272.
Lou, J.S., et al., 1995. Use of buspirone for treatment of cerebellar ataxia. An open-label study. Arch. Neurol. 52, 982–988.
Mathis, C.A., et al., 1994. [11C]WAY 100635: a radioligand for imaging 5-HT1A receptors with positron emission tomography. Life Sci. 55, PL403–7.
McCreary, A.C., et al., 2016. The novel 5-HT1A receptor agonist, NLX-112 reduces l-DOPA-induced abnormal involuntary movements in rat: a chronic administration study with microdialysis measurements. Neuropharmacology. 105, 651–660.
Mellatyar, H., et al., 2018. Targeted cancer therapy through 17-DMAG as an Hsp90 inhibitor: overview and current state of the art. Biomed. Pharmacother. 102, 608–617.
Mello, C.C., et al., 1991. Efficient gene transfer in C.elegans: extrachromosomal maintenance and integration of transforming sequences. EMBO J. 10, 3959–3970.
Mendonca, N., et al., 2018. Clinical features of Machado-Joseph disease. Adv. Exp. Med. Biol. 1049, 255–273.
Meyer, S., et al., 2019. Citalopram improves obsessive-compulsive crossword puzzling in frontotemporal dementia. Case Rep. Neurol. 11, 94–105.
Miyazaki, I., Asanuma, M., 2016. Serotonin 1A receptors on astrocytes as a potential target for the treatment of Parkinson's disease. Curr. Med. Chem. 23, 686–700.
Mohajjel Nayebi, A.A., Sheidaei, H., 2010. Buspirone improves haloperidol-induced Parkinson disease in mice through 5-HT(1A) recaptors. Daru. 18, 41–45.
Moulin-Sallanon, M., et al., 2009. Acute and chronic effects of citalopram on 5-HT1A receptor-labeling by [18F]MPPF and -coupling to receptors-G proteins. Synapse. 63, 106–116.
Neves-Carvalho, A., et al., 2020. Polyglutamine spinocerebellar ataxias: emerging therapeutic targets. Expert Opin. Ther. Targets 24 (11), 1099–1119. https://doi.org/10.1080/14728222.2020.1827394.
Newman-Tancredi, A., et al., 2017. Distinctive in vitro signal transduction profile of NLX-112, a potent and efficacious serotonin 5-HT1A receptor agonist. J. Pharm. Pharmacol. 69, 1178–1190.
Notredame, C., et al., 2000. T-coffee: a novel method for fast and accurate multiple sequence alignment. J. Mol. Biol. 302, 205–217.
Nussbaum-Krammer, C.I., et al., 2015. Investigating the spreading and toxicity of prion-like proteins using the metazoan model organism *C. elegans*. J. Vis. Exp. 52321.
Ogawa, M., 2004. Pharmacological treatments of cerebellar ataxia. Cerebellum. 3, 107–111.
Ohno, Y., 2011. Therapeutic role of 5-HT1A receptors in the treatment of schizophrenia and Parkinson's disease. CNS Neurosci. Ther. 17, 58–65.
Ohno, Y., et al., 2008. Evaluation of the antibradykinetic actions of 5-HT1A agonists using the mouse pole test. Prog. Neuro-Psychopharmacol. Biol. Psychiatry 32, 1302–1307.
Ohno, Y., et al., 2015. New insight into the therapeutic role of the serotonergic system in Parkinson's disease. Prog. Neurobiol. 134, 104–121.
Olde, B., McCombie, W.R., 1997. Molecular cloning and functional expression of a serotonin receptor from *Caenorhabditis elegans*. J. Mol. Neurosci. 8, 53–62.
Oosterink, B.J., et al., 2003. Post-lesion administration of 5-HT1A receptor agonist 8-OH-DPAT protects cholinergic nucleus basalis neurons against NMDA excitotoxicity. Neuroreport. 14, 57–60.
Paillard, B.E., Del Frari, Laurence, Brunner, Valérie, Adrian, Newman Tancredi, Varney, Mark, 2020. Method for Treating Movement Disorders With Befiradol. Pierre Fabre Medicament (Boulogne-Billancourt, FR), United States.
Paix, A., et al., 2015. High efficiency, homology-directed genome editing in *Caenorhabditis elegans* using CRISPR-Cas9 ribonucleoprotein complexes. Genetics. 201, 47–54.
Paulson, H., 2012. Machado-Joseph disease/spinocerebellar ataxia type 3. Handb. Clin. Neurol. 103, 437–449.
Pena-Bautista, C., et al., 2020. Plasma alterations in cholinergic and serotonergic systems in early Alzheimer disease: diagnosis utility. Clin. Chim. Acta 500, 233–240.
Peralba, J.M., et al., 2003. Pharmacodynamic evaluation of CCI-779, an inhibitor of mTOR, in cancer patients. Clin. Cancer Res. 9, 2887–2892.
Pompeiano, M., et al., 1992. Distribution and cellular localization of mRNA coding for 5-HT1A receptor in the rat brain: correlation with receptor binding. J. Neurosci. 12, 440–453.
Prinssen, E.P., et al., 2002. 5-HT1A receptor activation and anti-cataleptic effects: high-efficacy agonists maximally inhibit haloperidol-induced catalepsy. Eur. J. Pharmacol. 453, 217–221.
Ramirez, M.J., et al., 2014. Serotonergic therapies for cognitive symptoms in Alzheimer's disease: rationale and current status. Drugs. 74, 729–736.
Ranganathan, R., et al., 2000. MOD-1 is a serotonin-gated chloride channel that modulates locomotory behaviour in *C. elegans*. Nature. 408, 470–475.
Ravi, B., et al., 2018a. Homeostatic feedback modulates the development of two-state patterned activity in a model serotonin motor circuit in *Caenorhabditis elegans*. J. Neurosci. 38, 6283–6298.
Ravi, B., et al., 2018 Feb 7. Ratiometric calcium imaging of individual neurons in behaving *Caenorhabditis elegans*. J. Vis. Exp. 7 (132), 56911. https://doi.org/10.3791/56911 (PMID: 29443112; PMCID: PMC5912386).
Riad, M., et al., 2000. Somatodendritic localization of 5-HT1A and preterminal axonal localization of 5-HT1B serotonin receptors in adult rat brain. J. Comp. Neurol. 417, 181–194.
Ross, C.A., Poirier, M.A., 2004. Protein aggregation and neurodegenerative disease. Nat. Med. 10 (Suppl), S10–S17.
Sato, S., et al., 2007. A preliminary open-label study of 5-HT1A partial agonist tandospirone for behavioural and psychological symptoms associated with dementia. Int. J. Neuropsychopharmacol. 10, 281–283.
Schatzberg, A.F., 2002. Pharmacological principles of antidepressant efficacy. Hum. Psychopharmacol. 17 (Suppl. 1), S17–S22.
Selvaraj, S., et al., 2018. Effect of citalopram on emotion processing in humans: a combined 5-HT1A [(11)C]CUMI-101 PET and functional MRI study. Neuropsychopharmacology. 43, 655–664.
Silva-Fernandes, A., et al., 2014. Chronic treatment with 17-DMAG improves balance and coordination in a new mouse model of Machado-Joseph disease. Neurotherapeutics. 11, 433–449.
Snowden, S.G., et al., 2019. Neurotransmitter imbalance in the brain and Alzheimer's disease pathology. J. Alzheimers Dis. 72, 35–43.
Stahl, S.M., 1998. Mechanism of action of serotonin selective reuptake inhibitors. Serotonin receptors and pathways mediate therapeutic effects and side effects. J. Affect. Disord. 51, 215–235.

Stothard, P., 2000. The sequence manipulation suite: JavaScript programs for analyzing and formatting protein and DNA sequences. Biotechniques. 28 (1102), 1104.
Sze, J.Y., et al., 2000. Food and metabolic signalling defects in a *Caenorhabditis elegans* serotonin-synthesis mutant. Nature. 403, 560–564.
Takei, A., et al., 2003. 'Drug holiday' effects of tandospirone in a patient with Machado-Joseph disease. Psychiatry Clin. Neurosci. 57, 607–608.
Takei, A., et al., 2004. Effects of tandospirone on "5-HT1A receptor-associated symptoms" in patients with Machado-Josephe disease: an open-label study. Clin. Neuropharmacol. 27, 9–13.
Takei, A., et al., 2005. Treatment of cerebellar ataxia with 5-HT1A agonist. Cerebellum. 4, 211–215.
Takei, A., et al., 2010. Difference in the effects of tandospirone on ataxia in various types of spinocerebellar degeneration: an open-label study. Cerebellum. 9, 567–570.
Tatum, M.C., et al., 2015. Neuronal serotonin release triggers the heat shock response in *C. elegans* in the absence of temperature increase. Curr. Biol. 25, 163–174.
Teixeira-Castro, A., et al., 2011a. Neuron-specific proteotoxicity of mutant ataxin-3 in *C. elegans*: rescue by the DAF-16 and HSF-1 pathways. Hum. Mol. Genet. 20, 2996–3009.
Teixeira-Castro, A., et al., 2011b. An Image Processing Application for Quantification of Protein Aggregates in *Caenorhabditis elegans*. Springer, Berlin Heidelberg, Berlin, Heidelberg, pp. 31–38.
Teixeira-Castro, A., et al., 2015. Serotonergic signalling suppresses ataxin 3 aggregation and neurotoxicity in animal models of Machado-Joseph disease. Brain. 138, 3221–3237.
Thampi, P., et al., 2012. The 5HT1a receptor agonist 8-Oh DPAT induces protection from lipofuscin accumulation and oxidative stress in the retinal pigment epithelium. PLoS One 7, e34468.
Trouillas, P., et al., 1997. Buspirone, a 5-hydroxytryptamine1A agonist, is active in cerebellar ataxia. Results of a double-blind drug placebo study in patients with cerebellar cortical atrophy. Arch. Neurol. 54, 749–752.
Tsalik, E.L., et al., 2003. LIM homeobox gene-dependent expression of biogenic amine receptors in restricted regions of the *C. elegans* nervous system. Dev. Biol. 263, 81–102.
Vermeiren, Y., et al., 2018. Serotonergic dysfunction in amyotrophic lateral sclerosis and Parkinson's disease: similar mechanisms, dissimilar outcomes. Front. Neurosci. 12, 185.
Vidal, B., et al., 2018. (18)F-F13640 preclinical evaluation in rodent, cat and primate as a 5-HT1A receptor agonist for PET neuroimaging. Brain Struct. Funct. 223, 2973–2988.
Vidal, B., et al., 2019. Pharmacological MRI to investigate the functional selectivity of 5-HT1A receptor biased agonists. Neuropharmacology 107867.
Vilchez, D., et al., 2012. RPN-6 determines *C. elegans* longevity under proteotoxic stress conditions. Nature. 489, 263–268.
Voisine, C., et al., 2007. Identification of potential therapeutic drugs for huntington's disease using *Caenorhabditis elegans*. PLoS One 2, e504.
Wang, Y.J., et al., 2016. Escitalopram attenuates beta-amyloid-induced tau hyperphosphorylation in primary hippocampal neurons through the 5-HT1A receptor mediated Akt/GSK-3beta pathway. Oncotarget. 7, 13328–13339.
Wang, P.S., et al., 2020a. Supratentorial and Infratentorial lesions in spinocerebellar ataxia type 3. Front. Neurol. 11, 124.
Wang, Y.J., et al., 2020b. Escitalopram alleviates Alzheimer's disease-type tau pathologies in the aged P301L tau transgenic mice. J. Alzheimers Dis. 77, 807–819.
Xie, Y., et al., 2019. The effect of selective serotonin reuptake inhibitors on cognitive function in patients with Alzheimer's disease and vascular dementia: focusing on fluoxetine with long follow-up periods. Signal Transduct Target Ther. 4, 30.
Yocca, F.D., 1990. Neurochemistry and neurophysiology of buspirone and gepirone: interactions at presynaptic and postsynaptic 5-HT1A receptors. J. Clin. Psychopharmacol. 10, 6S–12S.
van der Zande, J.J., et al., 2020. Serotonergic deficits in dementia with Lewy bodies with concomitant Alzheimer's disease pathology: an (123)I-FP-CIT SPECT study. Neuroimage Clin. 25, 102062.
Zhang, Q., et al., 2018. The mitochondrial unfolded protein response is mediated cell-non-autonomously by retromer-dependent Wnt signaling. Cell. 174 (870–883), e17.

Supplementary Material

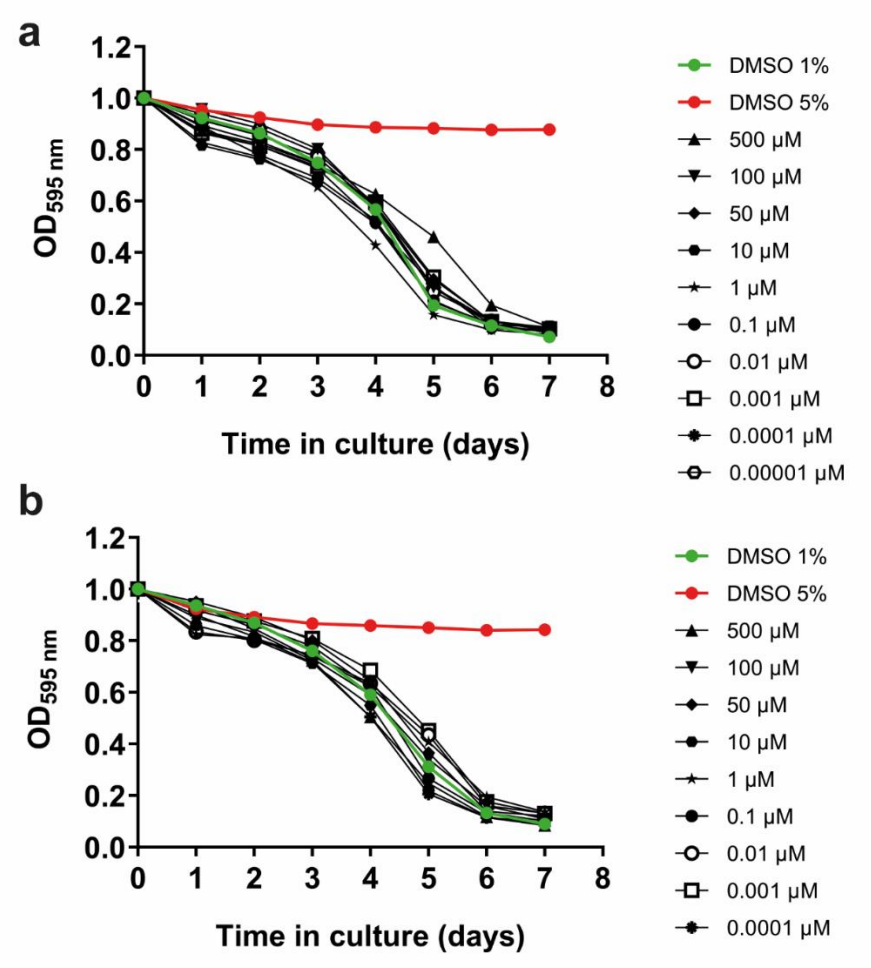

Supplementary figure 1. Befiradol and tandospirone toxicity evaluated using the food clearance assay.

The optical density of the *E. coli* OP50 suspension was measured daily in WT animals treated with **(a)** befiradol or **(b)** tandospirone at a 500 to 0.0001 µM concentration range. The mean OD was calculated for each day from triplicate samples and plotted during the 7 days of the experiment. DMSO 1% (green line) corresponds to drug vehicle and was used as negative (safe) control, conversely DMSO 5% (red line) was used as a positive (toxic) control. Despite the fact that the curves for all concentrations of both drugs are not different from the respective negative control in a statistically significant manner, visual inspection of animals treated with 500 µM of befiradol revealed some deficits in body fitness (data not shown) consistent with mild drug toxicity, being therefore this concentration classified as not safe. The other concentrations were classified as safe, as the OD decrease paralleled the one of vehicle control samples and visual inspection confirmed normal growth of the animals. WT – Wild-type. Statistical analysis: Application of a non-linear regression model for sigmoidal curves against DMSO 1% presented unique model for LogIC50 and HillSlope values, suggestive of no statistical differences between the curves (befiradol P = 0.1352; tandospirone P = 0.0836).

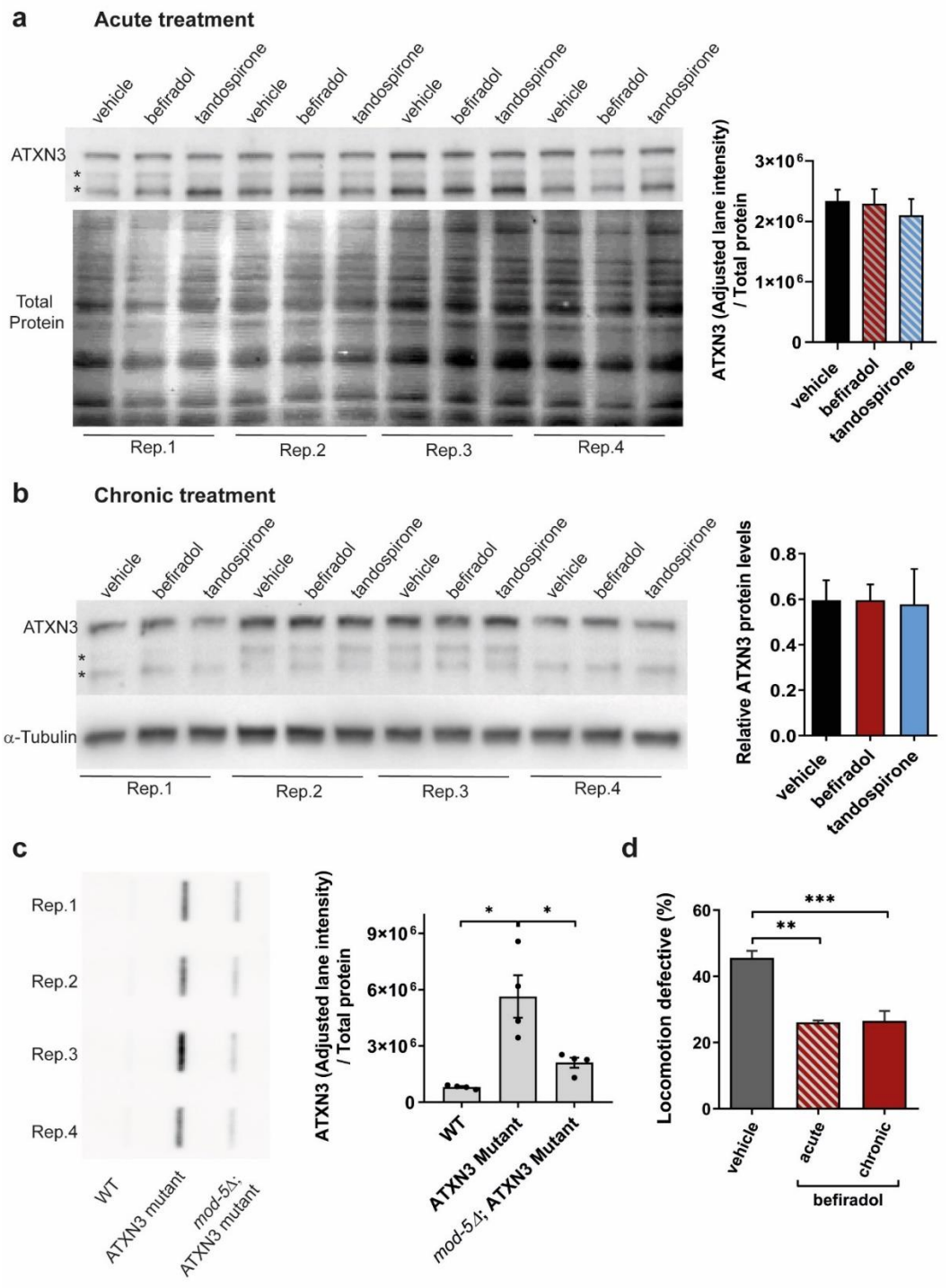

Supplementary figure 2. Total steady-state levels of ATXN3 protein.

Total steady-state levels of ATXN3 protein upon **(a)** acute or **(b)** chronic treatments was evaluated by Western blot and normalized by the total protein staining (AzureRed®, Azure Biosystems) or house-keeping protein (tubulin), respectively. No alterations were found in ATXN3 full length protein levels. **(c)** Filter trap assay membrane and quantification comparing WT, ATXN3 mutant and ATXN3 mutant strain with a deletion in *mod-5* gene. **(d)** Motility assay of animals treated with befiradol immediately before animals harvesting for filter trap assay, showing drug efficacy. Rep. – biological replicate. Steady-state levels acute: (n = 8, ± SEM); Steady-state levels chronic: (n = 4, ± SEM); For filter trap: (n = 4, ± SEM) *P<0.05, (ANOVA, Dunnett T3 test); For motility test: (n = 3-6, ± SEM) **P<0.01, ***P<0.001, ns – non significant (ANOVA, Dunnett test).

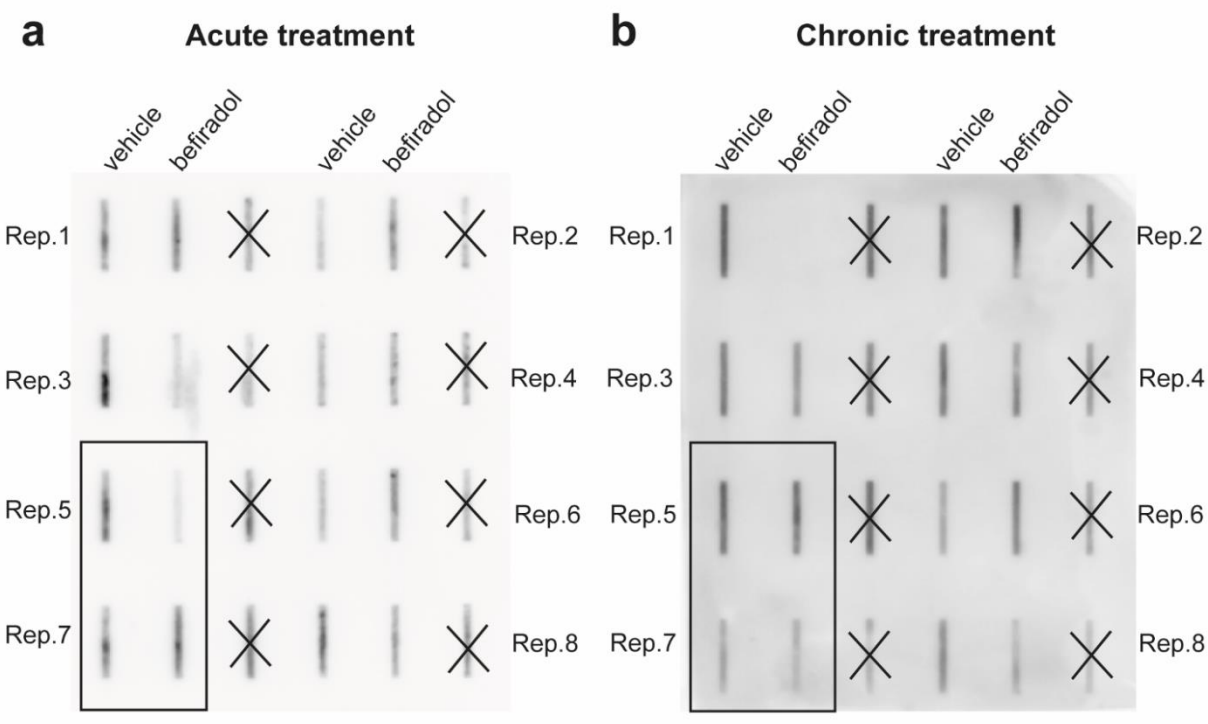

Supplementary figure 3. Filter trap membranes.

Filter trap membranes for befiradol **(a)** acute and **(b)** chronic treatments after ATXN3 Western blot probing. The highlighted rectangles are shown in the main figures 2g and 2h. Rep. – biological replicate.

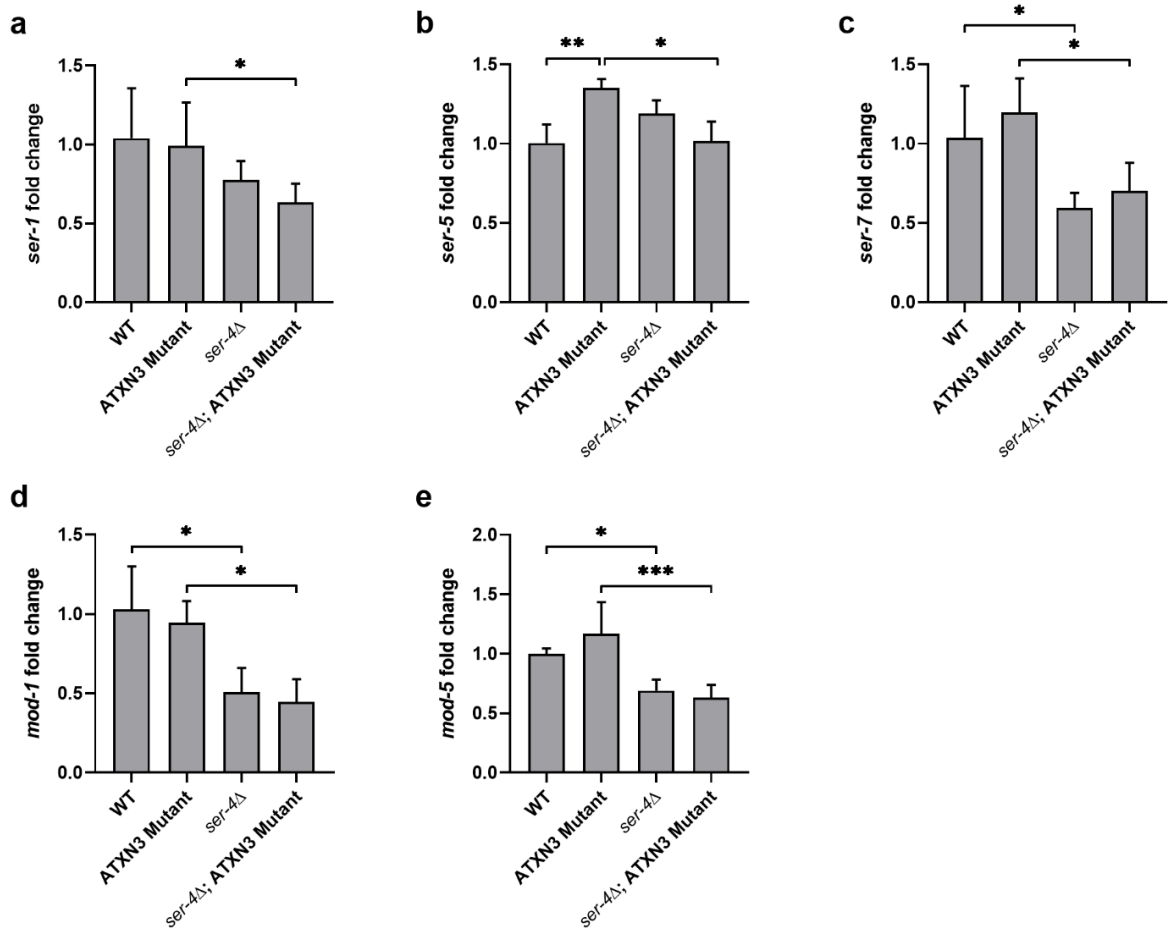

Supplementary figure 4. Whole animal mRNA levels.

Whole-animal mRNA levels of **(a)** *ser-1*, **(b)** *ser-5*, **(c)** *ser-7*, **(d)** *mod-1* receptors and **(e)** *mod-5* transporter in WT, ATXN3 mutant (AT3q130), *ser-4Δ* and *ser-4*Δ; ATXN3 mutant (*ser-4*Δ; AT3q130) animals suggest no compensatory mechanisms at the level of mRNA expression of the different receptors/transporter upon *ser-4* ablation (n = 5, ± SD), *P<0.05, ***P<0.001 [(a and b) Kruskal-Wallis, Dunn's; (c and e) ANOVA, Tukey; (d) ANOVA, Sidak].

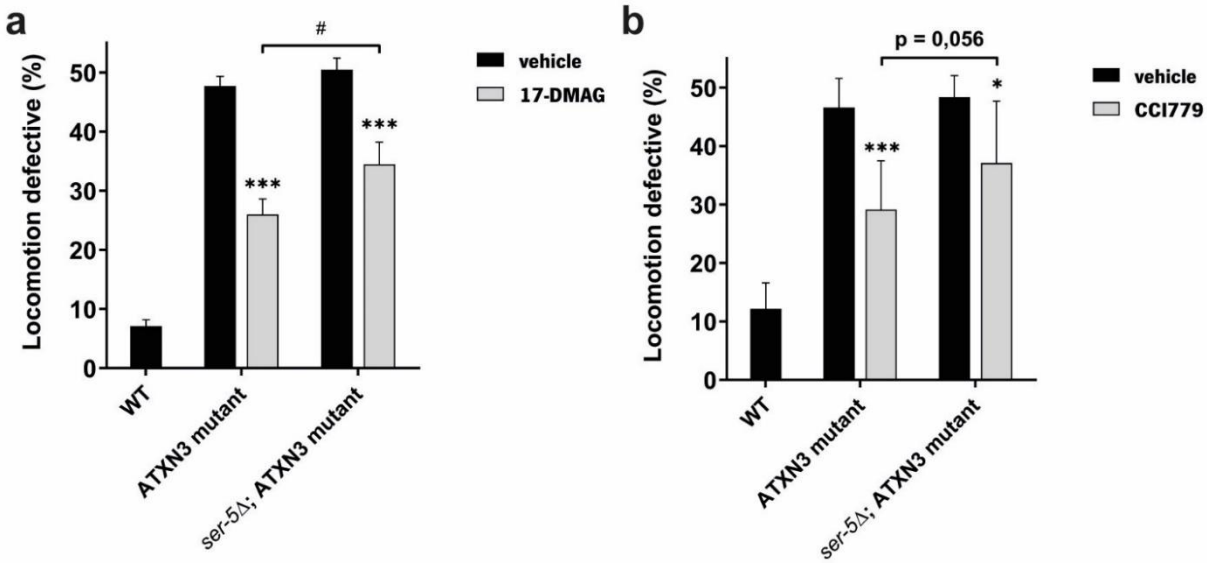

Supplementary figure 5. 17-DMAG and CCI779 actions on mutant ATXN3-mediated motor dysfunction decreases in the absence of SER-5.

The effect of **(a)** 17-DMAG, a HSP-90 inhibitor, and **(b)** CCI779, a m-TOR inhibitor, is decreased in *ser-5*Δ; ATXN3 mutant, suggesting intrinsic features of the strain that make it less amenable to phenotypic modification by different drugs, independently of their mode of action. For 17-DMAG treatment (n = 4, ± SEM), ***P<0.001 comparing drug treatment with vehicle, #P<0.05 comparing strain effect within the same drug treatment (Factorial ANOVA, Sidak post-hoc test). For CCI779 treatment (n = 6 - 7, ± SD), *P<0.05, ***P<0.001 comparing drug treatment with vehicle (Factorial ANOVA, Sidak post-hoc test).

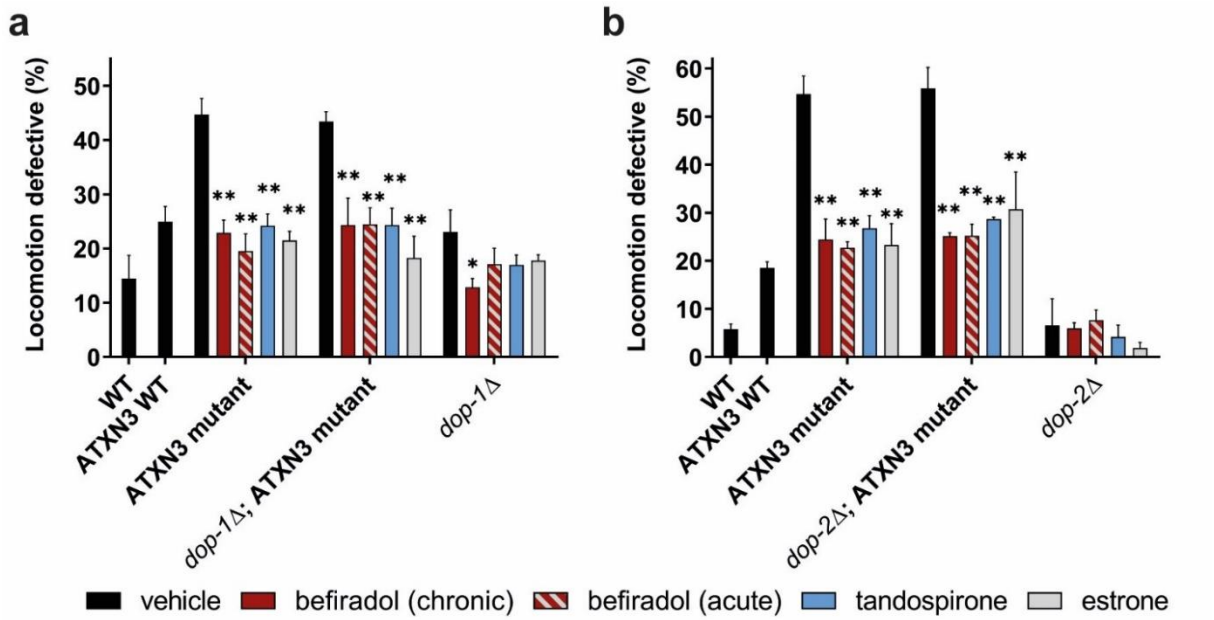

Supplementary figure 6. Befiradol and tandospirone actions on mutant ATXN3-mediated motor dysfunction are independent of dopaminergic receptors.

Genetic ablation of the dopaminergic receptors **(a)** *dop-1* or **(b)** *dop-2* did not impact on befiradol's or tandospirone's therapeutic effect on animals' motor behaviour. (n = 3–4, ± SD), *P<0.05, **P<0.01 (Factorial ANOVA, Sidak test corrected for BCA).

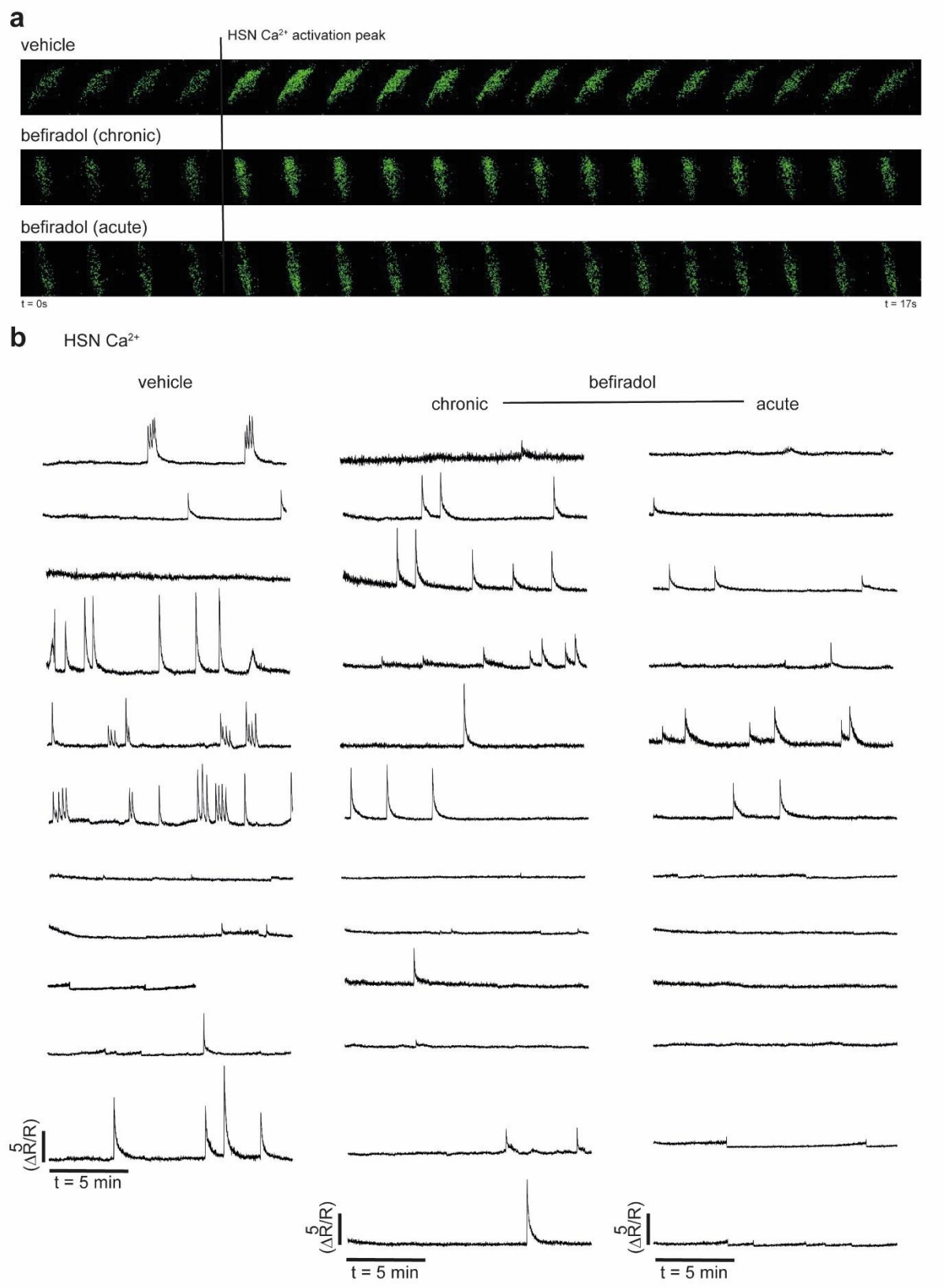

Supplementary figure 7. Ca^{2+} dynamics in HSN neuron upon befiradol chronic and acute treatment.

(a) Kymograph of HSN activation (maximum calcium peak) upon vehicle, chronic- and acute- befiradol treatment. **(b)** GCaMP5/mCherry ratio (ΔR/R) traces of HSN activity upon vehicle, chronic- and acute- befiradol treatment modalities. Each line represents the Ca^{2+} dynamics of an individual neuron, during 15 minutes.

Supplementary table 1. Strains used in the study.

*Strains generated in this work

ID number	Strain name	Genotype
N2 (Bristol)	WT	WT
MAC037/ AM520	ATXN3 WT (AT3q75)	*rmIs238*[$P_{rgef\text{-}1}$::AT3v1-1q75::YFP]
MAC001/ AM685	ATXN3 mutant (AT3q130)	*rmIs263*[$P_{rgef\text{-}1}$::AT3v1-1q130::YFP] II
DA1814	*ser-1*Δ	*ser-1*(*ok345*) X
MAC075	*ser-1*Δ; ATXN3 mutant	*rmIs263*[$P_{rgef\text{-}1}$::AT3v1-1q130::YFP]; *ser-1*(*ok345*) X
AQ866	*ser-4*Δ	*ser-4*(*ok512*) III
MAC072	*ser-4*Δ; ATXN3 mutant	*rmIs263*[$P_{rgef\text{-}1}$::AT3v1-1q130::YFP] II; *ser-4*(*ok512*) III
tm2654	*ser-5*Δ	*ser-5* (*tm2654*) I
MAC013*	*ser-5*Δ; ATXN3 mutant	*ser-5* (*tm2654*) I; *rmIs263*[$P_{rgef\text{-}1}$::AT3v1-1q130::YFP] II
MAC038*	ATXN3 mutant (*ser-5*WT)	*ser-5* (+) I; *rmIs263*[$P_{rgef\text{-}1}$::AT3v1-1q130::YFP] II
DA2100	*ser-7*Δ	*ser-7*(*tm1325*) X
MAC017*	*ser-7*Δ; ATXN3 mutant	*rmIs263*[$P_{rgef\text{-}1}$::AT3v1-1q130::YFP] II; *ser-7*(*tm1325*) X
MAC039*	ATXN3 mutant (*ser-7*WT)	*rmIs263*[$P_{rgef\text{-}1}$::AT3v1-1q130::YFP] II; *ser-7* (+) X
MT9668	*mod-1*Δ	*mod-1*(*ok103*) V
MAC019*	*mod-1*Δ; ATXN3 mutant	*rmIs263*[$P_{rgef\text{-}1}$::AT3v1-1q130::YFP] II; *mod-1*(*ok103*) V
MAC040*	ATXN3 mutant (*mod-1*WT)	*rmIs263*[$P_{rgef\text{-}1}$::AT3v1-1q130::YFP] II; *mod-1* (+) V
LX636	*dop-1*Δ	*dop-1*(*vs101*) X
MAC171*	*dop-1*Δ; ATXN3 mutant	*rmIs263*[$P_{rgef\text{-}1}$::AT3v1-1q130::YFP] II; *dop-1*(*vs101*) X
MAC168*	ATXN3 mutant (*dop-1*WT)	*rmIs263*[$P_{rgef\text{-}1}$::AT3v1-1q130::YFP] II; *dop-1* (+) X
LX702	*dop-2*Δ	*dop-2*(*vs105*) V
MAC222*	*dop-2*Δ; ATXN3 mutant	*rmIs263*[$P_{rgef\text{-}1}$::AT3v1-1q130::YFP] II; *dop-2*(*vs105*) V
MAC167*	ATXN3 mutant (*dop-2*WT)	*rmIs263*[$P_{rgef\text{-}1}$::AT3v1-1q130::YFP] II; *dop-2* (+) V
MAC390*	*tph-1*Δ; ATXN3 mutant	*rmIs263*[$P_{rgef\text{-}1}$::AT3v1-1q130::YFP] ; *tph-1*(*mnh5*) II
LX2004	HSN GCaMP5, mCherry	lite-1(ce314), vsIs183 lin-15(n765ts) X

Supplementary table 2. List of primers used in the generation of double mutant strains.

Gene	Primer ID	Sequence
ser-5	ser-5 F1	5'- CTTCGTCGATTTTGCTCACA - 3'
	ser-5 rev 3	5'- TGCGCCAGTAAAGTGTTAATGT - 3'
	ser-5 R2	5'- CCAACCAACTTGCTACATCG - 3'
ser-7	ser-7_for1	5'- TGGATCTGCTAGCACTGTGG - 3'
	ser-7_rev1	5'- CCGGAGATCCTAAGGTAGGC - 3'
	ser-7_rev2	5'- ACCCCATTTTGGGCCTATAC - 3'
mod-1	mod-1_for1	5'- AATACTCCAGGTGCCAATGC - 3'
	mod-1_rev2	5'- TTCCGTCGTTTTCCTTTAGC - 3'
	mod-1_rev3	5'- TCGAATTGAATACCAACACAATG - 3'
dop-1	dop-1_for1	5'- TGTGCTGAAATGAACGAATGA - 3'
	dop-1_rev1	5'- GGATTGGCAGAAGAGTTTGC - 3'
	dop-1_rev2	5'- CGGAATGGTTTCCTCGTTAT - 3'
dop-2	dop-2_for1	5'- ACGATTCCTTGCGATTCTGG - 3'
	dop-2_rev1	5'- CACAGCCAGGCCTAGGATAA - 3'
	dop-2_rev2	5'- GGAGCCTATGCTGCTATGGA - 3'
tph-1	tph-1_fulldel_F1	5'- ACCACGCCATCGGATATCTA - 3'
	tph-1_fulldel_F2	5'- GGATCGTGTTGTTGAGCAAG - 3'
	tph-1_fulldel_R1	5'- GGAGAATCAATGGTCAACTCG - 3'

Supplementary table 3. List of primers used in reverse-transcriptase quantitative PCR.

Gene	Primer ID	Sequence
ser-1	ser-1 F1	5'- CGTACACTTGCTCGAGGTCA - 3'
	ser-1 R1	5'- GTTGATGCCTCTGTCGTTGC - 3'
ser-5	ser-5 F1	5'- TTGCACTTGCTCAGTGGTGA - 3'
	ser-5 R1	5'- TCCCACCGAACTGTTGTGAG - 3'
ser-7	ser-7 F1	5'- TGTGGATCCCGGATTGGTTG - 3'
	ser-7 R1	5'- TTGCGTCGAGATAGAAGCGG - 3'
mod-1	mod-1 F1	5'- TGATCAGCTGCCAGTTTCCA - 3'
	mod-1 R1	5'- AGTGCCACCAGTAGACAAGA - 3'
mod-5	mod-5 F1	5'- AACTGCTATCGTGACGCCG - 3'
	mod-5 R1	5'- GAGCTTGGGGGTAGACGATG - 3'

Supplementary table 4. Statistical report.

Effect size calculated using Uanhoro, J. O. (2017). Effect size calculators. *Available online at:* https://effect-size-calculator.herokuapp.com/.

Figure		Statistical Report	Sample Size
Fig.1a	befiradol	$F(11, 70) = 12.965$, $p < 0.001$, $\omega^2p = 0.616$	7
	tandospirone	$F(11, 38.7) = 8.050$, $p = 0.005$, $\omega^2p = 0.605$	6
Fig.1b		$F(4, 173) = 6.115$, $p < 0.001$, $\omega^2p = 0.103$	18 to 43
Fig.1c		$F(4, 24) = 3.598$, $p = 0.0196$, $\omega^2p = 0.264$	3
Fig.1d		$F(10, 22) = 11.896$, $p < 0.001$, $\omega^2p = 0.844$	3
Fig.2b (number of aggregates / TA)	Acute + TD Chronic	$H(3) = 10.48$, $p = 0.0149$, $\eta^2 = 0.095$	11 to 32
	befiradol Chronic	$T(37) = 1.868$, $p = 0.0697$, $\eta^2 = 0.086$	17 to 22
Fig.2c (area of aggregates / TA)	Acute + TD Chronic	$H(3) = 5.887$, $p = 0.1173$, $\eta^2 = 0.037$	11 to 32
	befiradol Chronic	$T(37) = 2.257$, $p = 0.0300$, $\eta^2 = 0.121$	17 to 22
Fig.2d (total area)	Acute + TD Chronic	$F(3, 79) = 1.802$, $p = 0.1536$, $\omega^2p = 0.028$	11 to 32
	befiradol Chronic	$T(37) = 1.804$, $p = 0.0793$, $\eta^2 = 0.081$	17 to 22
Fig.2e	Soluble	$T(1) = 0.6667$, $p_{corrected} < 0.9999$, $d = 0.471$	2
	SDS - soluble	$T(1) = 0.000$, $p_{corrected} < 0.9999$, $d = 0$	2
	SDS - resistant	$T(1) = 1.000$, $p_{corrected} < 0.9999$, $d = 0.707$	2
Fig.2f	Soluble	$T(4) = 0.520$, $p_{corrected} = < 0.9999$, $d = -0.233$	5
	SDS - soluble	$T(3) = 7.437$, $p_{corrected} = 0.015$, $d = 3.722$	4
	SDS - resistant	$T(1) = 0.423$, $p_{corrected} = < 0.9999$, $d = -0.299$	2
Fig.2g		$F(2, 17) = 0.8325$, $p = 0.4519$, $\omega^2p = 0.000$	6 to 7
Fig.2h		$F(2 , 17) = 2.026$, $p = 0.1625$, $\omega^2p = 0.093$	6 to 7
Fig.3		$F(9, 52) = 2.398$, $p = 0.0234$, $\omega^2p = 0.168$	3
Fig.4b		$F(8, 34) = 8.683$, $p < 0.001$, $\omega^2p = 0.588$	3
Fig.4c		$F(8, 34) = 11.935$, $p < 0.001$, $\omega^2p = 0.670$	3
Fig.4d		$F(10, 40) = 2.878$, $p = 0.008$, $\omega^2p = 0.269$	3
Fig. 4e		$F(10, 60) = 3.237$, $p = 0.002$, $\omega^2p = 0.240$	4
Fig. 4f		$F(10, 40) = 4.257$, $p < 0.001$, $\omega^2p = 0.390$	3
Fig. 5a		$F(9, 6.160) = 6.039$, $p = 0.019$, $\omega^2p = 0.737$	2 -3
Fig. 5b		$F(6, 14) = 102.703$, $p < 0.001$, $\omega^2p = 0.966$	3
Fig. 5c		$F(2, 18.651) = 5.117$, $p = 0.017$, $\omega^2p = 0.275$	11 - 12
S1a		$F(40, 44) = 1.406$, $p = 0.1352$, $\omega^2p = 0.160$	5

S1b		$F(36, 40) = 1.568$, $p = 0.0836$, $\omega^2p = 0.210$	5
S2a		$F(2, 20) = 0.277$, $p = 0.7609$, $\omega^2p = 0$	7 - 8
S2b		$F(2, 9) = 0.471$, $p = 0.6387$, $\omega^2p = 0$	4
S2c		$F(2, 3.353) = 13.72$, $p = 0.0243$, $\omega^2p = 0.800$	4
S2d		$F(4, 20) = 8.233$, $p = 0.0004$, $\omega^2p = 0.536$	3 - 6
S4a		$H(3) = 9.571$, $p = 0.0226$, $\eta^2 = 0.411$	5
S4b		$H(3) = 14.12$, $p = 0.0027$, $\eta^2 = 0.695$	5
S4c		$F(3, 16) = 8.179$, $p = 0.0016$, $\omega^2p = 0.518$	5
S4d		$F(3, 16) = 5.598$, $p = 0.0081$, $\omega^2p = 0.408$	5
S4e		$F(3, 16) = 14.201$, $p < 0.001$, $\omega^2p = 0.664$	5
S5a		$F(4, 13) = 33.983$, $p < 0.001$, $\omega^2p = 0.880$	4
S5b		$F(4, 24) = 16.341$, $p < 0.001$, $\omega^2p = 0.680$	6 - 7
S6a		$F(16, 34.183) = 8.428$, $p < 0.001$, $\omega^2p = 0.699$	4
S6b		$F(16, 12.372) = 22.505$, $p < 0.001$, $\omega^2p = 0.921$	3

Chapter 4.

Addressing the role of serotonin receptors in the suppression of mutant ataxin-3 proteotoxicity

Addressing the role of serotonin receptors in the suppression of mutant ataxin-3 proteotoxicity

Joana Pereira-Sousa[1,2,3], Daniela Vilasboas-Campos[1,2], Carmén Vieira[1,2], Patricia Maciel[1,2], Andreia Teixeira-Castro[1,2]

[1]Life and Health Sciences Research Institute (ICVS), School of Medicine, University of Minho, Braga

[2]ICVS/3B's - PT Government Associate Laboratory Braga/Guimarães, Portugal

[3]Behavioural and Molecular Lab (Bn'ML), University of Minho, Braga

Abstract

Serotonin is a monoamine neurotransmitter produced, in the brain, by serotonergic neurons. These neurons project to virtually all brain regions exerting a tonic modulatory effect. The pleotropic effects exerted by serotonin, in the extensive target sites, is ensured by a vast repertoire of serotonin receptors (5-HTRs). In humans, seven types of 5-HTRs were reported, 5-HT_{1-7}, that can present subtypes, in a total of 14 receptors. Except for 5-HT_3, all the 5-HTRs are metabotropic G protein-coupled receptors (GPCRs). In *C. elegans*, the serotonergic system is composed by four metabotropic GPCRs, namely SER-1, SER-4, SER-5 and SER-7, orthologs of the mammalian receptors 5-HT_2, 5-HT_{1A}, 5-HT_6 and 5-HT_7, respectively, and by MOD-1, the nematode specific channel-gated serotonin receptor.

Previously, our laboratory described the modulation of serotonergic signalling as a potential therapeutic strategy for Machado-Joseph disease (MJD). Citalopram (CIT) treatment improved motor coordination and decreased mutant ATXN3 aggregation in several animal models of the disease. CIT's effect showed to be dependent on SERT, its molecular target, with an important contribution of the 5-HT_{1A}/SER-4, and also of 5-HT_2/SER-1 receptors in *C. elegans*. Furthermore, direct and specific modulation of the 5-HT_{1A}R alone was sufficient to reduce mutant ATXN3-mediated proteotoxicity. This led us to ask whether other 5-HTRs could also play a role in the suppression of MJD pathogenesis.

Here, we found a potential partial contribution of the 5-HT_6/SER-5 and 5-HT_7/SER-7 receptors, as in the absence of these receptors therapeutic effect of CIT was reduced. In contrast, ablation of MOD-1 seemed to be dispensable for CIT-mediated suppression of motor dysfunction in *C. elegans*. Next, using tool compounds likely targeting the different receptors, we observed that, surprisingly, antagonism of 5-HT_2R/SER-1, 5-HT_6R/SER-5 and 5-HT_7R/SER-7 ameliorated motor function of the mutant animals. Although these findings are promising, further studies are needed to support the contribution of 5-HT_2R/SER-1, 5-HT_6R/SER-5 and 5-HT_7R/SER-7 in MJD therapeutics and to dissect the specific pathways by which each receptor impacts on ATXN3 proteotoxicity.

1. Introduction

Serotonin is a monoamine neurotransmitter synthesised by the conversion of the amino acid L-tryptophan by tryptophane hydroxylase [1]. Serotonin can be found in central nervous system as well as in the enterochromaffin cells of the gastrointestinal tract, and in blood platelets [2; 3; 4]. Within the brain, serotonin is produced by cell bodies of the serotonergic neurons in the raphe nucleus [5; 6]. These neurons project, almost, to all brain regions exerting a tonic modulatory effect on its extensive target cells (reviewed in [7]). The pleiotropic effect exerted by serotonin in target cells leads to the modulation of several systems and to physiological and phenotypic responses. These events are ensured by the high diversity and number of serotonin receptors.

In humans, seven types of 5-HT receptors (5-HTRs) were reported, 5-HT_{1-7}. Over this, some receptor types present subtypes, including the 5-HT_{1A-F}, 5-HT_{2A-C}, 5-HT_{5A-B}, in a total of 14 subtypes. 5-HTRs are encoded by 17 genes, 12 of them encode metabotropic 5-HTRs and five encode ionotropic receptor subunits of the 5-HT_3R [8; 9].

5-HT metabotropic receptors are G protein-coupled receptors (GPCRs) that elicit, upon serotonin binding, canonical signalling pathways by association with G proteins [10]. Depending on the G protein subunit associated with the receptor, the signalling cascade elicited by its activation can have an inhibitory or excitatory effect on neurons (reviewed on [8; 11]).

5-HT_1 and 5-HT_5 receptors are associated with the $G_{i/o}$ subunit, which activation results in inhibition of adenylyl cyclase and decrease cAMP formation [12]. Furthermore, activation of these receptors opens G protein-gated inwardly rectifying potassium channels (GIRKs) leading to hyperpolarisation of the neuron and inhibits the opening of voltage-gated calcium channels [13]. Therefore, activation of 5-HT_1R and 5-HT_5R produce an inhibitory effect on neurons.

In contrast, 5-HT_2R, 5-HT_4R, 5-HT_6R and 5-HT_7R families are associated with $G_{q/11}$ or G_s subunits, eliciting an excitatory response. Conversely to $G_{i/o}$, G_s-coupled signalling activates adenylyl cyclase and increase cAMP formation. 5-HT_2Rs are the ones interacting with $G\alpha_q$ proteins, leading to the activation of phospholipase C to promote increasing formation of inositol trisphosphate (IP3) and diacylglycerol (DAG). This results in the activation of protein kinase C (PKC) by DAG and a cytosolic raise in Ca^{2+} levels by IP3 [14; 15; 16].

In addition to these canonical pathways, 5-HT metabotropic receptors reveal non-canonical signalling by diverse molecules, except for the 5-HT_5R. All 5-HTRs act through ERK, but also through small

G proteins (for 5-HT_1R and 5-HT_7R), PLA2, PLD, Src/Akt (for 5-HT_2R), and through mTOR, Cdk5 (for 5-HT_6R) [8; 11].

The *C. elegans* serotonergic system is composed of neurons expressing five types of receptors: SER-1, SER-4, SER-5, SER-7 and MOD-1 [17]. As in mammalian, these receptors are divided in metabotropic and ionotropic receptors. SER-1, SER-4, SER-5 and SER-7 are GPCRs with a high degree of homology to the mammalian receptors 5-HT_2, 5-HT_{1A}, 5-HT_6 and 5-HT_7 receptors, respectively [18; 19; 20; 21]. Therefore, throughout this chapter, the orthology of the receptors will be represented as follows: mammalian receptor/*C. elegans* orthologue. MOD-1 is a serotonin-gated chloride channel specific of *C. elegans* nematode [22].

Previous work from our laboratory showed that modulation of serotonergic signalling supressed MJD pathogenesis [23; 24]. Citalopram (CIT) is a selective serotonin reuptake inhibitor (SSRI) that blocks the serotonin reuptake transporter (SERT), increasing serotonin availability in the synaptic cleft. Long-term administration of CIT to pre-symptomatic MJD animal models ameliorated motor dysfunction and decreased ATXN3 aggregation [24]. The effect of CIT showed to be dependent on MOD-5, the *C. elegans* orthologue of SERT, but also on 5-HT_2R/SER-1 and 5-HT_{1A}R/SER-4, suggesting a role for the serotonin receptors in the suppression of MJD pathogenesis. 5-HT_{1A}R/SER-4 involvement was further supported by pharmacogenetic and pharmacological approaches. Acute and chronic administration of befiradol, a 5-HT_{1A}R/SER-4 potent and selective agonist [25; 26], ameliorated motor dysfunction and decreased mutant ATXN3 aggregation in a *C. elegans* model of mutant ATXN3 proteotoxicity [23].

Here, we started to explore the contribution of the different serotonin receptors to the suppression of MJD pathogenesis in *C. elegans* using tool compounds. Tool compounds (also known as chemical probes) are small molecules that are potent, selective to the target protein and with a known mode-of-action, that allows researchers to ask mechanistic and phenotypic questions about their molecular targets in biochemistry-based or animal studies. Arrowsmith et al defined a chemical probe based on the following criteria: (i) *in vitro* potency of <100 nM at the protein target, (ii) >30-fold selectivity against other protein targets, and (iii) demonstration of on-target effect in cells at <1 μM [27]. These compounds comprise different classes of molecules with distinct ability to influence receptor activity (intrinsic efficacy). Agonists are defined as compounds that, upon binding to the receptor, change receptor activity to produce a response. Antagonists are compounds that, although they can bind to the receptor with high affinity, do not produce alterations in receptor response, having no intrinsic efficacy. In biological systems, however, several principles may be considered to define the action of tool compounds. In organism-based research,

the presence of the endogenous ligand of the receptor will produce a baseline response with biological relevance. In the presence of a competitor, as a tool compound, the receptor-ligand equilibrium will be altered by increasing concentrations of the agonist or antagonist, which compete for the same receptor binding site, changing the receptor's response [28]. In addition, it has also been demonstrated that several receptors can signal even in the absence of a ligand, displaying a constitutive activity, independent of the binding of the endogenous ligand [11; 28]. Therefore, the impact of a compound on the receptor's response, in biological models, should consider the presence of the endogenous ligand and the presence (or absence) of a constitutive activity of the receptor, thus defining three major categories of tool compounds: a) agonists, b) neutral antagonists and c) inverse agonists. In such scenario, when added to the system, full agonists will elicit the maximum response by the receptor (Figure 1). Furthermore, assuming a receptor that does not have constitutive activity, both neutral antagonists and inverse agonists will compete with the endogenous ligand by the receptor binding site, decreasing the receptor's response to the same extent (Figure 1A). However, in the presence of a receptor with constitutive activity, the impact of neutral antagonists or inverse agonists will be different. Neutral antagonists decrease the response of the receptor by competition with endogenous ligand, but only inverse agonists will impact the constitutive activity of the receptor, further suppressing its response (Figure 1B) [28].

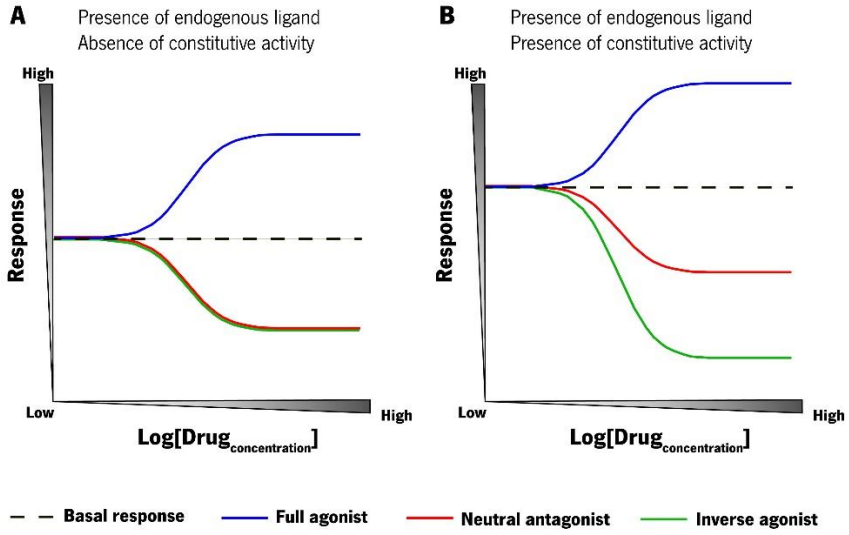

Figure 1. Schematic representation of the impact of tool compounds on a receptor's response.

In complex biological systems, receptors response is elicited by the endogenous ligand, however some receptors can also present a constitutive activity that influences basal response independently of the endogenous ligand stimulation. With increasing concentrations of full agonists (blue line) receptors response increase to a maximum, while the impact on receptors response by neutral antagonists (red line) or inverse agonists (green line) depends on the presence or absence of receptors' constitutive activity. **(A)** In the absence of constitutive activity of the receptor, neutral antagonists and inverse agonists compete by the binding site occupied by the endogenous ligand, that by displacement of endogenous ligand decrease receptors basal

response in the same extent. **(B)** However, since inverse agonists can suppress receptors constitutive activity, in its presence, inverse agonists further decrease receptors response, not only by the displacement of the endogenous ligand (as neutral antagonists) but also by impacting on receptor's constitutive activity. Based on [28].

Here, to address the role of serotonin receptors in the suppression of ATXN3 proteotoxicity, first we explored the contribution of each serotonin receptor on the action of CIT using genetics. Then, for the most relevant receptors, we took advantage of tool compounds with distinct pharmacological profiles. Agonists, neutral antagonists, and inverse agonists of mammalian serotonin receptors were selected, and their impact on motor behaviour was evaluated in animals expressing mutant ATXN3 protein.

2. Material and methods

2.1. Caenorhabditis elegans strains and maintenance

Caenorhabditis elegans (C. elegans) strains used and abbreviations are listed in Table 1. All the strains were backcrossed to the Bristol strain N2 (Wild-type - WT) five to twelve times. Standard methods were used for culturing and observing *C. elegans* [29]. Nematodes were grown on nematode growth medium (NGM) plates seeded with *Escherichia coli* (OP50 strain) at 20°C.

Table 1. *C. elegans* strains used in this study.

ID number	Strain name	Genotype
N2(Bristol)	WT	Wild-type
MAC037/AM599	ATXN3 WT (AT3q75)	*rmIs238* [P_{rgef-1}::AT3v1-1q75::YFP]
MAC001/AM685	ATXN3 mutant (AT3q130)	*rmIs263* [P_{rgef-1}::AT3v1-1q130::YFP] II
tm2654	*ser-5*Δ	*ser-5* (tm2654) I
MAC013	*ser-5*Δ; ATXN3 mutant	*ser-5* (tm2654) I; *rmIs263* [P_{rgef-1}::AT3v1-1q130::YFP] II
MAC038	ATXN3 mutant (*ser-5* WT)	*ser-5* (+) I; *rmIs263* [P_{rgef-1}::AT3v1-1q130::YFP] II
DA2100	*ser-7*Δ	*ser-7* (tm1325) X
MAC017	*ser-7*Δ; ATXN3 mutant	*rmIs263* [P_{rgef-1}::AT3v1-1q130::YFP] II; *ser-7* (tm1325) X
MAC039	ATXN3 mutant (*ser-7* WT)	*rmIs263* [P_{rgef-1}::AT3v1-1q130::YFP] II; *ser-7* (+) X
MT9668	*mod-1*Δ	*mod-1* (ok103) V
MAC019	*mod-1*Δ; ATXN3 mutant	*rmIs263* [P_{rgef-1}::AT3v1-1q130::YFP] II; *mod-1* (ok103) V
MAC040	ATXN3 mutant (*mod-1* WT)	*rmIs263* [P_{rgef-1}::AT3v1-1q130::YFP] II; *mod-1* (+) V

2.2. Tool compounds

Tool compounds were selected by (a) low *in vitro* constant of inhibition (K_i) indicative of high potency of the compound, (b) described selectivity against other receptors determined *in vitro* and (c) specificity of the compound to the target receptor in mammalian animal models [30; 31; 32; 33; 34; 35; 36; 37; 38; 39; 40; 41; 42; 43; 44; 45; 46; 47; 48; 49; 50; 51]. To mitigate the lack of information regarding drug specificity in *C. elegans*, the orthology between *C. elegans* and mammalian receptors was determined, based on the available literature [19; 20; 21; 52]. Tool compounds selected and target receptors are listed in Table 2.

Table 2. Tool compounds used in this study and mammalian target receptors.
C. elegans orthologue to each mammalian receptor is shown.

Mammalian receptor	*C. elegans* orthologue	Agonist	Antagonist	Inverse agonist
5-HT_{2A}	SER-1	TCB-2	————————	MDL 100907
5-HT_{2B}		————————	LY 266097	————————
5-HT_{6}	SER-5	EMDT oxalate	SB 399885 hydrochloride	SB-742457
5-HT_{7}	SER-7	LP44	DR 4485 hydrochloride	SB-269970

2.3. Compound preparation

Tool compounds used in this study were purchased from Tocris Bioscience (United Kingdom) and were used without further purification. To define the most efficient concentration of the compounds, tool compounds were serially diluted from 50 mM to 0.00001 mM in 100% dimethyl sulfoxide (DMSO, Sigma). Each concentration was then diluted in MiliQ water to obtain a final concentration ranging from 500 µM to 0.0001 nM in 1% DMSO. Estrone CAS 53-16-7 (Sigma) and citalopram CAS 59729-32-7 (Kemprotec) were diluted to a 25 µM and 5 µM concentration, respectively. For inverse agonists, MDL 100907 (Tocris Bioscience), SB-742457 (Cayman Chemical) and SB-269970 (Cayman Chemical) were diluted to a 10 µM, 1 µM and 0.1 µM concentrations.

2.4. Drug assay

The drug assay was performed in a 96-well plate format, in liquid culture, as previously described [53]. Briefly, each well contained a final volume of 60 µl, comprising 20–25 animals of wild-type (WT, N2) and wild-type ATXN3 (ATXN3 WT) strains, or 40-45 of ATXN3 mutant (AT3q130) animals in egg stage

in a volume of 15 µl (increased egg number of ATXN3 mutant animals are needed to ensure similar number of animals post-hatching, comparing with WT and ATXN3 WT), 25 µl of tool compounds, citalopram or estrone at the appropriate concentration, and 20 µl of OP50 inactivated bacteria to a final OD_{595} of 0.9 measured in the microplate reader (Tecan Infinite 200 Microplate Reader).

To obtain an age-synchronized population of eggs, four-day-old gravid adults were treated with alkaline hypochlorite solution (0.5 M NaOH, ~2.6% NaClO) for five minutes. The animals were then washed in M9 buffer, resuspended in S-medium complete (S-Basal buffer, 10 mM potassium citrate pH 6, 10X trace metal solution, 3 mM $CaCl_2$, 3 mM $MgSO_4$) to the appropriate egg number and transferred into the 96-well plate. The OP50 bacteria were grown overnight at 37°C and 150 rpm in Luria Broth (LB) medium, pelleted by centrifugation, inactivated by three cycles of freeze/thawing at 37°C, frozen at −80°C and then resuspended in S-medium complete supplemented with 0.004 mg/ml cholesterol, 0.5X Pen-strep (Sigma) and 0.5X nystatin (Sigma). Animals were grown with continuous shaking at 180 rpm at 20°C (Shel Lab) for four days.

2.5. Motility assay and drug efficacy determination

Four-day-old animals were transferred from the 96-well plates onto an unseeded NGM plate (equilibrated at 20°C). Plates dried for 45 minutes before starting the motility assays. Motility assays were performed at 20°C as previously described [54]. Briefly, ten animals were placed simultaneously in the centre of a freshly seeded 30 mm plate, equilibrated at 20°C. Animals remaining inside the 1 cm circle after one minute were scored as locomotion-defective. Motor behaviour assays were run in triplicates or quadruplicates (n = 3 or 4), with a total of at least 150 animals tested per compound concentration.

To quantify drug efficacy we established a score, in which treated animals that display the same motor impairment as ATXN3 mutant animals had a 0% efficacy score and when animals upon treatment ameliorated their motor behaviour, the efficacy score increases. All results shown in the figures are calculated using the following formula:

$$Efficacy\ (\%) = \frac{LD\ mutant\ ATXN3_{vehicle} - LD\ mutant\ ATXN3_{drug}}{LD\ mutant\ ATXN3_{vehicle}}$$

LD - % of locomotion-defective animals (animals that remain within a 1 cm circle after 1 min of observation)

2.6. Statistical analysis

Statistical analysis was performed using the IBM SPSS statistics 23 software (SPSS) and GraphPad Prism 8.0.1 software. Normal distribution of continuous variables was analysed according with Shapiro-Wilk or Kolmogorov-Smirnov normality test, depending on sample size. Levene's test assessment was applied to confirm homogeneity of variances between groups. When both assumptions were verified, groups were compared using one-way or two-way ANOVA followed by Dunnett (Fig. 3A – TCB2; Fig. 3D; Fig. 3E; Fig. 3F; Fig. 4; Fig. 5). When homogeneity of variances between groups was not displayed, groups were compared using One-Way ANOVA and Games-Howell or Dunnett T3 post-hoc test was performed (Fig. 3A – LY 266097; Fig. 3B – EDMT) and ANOVA with Welch correction was reported. When the previous assumptions were not displayed a robust ANOVA (using R batch for SPSS) with Brown-Forsythe (if sample size less than 6) or Welch correction was reported and bootstrap with BCA were performed. Bootstrap sampling was followed by factorial ANOVA with Sidak post-hoc test with bias correction (Fig. 2; Fig. 3B – SB 399885; Fig 3C).

Detailed statistics for all experiments are shown in Supplementary table 1.

3. Results

3.1. Citalopram action depends on serotonergic G protein-coupled receptors

As mentioned above, CIT was previously reported as a potent compound to suppress MJD pathogenesis in several animal models [24]. Interestingly, CIT's action was dependent not only on SERT, its molecular target, but also on the nematode orthologs of 5-HT_{1A}R and 5-HT_{2}R, SER-4 and SER-1, respectively [24], suggesting that a post-synaptic effect of serotonin may be involved, but not excluding a pre-synaptic one.

To evaluate the dependency of the therapeutic effect of CIT, on mutant ATXN3 proteotoxicity in *C. elegans*, on other serotonin receptors we used a chemical-genetics approach [23]. Ablation of 5-HT_{6}R/SER-5 and 5-HT_{7}R/SER-7 receptors in mutant ATXN3-expressing animals attenuated the positive impact of CIT on the motor dysfunction of the animals, suggesting at least a partial contribution of these receptors (Figure 2A and B). In contrast, absence of MOD-1, the nematode specific channel-gated serotonin receptor, still allows the action of CIT (Figure 2C). Taken together, these results pointed out a contribution of all serotonin GPCRs to the action of this drug suggesting a role of these receptors in the suppression of MJD pathogenesis in *C. elegans*.

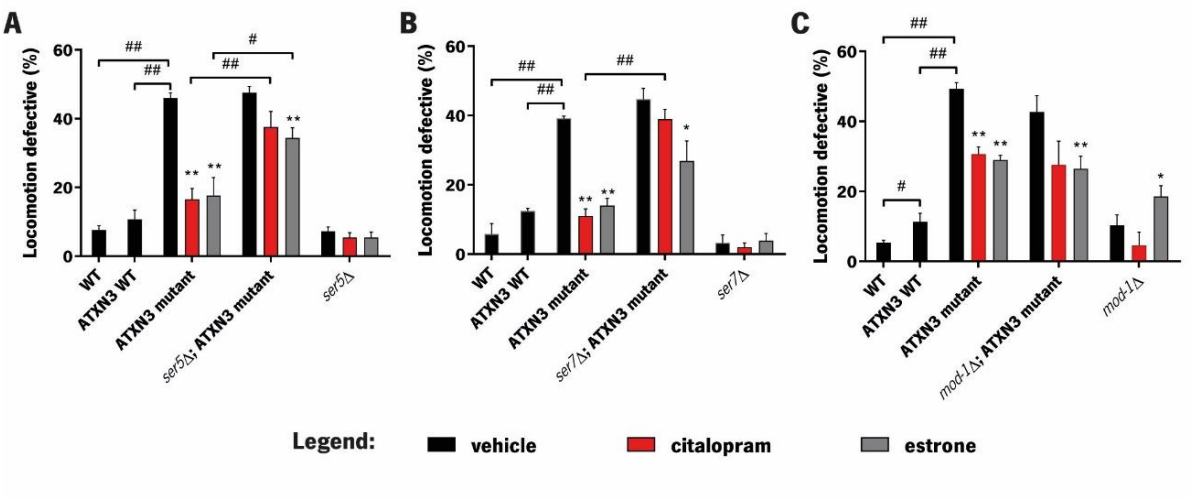

Figure 2. The effect of citalopram in the amelioration of motor dysfunction of AT3q130 animals is partially dependent on the G protein-coupled receptors SER-5 and SER-7 in *C. elegans*.

The amelioration of motor dysfunction by citalopram (CIT) was evaluated in mutant ATXN3-expressing animals lacking 5-HTRs. In the absence of **(A)** SER-5 and **(B)** SER-7, CIT (red bar) no longer significantly suppressed motor dysfunction **(C)** its effect being unchanged in the absence of the only channel gate 5-HTR in *C. elegans* MOD-1. Treatment with estrone, a steroid hormone, attenuated motor dysfunction of ATXN3 mutant animals even in the absence of 5-HTRs (grey bar), since its action is independent of serotonin receptors. (n = 3–4, ± SD), *P<0.05, **P<0.01, ***P<0.001 comparing drug treatment with vehicle, #P<0.05, ##P<0.01, ###P<0.001 comparing strain effect within the same drug treatment (Factorial ANOVA, Sidak test corrected for BCA).

3.2. Chronic antagonism of 5-HT$_2$R/SER-1, 5-HT$_6$R/SER-5 and 5-HT$_7$R/SER-7 alone, but not agonism nor inverse agonism, are sufficient to ameliorate motor dysfunction of the ATXN3-proteotoxicity C. elegans model

To further explore the role of 5-HTRs on the suppression of MJD pathogenesis, we used tool compounds, acting as agonists, antagonists or inverse agonists, chosen among those previously described as being specific and potent drugs for each serotonin receptor in mammals. In the previous chapter, we described the role of 5-HT$_{1A}$R/SER-4 using befiradol. This compound proved to be a potent and selective agonist of 5-HT$_{1A}$R/SER-4 receptors in *C. elegans* [23]. Furthermore, we showed that SER-4 heteroreceptor activation by befiradol, and the probable desensitisation of SER-4 autoreceptor by chronic exposure to this compound, impacted on ATXN3 aggregation and ameliorated motor dysfunction of mutant ATXN3-expressing animals [23], suggesting that modulation of 5-HT$_{1A}$R/SER-4 activity *per se* suppressed MJD pathogenesis.

Similarly, to investigate the contribution of other GPCR serotonin receptors, namely of 5-HT$_2$R/SER-1, 5-HT$_6$R/SER-5 and 5-HT$_7$R/SER-7, the following compounds were used: a) TCB-2 as an

agonist [34] and LY 266097 hydrochloride as an antagonist [32] of 5-HT_{2A}R and 5-HT_{2B}R, respectively; b) EMDT oxalate as an agonist [35] and SB 399885 hydrochloride as an antagonist [39] of 5-HT_6R; and c) LP44 as an agonist [45] and DR 4485 hydrochloride as an antagonist [43] of 5-HT_7R (Table 2).

To determine the most efficient concentration of each drug a dose-response assessment was performed. Chronic treatment over 4 days, since the egg stage to adulthood, with a 5-HT_2R/SER-1 antagonist significantly improved motor function of the animals in several concentrations (Figure 3A – red squares), displaying an overall drug efficacy of approximately 40% in all concentrations tested. In contrast, agonism of the same receptor did not impact motility of mutant ATXN3-expressing animals (Figure 3A – blue squares). Regarding 5-HT_6R/SER-5 and 5-HT_7R/SER-7, both chronic agonism and antagonism improved motor dysfunction with a drug efficacy between 20% to 40% (Figure 3B and C). However, in all cases of positive impact on motor dysfunction, we were unable to detect a clear dose-response profile for any of the drugs tested. Based on this, the concentrations that showed maximum efficacy for each drug (Table 3) were further assessed (new batch of the drugs) for their ability to ameliorate motility impairment of mutant ATXN3 animals, with simultaneous evaluation of their effect on motor behaviour of wild-type (WT) and wild-type animals expressing a non-expanded form of ATXN3 (ATXN3 WT). Chronic treatment with the most efficient concentration of agonists for all receptors, showed a limited impact on the suppression of motor dysfunction of mutant ATXN3 animals (Figure 3E and F). Conversely, chronic antagonism of 5-HT_2R/SER-1 (Figure 3D), 5-HT_6R/SER-5 (Figure 3E) and 5-HT_7R/SER-7 (Figure 3F) attenuated motor dysfunction of the animals, decreasing the percentage of locomotion defective mutant ATXN3 animals with no overall impact on the behaviour of WT and ATXN3 WT animals (Figure 3D, 3E and 3F), suggesting a disease-specific effect on motor behaviour.

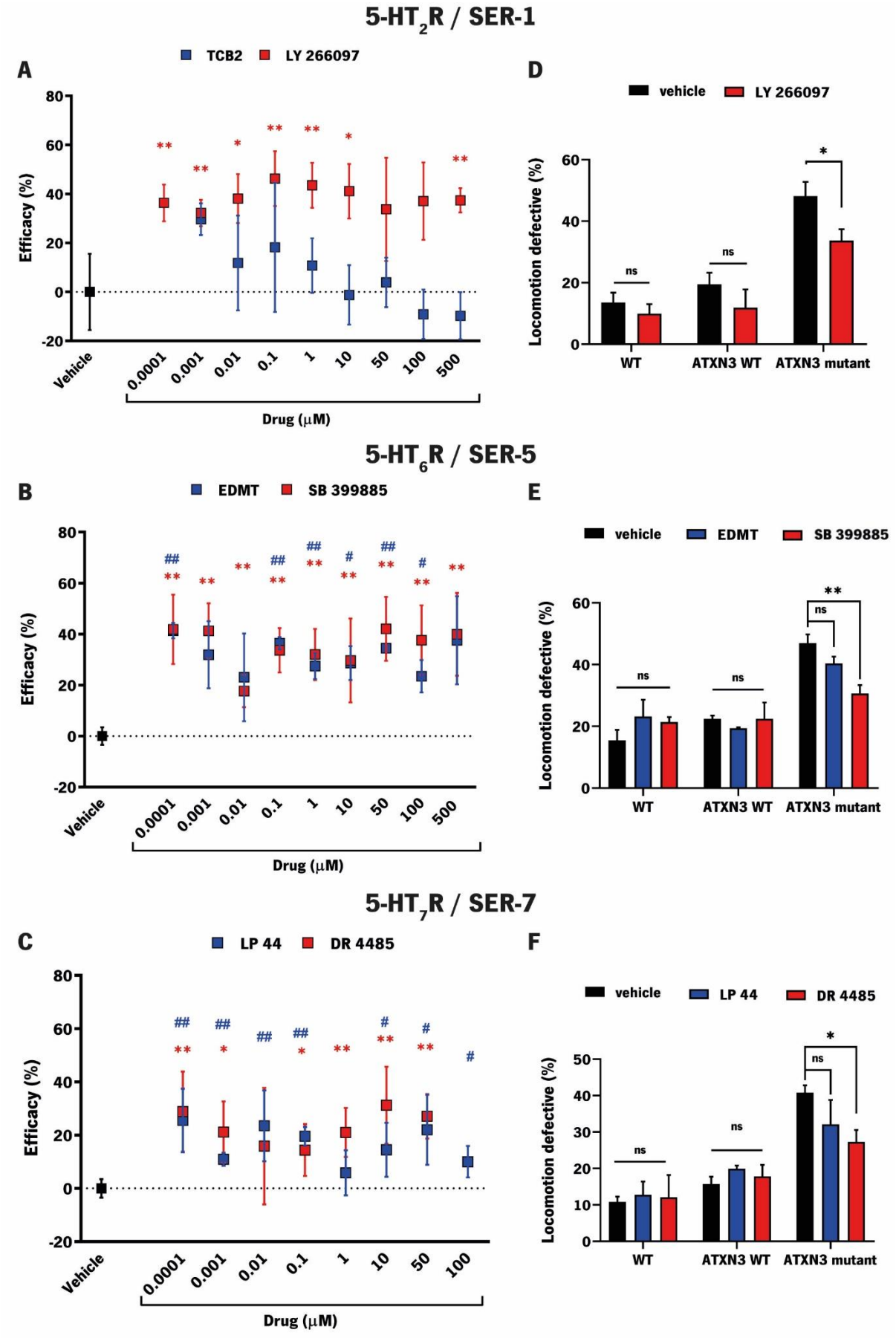
5-HT2R / SER-1
A
TCB2
LY 266097
Efficacy (%)
Vehicle
0.0001
0.001
0.01
0.1
1
10
50
100
500
Drug (μM)
D
vehicle
LY 266097
Locomotion defective (%)
ns
*
WT
ATXN3 WT
ATXN3 mutant
5-HT6R / SER-5
B
EDMT
SB 399885
E
vehicle
EDMT
SB 399885
**
5-HT7R / SER-7
C
LP 44
DR 4485
F
vehicle
LP 44
DR 4485

Figure 3. Chronic administration of antagonists, but not agonists of 5-HT$_2$R/SER-1, 5-HT$_6$R/SER-5 and 5-HT$_7$R/SER-7, ameliorates motor dysfunction of ATXN3 proteotoxicity model.

Dose-response curves of ATXN3 mutant animals treated with different concentrations of agonists (blue) and antagonists (red). **(A)** Antagonism of the 5-HT$_2$R/SER-1 positively impacted on motor dysfunction of mutant ATXN3-expressing animals in several concentrations tested, contrary to chronic treatment with an agonist. **(B)** 5-HT$_6$R/SER-5 and **(C)** 5-HT$_7$R/SER-7 treatment with agonists and antagonists ameliorated motor dysfunction of ATXN3 proteotoxicity model with an efficacy between 20% to 40%, in the absence of standard dose-response curves. The most efficient concentration of the compounds did not alter the motor behaviour of wild-type (WT) and non-expanded ATXN3 expressing animals (ATXN3 WT). Chronic treatment with antagonists, but not with agonists, of **(D)** 5-HT$_2$R/SER-1, **(E)** 5-HT$_6$R/SER-5 and **(F)** 5-HT$_7$R/SER-7 ameliorated motor dysfunction of ATXN3 mutant animals, using new drug batches. Agonist: blue squares/bars; Antagonists: red squares/bars. Statistical analysis: (A) TCB-2 (n = 3, ± SD) (ANOVA, Dunnett), LY 266097 (n = 4, ± SD) (ANOVA, Dunnett T3); (B) EDMT (n = 3, ± SD) (ANOVA, Games-Howell), SB399885 (n = 3, ± SD) (ANOVA, Sidak test corrected for BCA); (C) LP44 (n = 3, ± SD) (ANOVA, Sidak test corrected for BCA), DR 4485 (n = 3, ± SD) (ANOVA, Sidak test corrected for BCA). (D) (n =3, ± SD), ns – non significant, *P<0.05 (Two-Way ANOVA, Dunnett); (E) (n =3, ± SD), ns – non significant, **P<0.01 (Two-Way ANOVA, Dunnett); (F) (n = 5, ± SD), ns – non significant, *P<0.05 (Two-Way ANOVA, Dunnett).

Table 3. Most efficient concentration determined in dose-response curves, of each tool compound, used in the experiments summarized in figure 3.

Mammalian receptor	***C. elegans* orthologue**	**Tool compound**	**Concentration**
5-HT$_{2B}$	SER-1	LY 266097	0.1 µM
5-HT$_6$	SER-5	EMDT oxalate SB 399885 hydrochloride	50 µM 50 µM
5-HT$_7$	SER-7	LP44 DR 4485 hydrochloride	0.01 µM 10 µM

To further explore the role of 5-HT$_2$R/SER-1, 5-HT$_6$R/SER-5 and 5-HT$_7$R/SER-7 in the suppression of ATXN3 proteotoxicity, we used compounds with inverse agonism properties. MDL 100907, SB-742457 and SB-269970 were described as selective receptor blockers, with high potency on receptor binding, displaying inverse-agonism on 5-HT$_{2A}$R, 5-HT$_6$R and 5-HT$_7$R, respectively [11; 37; 40; 44].

In contrast with what was observed for 5-HT$_2$R/SER-1, 5-HT$_6$R/SER-5 and 5-HT$_7$R/SER-7 antagonists (LY 266097, SB 399885 and DR 4485 respectively), the inverse agonists used failed to impact the motor deficits of the animals at the three concentrations tested (Figure 4).

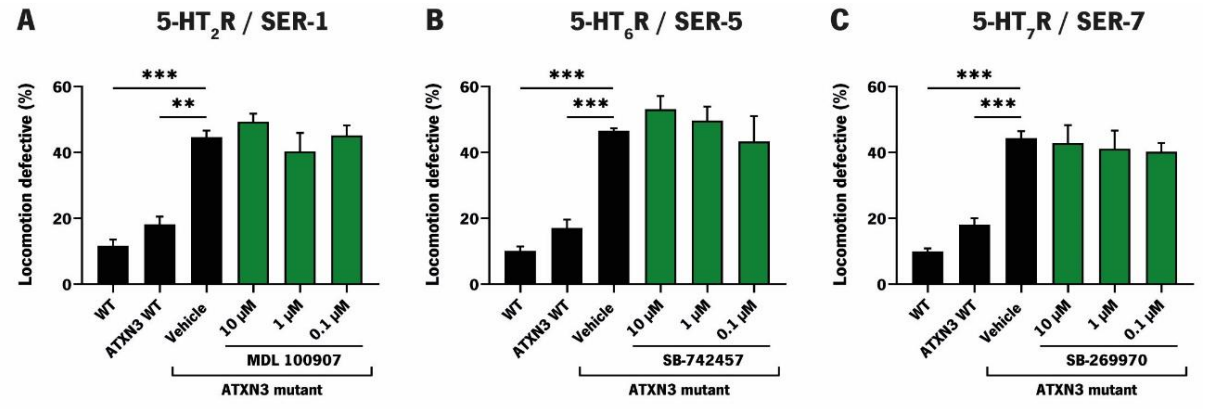

Figure 4. Chronic administration of 5-HT$_2$R/SER-1, 5-HT$_6$R/SER-5 and 5-HT$_7$R/SER-7 inverse agonists fail to impact motor dysfunction on ATXN3 mutant animals.

Egg stage to adulthood treatment of ATXN3 mutant animals with **(A)** 5-HT$_2$R/SER-1 inverse agonist, MLD 100907, **(B)** 5-HT$_6$R/SER-5 inverse agonist, SB-742457 or **(C)** 5-HT$_7$R/SER-7 inverse agonist, SB-269970 had no impact on locomotion with 10 µM, 1 µM and 0.1 µM concentration. (A) (n = 4, ± SEM), **P<0.01, ***P<0.001 (ANOVA, Dunnett). (B) (n = 3, ± SEM), ***P<0.001 (ANOVA, Dunnett). (C) (n = 4, ± SEM), ***P<0.001 (ANOVA, Dunnett).

3.3. Acute administration of 5-HT$_2$R/SER-1 antagonist, LY 266097, ameliorates motor dysfunction of ATXN3 mutant nematodes

Chronic administration of several drugs can lead to the desensitization of the receptors, as has been previously shown extensively [23; 55; 56; 57; 58; 59]. Therefore, we acutely treated the ATXN3 proteotoxicity model (ATXN3 mutant) with the most efficient concentration of 5-HT$_2$R/SER-1, 5-HT$_6$R/SER-5 and 5-HT$_7$R/SER-7 antagonists. The 2 hours treatment with 5-HT$_6$R/SER-5 and 5-HT$_7$R/SER-7 antagonists, SB 399885 and DR 4485, had a limited impact on motor function of mutant ATXN3 animals. However, acute administration of the 5-HT$_2$R/SER-1 antagonist LY 266097 attenuated motor deficits of the ATXN3 mutant animals, with an average efficacy of approximately 30% (Figure 5).

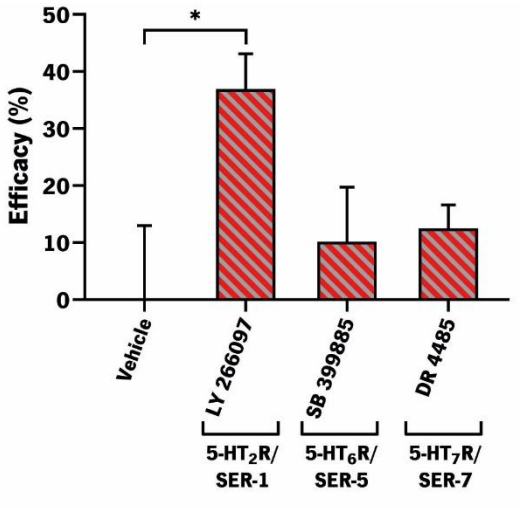

Figure 5. Acute administration of LY 266097, a 5-HT$_2$R/SER-1 antagonist, ameliorated mutant ATXN3-mediated motor dysfunction.

Acute treatment with LY 266097 decreased mutant ATXN3-mediated locomotion defects, although acute treatment with antagonists of 5-HT$_6$R/SER-5 and 5-HT$_7$R/SER-7 had a limited impact on the suppression of mutant ATXN3-induced motor dysfunction. (n = 3, ± SD) *P<0.05 (ANOVA, Dunnett).

4. Discussion

In this chapter, we started to address the role of 5-HTRs in the suppression of ATXN3-mediated proteotoxicity. Our results showed that *C. elegans* G protein-coupled serotonin receptors were indispensable for a maximal therapeutic action of citalopram (CIT). Teixeira-Castro and colleagues previously demonstrated the dependency of SER-1 and SER-4 to citalopram mediated suppression of mutant ATXN3 proteotoxicity [24]. Here, we suggested additional partial contributions of 5-HT$_6$R/SER-5 and 5-HT$_7$R/SER-7, the nematode-specific ion channel receptor MOD-1 being dispensable for this action.

Previous reports described alterations of 5-HTR activity or expression levels upon SSRI treatment. Chronic CIT administration increased the density and activity of 5-HT$_{1A}$R in the rat hippocampus and decreased 5-HT$_2$R density in the frontal cortex [60; 61], without any major changes in 5-HT$_4$R activity [61]. Regarding 5-HT$_7$R, a decrease in receptor binding in rat hypothalamus upon fluoxetine treatment was reported [62; 63]. However, other studies showed no changes in the expression levels of 5-HTRs upon prolonged SSRI treatment [64]. These apparently conflicting results likely can be explained by the different SSRIs used, treatment duration and brain areas in which the analyses were conducted.

We further explored the role of each individual 5-HTR in the suppression of ATXN3-mediated motor dysfunction, using tool compounds and a nematode model, and found that chronic antagonism of

5-HT_6R/SER-5 and 5-HT_7R/SER-7 ameliorated motor impairment of the animals, without any impact at acute administration. These results suggested that a remodelling of the serotonergic system, elicited by the chronic antagonism of 5-HT_6R/SER-5 and 5-HT_7R/SER-7 is needed for the therapeutic outcome. Interestingly, both chronic and acute antagonism of 5-HT_2R/SER-1 ameliorated motor dysfunction of ATXN3 mutant animals suggesting a more direct contribution of this receptor, probably dependent on its downstream signalling. The modulation of the serotonergic system is often associated with depression, being SSRIs the first line of treatment for this condition [65]. In the depression field, alterations in the serotonergic system, as well as anxiolytic and/or antidepressant amenability of drugs targeting 5-HTRs have been extensively described, *solo* or in combinatory therapy with SSRIs (reviewed in [66] and [67]). Paradoxically, both agonism and antagonism of 5-HT_{2C}R and 5-HT_6R elicited antidepressive like behaviour in mice or rats [68; 69; 70; 71; 72; 73; 74; 75]. This may be due to the double action of these receptors in the brain. On the one hand, stimulation of 5-HT_{2C}R and 5-HT_6R (as seen upon agonist treatment) may be an important component of the postsynaptic effects triggered by SSRI treatment. On the other hand, receptor antagonism may facilitate the release of other neurotransmitters, such as norepinephrine and dopamine, that are otherwise physiologically repressed by 5-HT_{2C}R activation, and similarly by 5-HT_6R activity [66]. In fact, the anxiolytic and antidepressive-like effects of the 5-HT_6R antagonist SB 399885 persisted in the absence of serotonin, favouring the hypothesis of an effect through the modulation of other neurotransmitters [76]. Antagonism of 5-HT_{2A}R and 5-HT_7R increased the effect of SSRIs and, alone, reduced depressive-like behaviour in mice. The mechanism through which blockage of 5-HT_{2A}R leads to amelioration of depressive symptoms is largely debated since many compounds, including MDL 100907, which display high affinity to 5-HT_{2A}R, augmented the effect of SSRIs [77]. The mechanism proposed was based on the impact, produced by the blockage of 5-HT_{2A}R, on the dopaminergic system [78]. Interestingly and in line with this hypothesis, co-administration of fluoxetine and MDL 100907 did not further increase serotonin levels in the prefrontal cortex of rats compared with fluoxetine alone, suggesting an impact of 5-HT_{2A}R antagonism outside serotonergic transmission [77]. However less explored, 5-HT_7R ablation or blockage with antagonists decreased immobility time in mouse models of depression [79; 80; 81] and potentiated the effect of CIT, increasing 5-HT concentration in the prefrontal cortex [82].

In MJD, we showed that not only CIT action was dependent on 5-HT_{1A}R/SER-4, but also that ablation or desensitization of SER-4 autoreceptor ameliorated ATXN3 proteotoxicity [23; 24], likely by increasing 5-HT availability. Furthermore, the contribution of the post-synaptic 5-HT_{1A}R/SER-4 heteroreceptors in suppression of ATXN3 proteotoxicity was shown, since activation of the SER-4 receptor, in the absence of serotonin, improved motor dysfunction and decreased ATXN3 aggregation [23].

Therefore, it is plausible that modulation of the activity of this and other 5-HT post-synaptic receptors, such as 5-HT_2R/SER-1, 5-HT_6R/SER-5 and 5-HT_7R/SER-7, could also impact on ATXN3 proteotoxicity by remodelling of the serotonergic system or by changing the release of other neurotransmitters.

Additionally, we showed here that inverse agonism of 5-HT_2R/SER-1, 5-HT_6R/SER-5 and 5-HT_7R/SER-7 - mediated by MDL 100907, SB-742457 and SB-269970, respectively [36; 47; 51; 83] - was inefficient in the suppression of the motor dysfunction seen in ATXN3 mutant animals, contrasting with the positive effect elicited by the antagonism of the same receptors (by LY 266097, SB 399885 and DR 4485). Keeping in mind that the intrinsic efficacy of an antagonist and an inverse agonist differ in the presence of a constitutive activity of the target receptors [28], our results suggest that a) *C. elegans* serotonin receptors SER-1, SER-5 and SER-7 can display constitutive activity *in vivo*, consistent with what was previously reported for SER-7 *in vitro* [21], and b) only a partial suppression of the activity of these receptors was beneficial for the suppression of ATXN3 proteotoxicity, the constitutive activity of the receptor being needed. However, the unspecific targeting of other receptor types, in *C. elegans*, by the antagonists LY 266097, SB 399885 and DR 4485, that elicited the positive effect in MJD pathogenesis, cannot be discarded. For that reason, although promising, the results presented here should be interpreted carefully and additional experiments are required to validate this hypothesis.

The selected tool compounds used in this study generally presented high affinity and selectivity to mammalian 5-HTRs. In functional studies, EMDT oxalate was demonstrated to behave as a 5-HT_6R agonist, with a potency equivalent to serotonin, and a reasonable selectivity profile versus other receptors, having 10- to 18-fold more selectivity to 5-HT_6R than other 5-HTRs [35; 41]. On the other hand, the 5-HT_6R antagonist and inverse agonist, SB 399885 and SB-742457, both present high affinity to 5-HT_6R receptor, the latter being the most potent (K_i = 0.28 nM) [39; 51]. Although both compounds displayed high selectivity (200-fold) to 5-HT_6R compared to other receptors [39], SB-742457 also presented some low affinity to 5-HT_{2A}R (K_i = 26 nM, 90-fold than 5-HT_6), and an inverse agonist profile for 5-HT_6R [36; 51].

For 5-HT_7R, LP44 is a potent receptor agonist with a K_i of 0.22 nM and a EC_{50} of 2.56 μM. This compound presents a 200-fold higher selectivity to 5-HT_7R over 5-HT_{1A}R and 1000-fold over 5-HT_{2A}R [45; 48]. However, the antagonist, DR 4485 presented high affinity to 5-HT_7R (K_i = 7.24 nM) but also some low affinity for the 5-HT_{1A}R (K_i = 316 nM, 40-fold than 5-HT_7R) [43; 50]. The inverse agonist of 5-HT_7R SB-269970 [30; 47] presents high potency (K_i = 1.3 nM) and a 250-fold selectivity to 5-HT_7R comparing with other receptors, except for 5-HT_{5A}R (50-fold) [37; 46].

For 5-HT_2R, both the antagonist and the inverse agonist compounds used in this study proved to be potent and specific in mammals [42; 49]. LY 266097 possesses high affinity for the 5-HT_{2B}R and at least 100-fold selectivity over the 5-HT_{2A}R and 5-HT_{2C}R, as well as over numerous other receptors [31; 32]. MDL 100907 displays a K_i of 0.36 nM for 5-HT_{2A}R and at least 200-fold selectivity to this over other receptors, such as 5-HT_{1A}R, 5-HT_{2C}R, D_2R or α_1R [38]. TCB-2, the 5-HT_{2A}R agonist, presents high potency to the receptor [34], although the pharmacological interactions of this compound with other receptors were never explored deeply (reviewed in [33]) and some affinity to the other 5-HT_2 subtypes, at least, cannot be discarded. Therefore, and since *C. elegans* has a single orthologue for all 5-HT_2 subtypes, the SER-1 receptor [52], a specific characterization of the binding and activation profile of this tool compound in the nematode model is needed.

As in this work, studies of receptor activity and cellular pathway characterization relies on tool compounds that should be potent and selective for the receptor but also have a proven mechanism of action [27]. Although the antagonists that impact ATXN3 proteotoxicity are potent and specific for 5-HT_2R, 5-HT_6R and 5-HT_7R mammalian receptors (LY 266097, SB-399885 and DR4485 respectively) the specificity of these drugs is model organism-dependent, since its mode of action can vary among species. In the case of DR 4485, the possible effect through its weak affinity to 5-HT_{1A}R could not be excluded in *C. elegans*. Therefore, in the future further studies are needed to confirm the contribution of 5-HT excitatory receptors to the suppression of ATXN3 proteotoxicity in *C. elegans* and to determine which molecular pathways mediate the beneficial effect.

Future experiments

To address these issues, we propose, in the future, to 1) using heterologous expression systems, evaluate the affinity and specificity of the ligation of the tool compounds to *C. elegans* serotonin receptors; 2) using pharmacogenetic approaches and competition pharmacotherapeutic assays, evaluate the contribution of each receptor-drug pair to the amelioration of ATXN3-mediated motor dysfunction and 3) by qRT-PCR and Western blot analysis or broader transcriptomic/ proteomic analysis techniques explore *in vivo* the activation of specific pathways upon serotonin receptor activation.

To explore the specificity of the ligation of the tool compounds to *C. elegans* receptors, a thermal stability shift assay conjugated with protein identification can be used. In this technique, drug-treated and vehicle-treated cells are subjected to a series of increasing temperatures. Cells are collected and lysed, the soluble proteome being conjugated with fluorophores to distinguish the treated and non-treated

proteomes. After a 2D gel electrophoresis, proteins that presented a thermal shift, that represents protein stabilization by drug-receptor engagement, will be excised from the gel and identified by mass-spectrometry [84]. This would allow a full characterization of the possible drug targets on the nematode *C. elegans*. Additionally, and to determine the association and potency of binding of each drug to the receptors we could use Tag-lite® assay platform (Cisbio), a HTRF based assay [85]. This *in vitro* system allows not only the study of the engagement of the serotonergic *C. elegans* receptors with each drug but also the measurement of GPCR activation products in canonical and non-canonical pathways (as Ca^{+}, cAMP, AKT and MAPK phosphorylation, etc).

After the validation of the specificity of the tool compounds' target receptor in *C. elegans*, the contribution of the receptor activation or inactivation by the drug to the suppression of MJD pathogenesis can be evaluated *in vivo* by pharmacogenetics or competition pharmacological assays, using specific agonists and antagonists, as previously described [23; 24]. Furthermore, the evaluation of the pathways elicited by drug treatment *in vivo* can be done by qRT-PCR or Western blot by measuring gene expression changes or protein phosphorylation of key molecules associated to each receptor. With these experiments we will be able to assess drug-receptor specificity and discriminate the biological molecular pathways involved in the suppression of ATXN3 proteotoxicity in *C. elegans*.

Acknowledgments

We are grateful to members of the Maciel laboratory for sharing reagents, for critical analysis of the data and results discussion. Thanks to the *Caenorhabditis Genetics Center* (CGC), which is funded by NIH Office of Research Infrastructure Programs (P40 OD010440) for providing some of the nematode strains used in this study.

Funding

This work was funded by FEDER, through the Competitiveness Internationalization Operational Programme (POCI), and by National funds, through the Foundation for Science and Technology (FCT), under the scope of the project POCI-01-0145-FEDER-031987, NORTE-010145-FEDER-000013 and NORTE-01-0145-FEDER-000023, supported by the Northern Portugal Regional Operational Programme (NORTE 2020), under the Portugal 2020 Partnership Agreement, through the European Regional Development Fund (ERDF); by National funds, through the Foundation for Science and Technology (FCT) - project UIDB/50026/2020 and UIDP/50026/2020. Additionally, this project was supported by

National Ataxia Foundation (NAF) and the FCT individual fellowship PD/BDE/127834/2016 (For Pereira-Sousa, J).

References

[1] D.M. Kuhn, and H. Hasegawa, Chapter 12 - Tryptophan hydroxylase and serotonin synthesis regulation. in: C.P. Müller, and K.A. Cunningham, (Eds.), Handbook of Behavioral Neuroscience, Elsevier, 2020, pp. 239-256.Book Section doi: 10.1016/B978-0-444-64125-0.00012-8.

[2] V. Erspamer, and B. Asero, Identification of enteramine, the specific hormone of the enterochromaffin cell system, as 5-hydroxytryptamine. Nature 169 (1952) 800-1. doi: 10.1038/169800b0.

[3] P.P. Bertrand, and R.L. Bertrand, Serotonin release and uptake in the gastrointestinal tract. Auton Neurosci 153 (2010) 47-57. doi: 10.1016/j.autneu.2009.08.002.

[4] T. Audhya, J.B. Adams, and L. Johansen, Correlation of serotonin levels in CSF, platelets, plasma, and urine. Biochim Biophys Acta 1820 (2012) 1496-501. doi: 10.1016/j.bbagen.2012.05.012.

[5] A. Parent, L. Descarries, and A. Beaudet, Organization of ascending serotonin systems in the adult rat brain. A radioautographic study after intraventricular administration of [3H]5-hydroxytryptamine. Neuroscience 6 (1981) 115-38. doi: 10.1016/0306-4522(81)90050-6.

[6] E.C. Azmitia, and M. Segal, An autoradiographic analysis of the differential ascending projections of the dorsal and median raphe nuclei in the rat. J Comp Neurol 179 (1978) 641-67. doi: 10.1002/cne.901790311.

[7] B.L. Jacobs, and E.C. Azmitia, Structure and function of the brain serotonin system. Physiol Rev 72 (1992) 165-229. doi: 10.1152/physrev.1992.72.1.165.

[8] T. Sharp, and N.M. Barnes, Central 5-HT receptors and their function; present and future. Neuropharmacology 177 (2020) 108155. doi: 10.1016/j.neuropharm.2020.108155.

[9] J. Bockaert, S. Claeysen, A. Dumuis, and P. Marin, CHAPTER 1.5 - Classification and Signaling Characteristics of 5-HT Receptors. in: C.P. Müller, and B.L. Jacobs, (Eds.), Handbook of Behavioral Neuroscience, Elsevier, 2010, pp. 103-121.Book Section doi: 10.1016/S1569-7339(10)70073-4.

[10] M.J. Millan, P. Marin, J. Bockaert, and C. Mannoury la Cour, Signaling at G-protein-coupled serotonin receptors: recent advances and future research directions. Trends Pharmacol Sci 29 (2008) 454-64. doi: 10.1016/j.tips.2008.06.007.

[11] P. De Deurwaerdere, R. Bharatiya, A. Chagraoui, and G. Di Giovanni, Constitutive activity of 5-HT receptors: Factual analysis. Neuropharmacology 168 (2020) 107967. doi: 10.1016/j.neuropharm.2020.107967.

[12] M. Noda, H. Higashida, S. Aoki, and K. Wada, Multiple signal transduction pathways mediated by 5-HT receptors. Mol Neurobiol 29 (2004) 31-9. doi: 10.1385/MN:29:1:31.

[13] A. Montalbano, R. Corradetti, and B. Mlinar, Pharmacological Characterization of 5-HT1A Autoreceptor-Coupled GIRK Channels in Rat Dorsal Raphe 5-HT Neurons. PLoS One 10 (2015) e0140369. doi: 10.1371/journal.pone.0140369.

[14] K.A. Berg, S. Maayani, J. Goldfarb, C. Scaramellini, P. Leff, and W.P. Clarke, Effector pathway-dependent relative efficacy at serotonin type 2A and 2C receptors: evidence for agonist-directed trafficking of receptor stimulus. Mol Pharmacol 54 (1998) 94-104. doi: 10.1124/mol.54.1.94.

[15] D. Hoyer, D.E. Clarke, J.R. Fozard, P.R. Hartig, G.R. Martin, E.J. Mylecharane, P.R. Saxena, and P.P. Humphrey, International Union of Pharmacology classification of receptors for 5-hydroxytryptamine (Serotonin). Pharmacol Rev 46 (1994) 157-203. http://www.ncbi.nlm.nih.gov/pubmed/7938165

[16] D. Hoyer, J.P. Hannon, and G.R. Martin, Molecular, pharmacological and functional diversity of 5-HT receptors. Pharmacol Biochem Behav 71 (2002) 533-54. doi: 10.1016/s0091-3057(01)00746-8.

[17] D.L. Chase, and M.R. Koelle, Biogenic amine neurotransmitters in C. elegans. WormBook (2007) 1-15. doi: 10.1895/wormbook.1.132.1.

[18] B. Olde, and W.R. McCombie, Molecular cloning and functional expression of a serotonin receptor from Caenorhabditis elegans. Journal of Molecular Neuroscience : MN 8 (1997) 53-62. doi: 10.1007/bf02736863.

[19] F.F. Hamdan, M.D. Ungrin, M. Abramovitz, and P. Ribeiro, Characterization of a novel serotonin receptor from Caenorhabditis elegans: cloning and expression of two splice variants. J Neurochem 72 (1999) 1372-83. doi: 10.1046/j.1471-4159.1999.721372.x.

[20] G.P. Harris, V.M. Hapiak, R.T. Wragg, S.B. Miller, L.J. Hughes, R.J. Hobson, R. Steven, B. Bamber, and R.W. Komuniecki, Three distinct amine receptors operating at different levels within the locomotory circuit are each essential for the serotonergic modulation of chemosensation in Caenorhabditis elegans. J Neurosci 29 (2009) 1446-56. doi: 10.1523/JNEUROSCI.4585-08.2009.

[21] R.J. Hobson, J. Geng, A.D. Gray, and R.W. Komuniecki, SER-7b, a constitutively active Galphas coupled 5-HT7-like receptor expressed in the Caenorhabditis elegans M4 pharyngeal motorneuron. J Neurochem 87 (2003) 22-9. doi: 10.1046/j.1471-4159.2003.01967.x.

[22] R. Ranganathan, S.C. Cannon, and H.R. Horvitz, MOD-1 is a serotonin-gated chloride channel that modulates locomotory behaviour in C. elegans. Nature 408 (2000) 470-5. doi: 10.1038/35044083.

[23] J. Pereira-Sousa, B. Ferreira-Lomba, A. Bellver-Sanchis, D. Vilasboas-Campos, J.H. Fernandes, M.D. Costa, M.A. Varney, A. Newman-Tancredi, P. Maciel, and A. Teixeira-Castro, Identification of the 5-HT1A serotonin receptor as a novel therapeutic target in a C. elegans model of Machado-Joseph disease. Neurobiol Dis (2021) 105278. doi: 10.1016/j.nbd.2021.105278.

[24] A. Teixeira-Castro, A. Jalles, S. Esteves, S. Kang, L. da Silva Santos, A. Silva-Fernandes, M.F. Neto, R.M. Brielmann, C. Bessa, S. Duarte-Silva, A. Miranda, S. Oliveira, A. Neves-Carvalho, J. Bessa, T. Summavielle, R.B. Silverman, P. Oliveira, R.I. Morimoto, and P. Maciel, Serotonergic signalling suppresses ataxin 3 aggregation and neurotoxicity in animal models of Machado-Joseph disease. Brain 138 (2015) 3221-37. doi: 10.1093/brain/awv262.

[25] F.C. Colpaert, J.P. Tarayre, W. Koek, P.J. Pauwels, L. Bardin, X.J. Xu, Z. Wiesenfeld-Hallin, C. Cosi, E. Carilla-Durand, M.B. Assie, and B. Vacher, Large-amplitude 5-HT1A receptor activation: a new mechanism of profound, central analgesia. Neuropharmacology 43 (2002) 945-58. doi: 10.1016/s0028-3908(02)00119-3.

[26] A. Newman-Tancredi, J.C. Martel, C. Cosi, P. Heusler, F. Lestienne, M.A. Varney, and D. Cussac, Distinctive in vitro signal transduction profile of NLX-112, a potent and efficacious serotonin 5-HT1A receptor agonist. J Pharm Pharmacol 69 (2017) 1178-1190. doi: 10.1111/jphp.12762.

[27] C.H. Arrowsmith, J.E. Audia, C. Austin, J. Baell, J. Bennett, J. Blagg, C. Bountra, P.E. Brennan, P.J. Brown, M.E. Bunnage, C. Buser-Doepner, R.M. Campbell, A.J. Carter, P. Cohen, R.A. Copeland, B. Cravatt, J.L. Dahlin, D. Dhanak, A.M. Edwards, M. Frederiksen, S.V. Frye, N. Gray, C.E. Grimshaw, D. Hepworth, T. Howe, K.V. Huber, J. Jin, S. Knapp, J.D. Kotz, R.G. Kruger, D. Lowe, M.M. Mader, B. Marsden, A. Mueller-Fahrnow, S. Muller, R.C. O'Hagan, J.P. Overington, D.R. Owen, S.H. Rosenberg, B. Roth, R. Ross, M. Schapira, S.L. Schreiber, B. Shoichet, M. Sundstrom, G. Superti-Furga, J. Taunton, L. Toledo-Sherman, C. Walpole, M.A. Walters, T.M. Willson, P. Workman, R.N. Young, and W.J. Zuercher, The promise and peril of chemical probes. Nat Chem Biol 11 (2015) 536-41. doi: 10.1038/nchembio.1867.

[28] K.A. Berg, and W.P. Clarke, Making Sense of Pharmacology: Inverse Agonism and Functional Selectivity. Int J Neuropsychopharmacol 21 (2018) 962-977. doi: 10.1093/ijnp/pyy071.
[29] S. Brenner, The genetics of Caenorhabditis elegans. Genetics 77 (1974) 71-94. http://www.ncbi.nlm.nih.gov/pubmed/4366476
[30] K.W. Andressen, O. Manfra, C.H. Brevik, A.H. Ulsund, P. Vanhoenacker, F.O. Levy, and K.A. Krobert, The atypical antipsychotics clozapine and olanzapine promote down-regulation and display functional selectivity at human 5-HT7 receptors. Br J Pharmacol 172 (2015) 3846-60. doi: 10.1111/bph.13169.
[31] J.E. Audia, D.A. Evrard, G.R. Murdoch, J.J. Droste, J.S. Nissen, K.W. Schenck, P. Fludzinski, V.L. Lucaites, D.L. Nelson, and M.L. Cohen, Potent, selective tetrahydro-beta-carboline antagonists of the serotonin 2B (5HT2B) contractile receptor in the rat stomach fundus. J Med Chem 39 (1996) 2773-80. doi: 10.1021/jm960062t.
[32] D. Cussac, A. Newman-Tancredi, Y. Quentric, N. Carpentier, G. Poissonnet, J.G. Parmentier, S. Goldstein, and M.J. Millan, Characterization of phospholipase C activity at h5-HT2C compared with h5-HT2B receptors: influence of novel ligands upon membrane-bound levels of [3H]phosphatidylinositols. Naunyn Schmiedebergs Arch Pharmacol 365 (2002) 242-52. doi: 10.1007/s00210-001-0505-y.
[33] G. Di Giovanni, and P. De Deurwaerdere, TCB-2 [(7R)-3-bromo-2, 5-dimethoxy-bicyclo[4.2.0]octa-1,3,5-trien-7-yl]methanamine]: A hallucinogenic drug, a selective 5-HT2A receptor pharmacological tool, or none of the above? Neuropharmacology 142 (2018) 20-29. doi: 10.1016/j.neuropharm.2017.10.004.
[34] M.A. Fox, H.T. French, J.L. LaPorte, A.R. Blackler, and D.L. Murphy, The serotonin 5-HT(2A) receptor agonist TCB-2: a behavioral and neurophysiological analysis. Psychopharmacology (Berl) 212 (2010) 13-23. doi: 10.1007/s00213-009-1694-1.
[35] R.A. Glennon, M. Lee, J.B. Rangisetty, M. Dukat, B.L. Roth, J.E. Savage, A. McBride, L. Rauser, S. Hufeisen, and D.K. Lee, 2-Substituted tryptamines: agents with selectivity for 5-HT(6) serotonin receptors. J Med Chem 43 (2000) 1011-8. doi: 10.1021/jm990550b.
[36] K. Grychowska, G. Satala, T. Kos, A. Partyka, E. Colacino, S. Chaumont-Dubel, X. Bantreil, A. Wesolowska, M. Pawlowski, J. Martinez, P. Marin, G. Subra, A.J. Bojarski, F. Lamaty, P. Popik, and P. Zajdel, Novel 1H-Pyrrolo[3,2-c]quinoline Based 5-HT6 Receptor Antagonists with Potential Application for the Treatment of Cognitive Disorders Associated with Alzheimer's Disease. ACS Chem Neurosci 7 (2016) 972-83. doi: 10.1021/acschemneuro.6b00090.
[37] J.J. Hagan, G.W. Price, P. Jeffrey, N.J. Deeks, T. Stean, D. Piper, M.I. Smith, N. Upton, A.D. Medhurst, D.N. Middlemiss, G.J. Riley, P.J. Lovell, S.M. Bromidge, and D.R. Thomas, Characterization of SB-269970-A, a selective 5-HT(7) receptor antagonist. Br J Pharmacol 130 (2000) 539-48. doi: 10.1038/sj.bjp.0703357.
[38] M.M. Herth, V. Kramer, M. Piel, M. Palner, P.J. Riss, G.M. Knudsen, and F. Rosch, Synthesis and in vitro affinities of various MDL 100907 derivatives as potential 18F-radioligands for 5-HT2A receptor imaging with PET. Bioorg Med Chem 17 (2009) 2989-3002. doi: 10.1016/j.bmc.2009.03.021.
[39] W.D. Hirst, T.O. Stean, D.C. Rogers, D. Sunter, P. Pugh, S.F. Moss, S.M. Bromidge, G. Riley, D.R. Smith, S. Bartlett, C.A. Heidbreder, A.R. Atkins, L.P. Lacroix, L.A. Dawson, A.G. Foley, C.M. Regan, and N. Upton, SB-399885 is a potent, selective 5-HT6 receptor antagonist with cognitive enhancing properties in aged rat water maze and novel object recognition models. Eur J Pharmacol 553 (2006) 109-19. doi: 10.1016/j.ejphar.2006.09.049.
[40] M.P. Johnson, B.W. Siegel, and A.A. Carr, [3H]MDL 100,907: a novel selective 5-HT2A receptor ligand. Naunyn Schmiedebergs Arch Pharmacol 354 (1996) 205-9. doi: 10.1007/BF00178722.

[41] D. Karila, T. Freret, V. Bouet, M. Boulouard, P. Dallemagne, and C. Rochais, Therapeutic Potential of 5-HT6 Receptor Agonists. J Med Chem 58 (2015) 7901-12. doi: 10.1021/acs.jmedchem.5b00179.

[42] J.H. Kehne, B.M. Baron, A.A. Carr, S.F. Chaney, J. Elands, D.J. Feldman, R.A. Frank, P.L. van Giersbergen, T.C. McCloskey, M.P. Johnson, D.R. McCarty, M. Poirot, Y. Senyah, B.W. Siegel, and C. Widmaier, Preclinical characterization of the potential of the putative atypical antipsychotic MDL 100,907 as a potent 5-HT2A antagonist with a favorable CNS safety profile. J Pharmacol Exp Ther 277 (1996) 968-81. http://www.ncbi.nlm.nih.gov/pubmed/8627580

[43] C. Kikuchi, H. Suzuki, T. Hiranuma, and M. Koyama, New tetrahydrobenzindoles as potent and selective 5-HT(7) antagonists with increased In vitro metabolic stability. Bioorg Med Chem Lett 13 (2003) 61-4. doi: 10.1016/s0960-894x(02)00842-9.

[44] H. Kristiansen, B. Elfving, P. Plenge, L.H. Pinborg, N. Gillings, and G.M. Knudsen, Binding characteristics of the 5-HT2A receptor antagonists altanserin and MDL 100907. Synapse 58 (2005) 249-57. doi: 10.1002/syn.20205.

[45] M. Leopoldo, F. Berardi, N.A. Colabufo, M. Contino, E. Lacivita, M. Niso, R. Perrone, and V. Tortorella, Structure-affinity relationship study on N-(1,2,3,4-tetrahydronaphthalen-1-yl)-4-aryl-1-piperazinealkylamides, a new class of 5-hydroxytryptamine7 receptor agents. J Med Chem 47 (2004) 6616-24. doi: 10.1021/jm049702f.

[46] P.J. Lovell, S.M. Bromidge, S. Dabbs, D.M. Duckworth, I.T. Forbes, A.J. Jennings, F.D. King, D.N. Middlemiss, S.K. Rahman, D.V. Saunders, L.L. Collin, J.J. Hagan, G.J. Riley, and D.R. Thomas, A novel, potent, and selective 5-HT(7) antagonist: (R)-3-(2-(2-(4-methylpiperidin-1-yl)ethyl)pyrrolidine-1-sulfonyl) phen ol (SB-269970). J Med Chem 43 (2000) 342-5. doi: 10.1021/jm991151j.

[47] C. Mahe, E. Loetscher, D. Feuerbach, W. Muller, M.P. Seiler, and P. Schoeffter, Differential inverse agonist efficacies of SB-258719, SB-258741 and SB-269970 at human recombinant serotonin 5-HT7 receptors. Eur J Pharmacol 495 (2004) 97-102. doi: 10.1016/j.ejphar.2004.05.033.

[48] J.M. Monti, M. Leopoldo, and H. Jantos, The serotonin 5-HT7 receptor agonist LP-44 microinjected into the dorsal raphe nucleus suppresses REM sleep in the rat. Behav Brain Res 191 (2008) 184-9. doi: 10.1016/j.bbr.2008.03.025.

[49] M.G. Palfreyman, C.J. Schmidt, S.M. Sorensen, M.W. Dudley, J.H. Kehne, P. Moser, M.W. Gittos, and A.A. Carr, Electrophysiological, biochemical and behavioral evidence for 5-HT2 and 5-HT3 mediated control of dopaminergic function. Psychopharmacology (Berl) 112 (1993) S60-7. doi: 10.1007/BF02245008.

[50] S.L. Thirumaran, A. Lepailleur, and C. Rochais, Structure-activity relationships of serotonin 5-HT7 receptors ligands: A review. Eur J Med Chem 183 (2019) 111705. doi: 10.1016/j.ejmech.2019.111705.

[51] D. Vanda, M. Soural, V. Canale, S. Chaumont-Dubel, G. Satala, T. Kos, P. Funk, V. Fulopova, B. Lemrova, P. Koczurkiewicz, E. Pekala, A.J. Bojarski, P. Popik, P. Marin, and P. Zajdel, Novel non-sulfonamide 5-HT6 receptor partial inverse agonist in a group of imidazo[4,5-b]pyridines with cognition enhancing properties. Eur J Med Chem 144 (2018) 716-729. doi: 10.1016/j.ejmech.2017.12.053.

[52] W. Kim, R.S. Underwood, I. Greenwald, and D.D. Shaye, OrthoList 2: A New Comparative Genomic Analysis of Human and Caenorhabditis elegans Genes. Genetics 210 (2018) 445-461. doi: 10.1534/genetics.118.301307.

[53] C. Voisine, H. Varma, N. Walker, E.A. Bates, B.R. Stockwell, and A.C. Hart, Identification of potential therapeutic drugs for huntington's disease using Caenorhabditis elegans. PLoS One 2 (2007) e504. doi: 10.1371/journal.pone.0000504.

[54] A. Teixeira-Castro, M. Ailion, A. Jalles, H.R. Brignull, J.L. Vilaca, N. Dias, P. Rodrigues, J.F. Oliveira, A. Neves-Carvalho, R.I. Morimoto, and P. Maciel, Neuron-specific proteotoxicity of mutant ataxin-3 in C. elegans: rescue by the DAF-16 and HSF-1 pathways. Hum Mol Genet 20 (2011) 2996-3009. doi: 10.1093/hmg/ddr203.

[55] N.J. Freedman, and R.J. Lefkowitz, Desensitization of G protein-coupled receptors. Recent Prog Horm Res 51 (1996) 319-51; discussion 352-3. http://www.ncbi.nlm.nih.gov/pubmed/8701085

[56] S. Allouche, F. Noble, and N. Marie, Opioid receptor desensitization: mechanisms and its link to tolerance. Front Pharmacol 5 (2014) 280. doi: 10.3389/fphar.2014.00280.

[57] D.E. Felsing, C.E. Canal, and R.G. Booth, Ligand-directed serotonin 5-HT2C receptor desensitization and sensitization. Eur J Pharmacol 848 (2019) 131-139. doi: 10.1016/j.ejphar.2019.01.037.

[58] S.M. Stahl, Mechanism of action of serotonin selective reuptake inhibitors. Serotonin receptors and pathways mediate therapeutic effects and side effects. J Affect Disord 51 (1998) 215-35. doi: 10.1016/s0165-0327(98)00221-3.

[59] M. Yamauchi, T. Miyara, T. Matsushima, and T. Imanishi, Desensitization of 5-HT2A receptor function by chronic administration of selective serotonin reuptake inhibitors. Brain Res 1067 (2006) 164-9. doi: 10.1016/j.brainres.2005.10.075.

[60] V. Klimek, J. Zak-Knapik, and M. Mackowiak, Effects of repeated treatment with fluoxetine and citalopram, 5-HT uptake inhibitors, on 5-HT1A and 5-HT2 receptors in the rat brain. J Psychiatry Neurosci 19 (1994) 63-7. http://www.ncbi.nlm.nih.gov/pubmed/8148368

[61] B. Bobula, K. Tokarski, A. Zahorodna, and G. Hess, Adaptive changes in the reactivity of 5-HT1A and 5-HT2 receptors induced in rat frontal cortex by repeated imipramine and citalopram. Naunyn Schmiedebergs Arch Pharmacol 367 (2003) 444-50. doi: 10.1007/s00210-003-0744-1.

[62] A.J. Sleight, C. Carolo, N. Petit, C. Zwingelstein, and A. Bourson, Identification of 5-hydroxytryptamine7 receptor binding sites in rat hypothalamus: sensitivity to chronic antidepressant treatment. Mol Pharmacol 47 (1995) 99-103. http://www.ncbi.nlm.nih.gov/pubmed/7838138

[63] U.L. Mullins, G. Gianutsos, and A.S. Eison, Effects of antidepressants on 5-HT7 receptor regulation in the rat hypothalamus. Neuropsychopharmacology 21 (1999) 352-67. doi: 10.1016/S0893-133X(99)00041-X.

[64] J.M. Massou, C. Trichard, D. Attar-Levy, A. Feline, E. Corruble, B. Beaufils, and J.L. Martinot, Frontal 5-HT2A receptors studied in depressive patients during chronic treatment by selective serotonin reuptake inhibitors. Psychopharmacology (Berl) 133 (1997) 99-101. doi: 10.1007/s002130050377.

[65] F.C. Gabriel, D.O. de Melo, R. Fraguas, N.C. Leite-Santos, R.A. Mantovani da Silva, and E. Ribeiro, Pharmacological treatment of depression: A systematic review comparing clinical practice guideline recommendations. PLoS One 15 (2020) e0231700. doi: 10.1371/journal.pone.0231700.

[66] G.V. Carr, and I. Lucki, The role of serotonin receptor subtypes in treating depression: a review of animal studies. Psychopharmacology (Berl) 213 (2011) 265-87. doi: 10.1007/s00213-010-2097-z.

[67] C.N. Yohn, M.M. Gergues, and B.A. Samuels, The role of 5-HT receptors in depression. Mol Brain 10 (2017) 28. doi: 10.1186/s13041-017-0306-y.

[68] A. Wesolowska, Potential role of the 5-HT6 receptor in depression and anxiety: an overview of preclinical data. Pharmacol Rep 62 (2010) 564-77. doi: 10.1016/s1734-1140(10)70315-7.

[69] A. Wesolowska, and A. Nikiforuk, Effects of the brain-penetrant and selective 5-HT6 receptor antagonist SB-399885 in animal models of anxiety and depression. Neuropharmacology 52 (2007) 1274-83. doi: 10.1016/j.neuropharm.2007.01.007.

[70] M. Jastrzebska-Wiesek, A. Siwek, A. Partyka, B. Szewczyk, M. Sowa-Kucma, A. Wasik, M. Kolaczkowski, and A. Wesolowska, Antidepressant-like activity of EMD 386088, a 5-HT6 receptor partial agonist, following systemic acute and chronic administration to rats. Naunyn Schmiedebergs Arch Pharmacol 388 (2015) 1079-88. doi: 10.1007/s00210-015-1141-2.

[71] N. Asaoka, K. Nagayasu, N. Nishitani, M. Yamashiro, H. Shirakawa, T. Nakagawa, and S. Kaneko, Olanzapine augments the effect of selective serotonin reuptake inhibitors by suppressing GABAergic inhibition via antagonism of 5-HT(6) receptors in the dorsal raphe nucleus. Neuropharmacology 95 (2015) 261-8. doi: 10.1016/j.neuropharm.2015.03.032.

[72] G.V. Carr, L.E. Schechter, and I. Lucki, Antidepressant and anxiolytic effects of selective 5-HT6 receptor agonists in rats. Psychopharmacology (Berl) 213 (2011) 499-507. doi: 10.1007/s00213-010-1798-7.

[73] M.J. Millan, Serotonin 5-HT2C receptors as a target for the treatment of depressive and anxious states: focus on novel therapeutic strategies. Therapie 60 (2005) 441-60. doi: 10.2515/therapie:2005065.

[74] M.D. Wood, Therapeutic potential of 5-HT2C receptor antagonists in the treatment of anxiety disorders. Curr Drug Targets CNS Neurol Disord 2 (2003) 383-7. doi: 10.2174/1568007033482698.

[75] A.L. Werneck, A.L. Rosso, and M.B. Vincent, The use of an antagonist 5-HT2a/c for depression and motor function in Parkinson' disease. Arq Neuropsiquiatr 67 (2009) 407-12. doi: 10.1590/s0004-282x2009000300007.

[76] A. Wesolowska, Study into a possible mechanism responsible for the antidepressant-like activity of the selective 5-HT6 receptor antagonist SB-399885 in rats. Pharmacol Rep 59 (2007) 664-71. http://www.ncbi.nlm.nih.gov/pubmed/18195455

[77] G.J. Marek, R. Martin-Ruiz, A. Abo, and F. Artigas, The selective 5-HT2A receptor antagonist M100907 enhances antidepressant-like behavioral effects of the SSRI fluoxetine. Neuropsychopharmacology 30 (2005) 2205-15. doi: 10.1038/sj.npp.1300762.

[78] P. Celada, M. Puig, M. Amargos-Bosch, A. Adell, and F. Artigas, The therapeutic role of 5-HT1A and 5-HT2A receptors in depression. J Psychiatry Neurosci 29 (2004) 252-65. http://www.ncbi.nlm.nih.gov/pubmed/15309042

[79] P.B. Hedlund, S. Huitron-Resendiz, S.J. Henriksen, and J.G. Sutcliffe, 5-HT7 receptor inhibition and inactivation induce antidepressantlike behavior and sleep pattern. Biol Psychiatry 58 (2005) 831-7. doi: 10.1016/j.biopsych.2005.05.012.

[80] A. Wesolowska, A. Nikiforuk, and K. Stachowicz, Potential anxiolytic and antidepressant effects of the selective 5-HT7 receptor antagonist SB 269970 after intrahippocampal administration to rats. Eur J Pharmacol 553 (2006) 185-90. doi: 10.1016/j.ejphar.2006.09.064.

[81] A. Wesolowska, A. Nikiforuk, K. Stachowicz, and E. Tatarczynska, Effect of the selective 5-HT7 receptor antagonist SB 269970 in animal models of anxiety and depression. Neuropharmacology 51 (2006) 578-86. doi: 10.1016/j.neuropharm.2006.04.017.

[82] P. Bonaventure, L. Kelly, L. Aluisio, J. Shelton, B. Lord, R. Galici, K. Miller, J. Atack, T.W. Lovenberg, and C. Dugovic, Selective blockade of 5-hydroxytryptamine (5-HT)7 receptors enhances 5-HT transmission, antidepressant-like behavior, and rapid eye movement sleep suppression induced by citalopram in rodents. J Pharmacol Exp Ther 321 (2007) 690-8. doi: 10.1124/jpet.107.119404.

[83] J.X. Li, A. Unzeitig, M.A. Javors, K.C. Rice, W. Koek, and C.P. France, Discriminative stimulus effects of 1-(2,5-dimethoxy-4-methylphenyl)-2-aminopropane (DOM), ketanserin, and (R)-(+)-{alpha}-(2,3-dimethoxyphenyl)-1-[2-(4-fluorophenyl)ethyl]-4-pipidinemetha nol (MDL100907) in rats. J Pharmacol Exp Ther 331 (2009) 671-9. doi: 10.1124/jpet.109.157560.

[84] H. Park, J. Ha, J.Y. Koo, J. Park, and S.B. Park, Label-free target identification using in-gel fluorescence difference via thermal stability shift. Chem Sci 8 (2017) 1127-1133. doi: 10.1039/c6sc03238a.

[85] F. Degorce, A. Card, S. Soh, E. Trinquet, G.P. Knapik, and B. Xie, HTRF: A technology tailored for drug discovery - a review of theoretical aspects and recent applications. Curr Chem Genomics 3 (2009) 22-32. doi: 10.2174/1875397300903010022.

Supplementary Material

Supplementary table 1. Statistical report.

Effect size calculated using Uanhoro, J. O. (2017). Effect size calculators. Available online at: https://effect-size-calculator.herokuapp.com/.

Figure			Statistical report	Sample size
Fig. 2	A		F(19, 29.771) = 24.717, p < 0.001, ω^2p = 0.900	4
	B		F(19, 14.324) = 20.101, p < 0.001, ω^2p = 0.914	3
	C		F(19, 18.523) = 14.780, p < 0.001, ω^2p = 0.872	3
Fig. 3	A	TCB-2	F(8, 18) = 2.830, p = 0.0318, ω^2p = 0.351	3
		LY 266097	F(11, 16.301) = 6.764, p > 0.001, ω^2p = 0.691	4
	B	EDMT	F(10, 22) = 5.807, p > 0.001, ω^2p = 0.593	3
		SB 399885	F(11, 16.337) = 10.266, p > 0.001, ω^2p = 0.782	3
	C	LP 44	F(9, 11.119) = 8.148, p = 0.001, ω^2p = 0.753	3
		DR 4485	F(8, 12.252) = 14.780, p = 0.008, ω^2p = 0.838	3
	D		F (4, 23) = 1.414; p = 0.2608, ω^2p = 0.056	3
	E		F (4, 22) = 4.133, p = 0.0120; ω^2p = 0.317	3
	F		F (4, 24) = 1.327, p = 0.2885, ω^2p = 0.043	3 - 5
Fig. 4	A		F (9, 30) = 8.925, p < 0.001, ω^2p = 0.641	4
	B		F (9, 20) = 15.70, p < 0.001, ω^2p = 0.815	3
	C		F (9, 30) = 9.827, p < 0.001, ω^2p = 0.665	4
Fig. 5			F (7, 16) = 2.553, p = 0.0571, ω^2p = 0.312	3

Chapter 5.

General discussion and conclusions

Discussion and future perspectives

Machado-Joseph disease (MJD) is one of the so called proteinopathies [1]. This group of diseases, that comprises Parkinson's, Alzheimer's and Huntington's diseases, among others, have protein aggregation as a common hallmark. Although the genetic alterations underlying each disease are different, this common feature establishes the study of protein misfolding and aggregation, and the impact of this phenomenon in cells and organisms, as a central process. In MJD, the abnormal expansion of the CAG-repeat in the ataxin-3 gene translates into a pathological polyglutamine (polyQ) tract that prone ataxin-3 protein (ATXN3) to form aggregates. Several transgenic model organisms expressing the expanded human protein mimic the hallmarks of the disease, including motor impairment and protein aggregation, which correlate with the CAG repeat length and age at onset, as in the human disease [2; 3; 4].

Over the last decade, several efforts have been conducted to unravel the disease mechanism(s) and to find a cure for this untreatable pathology. One of the potential therapeutical approaches discovered was the modulation of serotonergic neurotransmission. Hypothesis-free approaches based on the screening of commercially available drugs showed modulators of serotonergic signalling such as antidepressants (citalopram), antipsychotics (aripiprazole) or anxiolytic drugs (buspirone and tandospirone) as candidate therapeutic agents, having beneficial impact in several dimensions of MJD pathogenesis [5; 6; 7; 8; 9; 10; 11; 12]. However, the exact mechanism by which these drugs impact on MJD is mostly unknown.

In this thesis, we contributed to further deepen the understanding of how modulation of the serotonergic system suppresses MJD pathogenesis, assessing its impact on mutant ATXN3-mediated motor dysfunction and aggregation in *C. elegans* [4]. First, we further developed the existing biochemical techniques filter retardation assay and biochemical fractionation and applied them to a *C. elegans* model of mutant ATXN3 proteotoxicity, allowing a better assessment of ATXN3 aggregation states in this model (Chapter 2). Using this and other approaches, we explored the contribution of the different serotonin receptors to the suppression of MJD pathogenesis (Chapter 3 and 4).

Our results suggest that specific targeting of individual 5-HT receptors, either by the activation of SER-4/5-HT_{1A}R (Chapter 3), or by the chronic antagonism of SER-1/5-HT_2R, SER-5/5-HT_6R or SER-7/5-HT_7R (Chapter 4) is beneficial in the context of MJD pathogenesis. Our work thus opens new avenues in the study of the impact of the modulation of serotonergic system in MJD pathogenesis, including the

determination of the specific pathways by which each individual serotonin receptor impacts on ATXN3 proteotoxicity, raising a number of new questions that will be discussed below.

Possible serotonergic system deregulation in MJD

Although an extensive study of the serotonergic system has never been performed in the context of MJD, the amino acid L-tryptophan, the precursor of serotonin (5-HT), was found to be decreased in the serum of patients [13] and in a transgenic mouse model of the disease [14]. Importantly, L-tryptophan integrated a panel of four serum metabolites that confidently detected the disease state, discriminating MJD patients from controls, being therefore proposed as a promising biomarker [13]. Tryptophan is an essential component of the human diet but, since its storage is low, it is found in low concentrations in the body. This amino acid is involved not only in protein biogenesis but also in the 5-HT and kynurenine biosynthetic pathways [15]. Interestingly, metabolites of the kynurenine pathway have been proposed as novel prognostic markers and/or therapeutic targets for other neurodegenerative diseases, such as Parkinson's disease (PD) and Huntington's disease [16; 17; 18; 19; 20; 21]. Tryptophan is the precursor of 5-HT, and in some tissues, such as the pineal gland, 5-HT is further metabolized to melatonin [15]. Although to our knowledge, 5-HT levels were never measured in the serum or cerebrospinal fluid of MJD patients, a study from Takei and colleagues showed a negative correlation between serum melatonin levels and insomnia in patients [22]. This observation suggested that not only tryptophan may be decreased in MJD, but also other tryptophan metabolites, such as kynurenine and serotonin could be altered.

MJD patients typically present an atrophy of the cerebellum, pons, and medulla oblongata, and neuropathological studies reveal neuronal loss in the cerebellar dentate nuclei, pons, substantia nigra, thalamus, globus pallidus and in the brainstem nuclei, among others [23; 24]. Volumetric analyses by MRI of these patients demonstrated atrophy of the cerebellum, brainstem, caudate nuclei and thalamus [23; 25; 26]. Importantly, some of these brain regions were also shown to be involved in the pathophysiology of depression, including the thalamus, basal ganglia and brainstem [27; 28]. Brainstem can be considered the nuclei of neurotransmitters. This brain structure comprises the raphe nucleus - that contain serotonergic neurons, the locus coeruleus - with norepinephrinergic neurons, and the substantia nigra and ventral tegmentum - with dopaminergic neurons [27]. Therefore, it is possible that brainstem degeneration, in MJD patients, can contribute to imbalances in neurotransmission, namely by impacting serotonin production. Serotonergic signalling is involved in depression or depressive symptoms

[29; 30]. Indeed, SSRIs are the most common used pharmacological therapies for depression. Interestingly, MJD patients present a higher risk to develop depression than the general population, depression being an established comorbidity in MJD. The inverse correlation between motor performance of these patients and the development of depression was extensively reported, depressive symptoms increasing with disease progression [31; 32; 33; 34; 35]. This has been attributed to the negative psychological impact of the disease. However, it has been proposed that depression could be a primary effect of the neurodegeneration process also [36; 37]. Recent studies in the depression field suggested a more complicated origin of the depressive pathology, involving multiple pathways, among which an imbalance in kynurenine/serotonergic pathways [38; 39; 40; 41; 42]. Even though MJD patients show an increased susceptibility to depression, and a possible impairment in tryptophan levels or in its metabolites, MJD mouse models did not present decreased serotonin levels, at least in the brain regions analysed [11; 43], neither a major anxious- or depressive-like behaviour when assessed post-symptomatically, at 16 weeks of age (Correia J., personal communication).

Serotonergic signalling dysfunction was reported in other neurodegenerative disorders, such as PD [44], AD [45; 46] and ALS [47]. Low SERT binding in the brain limbic regions of AD patients [48] and decreased expression of the 5-HT_{1A}R were reported [49]. In the striatum of MJD transgenic mice, the RNA expression profile analysis by RNA sequencing, performed by our laboratory, also showed a downregulation of 5-HT_{1A}R heteroreceptor (Oliveira S., personal communication), without any other major alterations in expression of genes encoding enzymes that play a role in the biosynthetic pathways of serotonin, kynurenine, or melatonin.

In summary, more studies with the evaluation of the levels of neurotransmitter and their metabolites, and to dissect serotonergic signalling dysfunction are needed in MJD, particularly in patients.

The role of 5-HT receptors on the suppression of MJD pathogenesis

As referred above, serotonergic signalling modulation by chronic citalopram (CIT) administration suppressed MJD pathogenesis [11]. We showed that CIT treatment of two different MJD animal models ameliorated motor impairment and suppressed mutant ATXN3 aggregation, and more importantly, that these effects persisted after drug withdrawal [11]. The validation of these findings by an independent laboratory using a distinct transgenic mouse model [5] further supported the theory of serotonergic signalling modulation as a promising therapy for MJD.

In this thesis, we further supported these findings by establishing the 5-HT_{1A}R as a new therapeutic target for MJD (Chapter 3, published as [50]). By exploring the effect of befiradol, a specific and potent 5-HT_{1A}R agonist, we found that both chronic and acute administration of the compound ameliorated core features of the disease, including motor impairment and mutant ATXN3 aggregation. Importantly, and as seen for CIT administration, the beneficial effects of befiradol persisted after drug withdrawal [50], suggesting a disease modifying effect of serotonergic signalling modulation. Recent studies in our laboratory are showing promising results of befiradol treatment in MJD transgenic mice, in both chronic or sub-chronic treatment modalities (Ferreira-Lomba B. and Duarte-Silva S., personal communication).

Furthermore, our results showed that befiradol's effect on mutant ATXN3-mediated motor dysfunction was dependent specifically on the 5-HT_{1A}R orthologue in *C. elegans* SER-4, highlighting the specificity of compound binding in *C. elegans* [50]. 5-HT_{1A}Rs/SER-4 are present in the brain forming two distinct populations: i) the post-synaptic somatodendritic heteroreceptors expressed at 5-HT projecting areas [51; 52] and ii) the pre-synaptic autoreceptors at the cell body and dendrites of 5-HT producing neurons, namely of the dorsal raphe nuclei (DRN), in the case of mice and humans. Serotonin released from the DRN activates 5-HT_{1A} autoreceptors, exerting a feedback inhibition on the firing of 5-HT neurons, decreasing 5-HT production and negatively regulating the 5-HT system [53; 54; 55; 56]. Our results showed that both populations of 5-HT_{1A} auto- and heteroreceptors play a role in the suppression of ATXN3 proteotoxicity. First, we observed that in the absence of endogenous serotonin, caused by a full deletion of the *tph-1* gene generated by CRISPR-Cas9 technology in the ATXN3-proteotoxicity model, acute treatment with befiradol still ameliorated motor dysfunction of the animals, suggesting the contribution of 5-HT_{1A} heteroreceptors. Interestingly, chronic treatment with befiradol failed to ameliorate motor dysfunction in the absence of serotonin, highlighting a main role for 5-HT autoreceptor desensitization during chronic treatment. Consistently with this, by assessing neuronal activity of a serotonin-producing neuron, by ratiometric calcium imaging in live animals, we found a distinct activity profile between the two treatment modalities. Befiradol acute treatment displaying a neuronal inhibitory profile, comparing with chronic treatment and WT conditions, consistent with SER-4 activation. Taken together, our data led us to propose a model for befiradol's action through the desensitization of SER-4 autoreceptors and activation of SER-4 heteroreceptors expressed in serotonergic and non-serotonergic neurons, respectively [50]. The exact mechanism by which 5-HT_{1A}R/SER-4 desensitization impacts on MJD pathogenesis remains to be fully determined, however the desensitization of 5-HT_{1A}R has also been associated to SSRI's therapeutic action. Inhibition of SERT by treatment with SSRIs, likely increases 5-HT availability, with consequent activation of 5-HT_{1A} autoreceptors and the negative feedback against 5-HT production [53;

54; 55; 56], which was suggested to explain the delay in time to first response in the treatment of depression [57]. Upon chronic administration of SSRIs, there is a downregulation of the 5-HT_{1A} autoreceptors, and the subsequent increase in neuronal firing rates [56; 58]. Therefore, it is likely that post-synaptic 5-HT heteroreceptors mediate serotonergic signalling propagation, especially after 5-HT_{1A}R autoreceptor desensitization, as proposed for CIT's effect on the suppression of MJD pathogenesis.

Further exploration of the contribution of the post-synaptic 5-HTRs to the suppression of MJD pathogenesis suggested a potential common involvement of all 5-HT GPCRs (Chapter 4). CIT action showed to be dependent on all 5-HT GPCRs in *C. elegans*, namely of SER-1/5-HT_2R and SER-4/5-HT_{1A}R [11], SER-5/5-HT_6R and SER-7/5-HT_7R, being likely independent of the ion-channel receptor MOD-1. Surprisingly, the antagonism of SER-1/5-HT_2R, SER-5/5-HT_6R and SER-7/5-HT_7R, but not the inverse agonism of these receptors, were beneficial to motor behaviour of the animals. Antagonists and inverse agonists drug action differ from each other by its intrinsic efficacy. In complex systems, with the presence of the endogenous ligand and when the receptor has constitutive activity, antagonists impact on receptor's response by competing with endogenous ligand, while inverse agonists further reduce the receptor's response by the suppression of its constitutive activity [59]. This observation, together with our preliminary findings, suggest that there is an optimal level of activity for 5-HTRs and that their signalling should be tightly controlled/regulated to achieve the beneficial effect in the context of MJD. Interestingly, ERK signalling is a common non-canonical pathway to all 5-HTRs described in our work, 5-HT_{1A}R, 5-HT_2R, 5-HT_6R and 5-HT_7R [60; 61]. Long lasting neuronal ERK activation was found associated to neurodegenerative disorders, such as PD and AD [62; 63; 64; 65], and ERK signalling inhibitors were suggested as therapeutic strategies to these diseases [66]. Interestingly, it was shown that ERK1/2 pathway can regulate pathogenic ATXN3 protein levels in cells [67] the ERK signalling status being changed in MJD models [68]. Therefore, in the future we intend to assess the profile of proteins that are involved in ERK signalling upon CIT and befiradol treatments.

In order to address if any of the 5-HTRs were more important to the therapeutic effect of SSRIs in depression, Carr and Lucki, in a review paper, analysed behavioural pharmacology studies, selecting 5-HTRs target drugs that suppressed the effect of SSRIs or mimicked antidepressive-like effects in models of depression. They concluded that either agonism of 5-HT_{1A}R, 5-HT_{1B}R, 5-HT_{2C}R, 5-HT_4R, and 5-HT_6R or antagonism of 5-HT_{2A}R, 5-HT_{2C}R, 5-HT_3R, 5-HT_6R, and 5-HT_7R could produce antidepressive-like behaviours raising the hypothesis that none of the receptors exerted a prominent role in the action of SSRIs, being the beneficial effect probably a result of an orchestration of stimulation and blockage signals of the

different 5-HTRs [69]. Moreover, and aside the redundancy and apparent antagonic capacity of serotoninergic system, some receptors were indeed shown to be modulated, either in expression levels or activation status, by CIT administration [70; 71; 72]. Overall, our findings in MJD resemble what has been previous described in major depression disorders, suggesting that in spite of quite different outcome measures a common mechanism may underlie the therapeutic effects of 5-HT targeting drugs in neurodegenerative and neuropsychiatric disorders.

As previously referred, 5-HT_{1A}/SER-4 heteroreceptor agonism [50] and, possibly, acute antagonism of 5-HT_2R/SER-1 [Chapter 4] positively impacted on motor impairment of mutant ATXN3-expressing animals. CIT action was previously described to modulate these two receptors. On the one hand, as explained above the generally for SSRIs, short time treatment with CIT leads to activation of 5-HT_{1A} autoreceptors at DRN, that after a given time threshold become desensitized, with subsequent induction of the firing of serotonergic neurons [71; 72]. However, the desensitization of 5-HT_{1A}R, upon chronic CIT treatment, occurs preferentially at the DRN autoreceptors but not in 5-HT_{1A} heteroreceptors, at least at the hippocampus region, where, at the contrary, the responsivity of 5-HT_{1A}R was found increased [70; 72]. This observation was also verified for another SSRI, paroxetine [73]. The desensitization of 5-HT_{1A}R being needed for SSRIs action, it has been proposed that a co-treatment with a 5-HT_{1A}R antagonist would lead to a better outcome in depressive patients [74]. However, clinical trials employing this strategy of co-treatment failed to produce an enhancement in the effect of the SSRI alone [75; 76]. The justification given for this fact was its action on the 5-HT_{1A} heteroreceptors of the forebrain, that, upon treatment with the antagonist, could impact negatively the antidepressive response, regardless of the increased serotonin levels [76]. On the other hand, this study also shows that the positive effect of the SSRIs is maintained in the presence of 5-HT_{1A}R antagonist, suggesting the contribution of other serotonin receptors (other than the 5-HT_{1A}R) in SSRI action [76].

The increased responsivity of the 5-HT_{1A} heteroreceptor was found to be accompanied by a decrease in 5-HT_2R activation status or binding sites upon CIT treatment [70; 71]. Also, locomotion activity in mice exposed to a novel environment showed that CIT action was dependent on 5-HT_{1B}R and 5-HT_{2A}R, the response to this SSRI being augmented by 5-HT_{2C}R antagonist SB242084 [77]. In mice that were non-responders to SSRI treatment, the immobility in forced swimming test was also improved by the antagonism of 5-HT_{2C}R [78], the effect being attributed to the increased serotonin levels in pre-frontal cortex. This increased in serotonin availability was also found in the hippocampus of freely moving rats when treated with SB242084 prior to CIT administration [79]. Interestingly, buspirone, a 5-HT_{1A}R partial

agonist, alone or in combination with CIT, could mediate the alteration of high- to low- affinity status of 5-HT_{2C}R in rats [80]. In MJD, we found that CIT chronic treatment decreased the expression levels of 5-HT_{2A}R in the striatum, but the impact on receptor activity or binding affinity remains to be elucidated (Oliveira S., personal communication).

Less is known regarding the impact of CIT treatment on other 5-HTRs. In rats, co-treatment with CIT and the 5-HT_7R antagonist SB269970 augmented serotonin levels in the pre-frontal cortex and culminated in an enhancement of the antidepressive-like behaviour observed, when compared with the single therapies alone [81; 82]. Interestingly, the impact of 5-HT_7R antagonism on serotonin levels has been proposed as a cause for the improvement of depression symptoms in animal models, but the 5-HT_7R desensitization was also suggested to play a role, at least in part, in the mode of action of CIT [83; 84; 85] and, perhaps of other SSRIs, since chronic treatment with fluoxetine and 6-OH-DPAT (a 5-HT_{1A}R agonist) decreased the number of 5-HT_7R binding sites in the rats hypothalamus [83; 85]. To our knowledge, there are no descriptions of SSRI-mediated modulation of the 5-HT_6 receptor. However, several reports described the antidepressive effects of both 5-HT_6R agonists and antagonists [86; 87; 88; 89; 90]. Despite the fact that the mechanism of action of these drugs in depression is also mostly unknown, it was shown that 5-HT_6R inhibition, in GABAergic neurons, inhibited GABA release and therefore increased cholinergic, glutamatergic and monoaminergic neurotransmission [91]. Thus, it is hypothesized that the antidepressive properties of agonists and antagonists of this receptor could depend on receptor localization in different neuronal types, through the modulation of other neurotransmitters as acetylcholine, GABA and glutamate [92].

In conclusion, the serotonergic system encompasses a highly complex and robust network, that upon distinct pharmacological or genetical modulation can result in similar biologic outcomes/phenotypes, 5-HTRs possibly being the most relevant receptors for the mode-of-action of SSRIs, albeit the effect of these drugs is greatly dependent on cellular types and treatment modalities. Nevertheless, our results support the hypothesis, previously suggested by others [69; 93], that the increased serotonin levels by chronic CIT treatment, in a disease organism, can lead to a remodelling of serotonin receptors response and to a myriad of stimulations and inhibitions, namely through the desensitization of 5-HT_{1A}R/SER-4 autoreceptors, with augmentation of 5-HT_{1A}R/SER-4 heteroreceptors response and by decreasing 5-HT_2R/SER-1, 5-HT_6R/SER-5 and 5-HT_7R/SER-7 activity (Figure 1). The usage of multimodal drugs that target multiple 5-HTRs, as aripiprazole (APZ) or vortioxetine, helped to further validate this model. We showed that APZ chronic treatment ameliorated motor dysfunction of

mutant ATXN3 expressing animals the effect of the drug being dependent mainly on 5-HT_{1A}R/SER-4, 5-HT_2R/SER-1 and dopamine D2 receptors in *C. elegans* (Jalles, A. and Vieira, C. – under revision). Importantly, preliminary results showed a positive impact of vortioxetine on animals' motor dysfunction (Freitas, B. personal communication), this drug combining SERT/MOD-5 inhibition with antagonism of 5-HT_3R, 5-HT_{1D}R and 5-HT_7R, agonism of 5-HT_{1A}R and partial agonism of 5-HT_{1B}R [94; 95; 96].

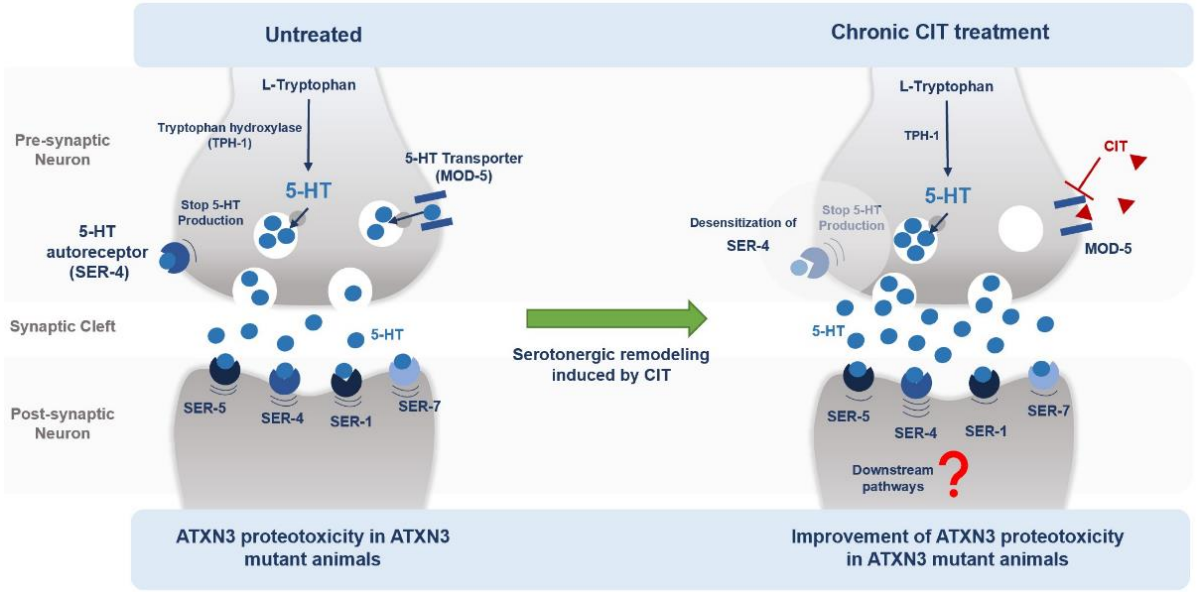

Figure 1. Hypothetical model of the beneficial effect induced by the remodelling of serotonergic signalling in the suppression of mutant ATXN3 proteotoxicity.

CIT administration, by the blockage of the serotonin transporter MOD-5, likely increases serotonin availability in the synaptic cleft and induces activation of the SER-4 autoreceptor. Prolonged activation of this autoreceptor likely results in its desensitization, decreasing the inhibitory signal exerted by SER-4 on 5-HT production. These actions on the pre-synaptic serotonergic neuron, may lead to a remodelling of the serotonergic system, impacting post-synaptic 5-HTR-mediated signalling. Agonism of SER-4 and/or antagonism of SER-1, SER-5 and SER-7 was beneficial to the suppression of ATXN3 proteotoxicity, however the downstream signalling pathways involved in 5-HTRs-mediated effects were not yet elucidated [11; 50] (Jalles, A. and Vieira, C. – under revision).

In spite of the clear need for further confirmatory studies and to dissect the molecular pathways involved in the suppression of MJD pathogenesis by 5-HTRs-mediated signalling, with this work, we proposed a new therapeutic target in MJD, the 5-HT_{1A}R. Moreover, we strengthened the finding of a possible role for other receptor types, such as 5-HT_2R, 5-HT_6R and 5-HT_7R, which can also constitute valuable targets, to be validated in the future, using a single molecule treatment or in combinatory therapies for MJD.

Main conclusions

- The 5-HT_{1A} receptor is a promising therapeutic target in MJD.
- Not only the 5-HT_{1A} autoreceptor desensitization but also 5-HT_{1A} heteroreceptor activation impact MJD pathogenesis in a *C. elegans* model of ATXN3-proteotoxicity.
- The mode-of-action of citalopram probably involves the remodelling of serotonin receptors, and the stimulation and inhibition of several receptors, simultaneously or sequentially, and depending on the brain region/cellular type, can account for the impact of citalopram treatment on MJD pathogenesis.
- The improved techniques to assess protein aggregation here developed are valuable to further understand the impact of drugs or genetic alterations in the disease context and can be used in models of other proteinopathies.

References

[1] T.A. Bayer, Proteinopathies, a core concept for understanding and ultimately treating degenerative disorders? Eur Neuropsychopharmacol 25 (2015) 713-24. doi: 10.1016/j.euroneuro.2013.03.007.

[2] J. Schmidt, and T. Schmidt, Animal Models of Machado-Joseph Disease. Adv Exp Med Biol 1049 (2018) 289-308. doi: 10.1007/978-3-319-71779-1_15.

[3] A. Silva-Fernandes, S. Duarte-Silva, A. Neves-Carvalho, M. Amorim, C. Soares-Cunha, P. Oliveira, K. Thirstrup, A. Teixeira-Castro, and P. Maciel, Chronic treatment with 17-DMAG improves balance and coordination in a new mouse model of Machado-Joseph disease. Neurotherapeutics 11 (2014) 433-49. doi: 10.1007/s13311-013-0255-9.

[4] A. Teixeira-Castro, M. Ailion, A. Jalles, H.R. Brignull, J.L. Vilaca, N. Dias, P. Rodrigues, J.F. Oliveira, A. Neves-Carvalho, R.I. Morimoto, and P. Maciel, Neuron-specific proteotoxicity of mutant ataxin-3 in C. elegans: rescue by the DAF-16 and HSF-1 pathways. Hum Mol Genet 20 (2011) 2996-3009. doi: 10.1093/hmg/ddr203.

[5] N.S. Ashraf, S. Duarte-Silva, E.D. Shaw, P. Maciel, H.L. Paulson, A. Teixeira-Castro, and M.D.C. Costa, Citalopram Reduces Aggregation of ATXN3 in a YAC Transgenic Mouse Model of Machado-Joseph Disease. Mol Neurobiol 56 (2019) 3690-3701. doi: 10.1007/s12035-018-1331-2.

[6] M.D.C. Costa, N.S. Ashraf, S. Fischer, Y. Yang, E. Schapka, G. Joshi, T.J. McQuade, R.M. Dharia, M. Dulchavsky, M. Ouyang, D. Cook, D. Sun, M.J. Larsen, J.E. Gestwicki, S.V. Todi, M.I. Ivanova, and H.L. Paulson, Unbiased screen identifies aripiprazole as a modulator of abundance of the polyglutamine disease protein, ataxin-3. Brain 139 (2016) 2891-2908. doi: 10.1093/brain/aww228.

[7] J.S. Lou, L. Goldfarb, L. McShane, P. Gatev, and M. Hallett, Use of buspirone for treatment of cerebellar ataxia. An open-label study. Arch Neurol 52 (1995) 982-8. doi: 10.1001/archneur.1995.00540340074015.

[8] A. Takei, T. Fukazawa, T. Hamada, H. Sohma, I. Yabe, H. Sasaki, and K. Tashiro, Effects of tandospirone on "5-HT1A receptor-associated symptoms" in patients with Machado-Josephe disease: an open-label study. Clin Neuropharmacol 27 (2004) 9-13. doi: 10.1097/00002826-200401000-00005.

[9] A. Takei, T. Fukazawa, T. Hamada, I. Yabe, and K. Tashiro, 'Drug holiday' effects of tandospirone in a patient with Machado-Joseph disease. Psychiatry Clin Neurosci 57 (2003) 607-8. doi: 10.1046/j.1440-1819.2003.01176.x.

[10] A. Takei, S. Hamada, S. Homma, K. Hamada, K. Tashiro, and T. Hamada, Difference in the effects of tandospirone on ataxia in various types of spinocerebellar degeneration: an open-label study. Cerebellum 9 (2010) 567-70. doi: 10.1007/s12311-010-0199-0.

[11] A. Teixeira-Castro, A. Jalles, S. Esteves, S. Kang, L. da Silva Santos, A. Silva-Fernandes, M.F. Neto, R.M. Brielmann, C. Bessa, S. Duarte-Silva, A. Miranda, S. Oliveira, A. Neves-Carvalho, J. Bessa, T. Summavielle, R.B. Silverman, P. Oliveira, R.I. Morimoto, and P. Maciel, Serotonergic signalling suppresses ataxin 3 aggregation and neurotoxicity in animal models of Machado-Joseph disease. Brain 138 (2015) 3221-37. doi: 10.1093/brain/awv262.

[12] P. Trouillas, J. Xie, P. Adeleine, D. Michel, A. Vighetto, J. Honnorat, R. Dumas, N. Nighoghossian, and B. Laurent, Buspirone, a 5-hydroxytryptamine1A agonist, is active in cerebellar ataxia. Results of a double-blind drug placebo study in patients with cerebellar cortical atrophy. Arch Neurol 54 (1997) 749-52. doi: 10.1001/archneur.1997.00550180059013.

[13] Z.H. Yang, C.H. Shi, L.N. Zhou, Y.S. Li, J. Yang, Y.T. Liu, C.Y. Mao, H.Y. Luo, G.W. Xu, and Y.M. Xu, Metabolic Profiling Reveals Biochemical Pathways and Potential Biomarkers of Spinocerebellar Ataxia 3. Front Mol Neurosci 12 (2019) 159. doi: 10.3389/fnmol.2019.00159.

[14] L.J.A. Toonen, M. Overzier, M.M. Evers, L.G. Leon, S.A.J. van der Zeeuw, H. Mei, S.M. Kielbasa, J.J. Goeman, K.M. Hettne, O.T. Magnusson, M. Poirel, A. Seyer, P.A.C. t Hoen, and W.M.C. van Roon-Mom, Transcriptional profiling and biomarker identification reveal tissue specific effects of expanded ataxin-3 in a spinocerebellar ataxia type 3 mouse model. Mol Neurodegener 13 (2018) 31. doi: 10.1186/s13024-018-0261-9.

[15] S. Comai, A. Bertazzo, M. Brughera, and S. Crotti, Tryptophan in health and disease. Adv Clin Chem 95 (2020) 165-218. doi: 10.1016/bs.acc.2019.08.005.

[16] T. Ogawa, W.R. Matson, M.F. Beal, R.H. Myers, E.D. Bird, P. Milbury, and S. Saso, Kynurenine pathway abnormalities in Parkinson's disease. Neurology 42 (1992) 1702-6. doi: 10.1212/wnl.42.9.1702.

[17] F.J.H. Sorgdrager, Y. Vermeiren, M. Van Faassen, C. van der Ley, E.A.A. Nollen, I.P. Kema, and P.P. De Deyn, Age- and disease-specific changes of the kynurenine pathway in Parkinson's and Alzheimer's disease. J Neurochem 151 (2019) 656-668. doi: 10.1111/jnc.14843.

[18] D. Venkatesan, M. Iyer, A. Narayanasamy, K. Siva, and B. Vellingiri, Kynurenine pathway in Parkinson's disease-An update. eNeurologicalSci 21 (2020) 100270. doi: 10.1016/j.ensci.2020.100270.

[19] M.F. Beal, W.R. Matson, K.J. Swartz, P.H. Gamache, and E.D. Bird, Kynurenine Pathway Measurements in Huntington's Disease Striatum: Evidence for Reduced Formation of Kynurenic Acid. Journal of Neurochemistry 55 (1990) 1327-1339. doi: 10.1111/j.1471-4159.1990.tb03143.x.

[20] S. Campesan, Edward W. Green, C. Breda, Korrapati V. Sathyasaikumar, Paul J. Muchowski, R. Schwarcz, Charalambos P. Kyriacou, and F. Giorgini, The Kynurenine Pathway Modulates Neurodegeneration in a Drosophila Model of Huntington's Disease. Current Biology 21 (2011) 961-966. doi: 10.1016/j.cub.2011.04.028.

[21] K.V. Sathyasaikumar, E.K. Stachowski, L. Amori, P. Guidetti, P.J. Muchowski, and R. Schwarcz, Dysfunctional kynurenine pathway metabolism in the R6/2 mouse model of Huntington's disease. Journal of Neurochemistry (2010). doi: 10.1111/j.1471-4159.2010.06675.x.

[22] A. Takei, T. Fukazawa, T. Hamada, H. Sohma, I. Yabe, H. Sasaki, and M. Okawa, Serum melatonin levels and insomnia in patients with Machado-Joseph Disease. Sleep and Biological Rhythms 2 (2004) 209-214. doi: 10.1111/j.1479-8425.2004.00144.x.

[23] C. Bettencourt, and M. Lima, Machado-Joseph Disease: from first descriptions to new perspectives. Orphanet J Rare Dis 6 (2011) 35. doi: 10.1186/1750-1172-6-35.
[24] J.D. Fratkin, and P.J.S. Vig, Neuropathology of degenerative ataxias. 103 (2012) 111-125. doi: 10.1016/b978-0-444-51892-7.00005-x.
[25] W.O. Arruda, A.T. Meira, S.E. Ono, A. de Carvalho Neto, L. Betting, S. Raskin, C.H.F. Camargo, and H.A.G. Teive, Volumetric MRI Changes in Spinocerebellar Ataxia (SCA3 and SCA10) Patients. Cerebellum 19 (2020) 536-543. doi: 10.1007/s12311-020-01137-3.
[26] P.S. Wang, Y.T. Wu, T.Y. Wang, H.M. Wu, B.W. Soong, and C.W. Jao, Supratentorial and Infratentorial Lesions in Spinocerebellar Ataxia Type 3. Front Neurol 11 (2020) 124. doi: 10.3389/fneur.2020.00124.
[27] M. Pandya, M. Altinay, D.A. Malone, Jr., and A. Anand, Where in the brain is depression? Curr Psychiatry Rep 14 (2012) 634-42. doi: 10.1007/s11920-012-0322-7.
[28] F.F. Zhang, W. Peng, J.A. Sweeney, Z.Y. Jia, and Q.Y. Gong, Brain structure alterations in depression: Psychoradiological evidence. CNS Neurosci Ther 24 (2018) 994-1003. doi: 10.1111/cns.12835.
[29] C. Kerr, The Serotonin Theory of Depression. Jefferson Journal of Psychiatry 12 (1994). doi: 10.29046/jjp.012.1.001.
[30] R.A. Daut, and L.K. Fonken, Circadian regulation of depression: A role for serotonin. Front Neuroendocrinol 54 (2019) 100746. doi: 10.1016/j.yfrne.2019.04.003.
[31] A.R. Martinez, M.B. Nunes, I. Faber, A. D'Abreu, I. Lopes-Cendes, and M.C. Franca, Jr., Fatigue and Its Associated Factors in Spinocerebellar Ataxia Type 3/Machado-Joseph Disease. Cerebellum 16 (2017) 118-121. doi: 10.1007/s12311-016-0775-z.
[32] J.A. Saute, A.C. da Silva, K.C. Donis, L. Vedolin, M.L. Saraiva-Pereira, and L.B. Jardim, Depressive mood is associated with ataxic and non-ataxic neurological dysfunction in SCA3 patients. Cerebellum 9 (2010) 603-5; author reply 606-7. doi: 10.1007/s12311-010-0205-6.
[33] T. Schmitz-Hubsch, M. Coudert, S. Tezenas du Montcel, P. Giunti, R. Labrum, A. Durr, P. Ribai, P. Charles, C. Linnemann, L. Schols, M. Rakowicz, R. Rola, E. Zdzienicka, R. Fancellu, C. Mariotti, L. Baliko, B. Melegh, A. Filla, E. Salvatore, B.P. van de Warrenburg, S. Szymanski, J. Infante, D. Timmann, S. Boesch, C. Depondt, J.S. Kang, J.B. Schulz, T. Klopstock, N. Lossnitzer, B. Lowe, C. Frick, D. Rottlander, T.E. Schlaepfer, and T. Klockgether, Depression comorbidity in spinocerebellar ataxia. Mov Disord 26 (2011) 870-6. doi: 10.1002/mds.23698.
[34] C.R. Cecchin, A.P. Pires, C.R. Rieder, T.L. Monte, I. Silveira, T. Carvalho, M.L. Saraiva-Pereira, J. Sequeiros, and L.B. Jardim, Depressive symptoms in Machado-Joseph disease (SCA3) patients and their relatives. Community Genet 10 (2007) 19-26. doi: 10.1159/000096276.
[35] A. Moro, M. Moscovich, M. Farah, C.H.F. Camargo, H.A.G. Teive, and R.P. Munhoz, Nonmotor symptoms in spinocerebellar ataxias (SCAs). Cerebellum Ataxias 6 (2019) 12. doi: 10.1186/s40673-019-0106-5.
[36] M.T. Lin, J.S. Yang, P.P. Chen, M.Z. Qian, H.X. Lin, X.P. Chen, X.J. Shang, D.N. Wang, Y.C. Chen, B. Jiang, Y.J. Chen, W.J. Chen, N. Wang, and S.R. Gan, Bidirectional Connections between Depression and Ataxia Severity in Spinocerebellar Ataxia Type 3 Patients. Eur Neurol 79 (2018) 266-271. doi: 10.1159/000489398.
[37] R.Y. Lo, K.P. Figueroa, S.M. Pulst, S. Perlman, G. Wilmot, C. Gomez, J. Schmahmann, H. Paulson, V.G. Shakkottai, S. Ying, T. Zesiewicz, K. Bushara, M. Geschwind, G. Xia, J.T. Yu, L.E. Lee, T. Ashizawa, S.H. Subramony, and S.H. Kuo, Depression and clinical progression in spinocerebellar ataxias. Parkinsonism Relat Disord 22 (2016) 87-92. doi: 10.1016/j.parkreldis.2015.11.021.
[38] L. Dell'Osso, C. Carmassi, F. Mucci, and D. Marazziti, Depression, Serotonin and Tryptophan. Curr Pharm Des 22 (2016) 949-54. doi: 10.2174/1381612822666151214104826.

[39] W. Marx, A.J. McGuinness, T. Rocks, A. Ruusunen, J. Cleminson, A.J. Walker, S. Gomes-da-Costa, M. Lane, M. Sanches, A.P. Diaz, P.T. Tseng, P.Y. Lin, M. Berk, G. Clarke, A. O'Neil, F. Jacka, B. Stubbs, A.F. Carvalho, J. Quevedo, J.C. Soares, and B.S. Fernandes, The kynurenine pathway in major depressive disorder, bipolar disorder, and schizophrenia: a meta-analysis of 101 studies. Mol Psychiatry (2020). doi: 10.1038/s41380-020-00951-9.

[40] H. Miura, N. Ozaki, M. Sawada, K. Isobe, T. Ohta, and T. Nagatsu, A link between stress and depression: shifts in the balance between the kynurenine and serotonin pathways of tryptophan metabolism and the etiology and pathophysiology of depression. Stress 11 (2008) 198-209. doi: 10.1080/10253890701754068.

[41] A. Muneer, Kynurenine Pathway of Tryptophan Metabolism in Neuropsychiatric Disorders: Pathophysiologic and Therapeutic Considerations. Clin Psychopharmacol Neurosci 18 (2020) 507-526. doi: 10.9758/cpn.2020.18.4.507.

[42] L.A. Ramirez, E.A. Perez-Padilla, F. Garcia-Oscos, H. Salgado, M. Atzori, and J.C. Pineda, A new theory of depression based on the serotonin/kynurenine relationship and the hypothalamicpituitary- adrenal axis. Biomedica 38 (2018) 437-450. doi: 10.7705/biomedica.v38i3.3688.

[43] U. Bichelmeier, T. Schmidt, J. Hubener, J. Boy, L. Ruttiger, K. Habig, S. Poths, M. Bonin, M. Knipper, W.J. Schmidt, J. Wilbertz, H. Wolburg, F. Laccone, and O. Riess, Nuclear localization of ataxin-3 is required for the manifestation of symptoms in SCA3: in vivo evidence. J Neurosci 27 (2007) 7418-28. doi: 10.1523/JNEUROSCI.4540-06.2007.

[44] P. Fazio, D. Ferreira, P. Svenningsson, C. Halldin, L. Farde, E. Westman, and A. Varrone, High-resolution PET imaging reveals subtle impairment of the serotonin transporter in an early non-depressed Parkinson's disease cohort. Eur J Nucl Med Mol Imaging 47 (2020) 2407-2416. doi: 10.1007/s00259-020-04683-4.

[45] C. Pena-Bautista, L. Flor, M. Lopez-Nogueroles, L. Garcia, I. Ferrer, M. Baquero, M. Vento, and C. Chafer-Pericas, Plasma alterations in cholinergic and serotonergic systems in early Alzheimer Disease: Diagnosis utility. Clin Chim Acta 500 (2020) 233-240. doi: 10.1016/j.cca.2019.10.023.

[46] S.G. Snowden, A.A. Ebshiana, A. Hye, O. Pletnikova, R. O'Brien, A. Yang, J. Troncoso, C. Legido-Quigley, and M. Thambisetty, Neurotransmitter Imbalance in the Brain and Alzheimer's Disease Pathology. J Alzheimers Dis 72 (2019) 35-43. doi: 10.3233/JAD-190577.

[47] Y. Vermeiren, J. Janssens, D. Van Dam, and P.P. De Deyn, Serotonergic Dysfunction in Amyotrophic Lateral Sclerosis and Parkinson's Disease: Similar Mechanisms, Dissimilar Outcomes. Front Neurosci 12 (2018) 185. doi: 10.3389/fnins.2018.00185.

[48] J.J. van der Zande, M. Joling, I.G. Happach, C. Vriend, P. Scheltens, J. Booij, and A.W. Lemstra, Serotonergic deficits in dementia with Lewy bodies with concomitant Alzheimer's disease pathology: An (123)I-FP-CIT SPECT study. Neuroimage Clin 25 (2020) 102062. doi: 10.1016/j.nicl.2019.102062.

[49] K.L. Lanctot, D.F. Hussey, N. Herrmann, S.E. Black, P.M. Rusjan, A.A. Wilson, S. Houle, N. Kozloff, N.P. Verhoeff, and S. Kapur, A positron emission tomography study of 5-hydroxytryptamine-1A receptors in Alzheimer disease. Am J Geriatr Psychiatry 15 (2007) 888-98. doi: 10.1097/JGP.0b013e3180488325.

[50] J. Pereira-Sousa, B. Ferreira-Lomba, A. Bellver-Sanchis, D. Vilasboas-Campos, J.H. Fernandes, M.D. Costa, M.A. Varney, A. Newman-Tancredi, P. Maciel, and A. Teixeira-Castro, Identification of the 5-HT1A serotonin receptor as a novel therapeutic target in a C. elegans model of Machado-Joseph disease. Neurobiol Dis 152 (2021) 105278. doi: 10.1016/j.nbd.2021.105278.

[51] H.K. Kia, M.C. Miquel, M.J. Brisorgueil, G. Daval, M. Riad, S. El Mestikawy, M. Hamon, and D. Verge, Immunocytochemical localization of serotonin1A receptors in the rat central nervous system. J

Comp Neurol 365 (1996) 289-305. doi: 10.1002/(SICI)1096-9861(19960205)365:2<289::AID-CNE7>3.0.CO;2-1.

[52] M. Riad, S. Garcia, K.C. Watkins, N. Jodoin, E. Doucet, X. Langlois, S. el Mestikawy, M. Hamon, and L. Descarries, Somatodendritic localization of 5-HT1A and preterminal axonal localization of 5-HT1B serotonin receptors in adult rat brain. J Comp Neurol 417 (2000) 181-94. http://www.ncbi.nlm.nih.gov/pubmed/10660896

[53] P.R. Albert, and F. Vahid-Ansari, The 5-HT1A receptor: Signaling to behavior. Biochimie 161 (2019) 34-45. doi: 10.1016/j.biochi.2018.10.015.

[54] R.W. Invernizzi, L. Cervo, and R. Samanin, 8-Hydroxy-2-(di-n-propylamino) tetralin, a selective serotonin1A receptor agonist, blocks haloperidol-induced catalepsy by an action on raphe nuclei medianus and dorsalis. Neuropharmacology 27 (1988) 515-8. doi: 10.1016/0028-3908(88)90134-7.

[55] E.P. Prinssen, F.C. Colpaert, and W. Koek, 5-HT1A receptor activation and anti-cataleptic effects: high-efficacy agonists maximally inhibit haloperidol-induced catalepsy. Eur J Pharmacol 453 (2002) 217-21. doi: 10.1016/s0014-2999(02)02430-5.

[56] S.M. Stahl, Mechanism of action of serotonin selective reuptake inhibitors. Serotonin receptors and pathways mediate therapeutic effects and side effects. J Affect Disord 51 (1998) 215-35. doi: 10.1016/s0165-0327(98)00221-3.

[57] A.F. Schatzberg, Pharmacological principles of antidepressant efficacy. Hum Psychopharmacol 17 Suppl 1 (2002) S17-22. doi: 10.1002/hup.399.

[58] A.V. Kulikov, R.R. Gainetdinov, E. Ponimaskin, A.V. Kalueff, V.S. Naumenko, and N.K. Popova, Interplay between the key proteins of serotonin system in SSRI antidepressants efficacy. Expert Opin Ther Targets 22 (2018) 319-330. doi: 10.1080/14728222.2018.1452912.

[59] K.A. Berg, and W.P. Clarke, Making Sense of Pharmacology: Inverse Agonism and Functional Selectivity. International Journal of Neuropsychopharmacology 21 (2018) 962-977. doi: 10.1093/ijnp/pyy071.

[60] N.M. Barnes, G.P. Ahern, C. Becamel, J. Bockaert, M. Camilleri, S. Chaumont-Dubel, S. Claeysen, K.A. Cunningham, K.C. Fone, M. Gershon, G. Di Giovanni, N.M. Goodfellow, A.L. Halberstadt, R.M. Hartley, G. Hassaine, K. Herrick-Davis, R. Hovius, E. Lacivita, E.K. Lambe, M. Leopoldo, F.O. Levy, S.C.R. Lummis, P. Marin, L. Maroteaux, A.C. McCreary, D.L. Nelson, J.F. Neumaier, A. Newman-Tancredi, H. Nury, A. Roberts, B.L. Roth, A. Roumier, G.J. Sanger, M. Teitler, T. Sharp, C.M. Villalon, H. Vogel, S.W. Watts, and D. Hoyer, International Union of Basic and Clinical Pharmacology. CX. Classification of Receptors for 5-hydroxytryptamine; Pharmacology and Function. Pharmacol Rev 73 (2021) 310-520. doi: 10.1124/pr.118.015552.

[61] T. Sharp, and N.M. Barnes, Central 5-HT receptors and their function; present and future. Neuropharmacology 177 (2020) 108155. doi: 10.1016/j.neuropharm.2020.108155.

[62] K.T. Dineley, M. Westerman, D. Bui, K. Bell, K.H. Ashe, and J.D. Sweatt, Beta-amyloid activates the mitogen-activated protein kinase cascade via hippocampal alpha7 nicotinic acetylcholine receptors: In vitro and in vivo mechanisms related to Alzheimer's disease. J Neurosci 21 (2001) 4125-33. http://www.ncbi.nlm.nih.gov/pubmed/11404397

[63] B.T. Hyman, T.E. Elvhage, and J. Reiter, Extracellular signal regulated kinases. Localization of protein and mRNA in the human hippocampal formation in Alzheimer's disease. Am J Pathol 144 (1994) 565-72. http://www.ncbi.nlm.nih.gov/pubmed/8129042

[64] S.M. Kulich, and C.T. Chu, Sustained extracellular signal-regulated kinase activation by 6-hydroxydopamine: implications for Parkinson's disease. J Neurochem 77 (2001) 1058-66. doi: 10.1046/j.1471-4159.2001.00304.x.

[65] C. Russo, V. Dolcini, S. Salis, V. Venezia, N. Zambrano, T. Russo, and G. Schettini, Signal transduction through tyrosine-phosphorylated C-terminal fragments of amyloid precursor protein

via an enhanced interaction with Shc/Grb2 adaptor proteins in reactive astrocytes of Alzheimer's disease brain. J Biol Chem 277 (2002) 35282-8. doi: 10.1074/jbc.M110785200.

[66] J. Sun, and G. Nan, The extracellular signal-regulated kinase 1/2 pathway in neurological diseases: A potential therapeutic target (Review). Int J Mol Med 39 (2017) 1338-1346. doi: 10.3892/ijmm.2017.2962.

[67] N.S. Ashraf, J.R. Sutton, Y. Yang, B. Ranxhi, K. Libohova, E.D. Shaw, A.J. Barget, S.V. Todi, H.L. Paulson, and M.d.C. Costa, Druggable genome screen identifies new regulators of the abundance and toxicity of ATXN3, the Spinocerebellar Ataxia type 3 disease protein. Neurobiology of Disease 137 (2020) 104697. doi: 10.1016/j.nbd.2019.104697.

[68] A.S. Sowa, T.G. Popova, T. Harmuth, J.J. Weber, P. Pereira Sena, J. Schmidt, J. Hübener-Schmid, and T. Schmidt, Neurodegenerative phosphoprotein signaling landscape in models of SCA3. Molecular Brain 14 (2021). doi: 10.1186/s13041-020-00723-0.

[69] G.V. Carr, and I. Lucki, The role of serotonin receptor subtypes in treating depression: a review of animal studies. Psychopharmacology (Berl) 213 (2011) 265-87. doi: 10.1007/s00213-010-2097-z.

[70] V. Klimek, J. Zak-Knapik, and M. Mackowiak, Effects of repeated treatment with fluoxetine and citalopram, 5-HT uptake inhibitors, on 5-HT1A and 5-HT2 receptors in the rat brain. J Psychiatry Neurosci 19 (1994) 63-7. http://www.ncbi.nlm.nih.gov/pubmed/8148368

[71] J. Maj, and E. Moryl, Effects of sertraline and citalopram given repeatedly on the responsiveness of 5-HT receptor subpopulations. J Neural Transm Gen Sect 88 (1992) 143-56. doi: 10.1007/BF01244819.

[72] M. El Mansari, C. Sanchez, G. Chouvet, B. Renaud, and N. Haddjeri, Effects of acute and long-term administration of escitalopram and citalopram on serotonin neurotransmission: an in vivo electrophysiological study in rat brain. Neuropsychopharmacology 30 (2005) 1269-77. doi: 10.1038/sj.npp.1300686.

[73] N. Haddjeri, P. Blier, and C. de Montigny, Long-term antidepressant treatments result in a tonic activation of forebrain 5-HT1A receptors. J Neurosci 18 (1998) 10150-6. http://www.ncbi.nlm.nih.gov/pubmed/9822768

[74] F. Artigas, 5-HT and antidepressants: new views from microdialysis studies. Trends Pharmacol Sci 14 (1993) 262. doi: 10.1016/0165-6147(93)90125-4.

[75] V. Perez, J. Soler, D. Puigdemont, E. Alvarez, and F. Artigas, A double-blind, randomized, placebo-controlled trial of pindolol augmentation in depressive patients resistant to serotonin reuptake inhibitors. Grup de Recerca en Trastorns Afectius. Arch Gen Psychiatry 56 (1999) 375-9. doi: 10.1001/archpsyc.56.4.375.

[76] M.C. Scorza, L. Llado-Pelfort, S. Oller, R. Cortes, D. Puigdemont, M.J. Portella, R. Perez-Egea, E. Alvarez, P. Celada, V. Perez, and F. Artigas, Preclinical and clinical characterization of the selective 5-HT(1A) receptor antagonist DU-125530 for antidepressant treatment. Br J Pharmacol 167 (2012) 1021-34. doi: 10.1111/j.1476-5381.2011.01770.x.

[77] M.J. Millan, S. Veiga, S. Girardon, and M. Brocco, Blockade of serotonin 5-HT1B and 5-HT2A receptors suppresses the induction of locomotor activity by 5-HT reuptake inhibitors, citalopram and fluvoxamine, in NMRI mice exposed to a novel environment: a comparison to other 5-HT receptor subtypes. Psychopharmacology (Berl) 168 (2003) 397-409. doi: 10.1007/s00213-003-1389-y.

[78] E. Calcagno, S. Guzzetti, A. Canetta, C. Fracasso, S. Caccia, L. Cervo, and R.W. Invernizzi, Enhancement of cortical extracellular 5-HT by 5-HT1A and 5-HT2C receptor blockade restores the antidepressant-like effect of citalopram in non-responder mice. Int J Neuropsychopharmacol 12 (2009) 793-803. doi: 10.1017/S1461145708009760.

[79] L.J. Boothman, S.N. Mitchell, and T. Sharp, Investigation of the SSRI augmentation properties of 5-HT(2) receptor antagonists using in vivo microdialysis. Neuropharmacology 50 (2006) 726-32. doi: 10.1016/j.neuropharm.2005.11.020.

[80] E. Syvalahti, J. Penttila, H. Majasuo, E.P. Palvimaki, A. Laakso, and J. Hietala, Combined treatment with citalopram and buspirone: effects on serotonin 5-HT2A and 5-HT2C receptors in the rat brain. Pharmacopsychiatry 39 (2006) 1-8. doi: 10.1055/s-2006-931470.

[81] P. Bonaventure, L. Kelly, L. Aluisio, J. Shelton, B. Lord, R. Galici, K. Miller, J. Atack, T.W. Lovenberg, and C. Dugovic, Selective blockade of 5-hydroxytryptamine (5-HT)7 receptors enhances 5-HT transmission, antidepressant-like behavior, and rapid eye movement sleep suppression induced by citalopram in rodents. J Pharmacol Exp Ther 321 (2007) 690-8. doi: 10.1124/jpet.107.119404.

[82] A. Wesolowska, A. Nikiforuk, K. Stachowicz, and E. Tatarczynska, Effect of the selective 5-HT7 receptor antagonist SB 269970 in animal models of anxiety and depression. Neuropharmacology 51 (2006) 578-86. doi: 10.1016/j.neuropharm.2006.04.017.

[83] U.L. Mullins, G. Gianutsos, and A.S. Eison, Effects of antidepressants on 5-HT7 receptor regulation in the rat hypothalamus. Neuropsychopharmacology 21 (1999) 352-67. doi: 10.1016/S0893-133X(99)00041-X.

[84] M. Okada, R. Matsumoto, Y. Yamamoto, and K. Fukuyama, Effects of Subchronic Administrations of Vortioxetine, Lurasidone, and Escitalopram on Thalamocortical Glutamatergic Transmission Associated with Serotonin 5-HT7 Receptor. Int J Mol Sci 22 (2021). doi: 10.3390/ijms22031351.

[85] A.J. Sleight, C. Carolo, N. Petit, C. Zwingelstein, and A. Bourson, Identification of 5-hydroxytryptamine7 receptor binding sites in rat hypothalamus: sensitivity to chronic antidepressant treatment. Mol Pharmacol 47 (1995) 99-103. http://www.ncbi.nlm.nih.gov/pubmed/7838138

[86] L.A. Dawson, and P. Li, Effects of 5-HT(6) receptor blockade on the neurochemical outcome of antidepressant treatment in the frontal cortex of the rat. J Neural Transm (Vienna) 110 (2003) 577-90. doi: 10.1007/s00702-003-0812-1.

[87] A. Nikiforuk, T. Kos, and A. Wesolowska, The 5-HT6 receptor agonist EMD 386088 produces antidepressant and anxiolytic effects in rats after intrahippocampal administration. Psychopharmacology (Berl) 217 (2011) 411-8. doi: 10.1007/s00213-011-2297-1.

[88] P. Svenningsson, E.T. Tzavara, H. Qi, R. Carruthers, J.M. Witkin, G.G. Nomikos, and P. Greengard, Biochemical and behavioral evidence for antidepressant-like effects of 5-HT6 receptor stimulation. J Neurosci 27 (2007) 4201-9. doi: 10.1523/JNEUROSCI.3110-06.2007.

[89] A. Wesolowska, Study into a possible mechanism responsible for the antidepressant-like activity of the selective 5-HT6 receptor antagonist SB-399885 in rats. Pharmacol Rep 59 (2007) 664-71. http://www.ncbi.nlm.nih.gov/pubmed/18195455

[90] A. Wesolowska, and A. Nikiforuk, Effects of the brain-penetrant and selective 5-HT6 receptor antagonist SB-399885 in animal models of anxiety and depression. Neuropharmacology 52 (2007) 1274-83. doi: 10.1016/j.neuropharm.2007.01.007.

[91] L.A. Dawson, The central role of 5-HT6 receptors in modulating brain neurochemistry. Int Rev Neurobiol 96 (2011) 1-26. doi: 10.1016/B978-0-12-385902-0.00001-2.

[92] G.R. Villas-Boas, S.N. Lavorato, M.M. Paes, P.M.G. de Carvalho, V.C. Rescia, M.S. Cunha, M.F. de Magalhaes-Filho, L.F. Ponsoni, A.A.V. de Carvalho, R.B. de Lacerda, S.L.L. da, S.T.-H.M. da, L.A.F. Lopes, L.G.R. Oliveira, S.E. Silva-Filho, A.P.S. da Silveira, R.K.N. Cuman, S.S.-C.F.M. de, J.F. Comar, A.B.L. do, J.N. Dos Santos, W.R. de Freitas, K.V. Leao, J.G. da Silva, R.C. Klein, M.H.F. Klein, S.R.B.H. da, C.K.C. Fernandes, L.R.D.G. de, and S.A. Oesterreich, Modulation of

the Serotonergic Receptosome in the Treatment of Anxiety and Depression: A Narrative Review of the Experimental Evidence. Pharmaceuticals (Basel) 14 (2021). doi: 10.3390/ph14020148.

[93] F. Artigas, Serotonin receptors involved in antidepressant effects. Pharmacol Ther 137 (2013) 119-31. doi: 10.1016/j.pharmthera.2012.09.006.

[94] B. Bang-Andersen, T. Ruhland, M. Jørgensen, G. Smith, K. Frederiksen, K.G. Jensen, H. Zhong, S.M. Nielsen, S. Hogg, A. Mørk, and T.B. Stensbøl, Discovery of 1-[2-(2,4-Dimethylphenylsulfanyl)phenyl]piperazine (Lu AA21004): A Novel Multimodal Compound for the Treatment of Major Depressive Disorder. Journal of Medicinal Chemistry 54 (2011) 3206-3221. doi: 10.1021/jm101459g.

[95] A. Mørk, A. Pehrson, L.T. Brennum, S.M. Nielsen, H. Zhong, A.B. Lassen, S. Miller, L. Westrich, N.J. Boyle, C. Sánchez, C.W. Fischer, N. Liebenberg, G. Wegener, C. Bundgaard, S. Hogg, B. Bang-Andersen, and T.B. Stensbøl, Pharmacological Effects of Lu AA21004: A Novel Multimodal Compound for the Treatment of Major Depressive Disorder. Journal of Pharmacology and Experimental Therapeutics 340 (2012) 666-675. doi: 10.1124/jpet.111.189068.

[96] C. Sanchez, K.E. Asin, and F. Artigas, Vortioxetine, a novel antidepressant with multimodal activity: Review of preclinical and clinical data. Pharmacology & Therapeutics 145 (2015) 43-57. doi: 10.1016/j.pharmthera.2014.07.001.

Appendix.

Permission of figures' usage

Consent to adaptation of Figure 2 of the Chapter 1. General Introduction

March 9, 2021

Joana Sousa
University of Minho
Rua das Alminhas, 48
4510-180 S. Pedro da Cova, Gondomar
Porto
Portugal

Email: id6531@alunos.uminho.pt

Dear Joana Sousa:

This is to grant you permission to include the following figures in your thesis titled "Suppression of Machado-Joseph disease pathogenesis by serotonergic signaling: the contribution of serotonin receptors" for the University of Minho:

> Figures 2 and 14 from NM Barnes, GP Ahern, C Becamel, J Bockaert, M Camilleri, S Chaumont-Dubel, S Claeysen, KA Cunningham, KC Fone, M Gershon, G Di Giovanni, NM Goodfellow, AL Halberstadt, RM Hartley, G Hassaine, K Herrick-Davis, R Hovius, E Lacivita, EK Lambe, M Leopoldo, FO Levy, SCR Lummis, P Marin, L Maroteaux, AC McCreary, DL Nelson, JF Neumaier, A Newman-Tancredi, H Nury, A Roberts, BL Roth, A Roumier, GJ Sanger, M Teitler, T Sharp, CM Villalón, H Vogel, SW Watts, and D Hoyer (2021) International Union of Basic and Clinical Pharmacology. CX. Classification of Receptors for 5-hydroxytryptamine; Pharmacology and Function, *Pharmacol Rev*, 73(1): 310-520; DOI: https://doi.org/10.1124/pr.118.015552

Permission to reproduce the figures is granted for one-time use in any format or medium including print and electronic. The authors and the source of the materials must be cited in full, including the article title, journal title, volume, year, and page numbers.

Sincerely yours,

Richard Dodenhoff
Journals Director